

**Studies on Effect of Different Parameters on
Dyeing of Eco-friendly Polyester Fibres**

Thesis submitted by

Arnab Sen

Doctor of Philosophy (Engineering)

Chemical Engineering Department

Faculty Council of Engineering & Technology

Jadavpur University,

Kolkata, India

2018

JADAVPUR UNIVERSITY

KOLKATA 700032

Index No: 276/14/E

1. Title of the thesis: **Studies on Effect of Different Parameters on Dyeing of
Eco-friendly Polyester Fibres.**

2. Name. Designation & Institution of the Supervisors:

Dr. Avijit Bhowal,

Professor,

Chemical Engineering Department,

Jadavpur University,

Kolkata- 700032, India.

&

Dr. Siddhartha Datta,

Professor,

Chemical Engineering Department,

Jadavpur University,

Kolkata- 700032, India.

3. **List of Publication:**

- (i) Arnab Sen, Avijit Bhowal, Siddhartha Datta, “Dyeing of PTT fibre with disperse dyes using Response surface methodology-I”, Asian Dyer, 2018, Vol. 15, No. 2, pp. 45-48.

- (ii) Arnab Sen, Avijit Bhowal, Siddhartha Datta, “Dyeing of PTT fibre with disperse dyes using Response surface methodology-II”, Asian Dyer, 2018, Vol. 15, No. 3, pp. 50-54.
- (iii) Arnab Sen, Avijit Bhowal, Siddhartha Datta, “Comparison of Dyeing of Polyester Fibers with Natural dye and Bio-Mordant”, Progress in Color, Colorants and Coatings Journal, 2018, Vol. 11, pp. 165-172.
- (iv) Arnab Sen, Avijit Bhowal, Siddhartha Datta, “Application of natural dye on polytrimethylene terephthalate fiber”, Research Journal of Textile and Apparel, 2019, Vol. 23 Issue: 1, pp. 71-90, <https://doi.org/10.1108/RJTA-06-2018-0041>.

4. List of Patents: Nil

5. List of Presentations in National Conferences:

- (i) Arnab Sen, Avijit Bhowal and Siddhartha Datta, “Dyeing of polytrimethylene terephthalate fiber with natural dyes and biomordants: Optimization using response surface methodology”, Proceedings of National Conference on Fashion Apparel and Textile (NCFAT), 2018, Amity School of Fashion Technology, Amity University, NOIDA, Uttar Pradesh, India, 27th March, 2018, ISBN- 978-93-86238-51-1, pp. 10-14.

CERTIFICATE FROM THE SUPERVISORS

This is to certify that the thesis entitled “Studies on Effect of Different Parameters on Dyeing of Eco-friendly Polyester Fibres” submitted by Shri Arnab Sen, who got his name registered on 27th February 2014 for the award of Ph. D. (Engineering) degree of Jadavpur University is absolutely based upon his own work under the supervision of Dr. Avijit Bhowal and Dr. Siddhartha Datta and that neither his thesis nor any part of the thesis has been submitted for any degree/diploma or any other academic award anywhere before.

Dr. Avijit Bhowal,

Professor,

Chemical Engineering Department,

Jadavpur University,

Kolkata- 700032, India.

Dr. Siddhartha Datta,

Professor,

Chemical Engineering Department,

Jadavpur University,

Kolkata- 700032, India.

Dedicated to

Maa, Baba, Ajinkya & Srirupa,
Thamma, Twinkle, Puffy & Whitey.

Acknowledgement

I would like to express my deepest gratitude towards my supervisors, Dr. Siddhartha Datta, Professor, and Dr. Avijit Bhowal, Professor, Chemical Engineering Department, Jadavpur University, Kolkata- 700032, India, for their valuable guidance and continual encouragement for my research. I am very grateful to Dr. Papita Das Saha, Associate Professor, Chemical Engineering Department, Jadavpur University, for extending the facility for FT-IR spectroscopy. I would very earnestly like to thank all the faculty members, staff members and research scholars of the department for extending their wholehearted cooperation whenever needed.

My mother, Smt. Bijoya Sen, made me dream of a Ph.D. and kept inspiring me, while my father, Shri Amitabha Sen, put all the hard work together to take care of almost everything in my life so that I remained focused. Whatever I could be today is because of their sacrifices, and I express my deepest sense of gratitude to my parents. The unexpected lifelines, when I needed them the most, kept coming from my in-laws, and I am ever thankful to Shri S. P. Kundu, Smt. Indrani Kundu and Shri Sabyasachi Kundu, for making the journey smoother.

My efforts could not culminate fruitfully without the mentoring, criticism, support, care and sufferings of my soulmate, Smt. Srirupa Kundu Sen, and the laughter of my son, Master Ajinkya Sen. I owe my whole life to them for what they have taken in, and thank them eternally.

I would also extend my gratefulness to Shri U. S. Tolia, Shri J. B. Modak, Shri D. Ganguly, Shri S. Halder and Dr. R. Tamrakar for their professional help. For many other people in my family circles and professional spheres of life, who contributed to this journey, I would very humbly extend my thankfulness, and also my sincere apologies for not being able to accommodate their names herein.

Arnab Sen.

Contents

Chapter	Title	Page No.
	List of Tables	i-v
	List of Figures	vii-xix
1.	Introduction	1
1.1	Poly-ethylene terephthalate (PET) fiber	2
1.2	Overview of ecofriendly polyester fibers	4
1.2.1	Poly-trimethylene terephthalate fiber	5
1.2.2	Poly-lactic acid fiber	7
1.3	Dyeing of textile fibers	8
1.3.1	Classes of dyes	8
1.3.1.1	Disperse Dyes	10
1.3.1.2	Natural dyes	11
2.	Review of Literature	17
2.1	Dyeing of textile fibers	17
2.1.1	Dyeing of PET	18
2.1.2	Dyeing of PTT	20
2.1.3	Dyeing of PLA	22
2.2	Dyes used for textile fibers	24
2.2.1	Disperse Dyes	24
2.2.2	Natural dyes	26
2.2.2.1	Lac	30

2.2.2.2	Catechu	32
2.2.2.3	Myrobalan	34
2.2.2.4	Pomegranate	35
2.3	Coloration properties	37
2.3.1	Adsorption isotherms	38
2.3.2	Fastness properties	40
2.4	Characterization of textile fibers	42
2.4.1	Thermogravimetric analysis	43
2.4.2	Scanning electron microscopy	45
2.4.3	Fourier Transform- Infra Red Spectroscopy	47
2.5	Design of experiments	50
2.5.1	Central Composite Design	50
2.5.2	Response Surface Methodology	52
3.	Aims and Objectives	55
3.1	Objectives	57
4.	Characterization of PTT and PLA fibers	61
4.1	Experimental	62
4.1.1	Materials	62
4.1.2	Methods	63
4.2	Results and discussion	63
4.2.1	Thermo-gravimetric analysis (TGA)	63
4.2.2	Scanning electron microscopy	67
4.2.3	Fourier Transform Infrared (FTIR) spectroscopy	68
4.3	Summary	73

5.	Dyeing and Optimization with Disperse Dyes	75
5.1	Materials and methods	75
5.1.1	Materials	75
5.1.2	Dyes	76
5.1.3	Equipment	77
5.1.3.1	Dyeing apparatus	77
5.1.3.2	Launder-o-meter	77
5.1.3.3	Spectrophotometer	78
5.1.3.4	Fiber fineness and tensile strength tester	79
5.1.4	Methods	79
5.1.4.1	Dyeing	79
5.1.4.2	Measurement of color strength	80
5.1.4.3	Measurement of wash fastness	81
5.1.4.4	Measurement of tensile properties	81
5.2	Results and Discussions	81
5.2.1	Effect of temperature	85
5.2.2	Effect of initial pH of the dye bath	90
5.2.3	Effect of time	94
5.2.4	Effect of material to liquor ratio	99
5.2.5	Effect of rate of heating	103
5.3	Optimization with disperse dyes	107
5.3.1	Optimization with Disperse Yellow 56	108
5.3.1.1	Optimization for PTT	109
5.3.1.2	Optimization for PLA	115

5.3.2	Optimization with Disperse Blue 79	120
5.3.2.1	Optimization for PTT	120
5.3.2.2	Optimization for PLA	126
5.3.3	Optimization with Disperse Red 167	131
5.3.3.1	Optimization for PTT	131
5.3.3.2	Optimization for PLA	137
5.3	Summary	142
6.	Application of Natural Dyes	147
6.1	Materials and methods	148
6.1.1	Materials	148
6.1.2	Dyes	148
6.1.3	Equipment	149
6.1.4	Methods	149
6.1.4.1	Dyeing	149
6.1.4.2	Measurement of color, wash fastness and tensile properties	151
6.1.4.3	Measurement of perspiration fastness	151
6.1.4.4	Measurement of fastness to acids and alkalis	152
6.1.4.5	Measurement of hydrogen peroxide bleaching fastness	152
6.2	Results and Discussions	152
6.2.1	Effect of various parameters on color strength and tensile properties	153
6.2.1.1	Effect of temperature	153
6.2.1.2	Effect of initial pH of the dye bath	158
6.2.1.3	Effect of time	162
6.2.1.4	Effect of material to liquor ratio	166

6.2.2	Evaluation of fastness properties	170
6.2.3	Evaluation of FTIR spectra after dyeing with natural dyes and biomordants	174
6.2.4	Evaluation of adsorption isotherms	176
6.2.5	Pre-mordanting, meta-mordanting and post-mordanting with biomordants	178
6.2.5.1	Identification of suitable mordanting technique	179
6.2.5.2	Evaluation of fastness properties	184
6.2.5.3	Measurement of color values of meta-mordanted samples	191
6.2.6	Comparison of color strength with inorganic mordants	192
6.2.6.1	Effect of temperature	197
6.2.6.2	Effect of initial pH of the dye bath	202
6.2.6.3	Effect of time	208
6.2.6.4	Effect of material to liquor ratio	213
6.2.6.5	Effect of mordant concentration	219
6.3	Summary	224
7.	Optimization with Natural Dyes and Biomordants	227
7.1	Optimization with natural dyes and biomordants	228
7.1.1	Optimization with Lac using Catechu as biomordant	229
7.1.1.1	Optimization for PTT	230
7.1.1.2	Optimization for PLA	235
7.1.2	Optimization with Lac using Myrobalan as biomordant	242
7.1.2.1	Optimization for PTT	242
7.1.2.2	Optimization for PLA	248

7.1.3	Optimization with Lac using Pomegranate as biomordant	253
7.1.3.1	Optimization for PTT	253
7.1.3.2	Optimization for PLA	259
7.1.4	Optimization with Catechu using Myrobalan as biomordant	266
7.1.4.1	Optimization for PTT	266
7.1.4.2	Optimization for PLA	271
7.1.5	Optimization with Catechu using Pomegranate as biomordant	277
7.1.5.1	Optimization for PTT	277
7.1.5.2	Optimization for PLA	283
7.1.6	Optimization with Myrobalan using Pomegranate as biomordant	289
7.1.6.1	Optimization for PTT	289
7.1.6.2	Optimization for PLA	294
7.2	Summary	300
8.	Conclusion	305
9.	Future Scope of Work	311
	References	313

List of Tables

Table No.	Title	Page No.
Table 1.1	Classification of textile fibers	2
Table 1.2	Different classes of dyes for textile fibers	9
Table 1.3	Natural dyes commonly used for textile fibers	12
Table 1.4	List of commonly used biomordants.	15
Table 2.1	Standard test methods for some fastness properties of dyed textile fibers	41
Table 2.2	Functional groups and wavenumbers at which their peaks occur in FTIR spectroscopy.	48
Table 4.1	Peaks observed in FTIR of PTT and functional groups indicated	70
Table 4.2	Peaks observed in FTIR of PLA and functional groups indicated	72
Table 5.1	CIE L*a*b* values of PTT and PLA fibers with three disperse dyes	82
Table 5.2	Factors for normal probability plot of PTT with Disperse Yellow 56	109
Table 5.3	Factors for RSM of PTT with Disperse Yellow 56	111
Table 5.4	Average values of experiments used for RSM	111
Table 5.5	Variance analysis (ANOVA) of factors on response	114
Table 5.6	Variance analysis (ANOVA) of quadratic regression model	114
Table 5.7	Factors for RSM of PLA with Disperse Yellow 56	116
Table 5.8	Average values of experiments used for RSM	116
Table 5.9	Variance analysis (ANOVA) of factors on response	119
Table 5.10	Variance analysis (ANOVA) of quadratic regression model	120
Table 5.11	Average values of experiments used for RSM	121

Table 5.12	Variance analysis (ANOVA) of factors on response	125
Table 5.13	Variance analysis (ANOVA) of quadratic regression model	125
Table 5.14	Average values of experiments used for RSM	127
Table 5.15	Variance analysis (ANOVA) of factors on response	129
Table 5.16	Variance analysis (ANOVA) of quadratic regression model	130
Table 5.17	Average values of experiments used for RSM	132
Table 5.18	Variance analysis (ANOVA) of factors on response	136
Table 5.19	Variance analysis (ANOVA) of quadratic regression model	136
Table 5.20	Average values of experiments used for RSM	138
Table 5.21	Variance analysis (ANOVA) of factors on response	141
Table 5.22	Variance analysis (ANOVA) of quadratic regression model	141
Table 6.1	CIE L*a*b* values of PTT and PLA fibers with three natural dyes	153
Table 6.2	Legend for Tables 6.3 to 6.5	170
Table 6.3	Results for wash fastness for PTT and PLA with natural dyes	171
Table 6.4	Results for perspiration fastness for PTT and PLA with natural dyes	172
Table 6.5	Results for fastness to acids, alkalis and hydrogen peroxide for PTT and PLA with natural dyes.	173
Table 6.6	Legend for Tables 6.7 and 6.12	184
Table 6.7	Results for wash fastness of PTT for pre-, meta- and post-mordanting	185
Table 6.8	Results for wash fastness of PLA for pre-, meta- and post-mordanting	186

Table 6.9	Results for perspiration fastness of PTT for pre-, meta- and post-mordanting	187
Table 6.10	Results for perspiration fastness of PLA for pre-, meta- and post-mordanting.	188
Table 6.11	Results for fastness to acids, alkalis and hydrogen peroxide Bleaching of PTT for pre-, meta- and post-mordanting.	189
Table 6.12	Results for fastness to acids, alkalis and hydrogen peroxide bleaching of PLA for pre-, meta- and post-mordanting	190
Table 6.13	CIE L*a*b* values of PTT and PLA fibers with three natural dyes and biomordants	191
Table 6.14	Coding used for dyed fiber samples	193
Table 7.1	Factors for normal probability plot of PTT with Lac using Catechu as biomordant	229
Table 7.2	Factors for normal probability plot of PLA with Lac using Catechu as biomordant.	229
Table 7.3	Factors for RSM of PTT with Lac using Catechu as biomordant	231
Table 7.4	Average values of experiments used for RSM	232
Table 7.5	Variance analysis (ANOVA) of factors on response	234
Table 7.6	Variance analysis (ANOVA) of quadratic regression model	235
Table 7.7	Factors for RSM of PLA with Lac using Catechu as biomordant	236
Table 7.8	Average values of experiments used for RSM	237
Table 7.9	Variance analysis (ANOVA) of factors on response	240
Table 7.10	Variance analysis (ANOVA) of quadratic regression model	241

Table 7.11	Average values of experiments used for RSM	243
Table 7.12	Variance analysis (ANOVA) of factors on response	246
Table 7.13	Variance analysis (ANOVA) of quadratic regression model	246
Table 7.14	Average values of experiments used for RSM	249
Table 7.15	Variance analysis (ANOVA) of factors on response	251
Table 7.16	Variance analysis (ANOVA) of quadratic regression model	252
Table 7.17	Average values of experiments used for RSM	255
Table 7.18	Variance analysis (ANOVA) of factors on response	257
Table 7.19	Variance analysis (ANOVA) of quadratic regression model	258
Table 7.20	Average values of experiments used for RSM	261
Table 7.21	Variance analysis (ANOVA) of factors on response	263
Table 7.22	Variance analysis (ANOVA) of quadratic regression model	264
Table 7.23	Average values of experiments used for RSM	266
Table 7.24	Variance analysis (ANOVA) of factors on response	269
Table 7.25	Variance analysis (ANOVA) of quadratic regression model	270
Table 7.26	Average values of experiments used for RSM	272
Table 7.27	Variance analysis (ANOVA) of factors on response	275
Table 7.28	Variance analysis (ANOVA) of quadratic regression model	276
Table 7.29	Average values of experiments used for RSM	278
Table 7.30	Variance analysis (ANOVA) of factors on response	281
Table 7.31	Variance analysis (ANOVA) of quadratic regression model	282
Table 7.32	Average values of experiments used for RSM	284
Table 7.33	Variance analysis (ANOVA) of factors on response	286

Table 7.34	Variance analysis (ANOVA) of quadratic regression model	287
Table 7.35	Average values of experiments used for RSM	290
Table 7.36	Variance analysis (ANOVA) of factors on response	292
Table 7.37	Variance analysis (ANOVA) of quadratic regression model	293
Table 7.38	Average values of experiments used for RSM	295
Table 7.39	Variance analysis (ANOVA) of factors on response	297
Table 7.40	Variance analysis (ANOVA) of quadratic regression model	299

List of Figures

Figure No.	Title	Page No.
Figure 1.1	Chemical structure of PET	3
Figure 1.2	Structure of PTT	6
Figure 1.3	Structure of PLA fiber polymer	7
Figure 2.1	Structures of Laccic acids A, B, C and E	31
Figure 2.2	Structures of stereoisomers of Catechin	33
Figure 2.3	Structure of chebulinic acid	35
Figure 2.4	Structure of punicalin	36
Figure 2.5	Typical adsorption isotherms obtained in dyeing of textile fibers	39
Figure 2.6	Typical TG and DTG traces	44
Figure 2.7	Typical response surface with contour plots	53
Figure 4.1	Thermo-gravimetric analysis of undyed PTT fiber	64
Figure 4.2	Thermo-gravimetric analysis of undyed PLA fiber	66
Figure 4.3	SEM of PTT	67
Figure 4.4	SEM of PLA	68
Figure 4.5	FT-IR spectroscopy of PTT	69
Figure 4.6	FT-IR spectroscopy of PLA	71
Figure 5.1	Structure of Disperse Yellow 56 (C.I. 216550)	76
Figure 5.2	Structure of Disperse Blue 79 (C.I. 11345)	76
Figure 5.3	Structure of Disperse Red 167 (C.I. 11338)	76
Figure 5.4	Superlab HTHP dyeing apparatus	77
Figure 5.5	Ramp Washometer for evaluation of wash fastness	78

Figure 5.6	Color i5 Spectrophotometer	78
Figure 5.7	Schematic diagram of the dyeing cycle	80
Figure 5.8	PTT fiber dyed with Disperse Yellow 56	83
Figure 5.9	PTT fiber dyed with Disperse Blue 79	83
Figure 5.10	PTT fiber dyed with Disperse Red 167	83
Figure 5.11	PLA fiber dyed with Disperse Yellow 56	84
Figure 5.12	PLA fiber dyed with Disperse Blue 79	84
Figure 5.13	PLA fiber dyed with Disperse Red 167	84
Figure 5.14	Effect of temperature on K/S value and dE value for Disperse Yellow 56	85
Figure 5.15	Effect of temperature on K/S value and dE value for Disperse Blue 79	86
Figure 5.16	Effect of temperature on K/S value and dE value for Disperse Red 167	86
Figure 5.17	Effect of temperature on tensile properties for Disperse Yellow 56	88
Figure 5.18	Effect of temperature on tensile properties for Disperse Blue 79	88
Figure 5.19	Effect of temperature on tensile properties for Disperse Red 167	89
Figure 5.20	Effect of initial pH of dye bath on K/S value and dE value for Disperse Yellow 56	90

Figure 5.21	Effect of initial pH of dye bath on K/S value and dE value for Disperse Blue 79	91
Figure 5.22	Effect of initial pH of dye bath on K/S value and dE value for Disperse Red 167	91
Figure 5.23	Effect of initial pH of dye bath on tensile properties for Disperse Yellow 56	92
Figure 5.24	Effect of initial pH of dye bath on tensile properties for Disperse Blue 79	93
Figure 5.25	Effect of initial pH of dye bath on tensile properties for Disperse Red 167	93
Figure 5.26	Effect of time on K/S value and dE value for Disperse Yellow 56	95
Figure 5.27	Effect of time on K/S value and dE value for Disperse Blue 79	95
Figure 5.28	Effect of time on K/S value and dE value for Disperse Red 167	96
Figure 5.29	Effect of time on tensile properties for Disperse Yellow 56	97
Figure 5.30	Effect of time on tensile properties for Disperse Blue 79	98
Figure 5.31	Effect of time on tensile properties for Disperse Red 167	98
Figure 5.32	Effect of material to liquor ratio on K/S value and dE value for Disperse Yellow 56	100
Figure 5.33	Effect of material to liquor ratio on K/S value and dE value for Disperse Blue 79	100
Figure 5.34	Effect of material to liquor ratio on K/S value and dE value for Disperse Red 167	101

Figure 5.35	Effect of material to liquor ratio on tensile properties for Disperse Yellow 56	102
Figure 5.36	Effect of material to liquor ratio on tensile properties for Disperse Blue 79	102
Figure 5.37	Effect of material to liquor ratio on tensile properties for Disperse Red 167	103
Figure 5.38	Effect of rate of heating on K/S value and dE value for Disperse Yellow 56	104
Figure 5.29	Effect of rate of heating on K/S value and dE value for Disperse Blue 79	104
Figure 5.40	Effect of rate of heating on K/S value and dE value for Disperse Red 167	105
Figure 5.41	Effect of rate of heating on tensile properties for Disperse Yellow 56	106
Figure 5.42	Effect of rate of heating on tensile properties for Disperse Blue 79	106
Figure 5.43	Effect of rate of heating on tensile properties for Disperse Red 167	107
Figure 5.44	Normal probability plot of Disperse Yellow 56 applied on PTT	110
Figure 5.45	Contour plot for K/S value (<i>y</i>) with temperature (<i>A</i>) and initial pH of dye bath (<i>B</i>)	112
Figure 5.46	Contour plot for K/S value (<i>y</i>) with initial pH of dye bath (<i>B</i>) and time (<i>C</i>)	13
Figure 5.47	Contour plot for K/S value (<i>y</i>) with temperature (<i>A</i>) and time (<i>C</i>)	113

Figure 5.48	Normal probability plot of Disperse Yellow 56 applied on PLA	115
Figure 5.49	Contour plot for K/S value (<i>y</i>) with temperature (<i>A</i>) and initial pH of dye bath (<i>B</i>)	117
Figure 5.50	Contour plot for K/S value (<i>y</i>) with initial pH of dye bath (<i>B</i>) and time (<i>C</i>)	117
Figure 5.51	Contour plot for K/S value (<i>y</i>) with temperature (<i>A</i>) and time (<i>C</i>)	118
Figure 5.52	Normal probability plot of Disperse Blue 79 applied on PTT	121
Figure 5.53	Contour plot for K/S value (<i>y</i>) with temperature (<i>A</i>) and initial pH of dye bath (<i>B</i>)	123
Figure 5.54	Contour plot for K/S value (<i>y</i>) with initial pH of dye bath (<i>B</i>) and time (<i>C</i>)	123
Figure 5.55	Contour plot for K/S value (<i>y</i>) with temperature (<i>A</i>) and time (<i>C</i>)	124
Figure 5.56	Normal probability plot of Disperse Blue 79 applied on PLA	126
Figure 5.57	Contour plot for K/S value (<i>y</i>) with temperature (<i>A</i>) and initial pH of dye bath (<i>B</i>)	128
Figure 5.58	Contour plot for K/S value (<i>y</i>) with initial pH of dye bath (<i>B</i>) and time (<i>C</i>)	128
Figure 5.59	Contour plot for K/S value (<i>y</i>) with temperature (<i>A</i>) and time (<i>C</i>)	129
Figure 5.60	Normal probability plot of Disperse Red 167 applied on PTT	131
Figure 5.61	Contour plot for K/S value (<i>y</i>) with temperature (<i>A</i>) and initial pH of dye bath (<i>B</i>)	133
Figure 5.62	Contour plot for K/S value (<i>y</i>) with initial pH of dye bath (<i>B</i>) and time (<i>C</i>)	134

Figure 5.63	Contour plot for K/S value (<i>y</i>) with temperature (<i>A</i>) and time (<i>C</i>)	134
Figure 5.64	Normal probability plot of Disperse Red 167 applied on PLA	137
Figure 5.65	Contour plot for K/S value (<i>y</i>) with temperature (<i>A</i>) and initial pH of dye bath (<i>B</i>)	139
Figure 5.66	Contour plot for K/S value (<i>y</i>) with initial pH of dye bath (<i>B</i>) and time (<i>C</i>)	139
Figure 5.67	Contour plot for K/S value (<i>y</i>) with temperature (<i>A</i>) and time (<i>C</i>)	140
Figure 6.1	AATCC Perspiration Tester	151
Figure 6.2	Effect of temperature on K/S value for Lac	154
Figure 6.3	Effect of temperature on K/S value for Catechu	154
Figure 6.4	Effect of temperature on K/S value for Myrobalan	155
Figure 6.5	Effect of temperature on tensile properties for Lac	156
Figure 6.6	Effect of temperature on tensile properties for Catechu	156
Figure 6.7	Effect of temperature on tensile properties for Myrobalan	157
Figure 6.8	Effect of initial pH of dye bath on K/S value for Lac	158
Figure 6.9	Effect of initial pH of dye bath on K/S value for Catechu	159
Figure 6.10	Effect of initial pH of dye bath on K/S value for Myrobalan	159
Figure 6.11:	Effect of initial pH of dye bath on tensile properties of Lac	160
Figure 6.12	Effect of initial pH of dye bath on tensile properties of Catechu	161
Figure 6.13	Effect of initial pH of dye bath on tensile properties of Myrobalan	161
Figure 6.14	Effect of time on K/S value for Lac	162
Figure 6.15	Effect of time on K/S value for Catechu	163
Figure 6.16	Effect of time on K/S value for Myrobalan	163

Figure 6.17	Effect of time on tensile properties for Lac	164
Figure 6.18	Effect of time on tensile properties for Catechu	165
Figure 6.19	Effect of time on tensile properties for Myrobalan	165
Figure 6.20	Effect of material to liquor ratio on K/S value for Lac	166
Figure 6.21	Effect of material to liquor ratio on K/S value for Catechu	167
Figure 6.22	Effect of material to liquor ratio on K/S value for Myrobalan	167
Figure 6.23	Effect of material to liquor ratio on tensile properties for Lac	168
Figure 6.24	Effect of material to liquor ratio on tensile properties for Catechu	169
Figure 6.25	Effect of material to liquor ratio on tensile properties for Myrobalan	169
Figure 6.26	FT-IR spectrum for PTT dyed with Lac	174
Figure 6.27	FT-IR spectrum for PTT dyed with Catechu	175
Figure 6.28	FT-IR spectrum for PTT dyed with Myrobalan	175
Figure 6.29	Adsorption isotherm of fibers dyed with Lac	176
Figure 6.30	Adsorption isotherm of fibers dyed with Catechu	177
Figure 6.31	Adsorption isotherm of fibers dyed with Myrobalan	177
Figure 6.32	K/S values with Lac and Catechu (biomordant)	181
Figure 6.33	K/S values with Lac and Myrobalan (biomordant)	181
Figure 6.34	K/S values with Lac and Pomegranate (biomordant)	182
Figure 6.35	K/S values with Catechu and Myrobalan (biomordant)	182
Figure 6.36	K/S values with Catechu and Pomegranate (biomordant)	183
Figure 6.37	K/S values with Myrobalan and Pomegranate (biomordant)	183
Figure 6.38	Shades of PTT with Lac using different mordants	194
Figure 6.39	Shades of PTT with Catechu using different mordants	194

Figure 6.40	Shades of PTT with Myrobalan using different mordants	195
Figure 6.41	Shades of PLA with Lac using different mordants	195
Figure 6.42	Shades of PLA with Catechu using different mordants	196
Figure 6.43	Shades of PLA with Myrobalan using different mordants	196
Figure 6.44	Effect of temperature on K/S value of PTT with Lac	197
Figure 6.45	Effect of temperature on K/S value of PLA with Lac	198
Figure 6.46	Effect of temperature on K/S value of PET with Lac.	198
Figure 6.47	Effect of temperature on K/S value of PTT with Catechu	199
Figure 6.48	Effect of temperature on K/S value of PLA with Catechu	199
Figure 6.49	Effect of temperature on K/S value of PET with Catechu	200
Figure 6.50	Effect of temperature on K/S value of PTT with Myrobalan	200
Figure 6.51	Effect of temperature on K/S value of PLA with Myrobalan	201
Figure 6.52	Effect of temperature on K/S value of PET with Myrobalan	201
Figure 6.53	Effect of initial pH of dye bath on K/S value of PTT with Lac	203
Figure 6.54	Effect of initial pH of dye bath on K/S value of PLA with Lac	203
Figure 6.55	Effect of initial pH of dye bath on K/S value of PET with Lac	204
Figure 6.56	Effect of initial pH of dye bath on K/S value of PTT with Catechu	204
Figure 6.57	Effect of initial pH of dye bath on K/S value of PLA with Catechu	205
Figure 6.58	Effect of initial pH of dye bath on K/S value of PET with Catechu	205
Figure 6.59	Effect of initial pH on K/S value of PTT with Myrobalan	206
Figure 6.60	Effect of initial pH on K/S value of PLA with Myrobalan	206
Figure 6.61	Effect of initial pH on K/S value of PET with Myrobalan	207
Figure 6.62	Effect of time on K/S value of PTT with Lac.	208

Figure 6.63	Effect of time on K/S value of PLA with Lac	209
Figure 6.64	Effect of time on K/S value of PET with Lac	209
Figure 6.65	Effect of time on K/S value of PTT with Catechu	210
Figure 6.66	Effect of time on K/S value of PLA with Catechu	210
Figure 6.67	Effect of time on K/S value of PET with Catechu	211
Figure 6.68	Effect of time on K/S value of PTT with Myrobalan	211
Figure 6.69	Effect of time on K/S value of PLA with Myrobalan	212
Figure 6.70	Effect of time on K/S value of PET with Myrobalan	212
Figure 6.71	Effect of material to liquor ratio on K/S value of PTT with Lac	214
Figure 6.72	Effect of material to liquor ratio on K/S value of PLA with Lac	214
Figure 6.73	Effect of material to liquor ratio on K/S value of PET with Lac	215
Figure 6.74	Effect of material to liquor ratio for PTT with Catechu	215
Figure 6.75	Effect of material to liquor ratio for PLA with Catechu	216
Figure 6.76	Effect of material to liquor ratio for PET with Catechu	216
Figure 6.77	Effect of material to liquor ratio for PTT with Myrobalan	217
Figure 6.78	Effect of material to liquor ratio for PLA with Myrobalan	217
Figure 6.79	Effect of material to liquor ratio for PET with Myrobalan	218
Figure 6.80	Effect of mordant concentration on K/S value of PTT with Lac	219
Figure 6.81	Effect of mordant concentration on K/S value of PLA with Lac	220
Figure 6.82	Effect of mordant concentration on K/S value of PET with Lac	220
Figure 6.83	Effect of mordant concentration on K/S value of PTT with Catechu2	221
Figure 6.84	Effect of mordant concentration on K/S value of PLA with Catechu	221
Figure 6.85	Effect of mordant concentration on K/S value of PET with Catechu	222

Figure 6.86	Effect of mordant concentration on K/S value of PTT with Myrobalan	222
Figure 6.87	Effect of mordant concentration on K/S value of PLA with Myrobalan	223
Figure 6.88	Effect of mordant concentration on K/S value of PET with Myrobalan	223
Figure 7.1	Normal probability plot of Lac applied on PTT using Catechu as biomordant	230
Figure 7.2	Contour plot for K/S value (<i>y</i>) with temperature (<i>A</i>) and initial pH of dye bath (<i>B</i>)	233
Figure 7.3	Contour plot for K/S value (<i>y</i>) with initial pH of dye bath (<i>B</i>) and time (<i>C</i>)	233
Figure 7.4	Contour plot for K/S value (<i>y</i>) with temperature (<i>A</i>) and time (<i>C</i>)	234
Figure 7.5	Normal probability plot of Lac applied on PLA using Catechu as biomordant	236
Figure 7.6	Contour plot for K/S value (<i>y</i>) with temperature (<i>A</i>) and initial pH of dye bath (<i>B</i>)	238
Figure 7.7	Contour plot for K/S value (<i>y</i>) with initial pH of dye bath (<i>B</i>) and time (<i>C</i>)	238
Figure 7.8	Contour plot for K/S value (<i>y</i>) with temperature (<i>A</i>) and time (<i>C</i>)	239
Figure 7.9	Normal probability plot of Lac applied on PTT using Myrobalan as biomordant	242

Figure 7.10	Contour plot for K/S value (<i>y</i>) with temperature (<i>A</i>) and initial pH of dye bath (<i>B</i>)	244
Figure 7.11	Contour plot for K/S value (<i>y</i>) with initial pH of dye bath (<i>B</i>) and time (<i>C</i>)	244
Figure 7.12	Contour plot for K/S value (<i>y</i>) with temperature (<i>A</i>) and time (<i>C</i>)	245
Figure 7.13	Normal probability plot of Lac applied on PLA using Myrobalan as biomordant	247
Figure 7.14	Contour plot for K/S value (<i>y</i>) with temperature (<i>A</i>) and initial pH of dye bath (<i>B</i>)	250
Figure 7.15	Contour plot for K/S value (<i>y</i>) with initial pH of dye bath (<i>B</i>) and time (<i>C</i>)	250
Figure 7.16	Contour plot for K/S value (<i>y</i>) with temperature (<i>A</i>) and time (<i>C</i>)	251
Figure 7.17	Normal probability plot of Lac applied on PTT using Pomegranate as biomordant	253
Figure 7.18	Contour plot for K/S value (<i>y</i>) with temperature (<i>A</i>) and initial pH of dye bath (<i>B</i>)	256
Figure 7.19:	Contour plot for K/S value (<i>y</i>) with initial pH of dye bath (<i>B</i>) and time (<i>C</i>)	256
Figure 7.20	Contour plot for K/S value (<i>y</i>) with temperature (<i>A</i>) and time (<i>C</i>)	257
Figure 7.21	Normal probability plot of Lac applied on PLA using Myrobalan as biomordant	259
Figure 7.22	Contour plot for K/S value (<i>y</i>) with temperature (<i>A</i>) and initial pH of dye bath (<i>B</i>)	262

Figure 7.23	Contour plot for K/S value (<i>y</i>) with initial pH of dye bath (<i>B</i>) and time (<i>C</i>)	262
Figure 7.24:	Contour plot for K/S value (<i>y</i>) with temperature (<i>A</i>) and time (<i>C</i>)	263
Figure 7.25	Normal probability plot of Catechu applied on PTT using Myrobalan as biomordant	264
Figure 7.26	Contour plot for K/S value (<i>y</i>) with temperature (<i>A</i>) and initial pH of dye bath (<i>B</i>)	268
Figure 7.27	Contour plot for K/S value (<i>y</i>) with initial pH of dye bath (<i>B</i>) and time (<i>C</i>)	268
Figure 7.28	Contour plot for K/S value (<i>y</i>) with temperature (<i>A</i>) and time (<i>C</i>)	269
Figure 7.29	Normal probability plot of Catechu applied on PLA using Myrobalan as biomordant	271
Figure 7.30	Contour plot for K/S value (<i>y</i>) with temperature (<i>A</i>) and initial pH of dye bath (<i>B</i>)	274
Figure 7.31	Contour plot for K/S value (<i>y</i>) with initial pH of dye bath (<i>B</i>) and time (<i>C</i>)	274
Figure 7.32	Contour plot for K/S value (<i>y</i>) with temperature (<i>A</i>) and time (<i>C</i>)	275
Figure 7.33	Normal probability plot of Catechu applied on PTT using Pomegranate as biomordant	277
Figure 7.34	Contour plot for K/S value (<i>y</i>) with temperature (<i>A</i>) and initial pH of dye bath (<i>B</i>)	279
Figure 7.35	Contour plot for K/S value (<i>y</i>) with initial pH of dye bath (<i>B</i>) and time (<i>C</i>)	280

Figure 7.36	Contour plot for K/S value (<i>y</i>) with temperature (<i>A</i>) and time (<i>C</i>)	280
Figure 7.37	Normal probability plot of Catechu applied on PLA using Pomegranate as biomordant	283
Figure 7.38	Contour plot for K/S value (<i>y</i>) with temperature (<i>A</i>) and initial pH of dye bath (<i>B</i>)	285
Figure 7.39	Contour plot for K/S value (<i>y</i>) with initial pH of dye bath (<i>B</i>) and time (<i>C</i>)	285
Figure 7.40	Contour plot for K/S value (<i>y</i>) with temperature (<i>A</i>) and time (<i>C</i>)	286
Figure 7.41	Normal probability plot of Myrobalan applied on PTT using Pomegranate as biomordant	289
Figure 7.42	Contour plot for K/S value (<i>y</i>) with temperature (<i>A</i>) and initial pH of dye bath (<i>B</i>)	291
Figure 7.43	Contour plot for K/S value (<i>y</i>) with initial pH of dye bath (<i>B</i>) and time (<i>C</i>)	291
Figure 7.44	Contour plot for K/S value (<i>y</i>) with temperature (<i>A</i>) and time (<i>C</i>)	292
Figure 7.45	Normal probability plot of Myrobalan applied on PLA using Pomegranate as biomordant	294
Figure 7.46	Contour plot for K/S value (<i>y</i>) with temperature (<i>A</i>) and initial pH of dye bath (<i>B</i>)	296
Figure 7.47	Contour plot for K/S value (<i>y</i>) with initial pH of dye bath (<i>B</i>) and time (<i>C</i>)	296
Figure 7.48	Contour plot for K/S value (<i>y</i>) with temperature (<i>A</i>) and time (<i>C</i>)	297

Chapter 1

Introduction

Textile fibers are used for making apparels as well as for non-apparel end products. Among the non-apparel usages, home furnishings are most common. The use of technical and industrial textiles is also on the rise. The desired properties for textile fibers include strength and durability, elasticity, drape and abrasion resistance, among others. For apparels, the need for comfort, moisture absorption, ease of dyeing, wrinkle resistance and recovery, etc. also become equally important. Besides these, the aesthetic properties of textiles are also essential both in case of apparels and home furnishings.

All of the desirable properties in textiles could not be catered to by a universal fiber. Hence, human civilization has explored a large variety of fibers since long. Prior to the last century, fibers from natural resources were extensively used. These were classified as natural fibers, and included cotton, jute, ramie, hemp, silk, wool etc. Later on, with the advent of technology, newer fibers were developed. A brief classification of textile fibers is provided in Table 1.1 [1].

The last century has seen the use of synthetic fibers to a significant extent. The development of nylon and polyester fibers can be associated with the World Wars I & II respectively. Primarily, the need for synthetic fibers at such times was driven by the exponential growth in the demand of fibers for consumption worldwide. The production of natural fibers was limited by the capacity of the available agricultural land, their seasonal nature and high dependence on climatic conditions, besides others. Thus, they were mostly unable to meet the surging rise in consumption.

Table 1.1: Classification of textile fibers [1].

Type of fiber	Sub-class	Examples
Natural	Vegetable or Cellulosic	Cotton, jute, flax, hemp, ramie, coir etc.
	Animal or Protein	Silk, wool, cashmere, alpaca etc.
	Mineral or Inorganic	Asbestos
Regenerated	Cellulosic	Viscose & cuprammonium rayons, cellulose acetate and triacetate
	Protein	Casein
Manmade	Synthetic	Polyesters, polyamides, polyurethanes, polyvinyl, polyacrylonitrile, synthetic rubbers
	Refractory and related fibers	Glass, carbon, metal, silica etc.

1.1 Poly-ethylene terephthalate (PET) fiber

Over time, many of the synthetic fibers could not be popularized, partially owing to technological barriers in production, shortcomings in some of the properties of the fiber, etc. Among those that stood the test of time, the family of polyester fibers was the most significant. About 40% of total textile consumption has been attributed to this family of fibers [2]. They had the advantage of superior tensile properties, dimensional stability, easy care and weather resistance, to name a few, over other fibers [3]. Another advantage was the non-biodegradability of the fiber, adding to the high durability of products. In the polyester family, poly-ethylene terephthalate (PET) fiber, was commercially the most successful one and widely used in apparel manufacturing [2, 4]. It is an aromatic linear polyester fiber with high crystallinity [4, 5]. The ease of its production from mono-ethylene glycol and terephthalic acid (or its salts) contributed to

its very low cost. PET thus accounts for almost 80% of the volume of synthetic fibers produced globally.

PET is an aromatic linear polyester fiber with high crystallinity [4, 5]. It is produced from mono-ethylene glycol and terephthalic acid (or its salts). The chemical structure is given in Figure 1.1 [6].

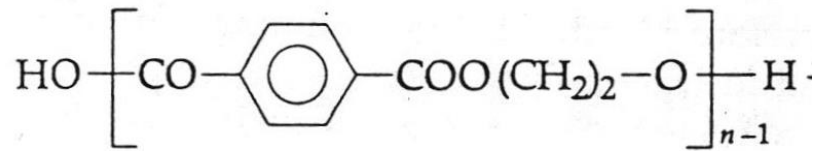


Figure 1.1: Chemical structure of PET [6].

PET is obtained as a textile fiber by melt spinning at 280°C. The non-biodegradability of PET was an advantage only until there was widespread awareness on waste management. Due to non-biodegradable nature, products made out of PET added to the waste generated over the years worldwide that would lay un-decomposed over time. On the other hand, developments in fashion consciousness as well as products were driving the global consumers to reject the older textile products and buy new ones more frequently. This only increased the contribution of PET to the volume of non-biodegradable waste across the world.

Besides non-biodegradability, PET was challenged by a few other inherent shortcomings too. One of them was the low moisture absorption capability because of which it was not comfortable to wear. As a result, the fiber had to be blended with various natural fibers so that the final product could have the favorable properties of both the fibers. However, this added to the cost of manufacturing as extra processes were

needed for blending, dyeing, finishing etc. This problem was closely related to another major hurdle that products made out of PET faced- that of dyeing.

The use of fossil fuels in manufacturing of PET and its non-biodegradable nature have been the causes of major concerns [2]. PET lacked the presence of functional groups, and as a result, could not present enough of reactive sites to the polar water molecules for satisfactory moisture absorption. This was also the reason why it could not form chemical bonds with any dye molecules in a way the natural fibers could be dyed [4, 7]. In order to dye PET, a separate set of dyes, viz. disperse dyes, had to be developed. These dyes mechanically penetrated the amorphous regions of PET during their process of coloration [5, 7-10]. It has been reported that PET can be dyed at above 110°C with disperse dyes [11]. In order to achieve better penetration, harsh conditions had to be resorted to during dyeing, like very high temperature, use of different auxiliary chemicals etc. The high temperature required made the process less eco-friendly due to excessive consumption of power [12]. Thus, environmental issues became important in determining acceptable industrial practices. Certain legislative requirements also followed that were to be conformed to in case of dyeing of polyester fibers with disperse dyes [13, 14].

1.2 Overview of ecofriendly polyester fibers

Over time, multidirectional research towards development of ecofriendly polyester fibers have been conducted. Some of the researches were aimed at exploring the natural resources that could be used to develop such fibers. If the source was natural, there would be various functional chemical groups present in the developed polyester fiber. These groups could enhance the biodegradability of the fiber, thereby helping in achieving one of the prime goals behind their development. Presence of such groups

could collaterally help in improving certain other properties of the fiber, like moisture absorption. It could also help in making dyeing easier and milder, thereby reducing pollution.

A number of ecofriendly polyester fibers were eventually developed, but only a few of them could stand the test of time owing to their commercial viability. Two of the most prominent ecofriendly polyester fibers were poly-trimethylene terephthalate (PTT) and poly-lactic acid (PLA). Both of the fibers were obtained from corn. This in a way also helped in fruitfully utilizing the corn that otherwise would be wasted. Although the fibers were obtained from a natural source, the process of their manufacturing was artificial, or man-made. Therefore, these fibers can be classified as regenerated polyester fibers.

1.2.1 Poly-trimethylene terephthalate fiber

Poly-trimethylene terephthalate (PTT) fiber is an aromatic thermoplastic polyester derived from 1,3- propanediol, obtained from corn derivatives, by reaction with terephthalic acid or its salts [15]. Its synthesis was first patented as early as the 1940s, but it regained commercial success only in the 1990s [16-20]. It has been found to retain most of the favorable properties of PET like weather resistance, dimensional stability, ease of processing, recyclability and easy care. The thermal and chemical resistances have also been reported to be superior [21]. Besides, it also offers some advantages like better stretch and recovery properties due to the zigzag structure of its linear polymer chains [3, 17, 19]. Under external stress, these chains tend to straighten by bending and twisting about the Carbon atoms of the chain, instead of simple stretching. As a result, the

extent up to which the polymer chains are broken is lesser. Also, when the external stress is removed, the chains can fold back to their original zigzag structure, thereby imparting high elastic recovery to the fiber. This has been attributed to the presence of odd-numbered methylene group in the macromolecular structure of PTT [Kurian 2005; Wu 2005].

The melting point (T_m) of PTT has been reported as 225°C and the glass transition temperature (T_g) as 45°C [22, 23]. Its thermal degradation occurs at 374°C , and maximum crystallinity obtained it 55% at 190°C [19]. The structure of PTT is given in Figure 1.2 [3].

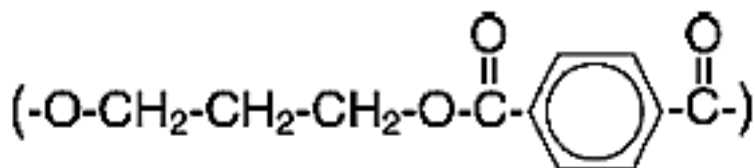


Figure 1.2: Structure of PTT [3].

PTT fiber has been reported to possess better elastic properties than PET [3, 17, 19, 24]. They can also be dyed at comparatively lower temperatures among the polyester fibers [24, 25]. However, its mass production was limited due to the high cost of raw materials [25]. The raw material used for PTT is 1,3-propanediol obtained from corn derivatives, which was earlier obtained chiefly from petroleum byproducts. It was therefore costly. The process of its separation and synthesis was also non-ecofriendly [3,26]. Attempts were made to derive the same from renewable natural resources in order to make the process less costly and environment friendly as well [15, 27, 28]

The superior elastic properties of PTT have led to development of various polyester block copolymers in combination with various co-monomer systems with different sets of properties. It has also been blended with other polymers like poly-lactic acid (PLA) in order to make textile fibers with its superior mechanical properties incorporated [29, 30]. PTT has also been reported to be used in making nano-composites owing to its attractive properties [15,31].

1.2.2 Poly-lactic acid fiber

PLA is an aliphatic thermoplastic polyester fiber, well known for its biodegradability [32, 33]. It is a renewable polymer that can replace conventional petroleum based polymers in a variety of end uses [34]. It is produced as a textile fiber through melt spinning at 240°C. The structure of PLA is given in Figure 1.3 [35].

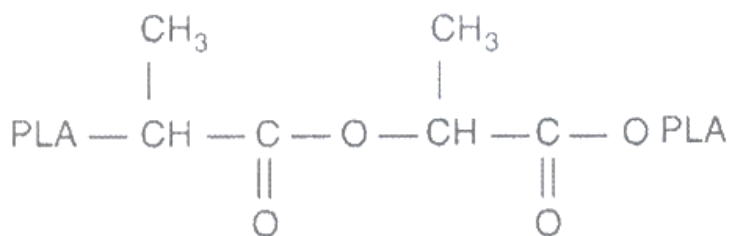


Figure 1.3: Structure of PLA fiber polymer [35]

PLA is the first textile fiber obtained from natural renewable resources (corn starch) that can be produced using melt spinning technology [36-40]. It is biodegradable as well as biocompatible [40, 41], but also has certain disadvantages like low brittleness and ductility, and tendency to hydrolyze [42, 43].

In the production of poly-lactic acid (PLA) fibers, the lactic acid monomer is subjected to ring opening polymerization in order to synthesize the fiber. The polymerization yields two isomeric varieties of PLA from D-lactide and L-lactide

respectively [44]. The poly-L-lactic acid (PLLA) variety is preferred for fiber formation [45]. The fiber inherits favorable properties like satisfactory stiffness and strength with low elongation at break [46]. In spite of a major drawback it exhibits is its brittle nature that demerits its products for durability [44, 47], it shows promising possibilities towards replacing petro-based fibers as an environmentally sustainable option [46].

1.3 Dyeing of textile fibers

Color, appearance and texture are some of the attributes of textile products included among these properties. Color is of primary importance since it makes textiles attractive. Various dyes have been used since history to color textiles in different forms, viz. fibers, yarns and fabrics, as required. In the earlier days, dyes obtained from natural resources were used. Dyeing of textile fibers in aqueous medium is generally guided by the following four steps [48, 49]:

- (i) Diffusion of dye into the solution.
- (ii) Adsorption of the dye onto the surface of the fiber.
- (iii) Diffusion of the dye inside the amorphous regions of the fiber polymer matrix.
- (iv) Fixation of the dye to the fiber through chemical bonding, mechanical entrapment or other means.

1.3.1 Classes of dyes

Dyes chemically constitute of two broad substructures, viz. the main skeleton or chromophore, and the substituent groups or auxochromes. The chromophore is mostly responsible for light fastness properties, besides imparting the main color developed [50]. It also helps in determining the wash fastness. The chromophore determines the molecular weight of the dye, and those with higher molecular weights tend to show better

wash and light fastness properties. The auxochromes are again responsible for chemical bonding with the substrate (fiber), which may be electrovalent, covalent or other weaker forces of attraction. Based on the nature of bonding with the fibers, the various dyes used in textiles may be classified as in Table 1.2 [1, 51].

Table 1.2 Different classes of dyes for textile fibers [1, 51].

Class of dye	Nature of bonding	Fibers applied on
Acid	Electrovalent	Wool, silk, nylon
Basic	Electrovalent	Wool, acrylic, modified polyester
Direct (Substantive)	van der Waal's forces, H-bonding	Cellulosic, wool, silk
Disperse	Physical	PET, acetate and other synthetic fibers
Metal complex	Electrovalent	Wool, silk, nylon
Mordant (Chrome)	Physical (through mordant)	Wool
Pigment	Physical (through binder)	Cotton, Cotton/PET blends
Reactive	Covalent	Cellulosic, wool, silk, nylon
Sulphur	Physical	Cotton
Vat	Physical	Cellulosic
Azoic (Naphthol)	Electrovalent	Cellulosic

1.3.1.1 Disperse Dyes

Disperse dyes are examples of dyes that depend on physical penetration into the amorphous regions of the fiber polymer matrix for coloration. Disperse dyes were invented in 1923-'24 for dyeing cellulose acetate fibers effectively. Cellulose acetate was the first of the hydrophobic fibers that had low moisture absorption capability. As a result, they could not be dyed with the existing dyes like acid, basic, natural, reactive and vat dyes, which were extensively used to color other fibers like cotton, silk, wool, nylon, etc. Contemporary researches were thus driven towards development of a new set of dyes suitable for cellulose acetate, which resulted in the development of disperse dyes. They were initially termed as cellulose acetate dyes. Since they were found to be suitable for dyeing a larger variety of fibers during the later stages of developments and modifications, the class of dyes was renamed as 'Disperse Dyes' by the Society of Dyers and Colorists, U.K., in 1953 [52].

Disperse dyes are often used to dye synthetic fibers, especially polyesters [9, 38-40]. Disperse dyes are low molecular weight organic compounds derived from azo, anthraquinone and others [53-55]. They are planar in structure and non-ionic in nature [53, 55]. They also have colloidal dispersion properties and very low solubility in water [5, 55-59]. They possess high tinctorial value and fastness properties [60].

Classification of disperse dyes was initially based on their sublimation characteristics. They were also classified based on their concomitant energy levels. Later on, with the introduction of disperse dyes for rapid dyeing in the 1980's, the earlier classification had to be discarded and replaced. Presently, they are classified based on the various end uses. Some of them are [52]:

- (i) Disperse dyes with superior light fastness or automotive textiles.
- (ii) Disperse dyes with excellent wash fastness for sportswear and heavy duty work wear.
- (iii) Disperse dyes that are fluorescent in nature for high visibility garments.
- (iv) Disperse dyes for home textiles that are highly compatible with good levelling properties, acceptable fastness etc.

There are disperse dyes for special purposes too, like those suitable for solvent dyeing, super critical carbon dioxide, etc. [52].

1.3.1.2 Natural dyes

Natural dyes have been in use since the early times of human civilization. In the absence of synthetic dyes, there was only one option to develop color, and that was the natural sources. Thus, various natural dyes were applied to textiles, fur and leather since the prehistoric times. Natural dyes are mostly obtained from plants, arthropods, marine invertebrates, algae, bacteria and fungi [61, 62]. The practical sources from where natural dyes are extracted include primary agro-based products, byproducts and waste materials from farming and forestry, and food and beverage wastes [62]. Among the many reasons for their decline were poor fastness properties, and lack of availability in huge volumes that suits industrial mass production. Also, the process of extraction was difficult from the natural resources, and hence, the costs of the dyes were higher as compared to the synthetic dyes. The synthetic dyes, on the other hand, could be modified in an easier and faster manner to suit the various end uses, which was not possible with the natural dyes. They had the advantages of ease of manufacturing, simple application process,

reproducibility of shades, better tinctorial properties, larger gamut of shades available, brighter colors, superior fastness properties and lower costs [5].

Natural dyes used for textile applications are generally classified into four different varieties based on their chemical nature. About 50% of the natural dyes that exist are flavonoid compounds. The other three classes are anthraquinones, naphthoquinones and indigoids [48]. Some researchers have further classified natural dyes into four other categories, viz. animal dyes, plant dyes, curcuminoid dyes and natural phenol dyes [59]. Some of the commonly used natural dyes for textile fibers are given in Table 1.3 [62-64]:

Table 1.3: Natural dyes commonly used for textile fibers

Sl. No.	Name of source	Extracted from	Chromophore	Class
1	<i>Acacia Arabica</i>	Bark	Catechin, epicatechin	Tannin
2	<i>Acacia catechu</i>	Wood	Catechin	Anthocyanin
3	<i>Alkanna tinctoria</i>	Root	Alkannin	Naphthoquinone
4	<i>Butea monosperma</i>	Flower	Butryin, Isobutryin	Flavonoid
5	<i>Bixa Orellana</i>	Seeds	Bixin	Carotenoid
6	<i>Coffea Arabica</i>	Beans	Caffeine	Alkaloid
7	<i>Curcuma longa</i>	Rhizome	Curcumin	Carotenoid
8	<i>Indigofera tinctoria</i>	Leaves	Indirubin, Indican	Indigoid

9	<i>Juglans regia</i>	Bark	Juglone	Naphthoquinone
10	<i>Lawsonia inermis</i>	Leaves	Lawsone	Naphthaquinone
11	<i>Mimosa tenuiflora</i>	Bark	Condensed tannins	Tannins
12	<i>Opuntia ficus-indica</i>	Fruit	Indicaxanthin	Betalain
13	<i>Punica granatum</i>	Fruit	Punicalgin	Tannin
14	<i>Quercus infectoria</i>	Rind	Gallic acid, Ellagic acid	Tannin
15	<i>Rubia cordifolia</i>	Root	Purpurin, Rubiaccordone	Anthraquinone
16	<i>Rubia tinctorum</i>	Root	Alizarin	Anthraquinone
17	<i>Solidago canadensis</i>	Plant	Quercetin, Quercitrin	Flavonoid
18	<i>Terminalia chebula</i>	Bark-fruit	Chebulinic acid	Tannin
19	<i>Tectona grandis</i>	Leaves	Tectoquinone, Tectoleafquinone	Anthraquinone
20	<i>Laccifer lacca</i>	Insect	Laccaic acid	Flavokermesic acid
21	<i>Dactylopius coccus</i>	Insect	Carminic acid	
22	<i>Murex trunculus</i>	Molluscs	Indigo, Indirubin	Indigoid

In order to achieve better fastness properties of natural dyes into textile fibers, mordants are used in dyeing [62, 65]. A mordant is an inorganic substance, mostly a metal salt that helps in creating affinity between the fiber and the dye molecules [62]. Some of the commonly used ones are aluminum sulfate, ferrous sulfate, potassium sodium tartrate etc. [65]. Besides, stannous chloride, potassium dichromate and copper sulfate have also been employed for mordanting [62].

Mordanting of textile fibers during dyeing can be carried out in three different ways [66]:

- (i) Pre-mordanting: fiber first treated with mordant in aqueous medium, followed by application of dye.
- (ii) Meta-mordanting: fiber treated simultaneously with dye and mordant in same bath.
- (iii) Post-mordanting: fiber dyed first and then treated with mordant.

The use of inorganic mordants in dyeing of textiles has been reported to impart harmful impacts on the environment. The dye effluent when drained into the aquatic ecosystems affects the biosphere as well as the qualities of water and soil adversely, chiefly due to the presence of the metal ions [62, 65]. In order to solve the environmental problems related to mordanting, use of biomordants has been proposed by many researchers. Biomordants are mostly obtained from plant sources. Plant products with either very high tannin content or obtained from plants that can hyperaccumulate metals have been found suitable as biomordants.

A list of commonly used biomordants is given in Table 1.4:

Table 1.4: List of commonly used biomordants.

Sl. No.	Name of biomordant	Name of species	Reference
1	Catechu	<i>Acacia catechu</i>	Shahid et al 2013
2	Myrobalan	<i>Terminalia chebula</i>	Shahid et al 2013
3	Powder of valex	<i>Quercus ithaburensis</i>	Ismal et al 2014
4	Pomegranate	<i>Punica granatum</i>	Ismal et al 2014
5	Rosemary	<i>Rosmarinus officinalis</i>	Ismal et al 2014
6	Thuja	<i>Thuja orientalis</i>	Ismal et al 2014
7	Cypress leaves	<i>Cupressus sempervirens</i>	Kilinc et al 2015

Chlorophyll- α has also been reported as an effective biomordant in dyeing of wool with natural dye, betanin, extracted from *Opuntia ficus-indica*. Among others, pH and temperature of the dye bath were found to be significant factors affecting coloring properties [61].

Chapter 2

Review of Literature

The end-uses of textile products can be broadly classified into commercial and industrial usages. The properties of textiles also can be divided into two categories- functional and aesthetic. A basic level has to be attained for both the categories in all sorts of end-uses for the textile products. However, their relative importance varies based on the specific end-use. Commercial products are driven by latest trends in fashion to a much greater extent. Thus, for such type of products, aesthetics become a primary area of concern. In case of industrial textiles, functionalities play a major role in determining the suitability of the product, although a minimum level of aesthetics also has to be achieved. When it comes to aesthetic appeal of textiles, the first thing that comes to the mind is its color.

2.1 Dyeing of textile fibers

A brief description of the dyes used for textiles have been given in the previous section 1.3.1. In case of textile fibers, the dyes bind together with the help of chemical or mechanical attachments. The mechanism of dyeing involves the penetration of dye molecules into the available inter-molecular spaces of the polymer matrix of textile fibers, followed by bonding at the reactive sites. There are some dyes that form covalent bonds with some fibers, and as a result, exhibit superior fastness properties. However, not all dyes are capable of this, and some of them can form less strong electrovalent bonds with certain fibers. These bonds are weak and hence the fastness properties exhibited lie in the range of average to unsatisfactory levels in different cases. Again, there are also some fibers that are incapable of forming any chemical bond with dye molecules owing to absence of any reactive site. In their cases, dyeing occurs as a result of mechanical penetration in the amorphous regions of the polymer matrix of the fibers.

Dyeing is a complex process. The nature of the complexity depends on the types of fibers and the classes of dyes used as well as the effects of different parameters controlling the process. Among the many parameters that determine the efficiency of dyeing are temperature, time, pH of dye bath, material to liquor ratio, rate of heating, concentration of mordant and other auxiliary chemicals, etc. The nature of the fiber also plays an important role. Natural fibers have a large number of functional groups present in order to bind with the dyes but in case of regenerated and synthetic fibers, it depends on the raw materials used.

2.1.1 Dyeing of PET

Dyeing of PET can happen both in finite and infinite dye bath conditions. In case of infinite dye bath conditions, the concentration of dye in the solution remains unchanged during the diffusion of the dye onto the fiber. In case of a finite dye bath, the dye concentration decreases gradually with diffusion of the dye into the fiber until equilibrium. The theoretical equation guiding the overall rate of diffusion of disperse dyes into PET have been based upon the dye diffusion rate within the fiber as a primary factor [67].

PET is dyed in aqueous phase at high temperatures in the range of 125-130°C with disperse dyes [12]. Not all of the dye is adsorbed by the fiber, resulting in wastage of dye along with water as the dye effluent [68, 69]. The effluent is also found to be toxic in nature. The disperse dyes also possess poor biodegradability [68, 69], and some of the azo-based ones are carcinogenic [10, 68].

In dyeing of PET, a few other auxiliary chemicals are often used for achieving certain functional properties and making the process of dyeing more effective. Carriers

are the significant ones among them. Due to environmental hazards posed by the carriers, they are often omitted in dyeing of PET, but to compensate for it, the dyeing temperature has to be raised [51]. If low temperature dyeing is preferred owing to reduction of power and related cost, use of carrier is a must [4]. In case of polyester-wool blend dyeing, carriers are still a must when using the disperse dyes [51]. Polyacrylates and alginates are also often added to the dye liquor when disperse dye is used in padding technique for dyeing of PET fabrics [4, 51]. In order to increase the stability and solubility of disperse dyes in the aqueous solution during the conventional way of dyeing PET, dispersing agents or dispersants may be further added [51, 70]. The reducing agent used as a final step to dyeing of PET with disperse dyes, often as sodium hydrosulfite, is very important as it hydrolyses and removes the unfixed dyes from the fiber surface, thereby improving wash fastness, and more importantly, the rubbing fastness. All of these auxiliaries leave hazardous footprints on the environment [51]. Thus, the use of chemical auxiliaries like dispersants and sodium hydrosulphite affect the environment adversely [56, 70, 71].

Since the use of water in conventional dyeing of PET is a cause of environmental pollution because of its constituents, various non-aqueous media has been attempted for the same [70]. Dyeing under super critical carbon dioxide (CO₂) environment has been attempted as an alternative method, and it was found to be successful with selected disperse dyes [72].

The application of disperse dyes on PET is most common, and natural dyes have hardly been attempted because of the nature of dyeing the fiber polymer construction allows. An attempt to dye PET with indigo, a natural vat dye, has been reported by Son et al (2004). The attempt was made in order to improve the wash fastness achieved with

disperse dyes. Since indigo, a vat dye, develops affinity towards textile fibers after oxidation, and is reduced after subsequent entrapment of the dye molecules within the fiber polymer matrix, becomes insoluble in water. As a result, vat dyes are expected to offer superior wash fastness. In the reported study, the color strength of dyed PET was found to increase with temperature owing to enhanced kinetic energy of indigo dye molecules. With temperature, the diffusion of dyes inside the fiber also increased, assisted by greater swelling of the fiber. The wash fastness ratings achieved were superior to disperse dyes and above the satisfactory level [73].

2.1.2 Dyeing of PTT

It has been reported that PTT fiber can be dyed satisfactorily with disperse dyes [74]. In a study, it was reported that the exhaustion of an azo disperse dye, C. I. Disperse Red 82, reached acceptable levels above 80°C when applied to PTT [24]. Dyeing with disperse dyes was possible at atmospheric conditions, i.e. without the application of pressure, and in the absence of any carrier. This indicated the possibility of dyeing PTT in an environment friendly manner, because carriers are one of the sources of pollution, extensively used in dyeing PET. This was explained to be due to the low glass transition temperature (T_g) of the fiber. The fastness properties were found to be satisfactory in spite of the low T_g [74].

Often, various auxiliary chemicals are used in dyeing of PTT with disperse dyes, similar to PET. The presence of heavy chemicals in the wastewater of dye effluents is harmful to the environment [75]. With the aim to reduce pollution from dye effluents, Jang et al (2009) investigated the dyeing of PTT with temporarily solubilized azo disperse dyes without the use of any dispersant. Good to excellent fastness properties

were achieved with optimum conditions of pH 5-6 and 110^oC. This indicated that dyeing of PTT was possible without the use of certain auxiliary chemicals that are common with dyeing of PET. Thus, there was a possibility of reduction in the pollution caused by the dye effluents in case of PTT [76].

Some studies have found temperature to be one of the primary parameters affecting dyeing of PTT with disperse dyes [24, 76]. The optimal temperature for satisfactory dyeing was reported to be between 100^oC to 110^oC [77]. The pH of the dye bath has also been reported as another significant influencing parameter [76]. The study by Ovejero et al (2007) also observed that the exhaustion of the dye reached satisfactory level only above 80^oC with C.I. Disperse Red 82, an azo based disperse dye. The dye exhaustion was fitted to different non-linear regression kinetic models in this study, and the Chrastil model was found to be the most appropriate [24].

In an attempt to obtain deeper shades of disperse dyes, PTT was surface treated, along with PET, with ultra-violet ozone exposure in order to introduce surface roughening at nano level. The results were encouraging with deeper shades obtained after nano-roughening. The fastness to laundering and rubbing were also observed to be superior, indicating this method as a replacement to plasma treatment and sputter etching techniques [78].

Shu and Hsiao (2006) reported comparison of various properties of different polyester fibers including PET and PTT. PTT was reported as a highly crystalline fiber with melting point lower than PET. Thus, its processing at various stages as textile fibers was opined to be easier as compared to PET. Not only were the elastic properties better but also dyeing of PTT was found to be easier. PTT could be dyed at atmospheric

conditions and there was no need for high pressure dyeing, unlike PET. Also, no pH adjustment and carrier was required. All of these attributes were indicative that satisfactory dyeing of PTT could be achieved under milder conditions of temperature and pressure. The absence of carriers and chemical auxiliaries for pH adjustments could make the process environment friendly by reducing the amount of pollutants in the effluents [79].

2.1.3 Dyeing of PLA

PLA is considered an eco-friendly biopolymer due to various reasons, one of which is the consumption of carbon dioxide in its manufacturing. Besides, it is also recyclable, compostable and biodegradable. It finds extensive usage in biomedical applications due to its notable biocompatibility. It does not have any toxic or carcinogenic effect on the local tissues when implanted inside a living body. It degrades to non-toxic byproducts that the body can easily reject through excretion. It also exhibits better thermal processibility as compared to many other polymers including biopolymers. It also enjoys the advantage of 25-55% savings in energy during its manufacturing as compared to other petroleum based polymers. Although the elastic modulus and tensile strength of PLA is in proximity to that of PET, it is brittle and has elongation at break of less than 10%. Its rate of degradation is also slow, thereby limiting the timeframe when it comes to biodegradability. It is also hydrophobic due to lack of side-chain groups, thereby asking for higher temperature when it comes to coloration of the fiber [80].

PLA shows low affinity towards conventional water soluble dyes. Thus, modified methods of dyeing have been proposed for the fiber [2]. PLA has been reported to be ideally dyed in aqueous medium using disperse dyes at 110-115^oC at pH 4.5-5 for 15-30

min. But, the exhaustion and absorption of disperse dyes is often found to be lower in PLA than for PET. The shades are however found to be brighter with better color yield.

PLA is susceptible to hydrolytic degradation at high temperatures, resulting in loss of strength [9, 32, 81]. This has also resulted in development of newer disperse dyes specific for application on PLA [81]. Thus, attempts have been made to dye PLA at lower temperatures by using alternative methods of dyeing. One such method, as reported by Burkinshaw and Jeong (2012), was ultrasonic dyeing. The color strength was found to increase with selective disperse dyes due to the easier disintegration of dye agglomerates. It was also due because the crystallinity percentage of PLA decreased during the process due to the thermal energy involved. An increase in the amorphous volume allowed more dye to enter the fiber polymer matrix. However, decrease in color values of some other disperse dyes due to breakdown of dye dispersions at such high energy levels and elevated temperatures was also reported [12, 81].

The susceptibility to hydrolysis of PLA is well known. Besides, application of dyes has been limited to disperse dyes for the fiber. It has been suggested that the application of other varieties of dyes like indigo may be studied [82]. This study also reported the application of various anthraquinone dyes on PLA. The exhaustion percentage was found to level beyond 90°C and fall above 120°C. The loss in strength kept increasing with temperature, and was very high above 120°C. A dyeing time of 20-30 min was reported to be suitable for satisfactory dyeing. It could also be presumed that longer dyeing time would lead to substantial loss of strength to the fiber. The hydrolysis was reported to accelerate under extreme acidic or alkaline conditions. The ideal range of pH was suggested as 4-5 based on dye exhaustion. However, considering both exhaustion

and strength loss, the best results obtained at pH 5. While wash fastness properties were found to be superior, light fastness was less than satisfactory and depended on dye-fiber interaction, dye crystallization and agglomeration as well as dye distribution inside the polymer matrix of the fiber [82].

2.2 Dyes used for textile fibers

In this study, dyeing of various polyester fibers is carried out. Disperse dyes are well known for application on PET, and also on PTT and PLA, the other fibers used in this study. Also, attempts have been made to apply some natural dyes on these fibers. Some recent developments on disperse and natural dyes are discussed in the following sections.

2.2.1 Disperse Dyes

Disperse dyes were initially developed for application on cellulose acetate fibers. Being synthetic in nature, it was possible to alter their chemical constitution by replacement of the substituent groups. As a result, the disperse dyes of today have undergone several experiments and modifications over time for their easy and cost effective applications on other synthetic fibers like polyester and nylon. Presently, this class of dyes is widely used for PET, PTT and PLA fibers [52]. Selected disperse dyes have also been applied successfully on silk [83].

The adsorption of disperse dyes on PET has been reported to be a function of the conformation of the dye in solid state and its interactions with the substrate. The performance of disperse dyes as a colorant has been found to be strongly guided by the particle size of the dye, and its morphology and conformation in the crystalline state [8, 9].

Disperse dyes have also been used for cellulose acetate, cellulose triacetate, polyamide and acrylic fibers, besides polyester fibers [54]. They are low molecular weight dyes and generally do not possess any solubilizing group. They have good to excellent light fastness while the wash fastness depends on the substrate fiber and is a result of the dye-fiber interaction. About 50% of disperse dyes are azo based, 25% are anthraquinone based and the remaining include methine, nitro and naphthoquinone groups [51, 83]. In case of disperse dyes, the dye-fiber interaction can be through hydrogen bonds, van der Waals forces and dipole-dipole interactions. Most of the disperse dyes can form hydrogen bonds with the oxygen and nitrogen atoms of the fibers through its own hydrogen atoms. The asymmetrical structures of the dye molecules can also form dipole-dipole interactions with the polarized bonds in the fiber. The van der Waals forces occur because of the proximity of the dye molecules to the fiber polymer chains [83].

Since modifying the disperse dye structures were easier than with other dyes, they were altered to achieve various desired properties. They were modified to improve the sublimation and gas fading fastness, although other common attributes like wash and rubbing fastness were already at superior levels. The light fastness property was found to be intermediate for the different varieties of the dye. Most of the modifications of disperse dyes were however aimed at making them suitable for dyeing of PET. Thus, alkali-clearing dyes, those with low thermos-migration, dyes with high wet fastness, etc. were subsequently developed [52].

Disperse dyes based on azo components have been used to dye PET since long [56]. About 3000 azo based dyes were in use in the 1990s, comprising of almost 60% of

the total volume of synthetic dyes annually produced globally [60, 84-86]. Aromatic heterocyclic azo dyes have been reported as highly suitable for dyeing of PET, imparting brilliant shades with satisfactory fastness properties [87-89]. But, azo based dyes have also been reported as detrimental to the environment due to its toxic and mutagenic effects on living beings, affecting even the process of photosynthesis adversely [14, 56, 59, 60, 84, 90, 91].

2.2.2 Natural dyes

The textile industry relies heavily on synthetic dyes for mass production. Not all of the dyes applied in the aqueous medium are absorbed by the fibers and a considerable amount is drained into the aquatic ecosystems. The synthetic dyes that they carry along with them contain carcinogenic and mutagenic components [34, 55, 92]. Thus, they can affect the DNA molecule of living beings adversely, causing damage to the nucleic acids, and thereby posing various threats related to health hazards. A report suggests reduction in such damages in the presence of the flavonoids, myricetin from green tea and apigenin from chamomile tea, both of which are varieties of flavonoids [55]. Natural dyes, on the other hand, have been reported to be non-toxic, non-carcinogenic and biodegradable [61, 66, 92, 93]. They are also renewable and sustainable bioresource products [94]. Thus, natural dyes can be a good substituent for synthetic dyes with respect to the harm caused to environment and the biosphere, since almost half of the natural dyes are based on flavonoids [48].

Natural dyes are mostly applied on natural fibers as the chemical bonds are formed easily due to presence of suitable functional groups in both the fibers and the dyes. However, they have also occasionally been applied to synthetic fibers like acrylic,

polyester and polyamide [95]. Guesmi et al., (2013) reported the application of indicaxanthin, a natural dye obtained from the fruits of the plant *Opuntia ficus-indica* on acrylic fibers using conventional as well as ultrasonic techniques of dyeing. The results indicated that ultrasonic dyeing gave better color properties, the optimal conditions of dyeing being 80°C and pH 3 for 30 min. The factors affecting dyeing have been reported as temperature, duration of dyeing, pH of the dye bath and salt concentration. The affinity of the dye towards acrylic fiber was found to be higher in case of ultrasonic dyeing. The fastness to rubbing, washing and light were found to be 4-5 and above on the rating scales, which denoted a satisfactory level [61].

Synthetic fibers are known to have no affinity with natural dyes. However, studies have revealed that anthraquinonoid based synthetic disperse dyes can color fibers like polyesters. Thus, further studies with anthraquinonoid based natural dyes, alizarin and purpurin extracted from *Rubia tinctorum* and *Rubia cordifolia*, were carried out to dye PET and PLA. The natural dyes were modified in order to suit the dyeing process. It was observed that with PET, the original dyes as well as their mono-alkylated derivatives exhibited higher color uptake than the bis-alkylated dyes. With PLA, the mono-alkylated dye with methyl-4-butanoate groups showed promising results. The wash and light fastness results were also the best with the mono-alkylated derivatives of the dyes [5].

In order to improve the fastness properties of natural dyes, mordants have been used in their applications in textile fibers. Mordants are chemical substances that help the dye molecules to attach more strongly with the fibers. They form chemical bonding with the fiber on one side and with the dye on the other [96]. Thus, the substantivity of the dye with the fiber is improved, thereby improving the fastness properties as well as color

depth [96]. There are three techniques in which mordants are applied in dyeing. They have been discussed in the earlier section 1.3.1.2.

The inorganic mordants used in application of natural dyes, however, leave harmful impact when drained into the aquatic ecosystems along with the dye effluents. The metal ions present in a mordant have been reported as harmful to the environment. As a result, there is a need to find eco-friendly alternatives to the existing range of inorganic mordants [62, 65]. The metal content in textiles as well as its effluents from dyeing has to comply with an upper limit of concentration as per international legislations. In this respect it has been found that mordants containing alum and ferrous sulfate were the safest among the inorganic mordants, closely followed by salts of tin. Salts of chromium and copper, however, are absolutely not suitable in this regard. It has been proposed that salts of rare earth chlorides in mordanting drastically reduced the possibility of environmental pollution by reducing the ionic concentration [62]. However, it could not totally nullify the adverse effects.

Haddar et al (2014) has reported dyeing of cotton with a natural dye eliminating the use of inorganic mordant. Aqueous extract from *Hibiscus mutabilis* was applied on previously cationized cotton. This pretreatment increased the dye affinity of cotton by introducing a large number of cationic reactive sites, as was revealed by the Fourier Transform- Infra Red (FT-IR) Spectroscopy. The surface modification was also visible through the Scanning Electron Microscopy (SEM). Cationization was found to enhance the dyeing as well as fastness properties. The important parameters affecting dyeing were identified as pH of the dye bath, temperature, duration of dyeing, nature of the cationizing

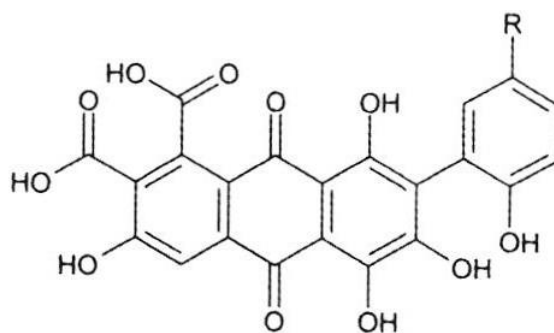
agent and its concentration. The study proposed an environment friendly application of a natural dye without the use of any mordant [91].

Mordants not only help in bridging between the fiber and the dye, they also affect the color properties of the dyed fiber. The effect is most prominent in terms of the tonal changes in the shades obtained with various mordants using the same dye in fixed amount [62]. It was reported in a study that silk when dyed with lac without mordant gave pink color, but in presence of inorganic mordants like alum and stannous chloride, red color was achieved. With copper sulfate, the tone changed to violet while with ferrous sulfate, dark grey shades were obtained [71]. Similar observations can be made with other inorganic mordants as well [97]. With biomordants, this effect may be even more pronounced. A close look at the biomordants would reveal that they themselves belong to the various categories of natural dyes. Hence, they also have chromophores in their skeleton that is capable of imparting color to textile materials. When a biomordant is used in combination with a natural dye, the final shade achieved would therefore be different from the shade that could be achieved with the dye alone, due to (a) higher dye fixation owing to the biomordant, causing a deeper shade; and (b) tonal change caused by the chromophore of the biomordant. This process of dyeing would closely resemble the development of mixed shades of color using more than one dye, as is often the case with disperse dyes.

In this study, three natural dyes were applied to PTT, PLA and PET for dyeing and comparison of coloring and other related properties. The three natural dyes chosen were Lac, Catechu and Myrobalan, and the latter two were also applied as a biomordant. They are discussed as follows.

2.2.2.1 Lac

Lac is a natural dye obtained from the dried bodies of an insect, *Coccus laccae* or *Laccifer lacca* [64, 97-100]. The insect is cultivated on various trees in India, Thailand, China and parts of south-east Asia [64]. The dye is also denoted as C. I. Natural Red 25 or C. I. 75450. The coloring matter of Lac is composed of two main components. One of them is Laccaic acid, which again is composed of the Laccaic acids varieties of A, B, C, D and E. They are soluble in water. The other component is erythrolaccin. It is soluble in alcohol and gives a pale yellow color on dissolution. The stick lac is used as a raw material for shellac, and the red pigment is rejected. This pigment when dissolved in water can produce a natural colorant that can be effectively used for textile fibers [64, 97, 98, 100]. Laccaic acid A is the main component of Lac with 51-57% presence, while Laccaic acid B content varies from 7-15%. Besides these, Lac also consists of flavokermesic acid and kermesic acid in small proportions (1-6%). Shades of red are obtained with the dye that can range up to purple depending on the mordant used. Figure 2.1 gives the structures of Laccaic acids A, B, C and E [64].



The laccaic acids A, B, C and E:

A: $R = \text{CH}_2\text{CH}_2\text{NHCOCH}_3$

B: $R = \text{CH}_2\text{CH}_2\text{OH}$

C: $R = \begin{array}{c} \text{CH}_2\text{CH}-\text{COOH} \\ | \\ \text{NH}_2 \end{array}$

E: $R = \text{CH}_2\text{CH}_2\text{NH}_2$

Figure 2.1: Structures of Laccaic acids A, B, C and E [64].

Lac has been reported to be in use for dyeing of wool, silk and cotton. Surface modification by plasma etching as well as ultrasonic dyeing has been found to improve dye uptake. The nature of dyeing was found to be of Langmuir type in case of silk [101]. However, the washing fastness of the dye obtained has been reported as low. In order to improve the same, various metal salts have been employed as inorganic mordants. These inorganic mordants in turn have been found to be hazardous to the environment and health of the living beings. Thus, a study was conducted to dye silk with Lac replacing the inorganic mordants with a biomordant, memecylon, obtained from *Memecylon scutellatum*. The results showed encouraging improvement in dye absorption as well as bonding with the fiber [98]. Dyeing of lac with silk in presence of inorganic mordants has been reported elsewhere too. While fastness to light, rubbing, water and perspiration were found to be satisfactory, wash fastness obtained was poor [97]. A comparison of K/S

values with the different inorganic mordants were found to be highest for ferrous sulfate, followed by alum, sodium chloride and stannous chloride. The K/S value without any mordant used was the lowest in this case [102].

In a study by Liu et al (2013), Lac was applied on chitosan fiber for dyeing. The absorption of the dye was observed to be dependent on temperature, electrolyte dosage and initial dye concentration. An interesting inference was that the dye absorption was guided by a hybrid mechanism of absorption, the Langmuir-Nernst isotherm. Whereas the electrostatic bonding guided isotherm to be of Langmuir type, the non-electrostatic ones were responsible for the isotherm to be of Nernst type [101].

The adsorption isotherms obtained for Lac on wool, silk and nylon were discussed in a study by Wei et al (2013). The isotherms were found to follow the Langmuir model in all cases, indicating ion-ion interaction between Lac and the fibers. The rate of adsorption was fastest for silk and slowest for wool. The saturation values were found to be highest for wool, followed by silk and nylon in sequence [99].

2.2.2.2 Catechu

Catechu is a natural dye obtained from the bark of the plant, *Acacia catechu* [64, 103]. The main component of the dye is Catechin, which is available in two minor image forms- positive and negative. The positive version acts as an antioxidant [103].

Catechu is composed of flavonoids including quercetin, and 55-60% of tannins. Besides, it also contains various derivatives of catechin based on flavon-3-ol polymers like catechin and *ent*-catechin, epicatechin and *ent*-epicatechin, gallocatechin and epigallocatechin. The high tannin content not only makes it an effective natural dye but

also a potential biomordant. The tones obtained by dyeing cotton with Catechu are ranges of brown from hazel to khaki, and even blackish brown. The final shade also depends on the nature of mordant used. The structures of the stereoisomers of catechin are given in Figure 2.2 [64].

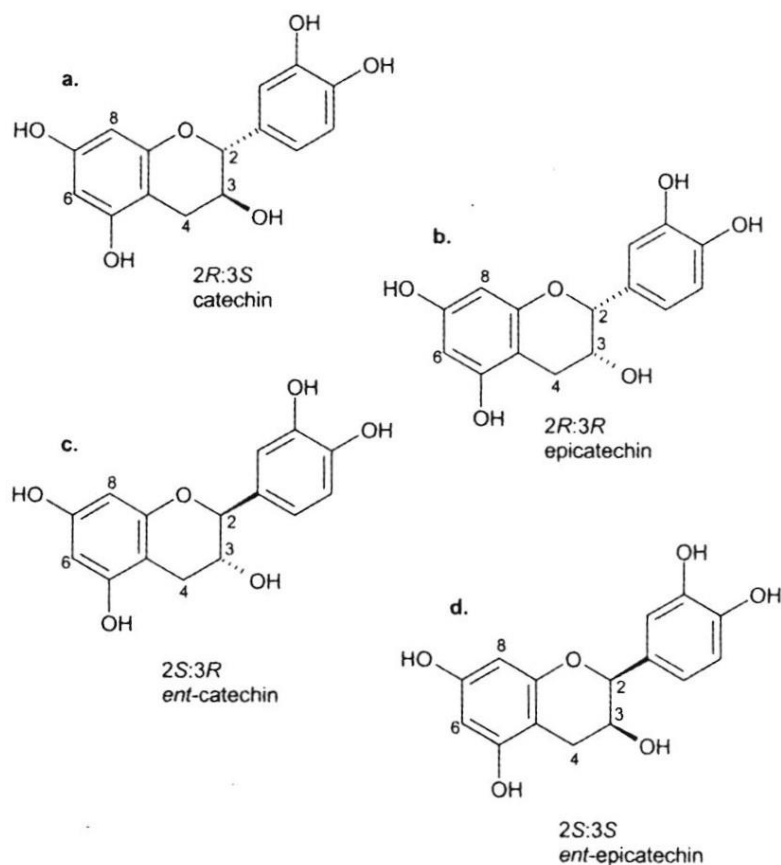


Figure 2.2: Structures of stereoisomers of Catechin [64].

Catechu is rich in tannin content. It was therefore applied as a biomordant in a study in which wool was dyed with *Rubia cordifolia*, a natural dye. The results were encouraging with the pre-mordanting technique, therefore indicating the possibility of

replacing or minimizing the use of metal salts as inorganic mordants, which are notorious for environmental pollution [96].

An attempt was made to dye cotton and silk with Catechu in an eco-friendly manner with the elimination of mordant, salts and other additives. Effective dyeing was reported with satisfactory wash fastness properties [103]. Another study reported the use of protease and amylase enzymes in the application of catechu on cotton. The wash and light fastness properties were found to improve largely than with inorganic mordants, offering an eco-friendly dyeing process. Enzymes are biodegradable and can be drained into the aquatic ecosystem along with the dye effluent without any special treatment for controlling pollution, unlike the metal based inorganic mordants. The use of ultrasound in dyeing in the same study reported 39% increase in exhaustion of Catechu [104].

2.2.2.3 Myrobalan

Myrobalan, also referred to as Chebulic Myrobalan, is obtained from the skin and pulp of the fruit of the plant, *Terminalia chebula* [64, 105]. It has been traditionally used in dyeing of cotton and imparts a buttery yellow color to the fiber [105]. The presence of polyphenols and ellagitannins has been identified as the coloring components in Myrobalan. Dyeing temperature and pH of the dye bath have been found to be the significant parameters affecting its coloring properties on wool. The adsorption isotherm was observed to resemble the Langmuir model closely [106].

Myrobalan is known to impart shades in the range of ochre to textile fibers, which changes to black when iron salts are used as mordants. Among the major components are corilagin, chebulinic acid, β -1,3,6-tri-*O*-galloyl-D-glucose, β -penta-*O*-galloyl-D-glucose,

chebulic and chebulagic acid. Figure 2.3 depict the structure of chebulinic acid, one of the main constituents of Myrobalan [64].

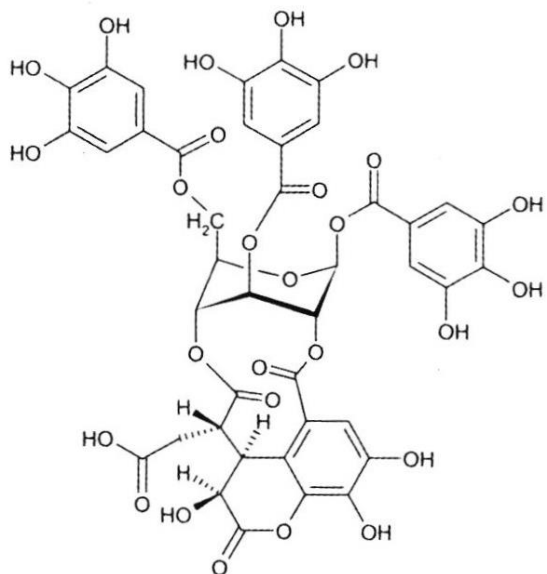


Figure 2.3: Structure of chebulinic acid [64].

The presence of tannins makes Myrobalan suitable as a biomordant in natural dyeing of textile fibers. Poorniammal et al (2013) has reported the use of Myrobalan as a mordant in dyeing of a natural yellow pigment obtained from *Thermomyces* sp. on silk. The light, wash and rubbing fastness were found to be highly satisfactory with this biomordant, along with high affinity [107].

2.2.2.4 Pomegranate

Pomegranate as a natural dye is obtained from the rind of the plant, *Punica granatum*. The dye is rich in tannin content with its main components as flavogallol, ellagitannins, punicalin, 2-*O*-galloylpunicalin, punicalagin, punicacorteins A, B, C and D, punigluconin, and granatins A and B. That Pomegranate can be used effectively as a biomordant lies in the fact that it can dye textile fibers without the use of any other

mordant to impart yellow and fawn shades. With alum as a mordant, the color changes to golden yellow while with iron salts, greys and blacks are obtained. The shades were found to exhibit satisfactory light and wash fastness properties as well. Figure 2.4 show the structure of punicalin, one of the main components of Pomegranate [64].

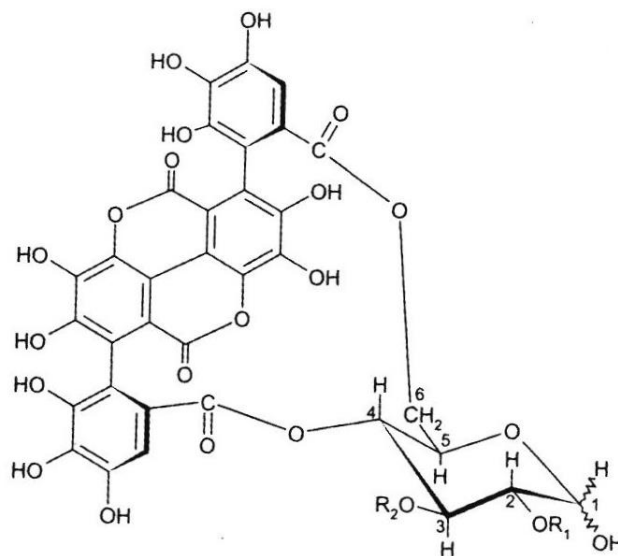


Figure 2.4: Structure of punicalin [64]

Pomegranate has been extensively used as a natural dye owing to the polyphenolic compounds, quercetin and tannin, which it contains. It has been used to dye wool, silk as well as polyester fibers [108]. It was applied to dye cotton in a study by Adeel et al (2009). Encouraging results were obtained with respect to color uptake and fastness properties [109].

Besides, Pomegranate has also been used as a biomordant. It has been reported that the use of Pomegranate as a biomordant enhances the light fastness property of textile fibers to a great extent, besides marginally improving the wash and rubbing fastness as well. The study also revealed that quercetin present in Pomegranate could act

as a chelating agent and could form metal complexes with Al^{3+} , Cu^{2+} , Fe^{3+} , etc. when the latter ions were available from the inorganic mordants applied [108].

2.3 Coloration properties

Although color on textiles is mostly assessed visually, attempts at quantification of the same have been done using a number of color theories. A primary reason for this was to nullify the human error in judging the color attributes that may vary based on the perceptions of individuals. An international body, the Commission Internationale de l'éclairage (CIE), set up in 1913, oversees the standardization of color measurements and evaluations at present.

In this study, the color strength of the dyed fibers are measured as the K/S value at the wavelength (λ_{max}) corresponding to its maximum, according to the Kubelka-Munk equation as follows [96, 110, 111]:

$$K/S = (1 - R^2) / 2R \quad (2.1)$$

where K is the absorption coefficient measured as the fractional absorption loss of radiant flux per unit basis weight, S is the scattering coefficient measured as the fractional scattering loss of radiant flux per unit basis weight, and R is the surface reflectance value at a particular wavelength where maximum absorption occurs.

The colorimetric properties of a dyed fiber are characterized by the CIE $L^*a^*b^*$ values. The various parameters measured are lightness-darkness (L^*), redness-greenness (a^*) and yellowness-blueness (b^*). The lightness scale is denoted by L^* ranging from 0 for black to 100 for white. Redness is denoted by $+a^*$ and greenness by $-a^*$; while yellowness denoted by $+b^*$ while blueness by $-b^*$. A further extension of these

measurements is given by the CIE $L^*C^*h^O$ system, where chroma (C^*) and hue (h^O) are measured as [62, 91, 104, 111, 112]:

$$C^* = \{(a^*)^2 + (b^*)^2\}^{1/2} \quad (2.2)$$

$$h^O = \tan^{-1}(b^*/a^*) \quad (2.3)$$

2.3.1 Adsorption isotherms

In a solid-solution interface, the amount of solute adsorbed, x , is defined as a function of the concentration of the solution at equilibrium, c , and the absolute temperature, T . It is often expressed as follows [113]:

$$x = f(c, T) \quad (2.4)$$

When the amount of solute adsorbed over a range of concentrations of the solution at various fixed temperatures is determined, adsorption isotherms are obtained, as follows [113]:

$$x = f(c), T = \text{constant} \quad (2.5)$$

In dyeing of textile fibers, the various adsorption isotherms observed with different dye-fiber interactions have been classified into three types- Langmuir, Freundlich and Nernst. The shapes of these isotherms in general are shown in Figure 2.5 [113].

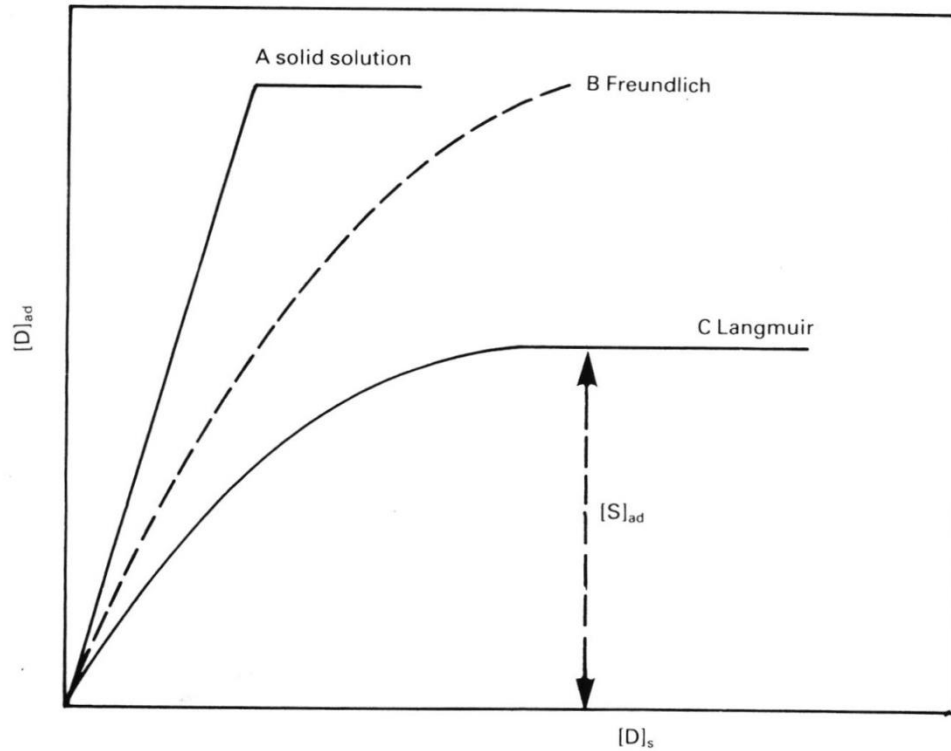


Figure 2.5: Typical adsorption isotherms obtained in dyeing of textile fibers [113].

In case of Langmuir adsorption isotherm, it is assumed that the adsorbed layers are uni-molecular, i.e. there is a single layer of dye adsorbed by the fiber. Also, this model assumes that dyeing happens in a localized manner only at the reactive sites available in the amorphous regions of the fiber polymer matrix. A typical Langmuir adsorption isotherm is governed by the equation as follows [113]:

$$1/[D]_f = (1/a[S]_f[D]_s) + 1/[S]_f \quad (2.6)$$

where $[D]_f$ is the concentration of the dye in the fiber (mol kg^{-1} or g kg^{-1}), $[D]_s$ is the concentration of the dye in solution (mol l^{-1} or g l^{-1}), $[S]_f$ is the saturation value of the dye on the fiber (mol kg^{-1} or g kg^{-1}), and a is a constant at constant temperature.

The Freundlich adsorption isotherm was developed as an empirical model following the equation [113],

$$[D]_f = K[D]_s^x \quad (2.7)$$

where $D]_f$ is the concentration of the dye in the fiber (mol kg^{-1} or g kg^{-1}), $[D]_s$ is the concentration of the dye in solution (mol l^{-1} or g l^{-1}), K is a constant and x is a fraction. The linear form of the equation 2.7 was obtained as follows [113]:

$$\log [D]_f = \log K + x \log [D]_s \quad (2.8)$$

The occurrence of isotherms close to Freundlich has often been observed in practical instances of textile dyeing. It can be distinguished from the Langmuir isotherm in a way that the initial slope of Freundlich adsorption isotherms is generally steeper than of the Langmuir isotherm [113].

The Nernst adsorption isotherm follows the equation,

$$[D]_f = K[D]_s \quad (2.9)$$

where $D]_f$ is the concentration of the dye in the fiber (mol kg^{-1} or g kg^{-1}), $[D]_s$ is the concentration of the dye in solution (mol l^{-1} or g l^{-1}), K is a constant at constant temperature, referred to as partition ratio or distribution coefficient. This isotherm is the simplest possible model for adsorption and gives a linear relationship. It is also referred to as partition isotherm. It is a special form of the Langmuir adsorption isotherm observed in case of very dilute solutions. It is often observed in cases of application of disperse dyes from solution [113].

2.3.2 Fastness properties

When a dye is applied to a textile fiber, it binds to the fiber in some way depending on its interaction with the fiber. There can be various external sources causing breakage of dye-fiber bonds or interactions. Some of them are mechanical abrasion,

solubility of dyes in water, reaction of salts, acids, alkalis and other chemicals on dye-fiber bonds, light incident on the fiber, etc. As a result, the dyes come out of the fiber, therefore decreasing its color values. Fastness property of a dye is defined as evaluation of the level of difficulty of breakage of the dye-fiber attachment.

Fastness properties are categorized into many types depending on the external forces. For evaluating each of these, the standardized procedures laid down by the American Association of Textile Chemists and Colorists, the U.S.A., are followed globally. Some of the test and the standard methods followed for them are given in Table 2.1 [114].

Table 2.1: Standard test methods for some fastness properties of dyed textile fibers.

Fastness property	Test method
Fastness to acids and alkalis	AATCC 6-2001
Fastness to crocking	AATCC 8-2004
Fastness to perspiration	AATCC 15-2002
Fastness to light	AATCC 16-2004
Fastness to burnt gas fumes	AATCC 23-2004
Fastness to laundering	AATCC 61-2003
Fastness to hydrogen peroxide bleaching	AATCC 101-2004
Fastness to ozone	AATCC 109-2002

The fastness properties are generally evaluated using the AATCC grey scales. Visual assessment is done and ratings given to the dyed samples, 5 being the best and 1 the worst. These are followed for almost all types of fastness, viz. rubbing, washing,

perspiration etc. except for light fastness, for which a separate system of blue wool scale exists, the ratings ranging from 1 to 9.

Fastness can also be evaluated by measuring the color difference between two dyed samples before and after fastness treatment, using the delta-E (dE) value, as follows [115, 116]:

$$dE = \{(L_1 - L_2)^2 + (a_1 - a_2)^2 + (b_1 - b_2)^2\}^{1/2} \quad (2.10)$$

There is no study to have reported the evaluation of fastness properties with this approach.

2.4 Characterization of textile fibers

In order to process a textile fiber, characterization of its various properties is needed for achieving the desired results with the minimal loss of the material and its properties. Chemical processes like dyeing and finishing of textiles require information about the crystallinity, presence of functional groups, surface morphology, etc. of the fibers. Characterization of the fibers can help in choosing the optimal conditions for processing, thereby minimizing the loss of strength, elongation, and other properties of the fiber as well as reducing waste of energy, chemicals, etc., along with achieving the desired quality.

Textile fibers are mostly characterized at three different stages as follows [117]:

- (i) Characterization at molecular level- measurement of molecular weight, molecular weight distribution, chemical structure, etc.
- (ii) Characterization of thermal properties- measurement of temperatures of glass transition, melting, crystallization, decomposition, etc.

- (iii) Characterization of physical structure and morphology- measurement of crystallinity, crystal size, crystal size distribution, amorphous orientation, microscopic morphological study, etc.

2.4.1 Thermogravimetric analysis

In order to determine the optimal dyeing parameters for a textile fiber, it is important to have knowledge of its glass transition temperature (T_g) and melting point (T_m). Several workers have reported about T_g and T_m of PTT and PLA fibers [3]. However, detailed thermogravimetric study of these polymers is scarce.

In order to characterize the glass transition temperature (T_g), melting point (T_m), thermal stability and other properties of polymers and fibers as a function of temperature, thermo-analytical techniques are often employed. The basic principle followed for these techniques is to measure some of the properties of a polymer as a function of temperature, using a programmed heating or cooling rate. The principle techniques used are as follows [117]:

- (i) Differential thermal analysis (DTA).
- (ii) Differential scanning calorimetry (DSC).
- (iii) Thermo-gravimetry (TG).
- (iv) Thermo-mechanical analysis (TMA).
- (v) Dynamic mechanical thermal analysis (DMTA).

The information obtained through DTA and DSC techniques are similar. As a result, DSC is preferred over DTA owing to its certain advantages. Properties of a polymer like glass transition temperature (T_g), melting and crystallization temperatures,

heat of melting as well as other parameters that are related to the crystalline structure of the polymer are revealed through DSC. The temperature of decomposition reactions are also obtained through DSC. TG tells us about the thermal stability of a polymer by providing the information about loss of weight as a function of temperature. In this technique, thermal balance is employed to assess the loss of weight of fiber samples very precisely and accurately in a controlled programmed temperature enclosure. The graphical trace obtained is a measure of the residual weight or weight loss as a function of temperature. The derivative of the weight loss, which is actually the rate of loss of weight with temperature, can also be obtained, referred to as the differential thermogravimetric (DTG) trace. It helps in detecting the steps of decomposition that involve very small loss of weight. A typical thermogravimetric trace is shown in Figure 2.6 [141]. It can be resolved into three main zones of decomposition. The zones T_1 and T_3 are smaller as compared to T_2 . The DTG trace corresponding to these three zones show peaks. The temperatures of decomposition also become clear from the TG trace- T_i being the initial decomposition temperature, T_f being the final one and T_{max} being the temperature corresponding to the maximum rate of loss of weight [117].

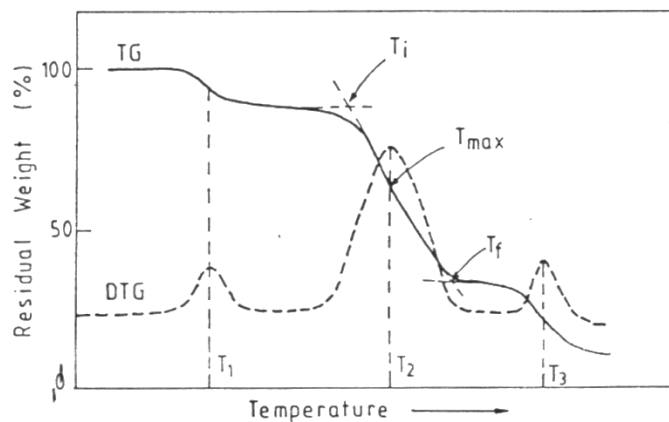


Figure 2.6: Typical TG and DTG traces [117].

Through TMA, the positions of glass transition and melting of a polymer can be measured through changes in certain mechanical properties as a function of temperature. DMTA provides information about the measurement of dynamic mechanical properties as a function of temperature. The positions of the principle secondary transitions in the polymer can be identified with its help [117].

In order to analyze the degradation kinetics of lac dyes, thermogravimetric analyses has been reported by researchers. The mass loss with temperature and time were observed using the TG, DTG and DSC curves [112].

2.4.2 Scanning electron microscopy

Microscopic analysis of polymers is done in order to reveal the visible characterization of the fibers in various ways. The microscopic techniques employed are generally of two types- light and electron microscopy. In electron microscopy, the electron beams are used as radiation. The wavelength applied is dependent on the energy of the electrons, which again depends on the voltage applied for their acceleration. The resolution employed depends on the wavelength of radiation, which may be as low as a few angstrom units in case of the most efficient electron microscopes. Electron microscopy can be performed using either reflection or transmission mode. In case of reflection mode, the electron beam is scanned over a specific area of the fiber and an image formed. This technique is therefore termed scanning electron microscopy (SEM). In case of the transmission mode, it is termed as transmission electron microscopy (TEM). Modern equipment possesses both the modes of transmission and scanning and is therefore termed as scanning transmission electron microscopy (STEM). In order to

characterize the morphology of fibers, Scanning Electron Microscopy (SEM) is often resorted to [117].

In SEM, scanning of the fiber surface is done by reflection. For effective measurement, the fiber surface has to be natural without any marking of the knife or blade. Thus, they are obtained by breaking the fiber with a force of deformation like an impact or a tensile fracture. Otherwise, fibers can also be manually flexed at cryogenic temperatures. Application of such low temperatures is done in order to avoid plastic deformation. Also, breaking of some fibers is difficult at temperatures higher than T_g . The fiber sample to be used for SEM is thus carefully cut in order to avoid any disturbance on the surface. Further, the surface is given an extremely thin coating with a metal. This helps in avoiding the accumulation of electrons or generation of static charges on the surface of the fibers tested owing to their poor conductivity. The thinness of the film is kept extremely thin so that it does not interfere with the readings of the test. It is performed by vacuum deposition of metals like silver, gold or platinum [117].

In electron microscopy, the practical limit for resolution is about 100 angstrom. Thus, it can be used to detect structural features of extremely small dimensions. SEM is used for the following applications in textiles [117]:

- (i) Fiber surface texture.
- (ii) Cross-section of fine filaments.
- (iii) Fibril structure and morphology.
- (iv) Single crystal structures.
- (v) Voids in fibers.
- (vi) Macroscopic features of two-phase morphology.

- (vii) Dispersion morphology of blends, especially in multi-component fibers.
- (viii) Measurement of particle size of additives.
- (ix) Interface morphology, adhesion and differential contraction of different phases of multicomponent fibers.
- (x) Fracture and deformation mechanism of fibers.

Its use has been reported on many occasions in order to evaluate a fiber before and after dyeing, surface modification treatments, finishing treatments, etc. [91, 104, 106, 118]. Changes in the fiber surface like twined morphology, shallow pith, etc. can be identified using SEM [106].

2.4.3 Fourier Transform- Infra Red Spectroscopy

Infra-red spectroscopy is used to obtain information about the structure of the fiber. The characteristic vibrational energies specific to the different functional groups present in the fiber are detected by scanning the transmitted intensity continuously through the range of frequency. The vibrational frequencies are sensitive to the chain conformation, molecular environment as well as the morphology of the polymer [117].

Table 2.2: Functional groups and wavenumbers at which their peaks occur in FTIR spectroscopy.

Functional group	Wavenumber (cm^{-1}) of peak	Reference
-CH stretching	2957	Gashti et al., 2013; Guesmi et al., 2013
Asymmetric and symmetric $-\text{CH}_2$ stretching	2910	Gashti et al., 2013
C=C asymmetric stretching	1958	Gashti et al., 2013
C-H in-plane wagging	1346	Gashti et al., 2013
Intermolecular $-\text{OH}$ stretching	3433	Gashti et al., 2013
Bending vibrations of $-\text{OH}$	1245	Gashti et al., 2013
H-bonded OH stretching	3550-3100	Guesmi et al., 2013
CH wagging	1385	Guesmi et al., 2013
C-N stretching vibration	1103	Haddar et al., 2014
Bending deformation of CH_2 group	1432	Haddar et al., 2014
Rocking vibrations of CH_2 group	1331	Haddar et al., 2014
Primary OH stretching	3368.61	Haddar et al., 2014
$-\text{OH}$ out of plane bending	662.24	Jabasingh et al., 2016
$-\text{C}-\text{O}-\text{C}$ and $-\text{C}=\text{O}$ stretching	1280.15	Jabasingh et al., 2016
$-\text{CH}$ bending	1312.45	Jabasingh et al., 2016
$-\text{CH}_2$ bending	1333.50	Jabasingh et al., 2016
$-\text{CH}_3$ bending	1425.67	Jabasingh et al., 2016

-C=O stretching of aldehyde group	1625.83	Jabasingh et al., 2016
-OH vibrations of carboxylate ions	2892.56	Jabasingh et al., 2016
H-bond between –OH group of dye and polymer	3736.48-3878.39	Jabasingh et al., 2016
Free phenolic OH stretching	3635, 3617	Yusuf et al., 2016
H-bonded phenolic OH stretching	3442	Yusuf et al., 2016
Carboxylic OH stretching	2895, 2822	Yusuf et al., 2016
C=O stretching of carbonyl group and carboxylic acid	1742, 1694, 1682	Yusuf et al., 2016
Aromatic C-C stretching	1506, 1461	Yusuf et al., 2016
Alcohol and carboxylic acid C-O stretching	1264, 1250	Yusuf et al., 2016
Carboxylic acid OH bending	964	Yusuf et al., 2016

In order to characterize the functional groups present in a polymer, Fourier Transform- Infra Red (FTIR) spectroscopy is often resorted to. The transmittance percentage is observed against the wavenumber and the sharp peaks are identified. These peaks occur at different wavenumbers corresponding to specific functional groups. The presence of such peaks, therefore, can provide adequate information regarding the functional groups in a polymer [96]. The wavenumbers against which the molecular vibrational frequencies are detected range from 4000 cm^{-1} to 400 cm^{-1} . At times, observations are also extended to the boundaries of this range, in the region of wavenumber $14000\text{-}4000\text{ cm}^{-1}$, the near-infrared (NIR) zone, and between $200\text{-}12\text{ cm}^{-1}$, in the far-infrared (FIR) zone [117].

FT-IR spectral analysis of cotton fiber has been often reported, before and after various treatments [91, 106]. The peaks that occur due to the various functional groups remain universal across polymers. Not only can the presence of the functional groups be identified through FTIR spectroscopy but also their nature of vibrations and bending. The spectroscopy also helps us to identify whether the vibrations and bending are in-plane or out of plane. Information about such activity of the functional groups help in knowing about not only their presence but also their extent of reactivity. Some of the functional groups and the wavenumbers where their peaks occur are given in Table 2.2 [61, 91, 106, 119, 120].

2.5 Design of experiments

The gamut of statistical techniques often used for examining the interdependence between dependent and independent variables, and their modelling and optimization, is referred to as Design of Experiments (DoE). A wise choice of DoE for experimentation can help in achieving higher degrees of accuracy, simple interpretation friendly to the industry, and saving in cost and time for the experimenter [121]. The use of DoE has been applied in the fields of extraction of natural dyes, and dyeing of textile fibers using natural and synthetic dyes, in various researches over the recent times [91, 106, 122-124].

2.5.1 Central Composite Design

Often, a first order model is used to determine the interdependence of a response variable with the independent variables. This is called an orthogonal first-order design, and is well known for the ease of performing as well as simplicity in interpreting them. In dyeing of textile fibers also, this model has often been used for evaluation of color

properties based on various regulating parameters. The general equation follow in order to fit a first order model is as follows [121]:

$$y = \beta_0 + \beta_1 x_1 + \beta_2 x_2 + \dots + \beta_k x_k + \varepsilon \quad (2.11)$$

where y is the response function, β_0 is the constant coefficient, $\beta_0, \beta_2, \beta_3, \dots, \beta_k$ are the coefficients of linear effects, x_1, x_2, \dots, x_k are the independent variables, and ε is the error.

However, many researchers have reported the dependence of the response variables on not only the process parameters but also their interactions, which are overlooked while fitting a first order model [91, 94, 111, 123, 124]. In such cases, a second order model has to be used for evaluation and optimization of the response variables. There are many designs of experiments developed in order to fit in a second order model, but the most popular of them remains the Central Composite Design (CCD).

In order to develop a CCD model a 2^k factorial or fractional factorial design, sequential experimentation is often employed. The experimentation starts with the attempt to fit in a first order model, and if it exhibits a substantial lack of fit, the axial points are added in the experimentation to incorporate the quadratic terms. CCD is extensively used for fitting second order models due to the efficiency and accuracy that it offers. An important advantage of CCD over other designs of experiment is its rotatability. Box and Hunter (1957) had suggested rotatability as mandatory for a second order DoE. A second order model needs to predict with equal precision over the entire range of interest under consideration. Since one of the purposes of CCD is optimization and the optimal points may not be known prior to the experiments, the ability to predict with equal precision of estimation in all directions from the center point is desirable. Rotatability imparts CCD with such precision because of which it is preferred over the

others. It is a spherical property which can provide the best estimation when the region of interest is a sphere. The value of α for imparting rotatability to a CCD is dependent on the number of points in the factorial portion of the design. In case of a spherical region of interest, the design has to include the center points so that the variance of the predicted response is stable. In general, the number of center points is kept between 3 and 5. Since Response Surface Methodology (RSM) is a tool often used for optimization, it is often carried out based on CCD due to its property of rotatability [121].

2.5.2 Response Surface Methodology

Response Surface Methodology (RSM) is a collection of mathematical and statistical techniques used for analyses of problems in which the response is a function of several variables. The techniques are often resorted to for modelling and optimization of the responses in case of such interdependence with the variables. The expected response is generally not only a function of more than one variable but also the dependence is often found to be quadratic or second order. If the response is plotted in a three dimensional graph, the surface obtained is termed as the response surface. For easier understanding of the response surface, we often also plot the contours on the plane surface defined by the two independent variables [121].

In case of first order dependence of the response, also called the dependent variable, on the independent ones, a first order model is used to derive the response surfaces, as per equation 2.11. In case of a second order dependence, the model followed for deriving the response surface is as follows [121]:

$$y = \beta_0 + \beta_i x_i + \beta_j x_j + \beta_{ij} x_i x_j + \beta_{ii} x_{ii} + \beta_{jj} x_{jj} + \varepsilon \quad (2.12)$$

where y is the response function, β_0 is the constant coefficient, β_i and β_j are the coefficients of linear effects, β_{ii} and β_{jj} are the coefficients of quadratic effects, β_{ij} is the coefficient of interaction effect, x_i and x_j are the independent variables, and ε is the error.

It is unlikely that the true relationship between the dependent and independent variables will resemble the developed models over the entire space of the independent variables, but over small selected regions, they generally are in good agreement. Often, experimentation starts at ranges far away from the optimal regions finally arrived at. This, RSM is often dealt with as a sequential procedure in which the region for optimal conditions are gradually arrived at using various statistical approaches. A typical response surface with contour plots is shown in Figure 2.7 [121].

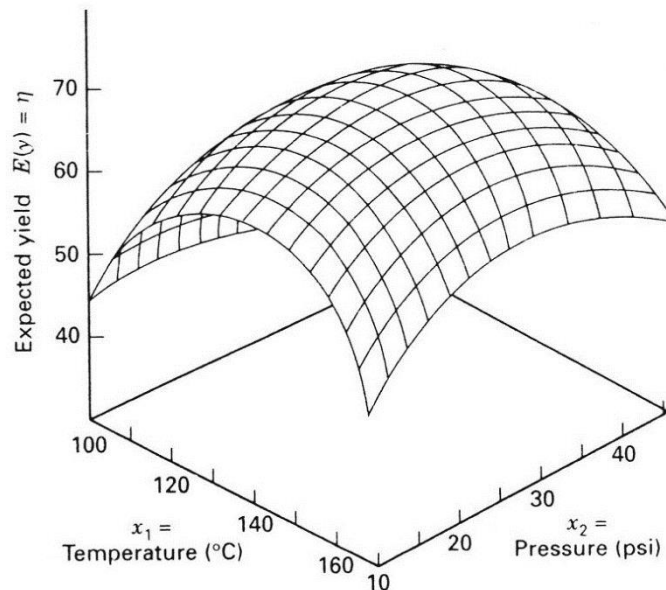


Figure 2.7: Typical response surface with contour plots [121].

There have been many instances of the use of RSM in textile dyeing over the recent times. Haddar et al. (2014) have used RSM to optimize pH of the dye bath, dyeing temperature and duration, nature and concentration of the cationic agent used in dyeing of

cotton with natural dye extracted from *Hibiscus mutabilis* [91]. The same technique was employed for optimization in another study that reported dyeing of cotton with natural dye from *Terminalia arjuna*. Mordant concentration, dye concentration, pH of the dye bath, dyeing temperature and time were the factors that were optimized [111]. It has also been used to optimize the process of extraction of natural dyes from various sources [111, 123-126].

Chapter 3

Aims and Objectives

While exhaustive researches have been carried out in the investigation of dyeing behavior of PET fibers since long, the volume of such work for eco-friendly polyesters like PTT and PLA is still scarce. A few works have been reported citing their dyeing behavior with temperature, pH of dye bath and time using disperse dyes [12, 24, 76, 82]. However, effects of some other parameters like material to liquor ratio and mordant concentration, wherever applicable, have not been investigated. Also, dyeing is a complex process influenced by more than one parameter at a time. Often, there remains a possibility of two or more dyeing parameters governing the color behavior collectively in a non-linear way. There is hardly any work reported dealing with the polynomial nature of the effects of various parameters on dyeing of ecofriendly polyester fibers like PTT and PLA. Various statistical tools based on design of experiments have been devised to explore the polynomial correlation between independent and dependent variables of a process. However, textile dyeing does not often cite such attempts to investigate the interdependence between dyeing and its affecting parameters, except for a few reported cases [91, 113]. In this study, an attempt towards investigating the non-linear effects of various parameters on dyeing of PTT and PLA fibers was felt, with the ultimate goal of optimization of the process parameters for most favorable results.

A closer look at the renewable natural sources of PTT and PLA indicated the possibility of some functional groups present in their polymer matrices. There existed a chance that PTT and PLA could be dyed under conditions that are milder as compared to dyeing of PET. An effective way of assessing this is to apply natural dyes in coloration of these fibers, and observe the results obtained. Incidentally, no research has so far been reported on application of natural dyes on PTT, and very few for PLA [5]. It was

therefore felt that investigation of dyeing behavior of PTT and PLA with natural dyes can be very significant in achieving an ecofriendly dyeing process for the family of polyester fibers, which this study has incorporated.

Natural dyes have been used on different textile fibers since historical times. But yet, they have failed to stand the test of time chiefly owing to poor fastness properties resulting from weak dye-fiber bonds. In order to overcome this shortcoming, mordant is often used in application of natural dyes. A mordant acts as a bridge in fixing the dye molecules strongly to the reactive sites on the fibers. Mostly, an inorganic mordant is preferred owing to superior properties achieved. But in doing so, one of the primary objectives in application of natural dyes, viz. eco-friendliness, is compromised, as an inorganic mordant also acts as a pollutant to the natural environment when drained away with the dye effluents [62, 65].

The usage of plant products as biomordants existed along with the application of natural dyes since long. But lack of proper documentation made it difficult for widespread application. The biomordants widely used mainly include vegetable tannins that are water soluble polyphenolic compounds. They are mostly obtained from bark wood, fruits, fruit pods, leaves, roots and plant galls. The presence of polyphenolic groups presents the possibility of crosslinking between the fibers and dyes using the available hydroxyl groups. Among the commonly used biomordants are *Acacia catechu*, *Punica granatum*, *Quercus infectoria*, *Terminalia chebula*, *Tamarindus indica*, *Emblica officinalis*, *Rhus coriaria*, *Rumex hymenosepolus*, etc. [62].

There are instances where selective natural dyes have been applied as a biomordant in natural dyeing [62, 65, 96], although all of such works report the cases of

natural fibers. Since the results were encouraging in most cases, it was felt in this study that a similar attempt may be made while applying natural dyes on PTT and PLA. Selective natural dyes with the potential to act as a biomordant were used along with other natural dyes used for coloration to evaluate the improvement in fastness properties as well as the effects on other properties. It was also expected that such attempts will enhance the gamut of colors achieved due to combinations of natural dyes.

3.1 Objectives

One of the objectives of this study was to investigate the effect of interactions of the main parameters that affect dyeing of PTT and PLA fibers with disperse dyes. For this purpose the color strength of the fibers achieved with three different disperse dyes, all based on anthraquinonoid structures, were evaluated as the *K/S* values. PET was also dyed under conditions similar to PTT and PLA with these dyes, so that the comparisons of the achieved color strengths for all the three fibers could be carried out. The evaluations were made under different conditions of the affecting parameters, viz. temperature, time, pH of the dye bath, material to liquor ratio and rate of heating. Initially, the effect of these factors on color strength was measured individually for the factors, keeping the other factors at constant levels. This was followed by statistical screening of the factors in order to identify the most significant ones affecting color strength. With three most significant factors, optimization was done using response surface methodology to obtain the most favorable conditions for dyeing. The interactions of these factors and their effects on dyeing were also studied.

In the next phase of this study, the focus was shifted to natural dyes. Four natural dyes were selected based on their reported performances in imparting color strength to

textile fibers, which were Lac, Catechu, Myrobalan and Pomegranate. Out of these, three were used for dyeing of PTT and PLA, viz. Lac, Catechu and Myrobalan. Catechu and Myrobalan, along with Pomegranate, was also used as biomordants in the application of the selected natural dyes on PTT and PLA. Dyeing of PET was also done under conditions similar to PTT and PLA, so that the color strengths achieved could be compared.

In these cases, the effects of temperature, time, pH of the dye bath, material to liquor ratio as well as mordant concentration were observed. The range of favorable conditions for each of the factors was identified from the results. These factors were screened statistically in order to identify the most significant parameters. With three most significant factors, optimization was done using response surface methodology.

Studies on color strength and optimization were carried out the combination of the natural dyes. In such cases, it was assumed that one of the natural dyes would act as a biomordant. Thus, results of optimization were obtained for Lac and Catechu, Lac and Myrobalan, and Lac and Pomegranate. Similar study was carried out with combinations of Catechu with Myrobalan, Catechu with Pomegranate, and Myrobalan with Pomegranate, in which both of the natural dyes were expected to act a biomordants.

The chief objective of this study was to establish optimized dyeing conditions for PTT and PLA fibers with each of the selected disperse and natural dyes, and combinations of natural dyes and bio-mordant. It also included a comparison of the optimized conditions with those of PET. The stepwise approach to achieve the objective could be summarized as follows:

- To study the effects of different parameters on dyeing of PTT and PLA fibers with disperse dyes without the use of any auxiliary chemical, and compare the results with that of PET,
- To study the effects of various parameters on dyeing of PTT and PLA fibers with natural dyes, and compare them with PET.
- To optimize the dyeing conditions for various combinations of natural dyes and biomordants for PTT and PLA fibers.

Chapter 4

**Characterization of PTT
and PLA Fibers**

Textile fibers are required to be chemically processed in order to achieve many of the desirable properties in their end uses. Dyeing is one such process in which various dyes along with auxiliary chemicals like dispersion agents, sequestering agents etc. are absorbed by the fibers. It thus involves mass transfer from solution into the amorphous regions of the fiber polymer matrix. For effectiveness of the process, thermal energy is required. The high temperature causes degradation of the fibers by lowering of its degree of polymerization. Also, with application of heat, the crystals in the fiber polymer matrix start to melt partially, thereby resulting in a reduction of crystallinity percentage [141]. Hence, the fibers tend to lose their tensile properties in dyeing. It is therefore important to deduce an effective range of temperature within which the fiber will achieve the desirable shade with minimal loss of tensile properties. Thus, characterization of thermal properties of a fiber is required. In case of dyeing, the temperature of application is always kept between the glass transition temperature (T_g) and the melting point (T_m) of the fibers. To get an idea of the thermal properties of a fiber, thermogravimetric analysis is often resorted to [141].

In case of dyeing of fibers, the steps involved have been discussed earlier in section 2.2 [87, 88]. An important step is the penetration of the dye molecules into the fiber. The ease of penetration may determine the effectivity of dyeing by reducing its duration as well as quantity of the dye required. The penetration of the dye molecules into the fiber is often governed by the surface morphology of the fibers. In order to gain information about the same, scanning electron microscopy (SEM), as discussed earlier in section 2.4.2, can be of immense importance.

The type of dye required in dyeing depends on the nature of the dye-fiber bonding, which may be electrovalent or covalent. In some cases, the dyes attach to the fiber only physically through mechanical penetration without any chemical bonding. The nature of bonding also helps to predict the level of fastness and its improvement. In case of chemical bonding, the dyes attach to some of the functional groups available in the fiber. In order to have information about the same, infrared spectroscopy is often found helpful. The most common infrared spectroscopy used in characterization of textile fibers is the mid-infrared (MIR) spectroscopy, also referred to as the Fourier Transform Infrared (FTIR) spectroscopy [141]. The spectral analysis can provide substantial information about the chemical nature of the fiber polymer. A comparison of the FT-IR spectra of a fiber before and after dyeing may also help us to detect the functional groups in the fiber where the dyes have attached, thereby helping in determining the nature of the dye-fiber bonds [18, 79, 82, 95, 142].

In this study, thermogravimetric analyses (TGA), scanning electron microscopy (SEM) and Fourier Transform Infrared (FT-IR) spectroscopy of PTT and PLA fibers were performed. The experimental set up, results obtained and discussion, as well as the summary of the findings are given in the following section.

4.1 Experimental

4.1.1 Materials

In this study, two of the three fibers used were subjected to characterization studies. One of them, poly-trimethylene terephthalate (PTT) fiber, was obtained from the DuPont Knowledge Centre, Hyderabad, India. It had fineness of 1.67 denier and average staple length of 80 mm. The other fiber tested in this section, poly-lactic acid (PLA), was

obtained as staple fiber from the University of Leeds, U.K. Its fineness was 1.75 denier and average staple length 75 mm.

4.1.2 Methods

The fibers were subjected to characterization tests in the forms obtained. The thermo-gravimetric analysis (TGA) of the fibers was done using the Pyris Diamond TG/DTA instrument of make PerkinElmer, Singapore. The scanning electron microscopy (SEM) was performed with the help of the JSM-6360 microscope with the electron accelerating voltage set at 20kV and using a scale of 5 μ m (for PTT) and 10 μ m (for PLA) under vacuum.

Fourier Transform Infrared (FTIR) spectroscopy was carried out using the Perkin Elmer Spectrum RXI FT-IR system. The fiber was cut into fine particles and powdered before mixing with Potassium bromide (KBr) as internal standard. Potassium bromide (KBr) is an alkali halide that turns into a transparent plastic-like sheet when pressurized. The sheet being transparent does not hinder the spectral analysis of the fibers embedded in it but acts as a bed holding them in place for the experiments. The test was performed in the mid-infrared (MIR) spectra across wavenumber range of 4000 cm^{-1} to 400 cm^{-1} with a resolution of 2 cm^{-1} to characterize the fiber.

4.2 Results and discussion

4.2.1 Thermo-gravimetric analysis (TGA)

The thermo-gravimetric analysis of undyed PTT fiber is shown in Figure 4.1. The green colored trace represents the loss of mass as a function of temperature and is referred to as the thermos-gravimetric (TG) trace, while the red colored trace shows the differential mass loss, or the rate of mass loss, against temperature, referred to as the differential thermos-gravimetric (DTG) trace [141]. It can be observed that in the DTG trace that a peak appears near the

commencement of the trace. This peak represents the glass transition temperature (T_g) of PTT, which lies very close to the room temperature at which the experiment commences. Another hump can be observed on the DTG trace with its onset at 197.99°C. It continues till 231.69°C with its peak recorded at 216.90°C.

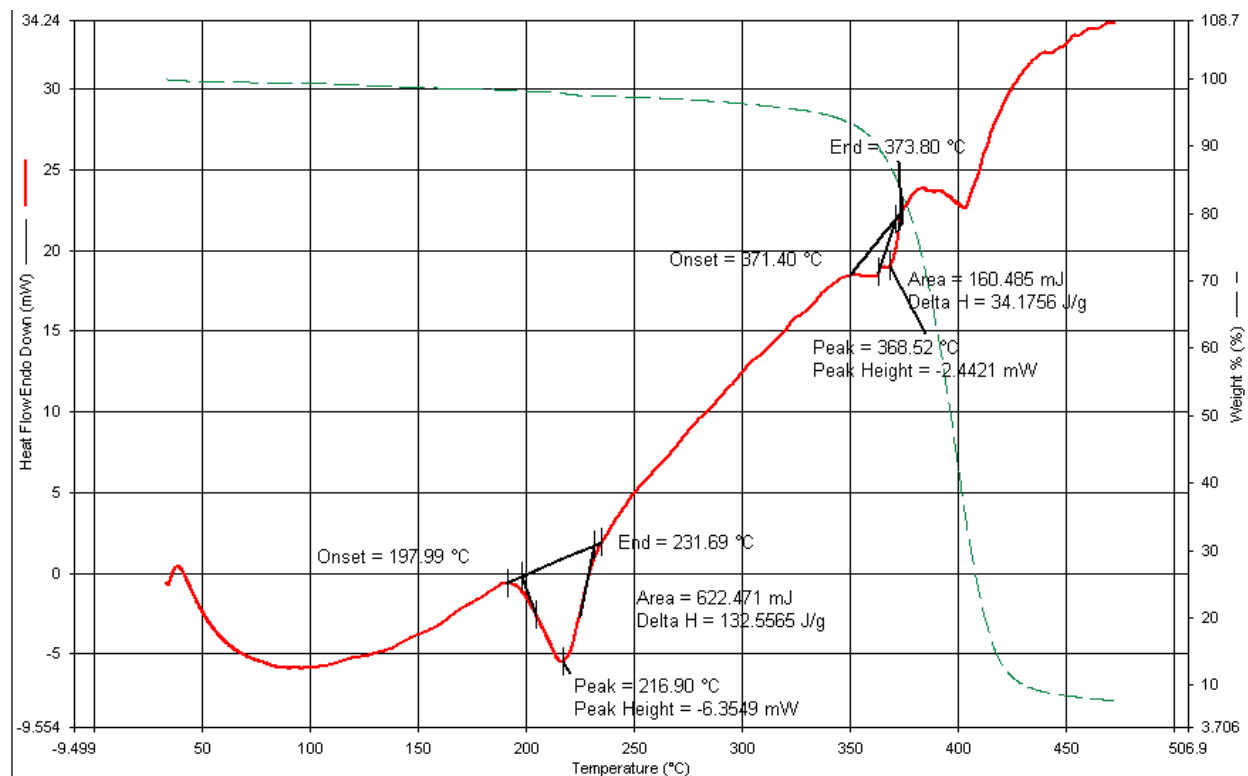


Figure 4.1: Thermo-gravimetric analysis of undyed PTT fiber.

It can be concluded from the TGA of undyed PTT that the glass transition temperature (T_g) of the fiber was just above 40°C. At this temperature, the segmental jump of the polymer chains was initiated, in which certain polymer segments in the amorphous regions could change their positions owing to a higher thermal energy available. But, such segmental jumps involved smaller segments of only a few carbon atoms of length. As a result of such movements inside the amorphous regions, the free volumes scattered in smaller proportions but larger numbers across the polymer matrix could coalesce to provide

comparatively larger free volumes, Hence, the space available for dye molecules to penetrate increased.

However, the steep slope of the TGA curve from around 40°C to about 80°C depicted too quick movements of the polymer chains about their covalent bonds involving a fewer number of carbon atoms, leading to a mechanically unstable condition inside the polymer. This could, therefore, lead to inferior tensile properties. From around 80°C to near-about 120°C, the slope of the curve was minimal, and above this range, it again became steeper with increase in temperature. This was due to the fact that above 120 °C, the movements of the carbon chains again became faster, this time involving more number of carbon atoms in each segmental jump. As a result, the polymer again entered a thermally and mechanically unstable state above this temperature.

It could thus be inferred that temperatures below 80°C and above 120°C were not suitable for dyeing. The faster segmental jumps in these ranges of temperatures would not only degrade the tensile properties of the fiber after dyeing; it would also result in less uniform dyeing due to larger variations in the diffusion of the dye into the fiber at different parts of the polymer matrix [25, 127].

From the second peak, the melting point (T_m) of PTT could be determined as 216.90°C. The glass transition temperature (T_g) and melting point (T_m) of PTT has been reported to be 45-55°C and 228°C respectively [3]. The above findings were in sync with the data cited in literature.

The thermo-gravimetric analysis of undyed PLA fiber is shown in Figure 4.2. The green and red colored traces represented the mass loss and the differential mass loss, as in case of Figure 4.1. The DTG trace was observed to have a small peak at its commencement at around 40°C. This was followed by a steep fall which stabilized by around 90°C. the stabilized region

continued till 145.40°C, wherefrom another region of steep fall initiated. This second region of steep fall gave a sharp peak at 156.97°C and ended at 168.38°C.

Similar to the case of PTT, it could be inferred that the initial region of steep slope of the DTG curve was a region where movements of small segments were initiated. During the second region of steep slope of the DTG trace, the movements of larger segments of the polymer chains occur. In between these two regions, a stable region is observed from around 90°C to 145.40°C. In this region, the segmental movements are eased out and the fiber remains thermally and mechanically stable. This region may thus be ideal for dyeing of PLA.

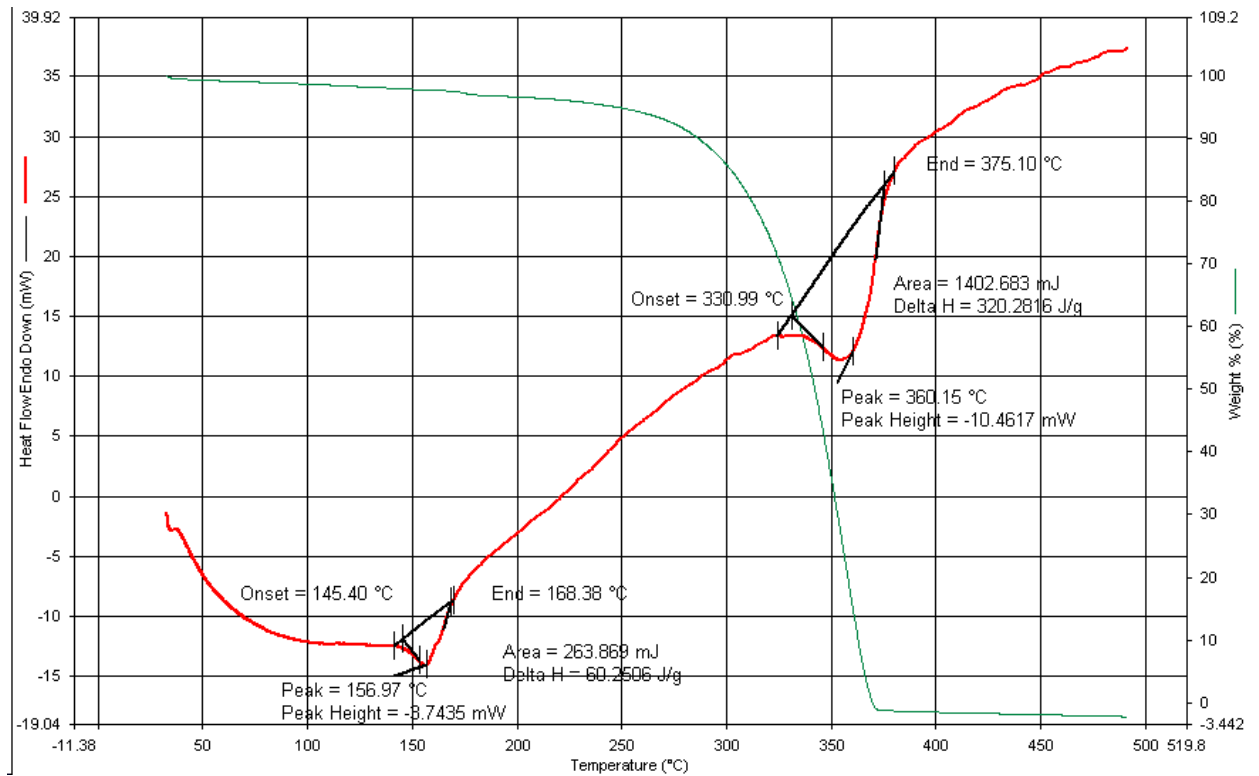


Figure 4.2: Thermo-gravimetric analysis of undyed PLA fiber.

From the TGA curve of PLA, it could also be inferred that the glass transition temperature (T_g) was around 40°C, and the melting point (T_m) was at 156.97°C. Literature

has reported the glass transition temperature (T_g) and melting point (T_m) of PLA as 55-60°C and 130-175°C. The findings are therefore in sync with the reported data [3].

4.2.2 Scanning electron microscopy

The views from scanning electron microscope (SEM) are shown for PTT in Figure 4.3 with a magnification of 5000, and for PLA in Figure 4.4 with a magnification of 2000.

The steps involved in dyeing have been described in section 2.2 earlier as well as above. Among them, the most difficult step is the diffusion of the dye into the fiber. This step is governed by many factors like the relative charges between the fiber and the dye in solution, zeta potential etc. In order to assist this step, many auxiliary chemicals are often resorted to. The nature of the fiber surface also plays a vital role in determining the efficacy of this step [87, 88].

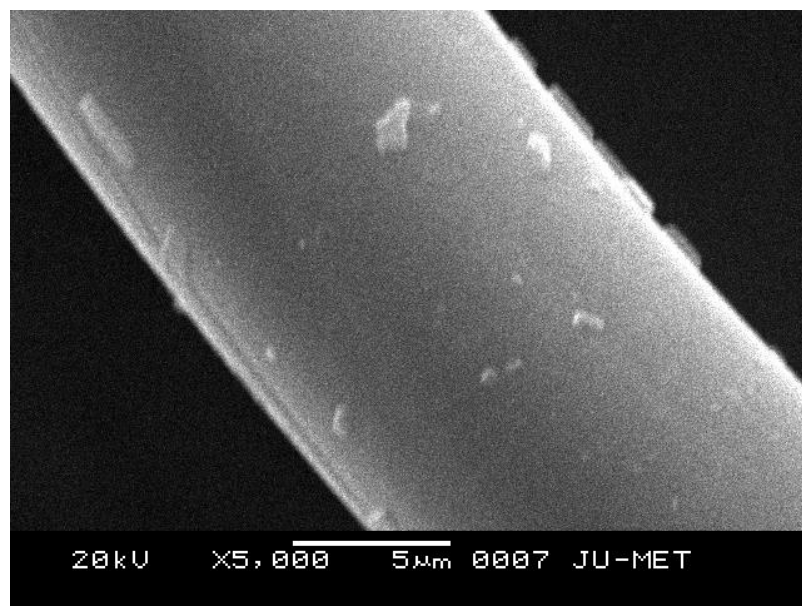


Figure 4.3: SEM of PTT.

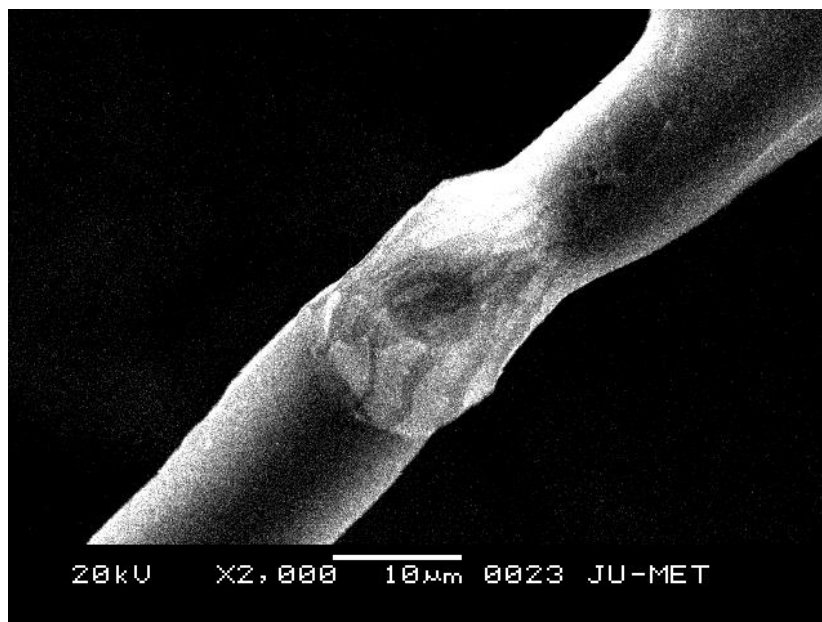


Figure 4.4: SEM of PLA.

In both of the SEM views, the presence of micropores on smooth surfaces was observed. Such smooth surfaces presented least hindrance to the diffusion of dyes at elevated temperatures. The micropores present may open up with temperature that can further assist the diffusion of the dye molecules into the fiber.

4.2.3 Fourier Transform Infrared (FTIR) spectroscopy

The spectral analysis of the FTIR spectroscopy of undyed PTT fiber is given in Figure 4.5. The interpretation of the same is provided in Table 4.1.

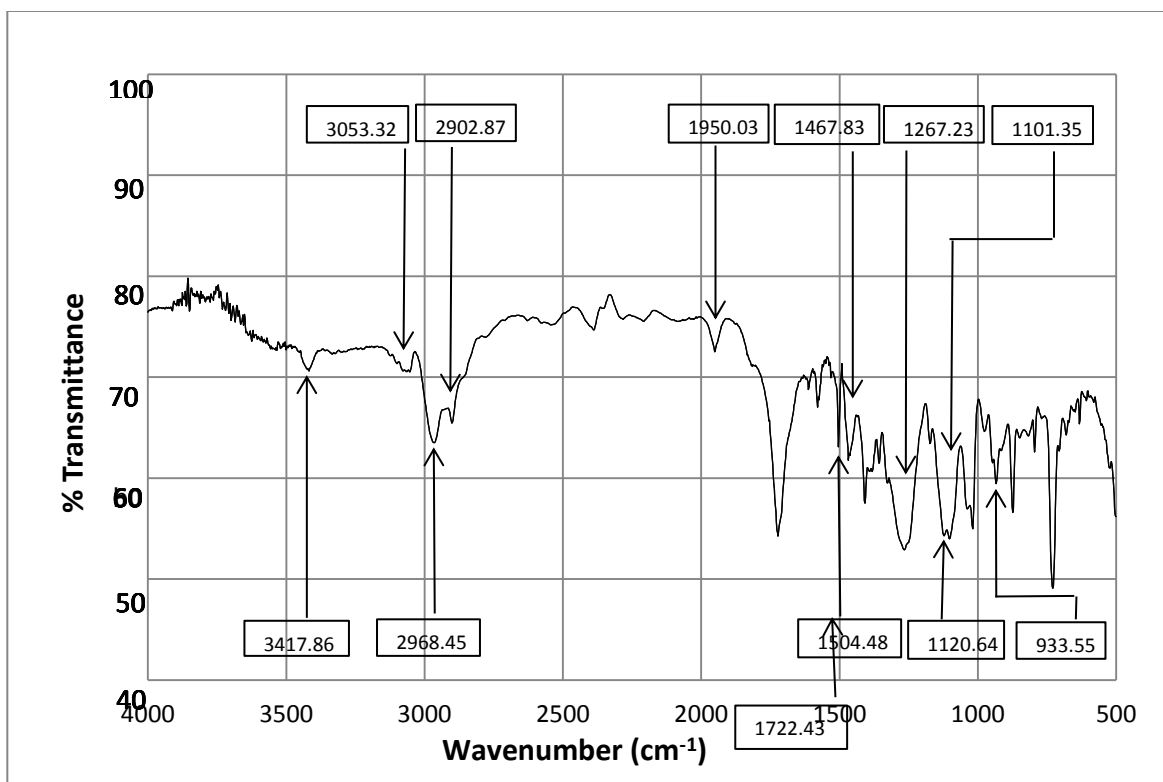


Figure 4.5: FTIR spectroscopy of PTT.

PET has been reported to be devoid of functional groups that can bond with polar water molecules. Their presence could have assisted in formation of chemical bonds with any dye molecule for effective coloration of the fiber. Due to their absence, coloration of the fiber depends on the extent of mechanical penetration of the dye molecules through its surface into the amorphous regions [5-9]. An effective penetration demands high temperatures during which the micropores on the fiber surface open up. Thus, the dyeing condition becomes harsher with a higher demand for power [10]. Also, many auxiliary chemicals are often used to help in penetration. These chemicals are harmful to the environment and cause pollution [10-18].

Table 4.1: Peaks observed in FTIR of PTT and functional groups indicated.

Wavenumber of peak observed (cm ⁻¹)	Nature of functional group	References
933.55	Rocking of -CH ₂ group	Yamen et al., 2008
1120.64, 1101.35	-OH from hydroxyl and carboxylic groups	Nacowong and Saikrasun, 2016
1467.83	Gauche conformation of -CH ₂ group	Yamen et al., 2008
1504.48	Aromatic ring in plane bending of -OH group	Gashti et al., 2013; Yamen et al., 2008
1722.43	-C=O stretching of carboxylic acid groups, or C=C aromatic ring	Yamen et al., 2008; Yusuf et al., 2016
1950.03	Symmetric stretching of -CH ₂	Gashti et al., 2013
2902.87	Asymmetric stretching of -CH ₂	Gashti et al., 2013
3417.86, 3053.32, 2968.45	Stretching and in plane bending of -CH group	Gashti et al., 2013; Nacowong and Saikrasun, 2016

In case of PTT, the presence of -OH in the hydroxyl and carboxyl groups may help in bonding with certain dye molecules. Thus, there appears to be a possibility of dyeing under milder conditions at temperatures lower than PET. Also, the use of auxiliary chemicals assisting dye penetration may be omitted, making the process of dyeing ecofriendly.

From the interpretation, it can also be deduced that there remains a possibility of application of natural dyes on PTT. The natural dyes have been historically used to dye natural fibers like cotton, jute, wool, silk etc. These dyeing processes are carried out above room temperatures but below the boiling point of water. Thus, the cost of power as well as infrastructure required for dyeing are minimal. This is possible owing to chemical bonding of natural dyes with these fibers at the available reactive sites.

If some reactive sites are present in PTT, they may make the fiber easier to dye with those dyes that can bind with these sites, such as the natural dyes. Hence, the dyeing temperature may come down to a great extent. Also, there may not be any need for the pollutant auxiliaries that are otherwise required to assist in dye diffusion. The results show a possibility of achieving ecofriendly dyeing process for PTT as compared to PET.

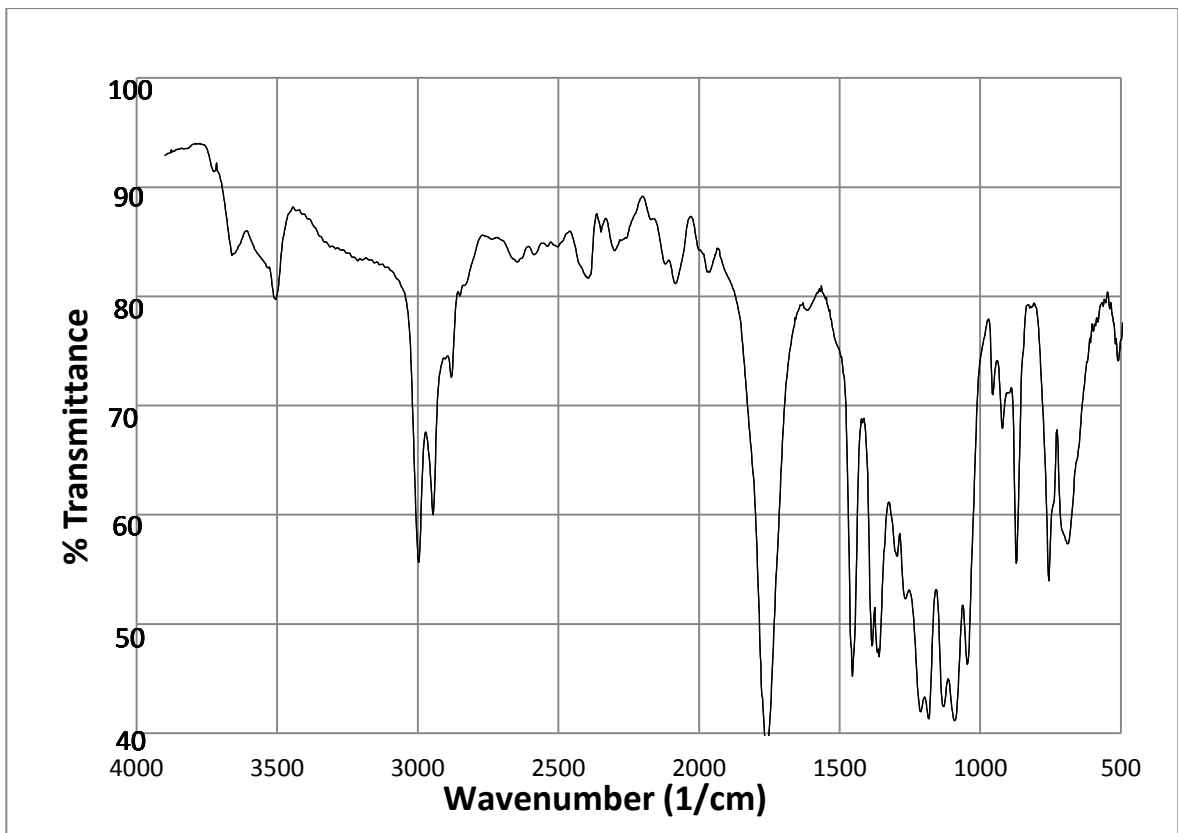


Figure 4.6: FTIR spectroscopy of PLA.

Table 4.2: Peaks observed in FTIR of PLA and functional groups indicated.

Wavenumber of peak observed (cm ⁻¹)	Nature of functional group	References
869.90	Meta-substituted compounds	Kaur, 2004-'05
1049.28	C-O stretching	Gashti et al., 2013; Yamen et al., 2008
1099.43	Weak C-O stretching	Gashti et al., 2013; Kaur, 2004-'05
1190.08	Weak C-O stretching	Yamen et al., 2008
1357.89	Gauche -CH ₂ wagging	Yamen et al., 2008
1452.40	Trans -CH ₂ wagging	Gashti et al., 2013; Yamen et al., 2008
1749.44	Strong -C=O stretching	Yamen et al., 2008; Yusuf et al., 2016; Kaur
2081.19	Stretching of -C≡C-	Kaur, 2004-'05
2385.95	Symmetric stretching and in plane bending of -CH group	Kaur, 2004-'05
2883.58	Asymmetric stretching and in plane bending of -CH group	Haddar et al., 2014; Kaur, 2004-'05
2995.45, 2943.37	Asymmetric stretching and in plane bending of -CH group	Gashti et al., 2013; Haddar et al., 2014; Nacowong and Saikrasun, 2016

4.3 Summary

From the characterization of the PTT and PLA fibers, the glass transition temperatures (T_g) and melting points (T_m) for PTT and PLA could be confirmed with the reported values from the thermo-gravimetric analysis performed in this study. The thermally and mechanically stable ranges of temperatures of PTT and PLA could be identified as 80 °C -120 °C and 90 °C -145 °C respectively.

The presence of a smooth surface with micropores could also be observed from SEM views. The FTIR spectroscopy revealed the possibility of presence of reactive sites in both the fibers. Their presence indirectly implied that there may be a possibility of chemical bonding between these fibers and certain dyes that can bind at the available reactive sites. The probability of natural dyes seemed to be high when applied on these fibers.

The above observations from the characterization studies of undyed PTT and PLA fibers indicated that there may be possibility of achieving milder dyeing conditions for these fibers in comparison to PET. However, it will depend on the nature of the dye selected as well. With an appropriate dye selected, the dyeing temperature may be lower than that of PET. It may even be lower than the dyeing temperatures of 100-110 °C reported for PTT and PLA with disperse dyes and auxiliaries, which remains to be studied. It also remains to be studied if satisfactory dyeing can be achieved with such selected dyestuffs for PTT and PLA without the use of harmful and pollutant auxiliary chemicals.

Chapter 5

**Dyeing and Optimization
with Disperse Dyes**

The effects of temperature, initial pH value of dye bath and dyeing time have been widely reported for PET, PT and PLA fibers with disperse dyes. However, material to liquor ratio and rate of heating may also have significant effects in dyeing of these fibers. In this chapter, dyeing was carried out using three disperse dyes with the fibers PET, PTT and PLA. The effect of the two additional parameters were carried out experimentally viz. material to liquor ratio, measured in percentage on the weight of the fiber (% owf), and the rate of heating, measured in °C/min.

The three disperse dyes chosen were Disperse Yellow 56, Disperse Blue 79 and Disperse Red 167. Although they are widely used for PET, the effects of the various factors on dyeing using these three dyes on PET as well as PTT and PLA have not been reported in literature.

Optimization was also performed in this chapter with the three selected dyes for PTT and PLA. Using normal probability plots, three statistically most significant factors were selected from the five, and optimization done with them using Response Surface Methodology based on Rotatable 2³-Factorial Central Composite Design..

5.1 Materials and methods

5.1.1 Materials

Poly-trimethylene terephthalate (PTT) and poly-ethylene terephthalate (PET) fibers were obtained from the DuPont Knowledge Center, Hyderabad, India. PTT had fiber fineness of 1.67 denier and average staple length of 80 mm. For PET, the fiber fineness was 1.85 denier and average staple length 75 mm. Poly-lactic acid (PLA) fiber was procured from the University of Leeds, U.K. It had a fiber fineness of 1.75 denier and average staple length of 72 mm.

Dyeing were carried out without the use of any auxiliary chemicals, carriers etc. Distilled water was used for all of the dyeing experiments and acetic acid (10% v/v) solution was used for maintaining the initial pH of the dye bath as well as for acid wash after dyeing. The acetic acid used was laboratory grade reagent.

5.1.2 Dyes

Three disperse dyes were used for dyeing of PTT, PLA and PET. They were Disperse Yellow 56 (C.I. 216550), Disperse Blue 79 (C.I. 11345) and Disperse Red 167 (C.I. 11338). All the three dyes were supplied by M/s. Jaychem Ind. Ltd., Mumbai, India. Their structures are given in Figures 5.1, 5.2 and 5.3 respectively [21].

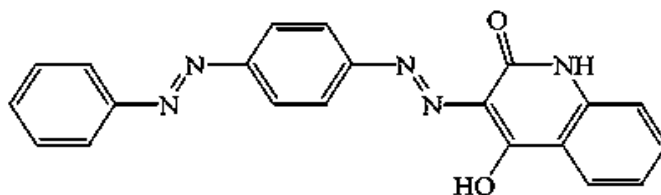


Figure 5.1: Structure of Disperse Yellow 56 (C.I. 216550) [21].

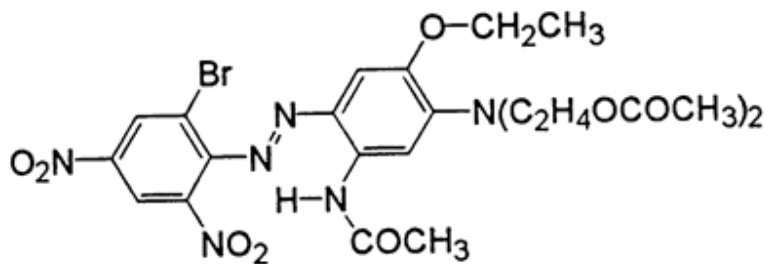


Figure 5.2: Structure of Disperse Blue 79 (C.I. 11345) [21].

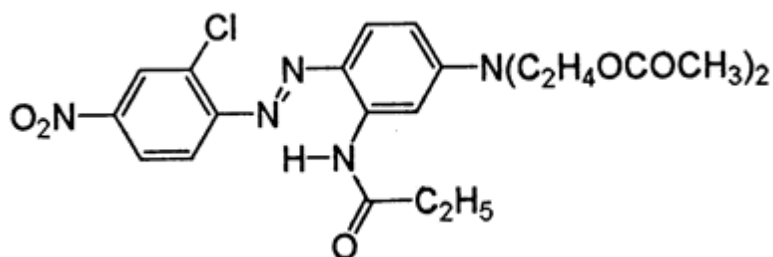


Figure 5.3: Structure of Disperse Red 167 (C.I. 11338) [21].

5.1.3 Equipment

5.1.3.1 Dyeing apparatus

For carrying out the dyeing experiments, a Superlab High Temperature and High Pressure (HTHP) dyeing equipment of laboratory scale from Supertech Textile Instruments Pvt. Ltd., New Delhi, India, was used. All dyeing experiments were started at room temperature and the dyeing temperature required was achieved with different rates of heating. The material to liquor ratio, dyeing time and initial pH of the dye bath were maintained as required in the different experiments. Figure 5.4 shows the dyeing apparatus used in this study.



Figure 5.4: Superlab HTHP dyeing apparatus.

5.1.3.2 Launder-o-meter

The wash fastness of the dyed fibers was evaluated using the Ramp Washometer equipment from Ramp Impex Pvt. Ltd., New Delhi, India. The tests were carried out as per the AATCC 61-2A-2007 test method. Figure 5.5 shows the Ramp Washometer used for the tests.



Figure 5.5: Ramp Washometer for evaluation of wash fastness.

5.1.3.3 Spectrophotometer

For measurements of color strength (K/S values) and dE values for wash fastness ratings, the Color i5 model made by Gretag MCBeth, U.S.A., was used. The aperture of the spectrophotometer that was used in all dyeing experiments was SAV (aperture diameter 6 mm). The mode of the measurements was kept as Specular Reflection Included, set at 10^0 observer and D65 illuminant. Figure 5.6 shows the spectrophotometer used in this study.

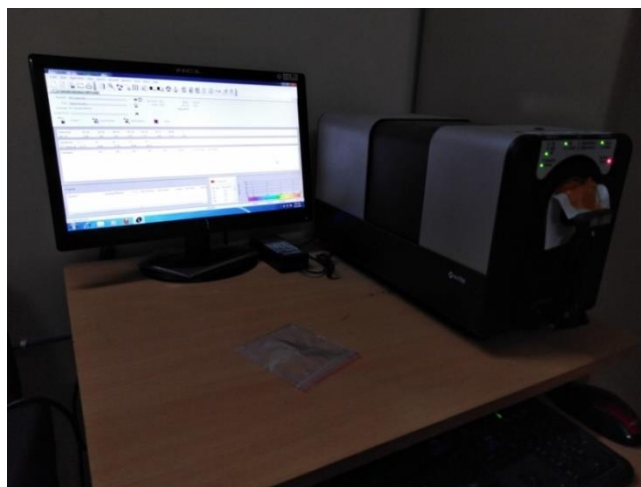


Figure 5.6: Color i5 Spectrophotometer.

5.1.3.4 Fiber fineness and tensile strength tester

In order to measure the tensile properties and fineness of fibers, the Vibrodyn-400 and Vibroscope-400 instruments from Lenzing, Austria, were used.

5.1.4 Methods

5.1.4.1 Dyeing

In case of each of the dyeing experiments, 1 g of fiber was taken and introduced into the empty dye baths. 1 g each of the three disperse dyes were added to 100 ml of distilled water so as to get a solution of 1% strength. 1 ml of this solution was introduced to each dye bath containing the undyed fibers, and the total volume inside the dye baths were made to the required volume by addition of distilled water. The total volume of liquor inside the dye bath was governed by the material to liquor ratio, and calculations were made accordingly. A schematic diagram of the dyeing cycle followed for the disperse dyes is given in Figure 5.7.

The dye baths were introduced to the HTHP apparatus at room temperature. Acetic acid (10% v/v) solution was added in required amounts to maintain the initial pH of the dye baths as predetermined. The HTHP apparatus was closed and the temperature was raised to the desired level. The rate of heating was also varied in different experiments as predetermined. Dyeing was carried out for the required duration of time, after which the machine was switched off and the dye baths drained. The dyed fibers were collected carefully and washed with distilled water. This was followed by an acid wash with acetic acid (10% v/v) solution, and then again distilled water wash to remove any residual acid. The dyed fibers were air dried at least for 8 hours before further testing.

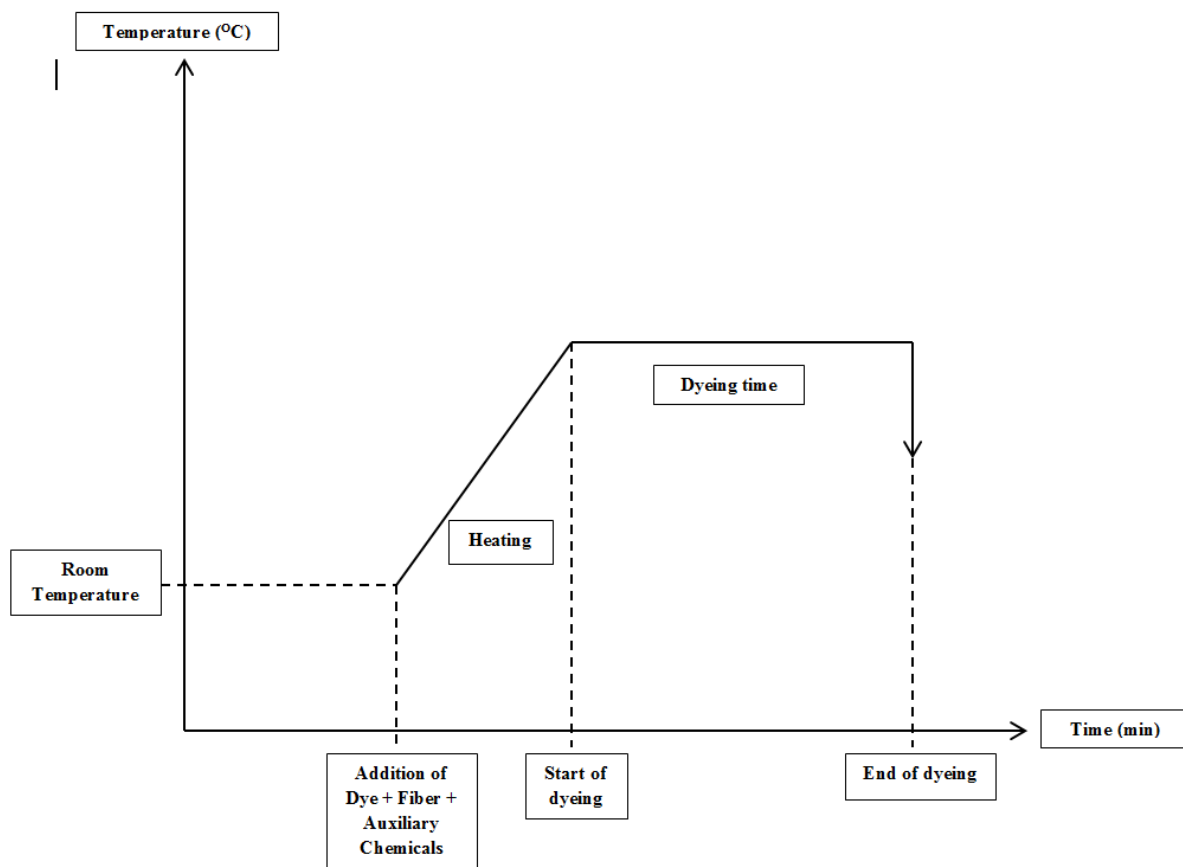


Figure 5.7: Schematic diagram of the dyeing cycle.

5.1.4.2 Measurement of color strength

The color strength of the dyed fibers was measured with the help of the K/S values. The K/S values, as defined by the equation 2.1 in the previous sections, were measured using the spectrophotometer. Dyed fibers were pasted on mounting boards and the SAV aperture was used for the evaluation. The K/S values were measured in the visible range of the spectrum (400-700 nm). The maximum K/S value and the corresponding wavelength of the spectrum were noted for each of the dyed fibers. For some of the samples, the L^* , a^* , b^* , C^* and h^o values were also measured, following the AATCC test method 173-1998.

5.1.4.3 Measurement of wash fastness

In order to measure the wash fastness, the launder-o-meter was used. Half of the dyed fiber samples were taken for each test. The tests were performed using the AATCC 61-2A-2007 test method. The tested samples were also evaluated for their dE values with respect to the untreated half of the dyed fiber. The dE value is defined as per the equation 2.10, as given in the earlier sections. The AATCC test method 173-1998 was followed for the measurements.

5.1.4.4 Measurement of tensile properties

The tensile properties were evaluated using the Vibrodyn-400 instrument from Lenzing, Austria. Single fibers were tested before and after dyeing for measuring the breaking strength (g) and elongation at break (%) as per ASTM D-3822:07 test method. The fineness (denier) of single fibers was also evaluated as per ASTM D-1577:07 test method using Vibroscope-400 instrument from Lenzing, Austria. The tenacity in grams per denier (gpd) of single fibers was determined as follows:

$$\text{Tenacity} = (\text{breaking strength}) / (\text{fiber fineness}).$$

(5.1)

5.2 Results and Discussions

The effects of temperature, initial pH of dye bath, dyeing time, material o liquor ratio and rate of heating on color strength, wash fastness as well as tensile properties of dyed PTT, PLA and PET were evaluated with disperse dyes in the following sections. The color strength was measured as K/S values and the wash fastness as dE values between the respective washed and unwashed samples of each experiment. The tenacity was measured in grams per denier (gpd) and the elongation at break as percentage (%) of

the initial length of the dyed fibers. Each experiment was carried out five times and the average values were used to plot the graphs. The CIE L*a*b*, C* and h° values of PTT and PLA fibers dyed with the three disperse dyes are given in Table 5.1. The dyed fibers are also shown in Figures 5.8-5.13. They were representative samples dyed at 120°C with initial pH of 5, dyeing time of 30 min, material to liquor ratio at 1:40 and rate of heating at 2 °C/min.

Table 5.1: CIE L*a*b* values of PTT and PLA fibers with three disperse dyes.

Fiber	Dye	L*	a*	b*	C*	h°	Figure no.
PTT	Disperse Yellow 56	53.70	34.90	71.93	79.95	64.12	5.9
	Disperse Blue 79	27.42	-5.00	-24.24	24.75	258.34	5.10
	Disperse Red 167	45.04	50.94	-3.03	51.03	356.60	5.11
PLA	Disperse Yellow 56	56.70	30.62	70.44	76.81	66.51	5.12
	Disperse Blue 79	29.54	-4.22	-24.08	24.44	260.07	5.13
	Disperse Red 167	45.95	54.36	-3.48	54.47	356.33	5.14



Figure 5.8: PTT fiber dyed with Disperse Yellow 56



Figure 5.9: PTT fiber dyed with Disperse Blue 79



Figure 5.10: PTT fiber dyed with Disperse Red 167



Figure 5.11: PLA fiber dyed with Disperse Yellow 56



Figure 5.12: PLA fiber dyed with Disperse Blue 79



Figure 5.13: PLA fiber dyed with Disperse Red 167

5.2.1 Effect of temperature

It has already been reported in chapter 4 that the thermally and mechanically stable ranges of temperatures of PTT and PLA were 80-120 °C and 90-145°C respectively, as could be concluded from the thermo-gravimetric analyses (TGA) of the two fibers. Earlier studies have also identified the range of 100-110°C as the optimal range of dyeing temperature. In this study, for measurement of color strength, a wide range of temperature was chosen. Dyeing was carried out at five different temperatures of 100 °C, 110 °C, 120 °C, 130 °C and 140 °C. Among the other factors, the initial pH of the dye bath was maintained at 5, time at 30 min, material to liquor ratio at 1:40 and rate of heating at 2 °C/min. The results for all of the three fibers, viz. PTT, PLA and PET, are shown in Figures 5.14, 5.15 and 5.16 for Disperse Yellow 56, Disperse Blue 79 and Disperse Red 167 respectively.

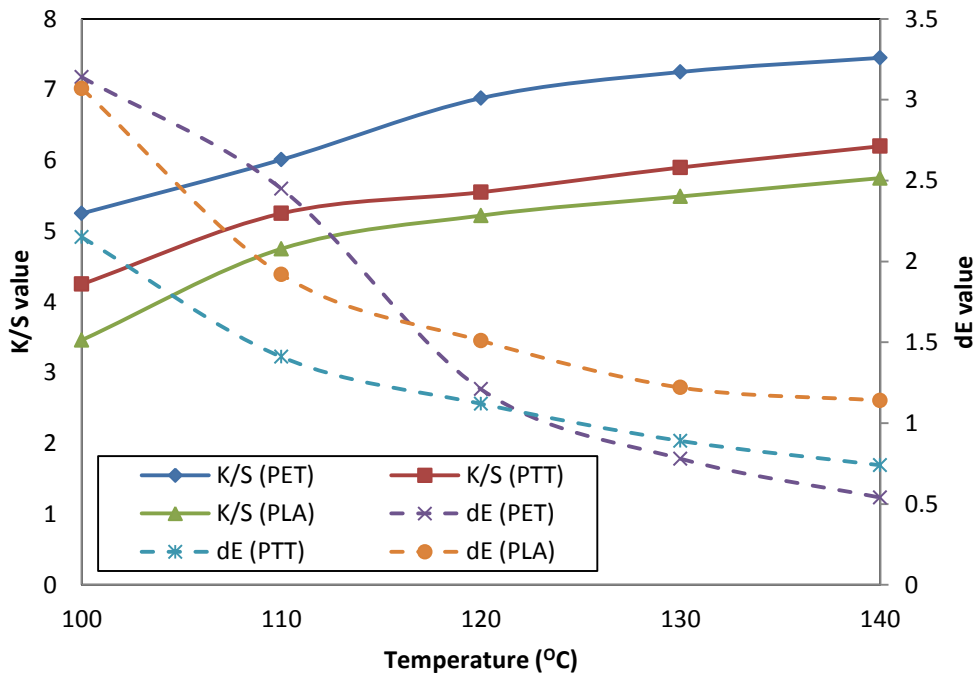


Figure 5.14: Effect of temperature on K/S value and dE value for Disperse Yellow 56.

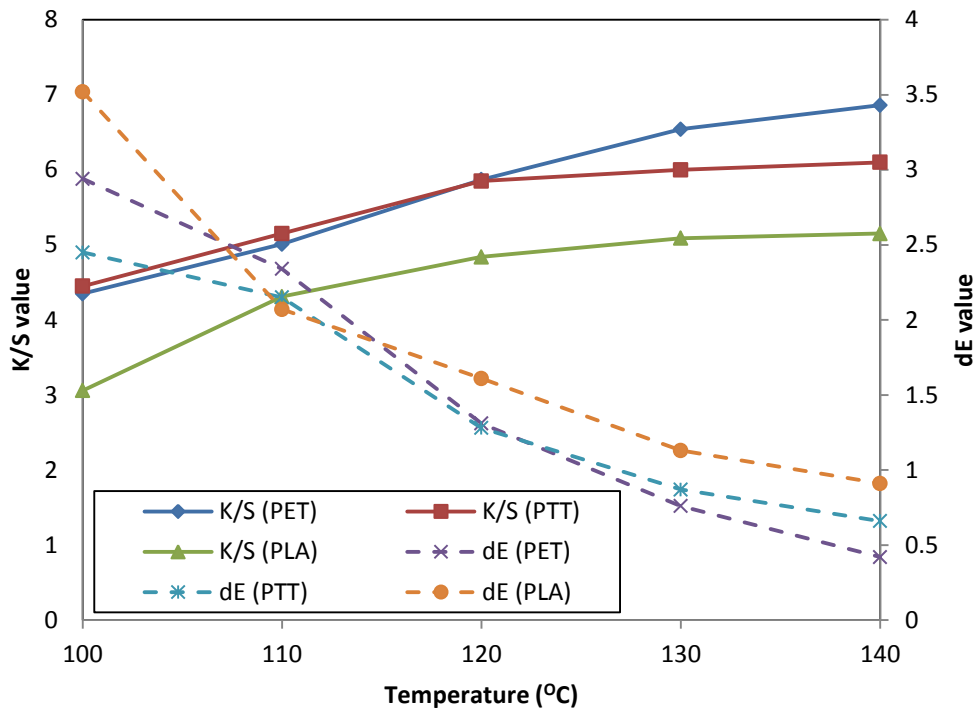


Figure 5.15: Effect of temperature on K/S value and dE value for Disperse Blue 79.

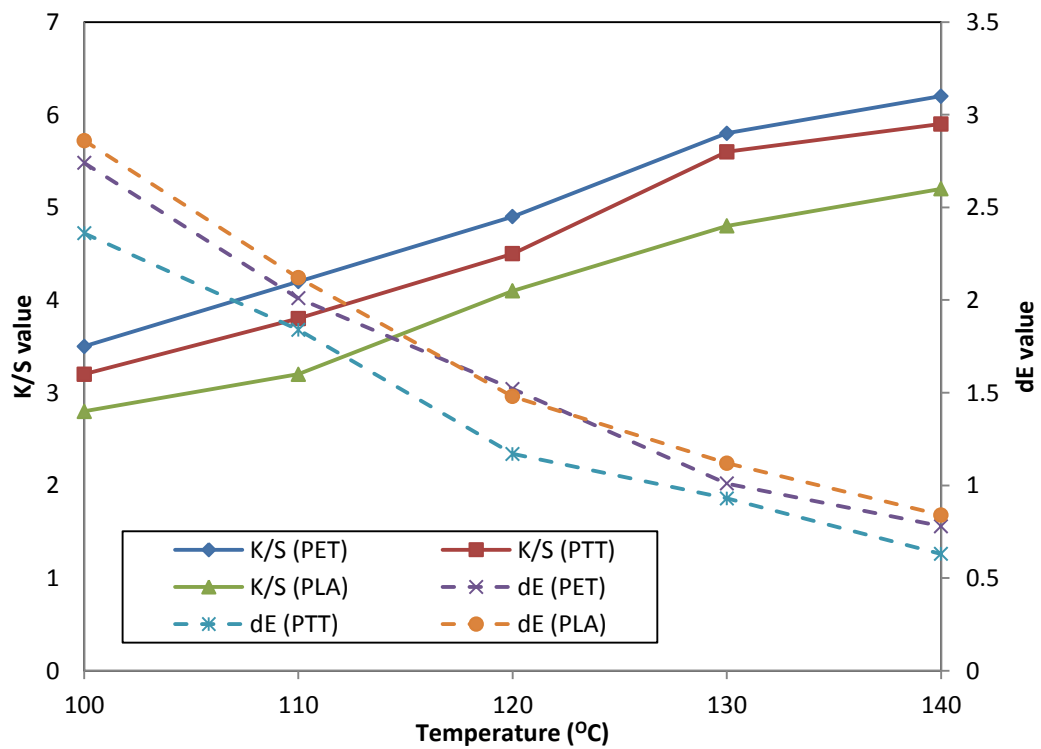


Figure 5.16: Effect of temperature on K/S value and dE value for Disperse Red 167.

It could be observed that the K/S value increased for all the three fibers with temperature. The values were highest for PET and lowest for PLA. The K/S values for PTT were very close to PET at lower temperatures. A higher K/S value was an indication of increased dye absorption by the fiber. It could thus be inferred that PET exhibited higher dye uptake for the dyes applied at this range of temperatures, but PTT was also close to PET in this regard.

The dE values decreased for all the three fibers with temperature. The dE values for PTT was found to be lower than the other two fibers at lower ranges of temperatures for all of the three dyes. A lower dE value indicated lesser color difference between the washed and unwashed dyed samples, thereby signifying better wash fastness. Thus, PTT exhibited better wash fastness than the PET and PLA at lower temperatures.

The effects of temperature on the tensile properties of the dyed fibers are also shown in Figures 5.17, 5.18 and 5.19 for Disperse Yellow 56, Disperse Blue 79 and Disperse Red 167 respectively.

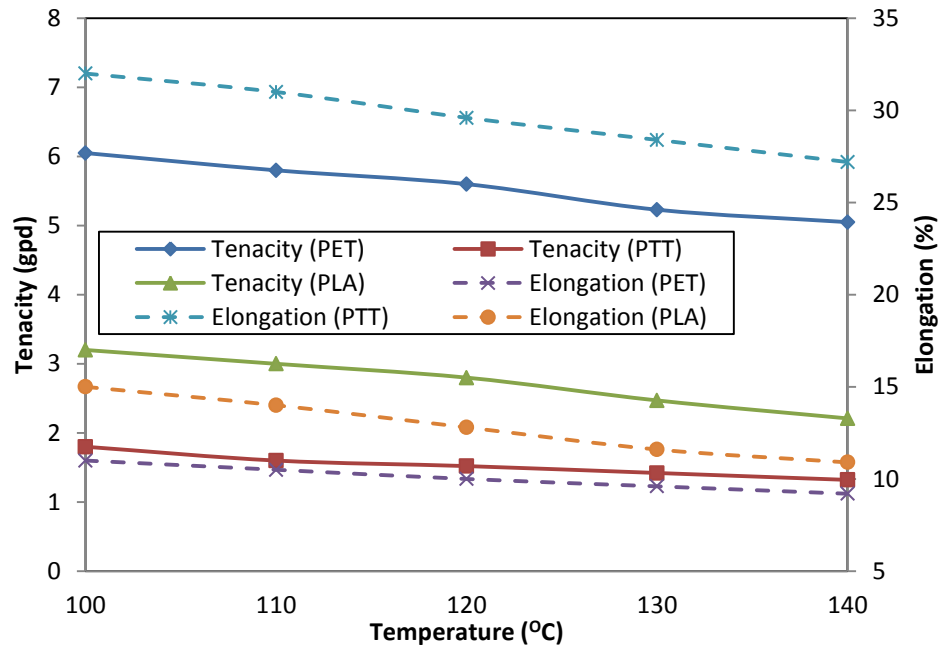


Figure 5.17: Effect of temperature on tensile properties for Disperse Yellow 56.

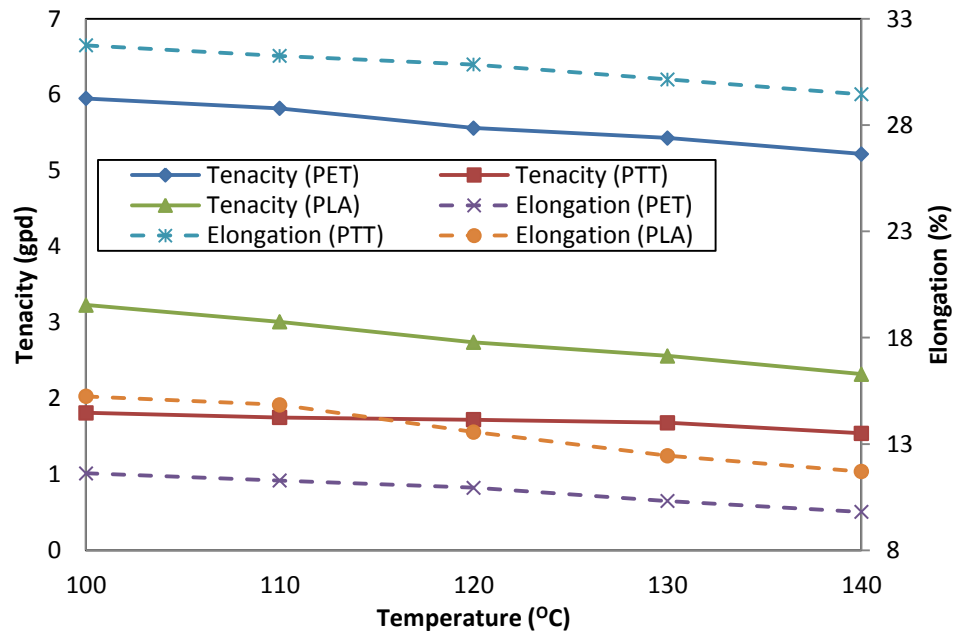


Figure 5.18: Effect of temperature on tensile properties for Disperse Blue 79.

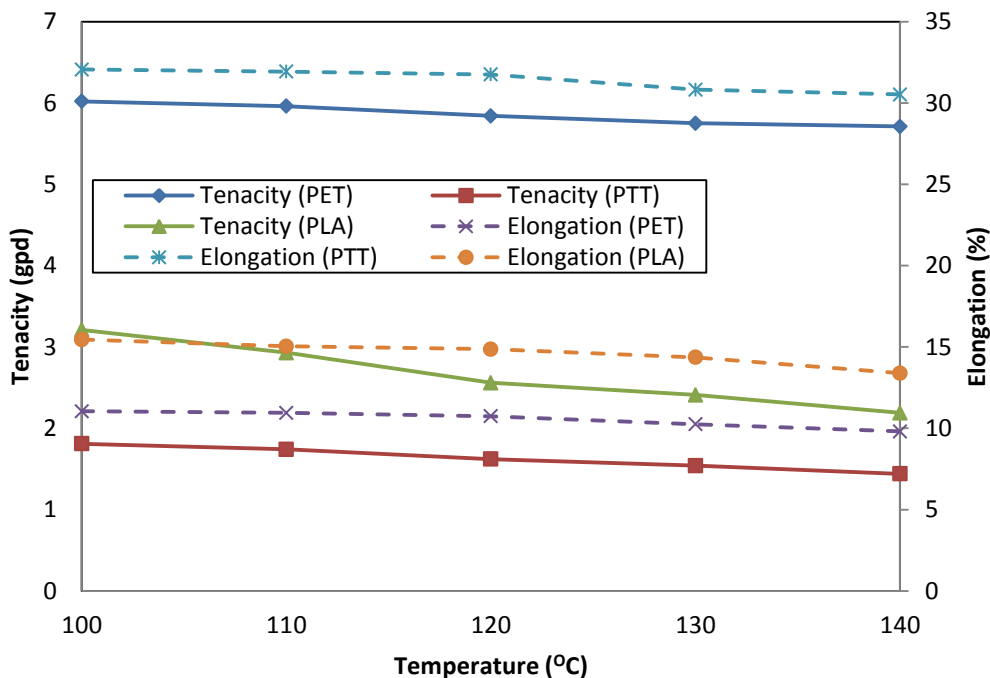


Figure 5.19: Effect of temperature on tensile properties for Disperse Red 167.

From the figures, it could be observed that the tenacity and elongation of all three fibers decreased with temperature. The fall in all cases was at a lower rate with lower temperatures, but at higher ones, the rate of decrease was enhanced. This indicated lowering of tensile properties with higher dyeing temperature for all of the fibers. It also indicated that with rise in dyeing temperature, the rate of fall of tensile properties was enhanced.

It could also be inferred that the tenacity of PTT was the lowest among the three fibers. However, the elongation was highest. This was due to the elastic property possessed by PTT as compared to other fibers including PET and PLA, as has been reported by many studies earlier. The tenacity of PET was the highest and the elongation lowest in all cases.

5.2.2 Effect of initial pH of the dye bath

Experiments were carried out at six different levels of initial pH of the dye bath for each of the three fibers with the three dyes chosen. The initial pH of the dye baths were kept at 2, 3, 4, 5, 6 and 7, keeping other factors constant. The dyeing temperature was kept at 110°C, time at 30 min, material to liquor ratio at 1:40 and rate of heating at 2°C/min for all of these experiments. The effects of initial pH of the dye bath on the color strength and wash fastness properties of the three fibers are depicted in Figures 5.20, 5.21 and 5.22 for Disperse Yellow 56, Disperse Blue 79 and Disperse Red 167 respectively.

From the figures, it could be seen that the K/S values of PTT and PLA were highest in the range of initial pH of 5-6. It decreased on both sides of this optimal range, but the fall was sharper at lower pH ranges below 5. Also, PTT exhibited higher K/S values than PLA indicating a higher dye uptake.

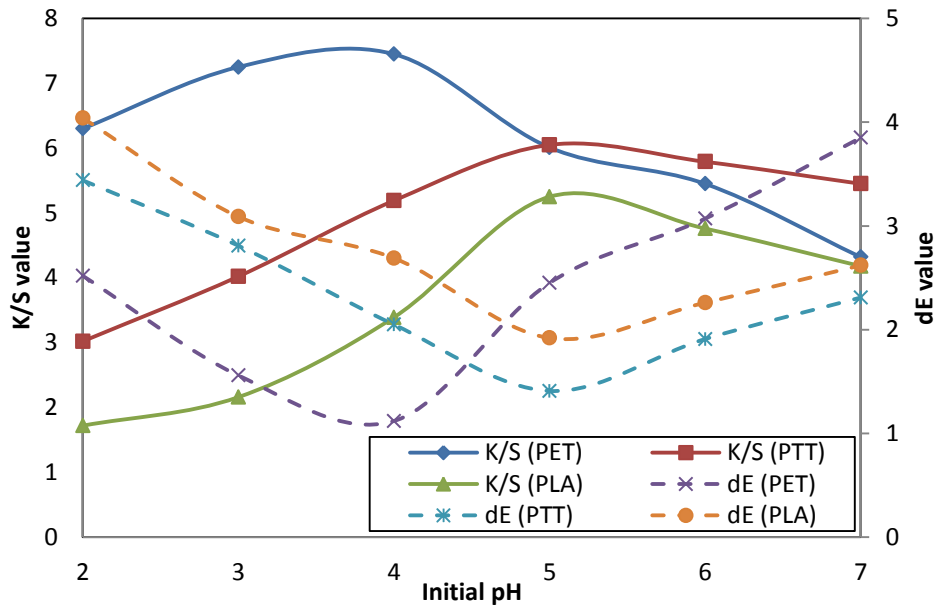


Figure 5.20: Effect of initial pH of dye bath on K/S value and dE value for Disperse Yellow 56.

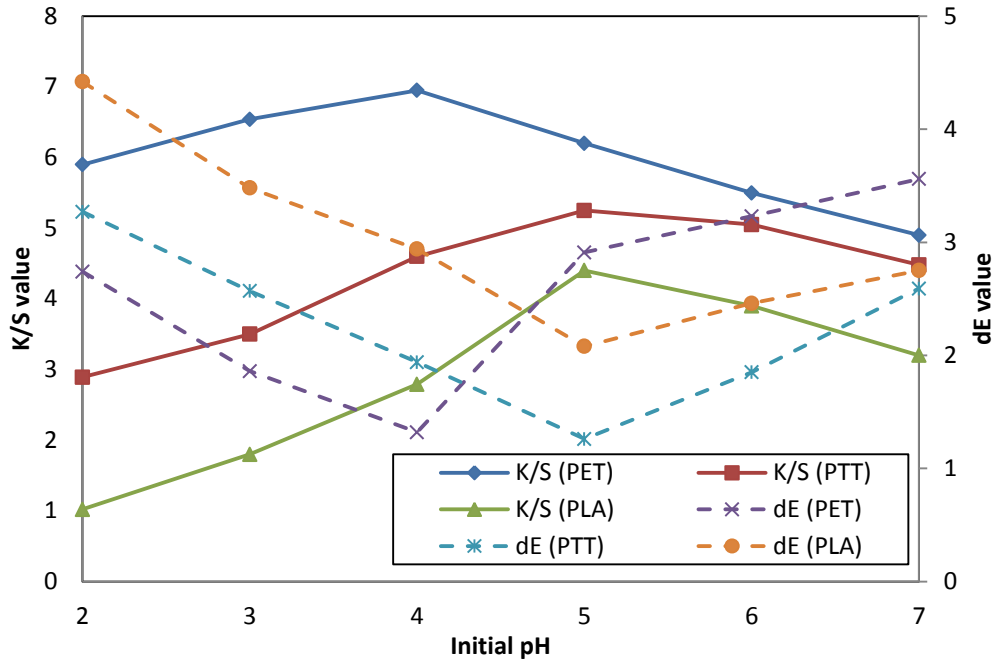


Figure 5.21: Effect of initial pH of dye bath on K/S value and dE value for Disperse Blue

79.

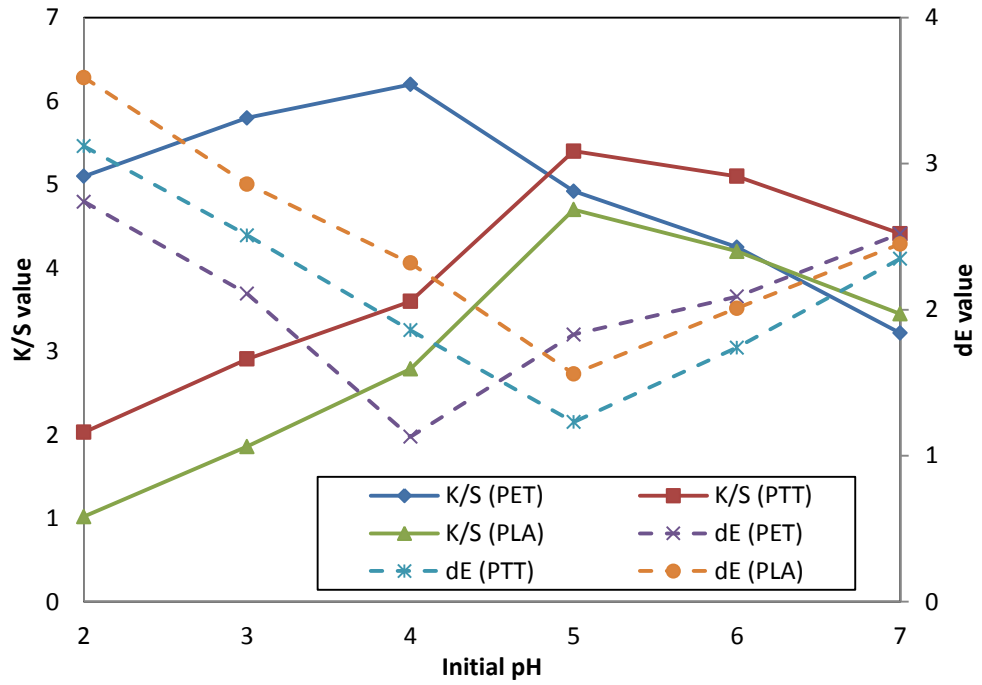


Figure 5.22: Effect of initial pH of dye bath on K/S value and dE value for Disperse Red

167.

For PET, the highest K/S values were observed in the pH range of 3-4. The values fell on both sides but the fall was sharper with higher pH ranges above 4. This was in accordance to the earlier studies that had reported 3-4 as the optimal pH range for dyeing of PET.

While observing the dE values also, it was found that the same trend was followed as for the K/S values. In case of PTT and PLA, lowest dE values were obtained in pH range of 5-6 which was 3-4 for PET with all the three dyes, indicating better dye-fiber bonding at these ranges.

The effects of initial pH of the dye bath on the tensile properties of the three fibers are depicted in Figures 5.23, 5.24 and 5.25 for Disperse Yellow 56, Disperse Blue 79 and Disperse Red 167 respectively.

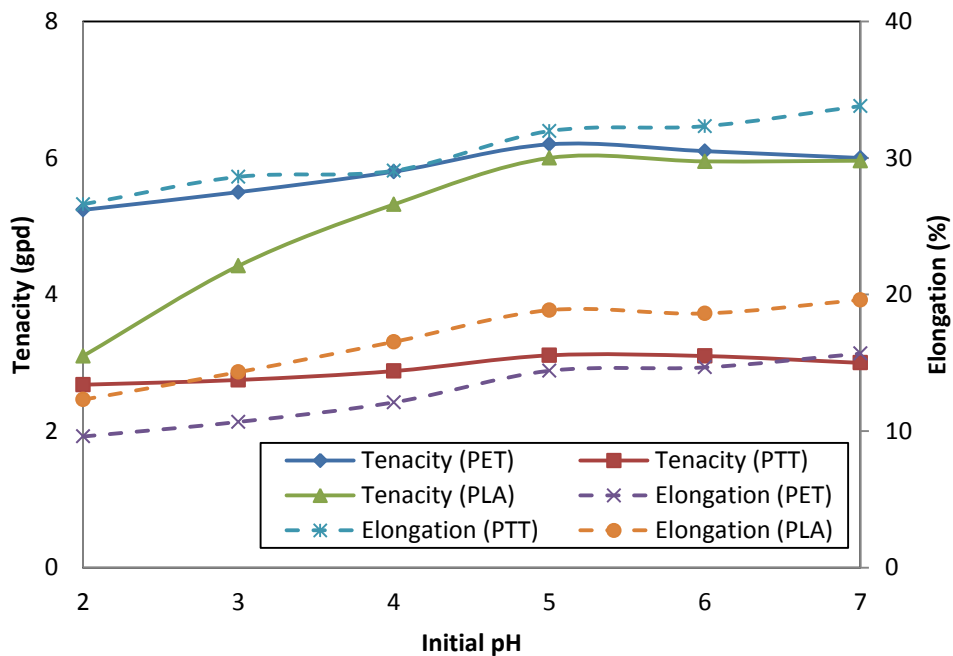


Figure 5.23: Effect of initial pH of dye bath on tensile properties for Disperse Yellow 56.

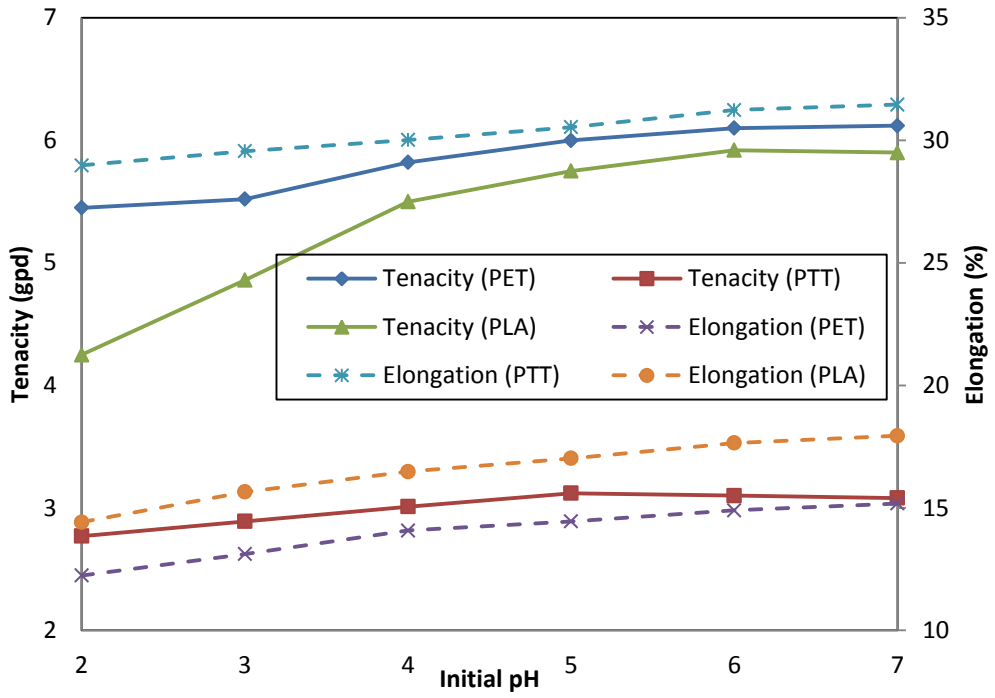


Figure 5.24: Effect of initial pH of dye bath on tensile properties for Disperse Blue 79.

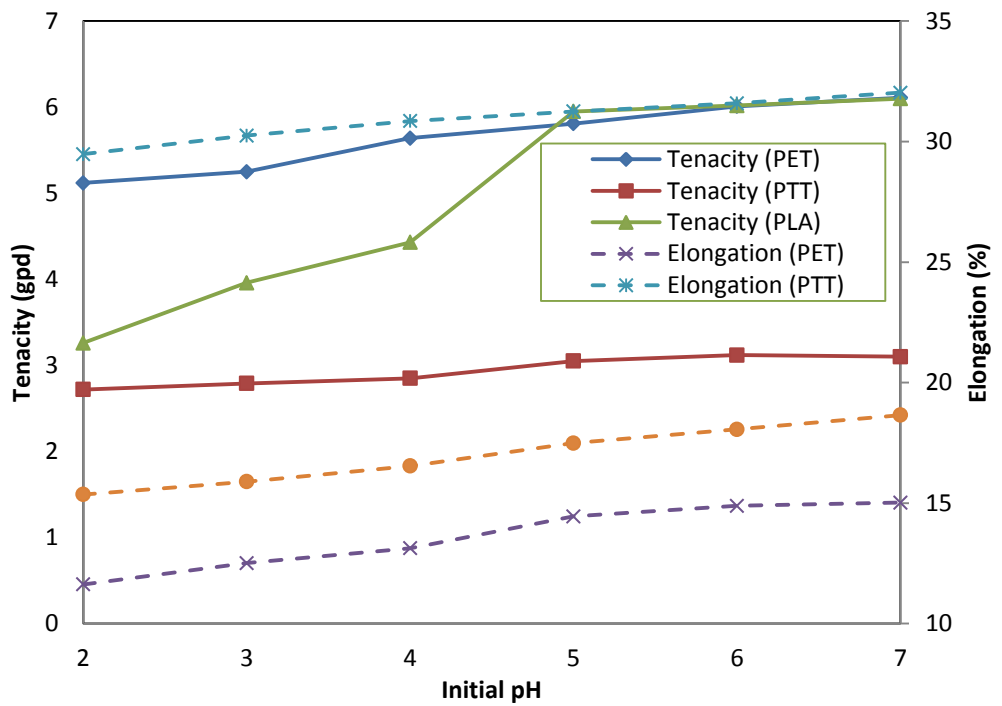


Figure 5.25: Effect of initial pH of dye bath on tensile properties for Disperse Red 167.

The graphs indicated that the tenacity (gpd) decreased for all the fibers with lowering of the pH. The fall for PLA was the most prominent with all the three dyes. The decrease for PET was the least, and that for PTT was close to it. In case of elongation too, the values decreased with lowering of the pH. The decrease in the elongation of PLA was at a higher rate than PET and PTT, but the steepness was lesser than the decrease in tenacity.

It could thus be concluded that PLA was most sensitive of the three fibers to the initial pH of the dye bath. PET was the least sensitive, justified by the lack of functional groups in it that would react to the changes in pH. PTT was more sensitive to pH changes than PET but not as much as PLA.

5.2.3 Effect of time

In order to find out the effect of dyeing time or duration on the properties of the dyed fibers, dyeing experiments were carried out at six different levels of time, viz. 15, 30, 45, 60, 75 and 90 min. other factors were kept at constant levels, which was 110°C for temperature, initial pH of 5 in the dye bath, material to liquor ratio of 1:40 and rate of heating of 2°C/min. The effects of dyeing time on the color strength and wash fastness properties of the three fibers are depicted in Figures 5.26, 5.27 and 5.28 for Disperse Yellow 56, Disperse Blue 79 and Disperse Red 167 respectively.

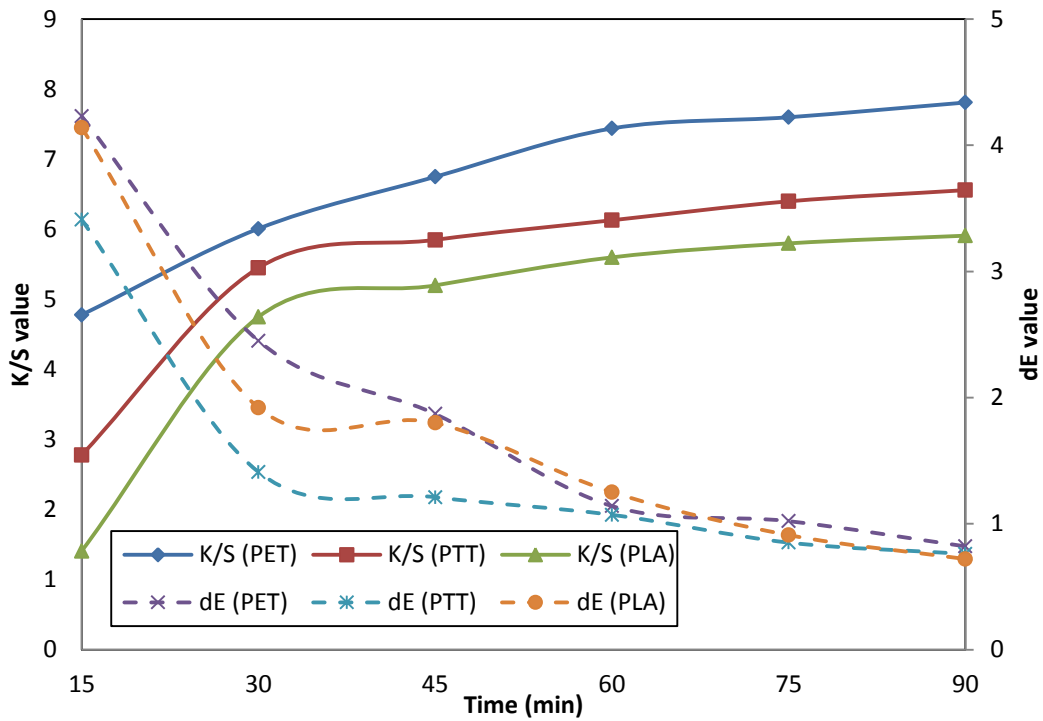


Figure 5.26: Effect of time on K/S value and dE value for Disperse Yellow 56.

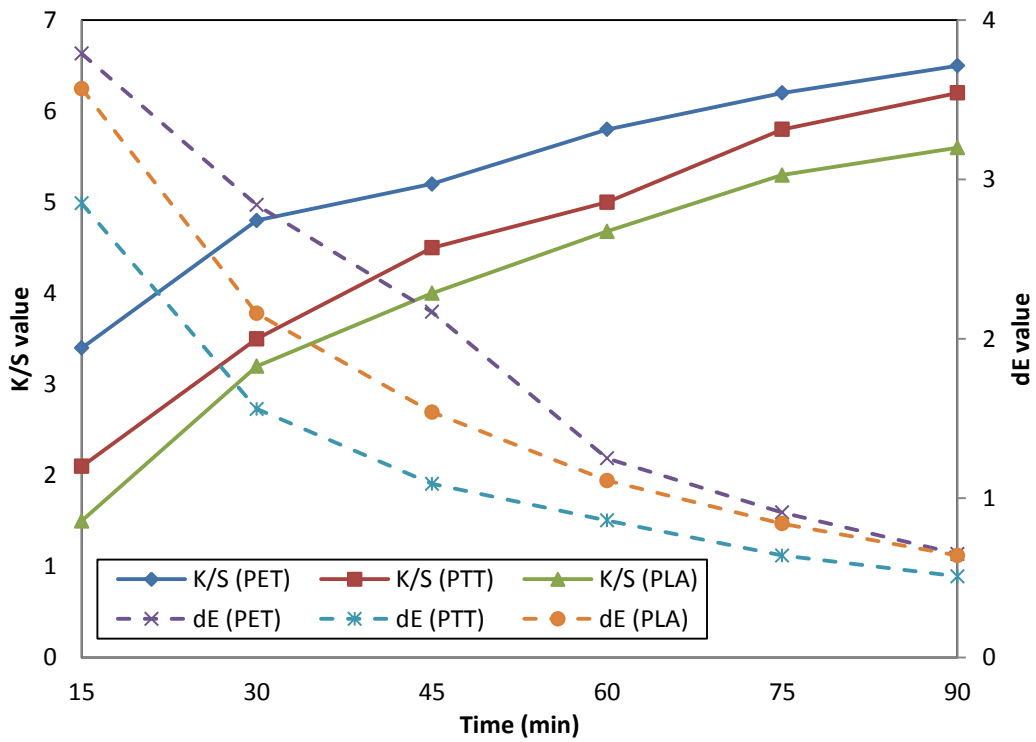


Figure 5.27: Effect of time on K/S value and dE value for Disperse Blue 79.

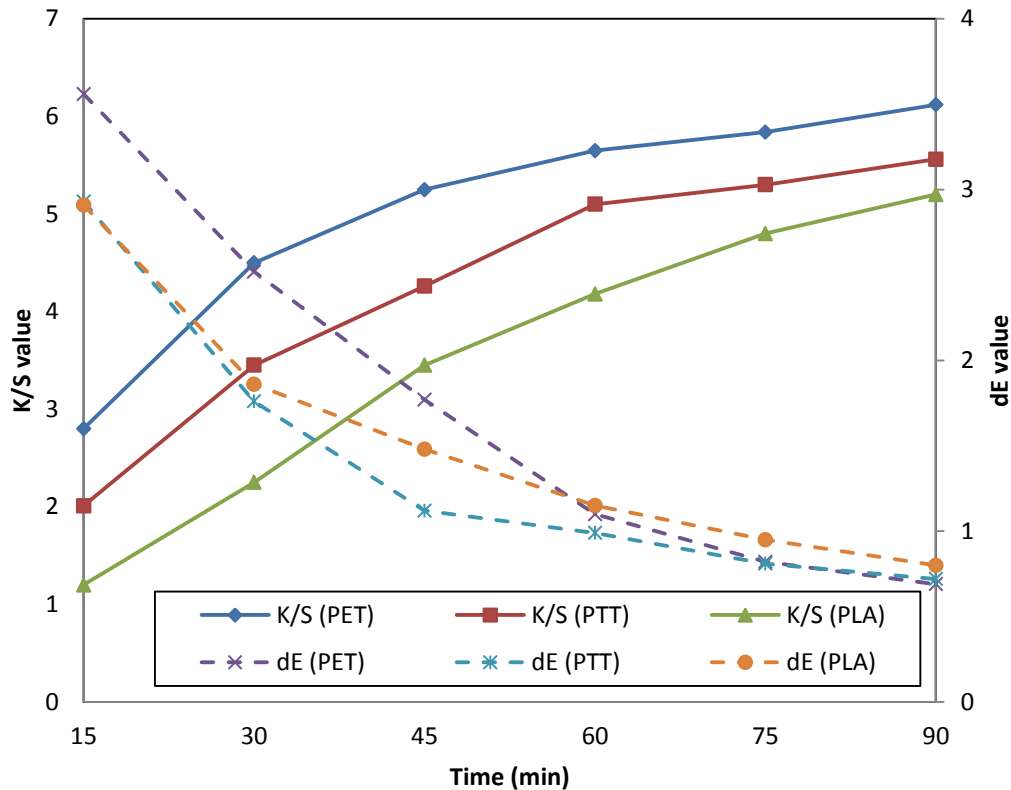


Figure 5.28: Effect of time on K/S value and dE value for Disperse Red 167.

Higher dyeing time supposedly expose the dyes for interaction with the fibers for longer duration, thereby facilitating the diffusion and adsorption. However, it also has adverse effects like destruction of the dye molecules due to exposure to higher temperatures for long. At the same time, the fibers undergo hydrolysis causing decrease in the degree of polymerization. This results in decrease of the tensile properties of the fibers as well.

It could be observed from the graphs in this case that K/S values increased for the fibers with all three dyes. With Disperse Yellow 56 and Disperse Red 167, the increase was sharper at lower temperatures but less steep at higher ones. However, for Disperse Blue 79, the rate of increase was found to be high even at higher temperatures. Also, the K/S values were highest for PET and lowest for PLA.

The dE values decreased sharply at lower temperatures indicating better dye fixation. The values tend to stabilize at higher temperatures thereby signifying that optimal dye-fiber bonding was achieved by the middle range of temperatures. Also, at lower temperatures, the dE values were lesser for PTT as compared to the other fibers. The values for PET were higher than PLA, indicating poorer wash fastness properties in this range of temperatures. At higher temperatures, the dE values of all the three fibers came close to each other, thereby indicating an improvement in wash fastness for all the fibers at higher temperatures.

The effects of dyeing time on the tensile properties of the three fibers are exhibited in Figures 5.29, 5.30 and 5.31 for Disperse Yellow 56, Disperse Blue 79 and Disperse Red 167 respectively.

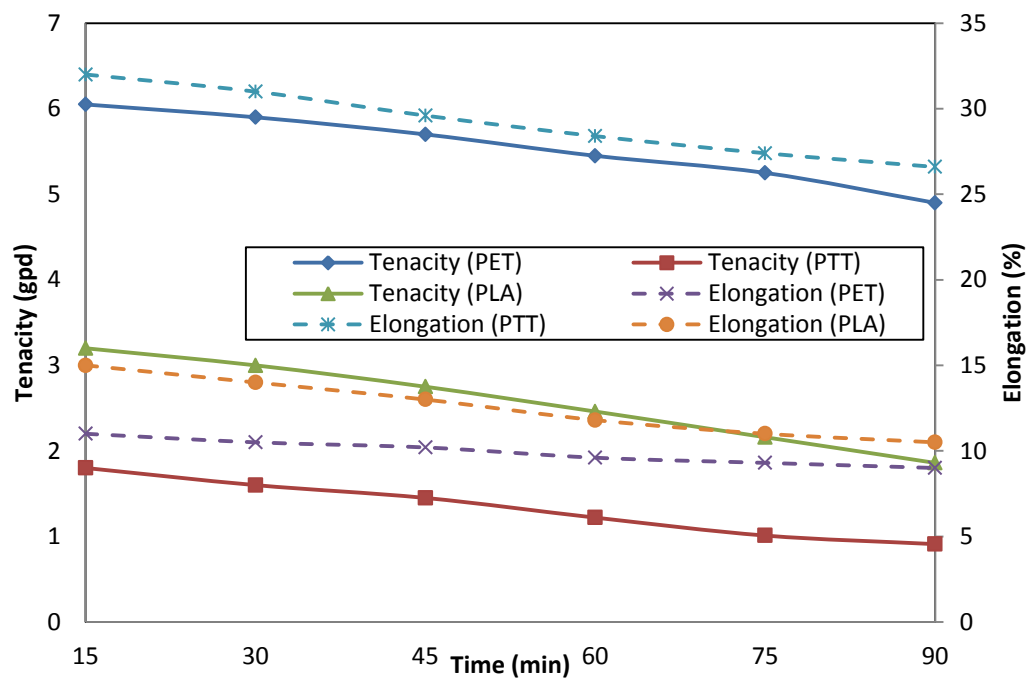


Figure 5.29: Effect of time on tensile properties for Disperse Yellow 56.

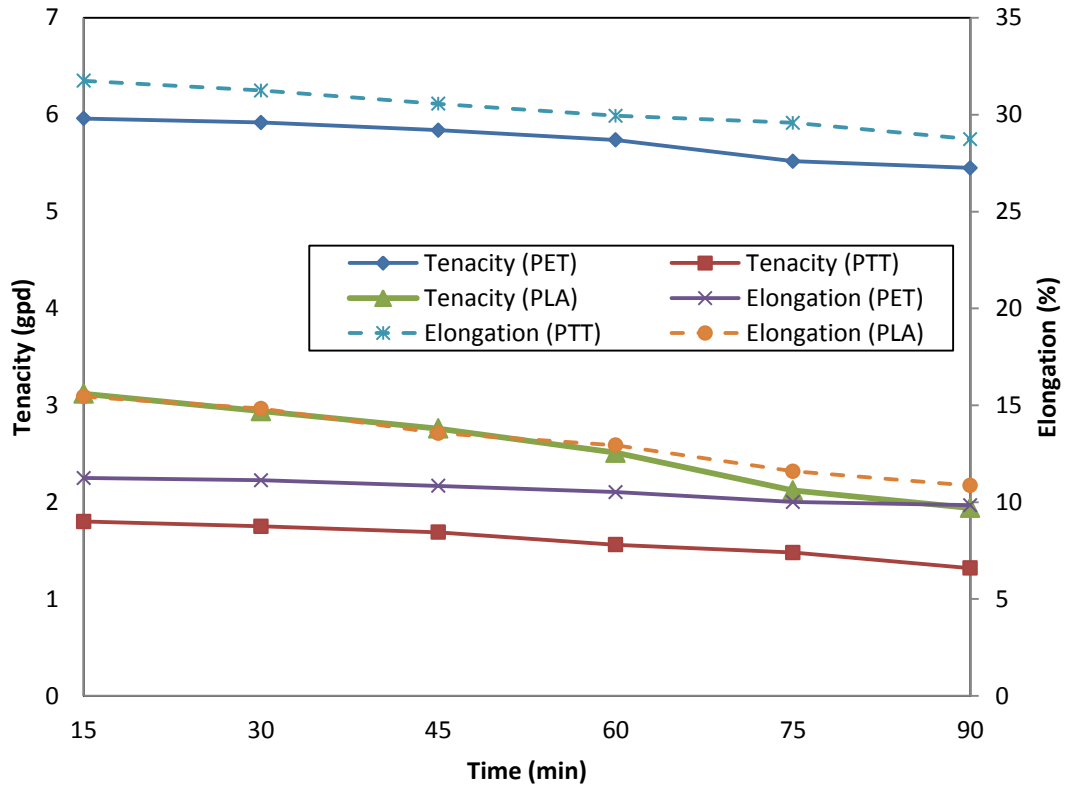


Figure 5.30: Effect of time on tensile properties for Disperse Blue 79.

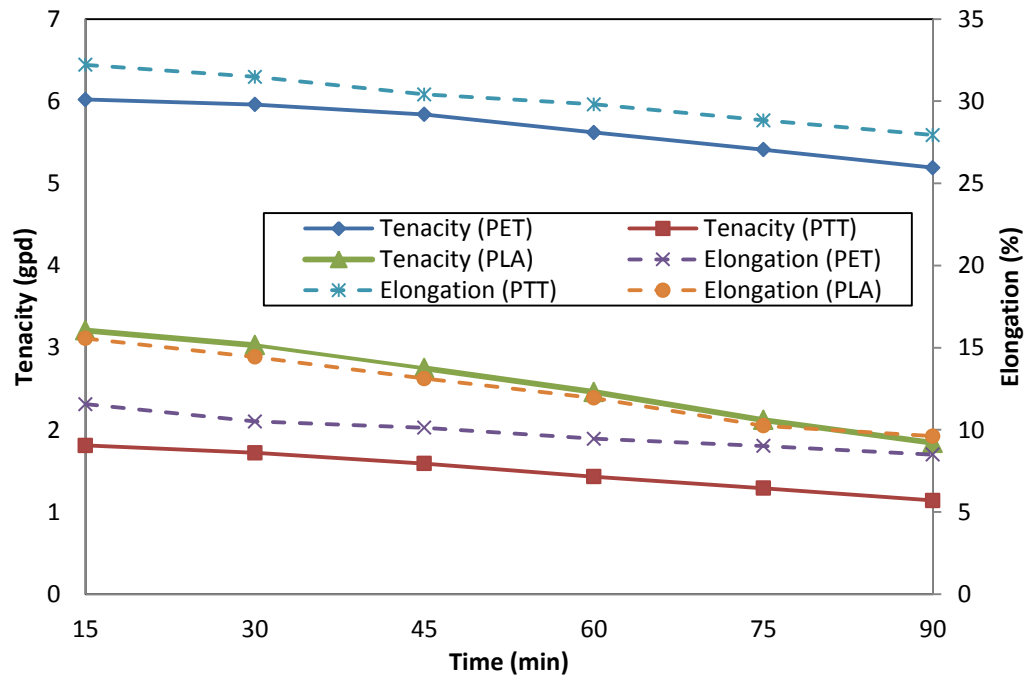


Figure 5.31: Effect of time on tensile properties for Disperse Red 167.

It was evident from the graphs that the tenacity (gpd) as well as elongation (%) of the three fibers decreased steadily with increase in dyeing time. Therefore, an optimal level of dyeing time has to be selected for all the fibers where the K/S values will be satisfactory without a significant fall in the tensile properties. The tenacity (gpd) of PET and elongation (%) of PTT were found to be higher than the other fibers.

5.2.4 Effect of material to liquor ratio

Dyeing experiments were also carried out in order to determine the effect of material to liquor ratio on the fiber properties. Five different ratios of material to liquor were chosen as 1:10 (=0.10), 1:20 (0.05), 1:30 (0.033), 1:40 (0.025) and 1:50 (0.02). Since 1 g of fiber was taken for dyeing in each case, the volume of liquor were kept at 10 ml, 20 ml, 30 ml, 40 ml and 50 ml respectively. The effects of material to liquor ratio on the color strength and wash fastness properties of the three fibers are given in Figures 5.32, 5.33 and 5.34 for Disperse Yellow 56, Disperse Blue 79 and Disperse Red 167 respectively.

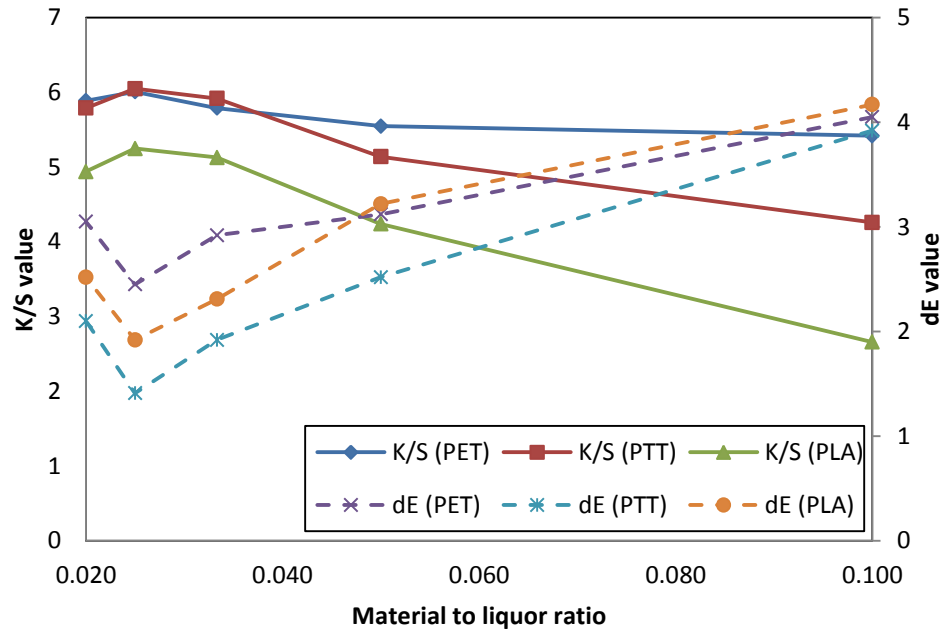


Figure 5.32: Effect of material to liquor ratio on K/S value and dE value for Disperse Yellow 56.

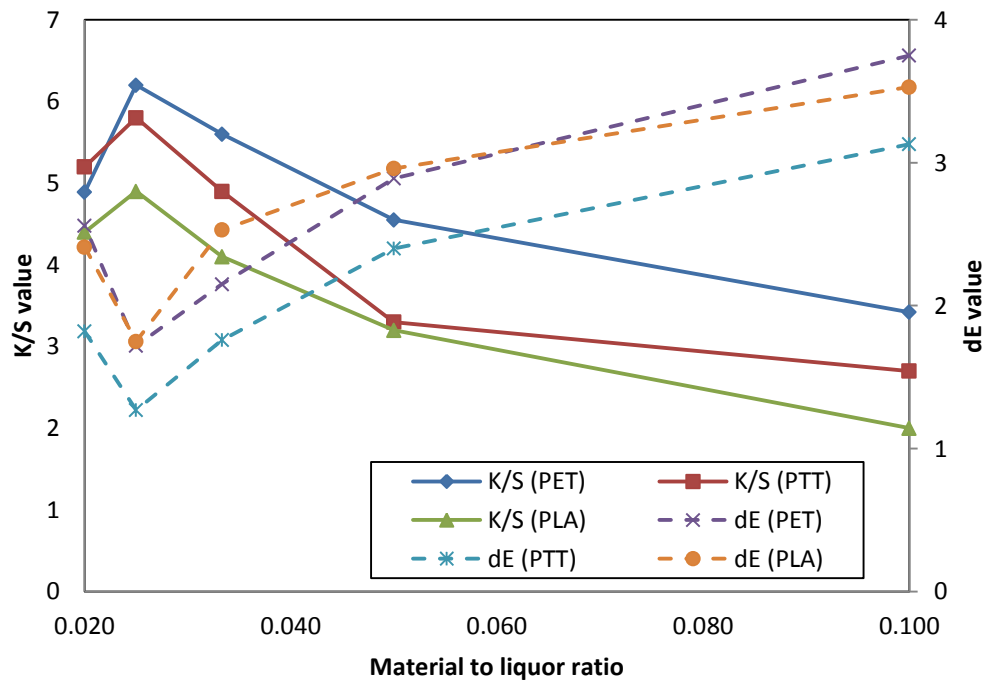


Figure 5.33: Effect of material to liquor ratio on K/S value and dE value for Disperse Blue 79.

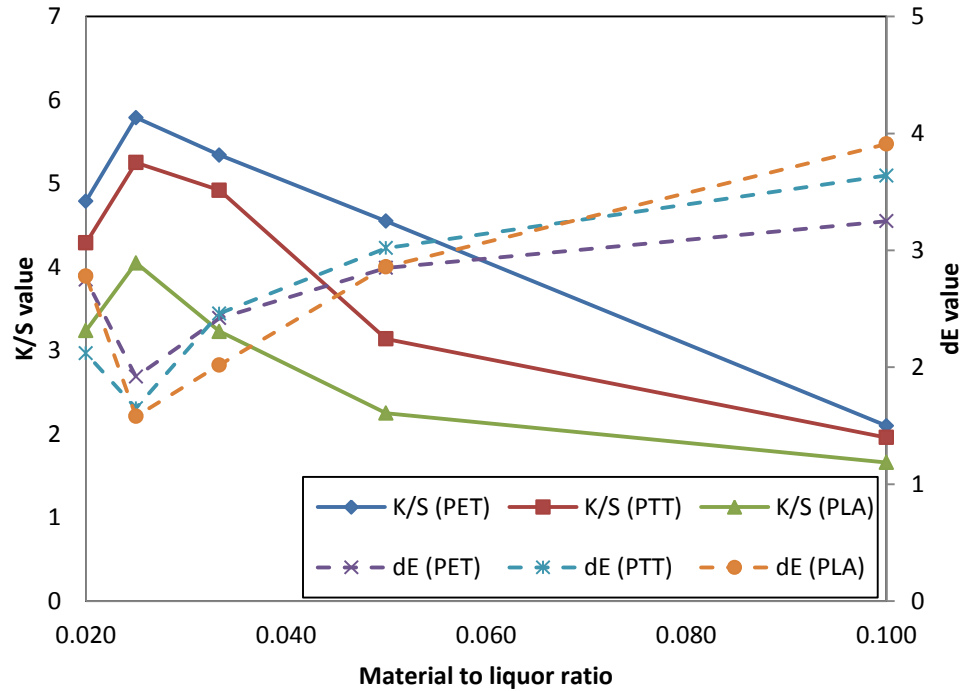


Figure 5.34: Effect of material to liquor ratio on K/S value and dE value for Disperse Red

167.

The figures exhibited that the K/S values increased for the three fibers with the material to liquor ratio up to 1:40 for Disperse Blue 79 and Disperse Red 167. For Disperse Yellow 56, the values stabilized after the ratio of 1:30. Similarly, the dE values decreased up to the ratio of 1:40 for all the dyes but increased at the ratio of 1:50. The results indicated that the range of 1:30 to 1:40 was optimal for both K/S values and dE values for all the fibers.

The effects of material to liquor ratio on the tensile properties of the three fibers are exhibited in Figures 5.35, 5.36 and 5.37 for Disperse Yellow 56, Disperse Blue 79 and Disperse Red 167 respectively.

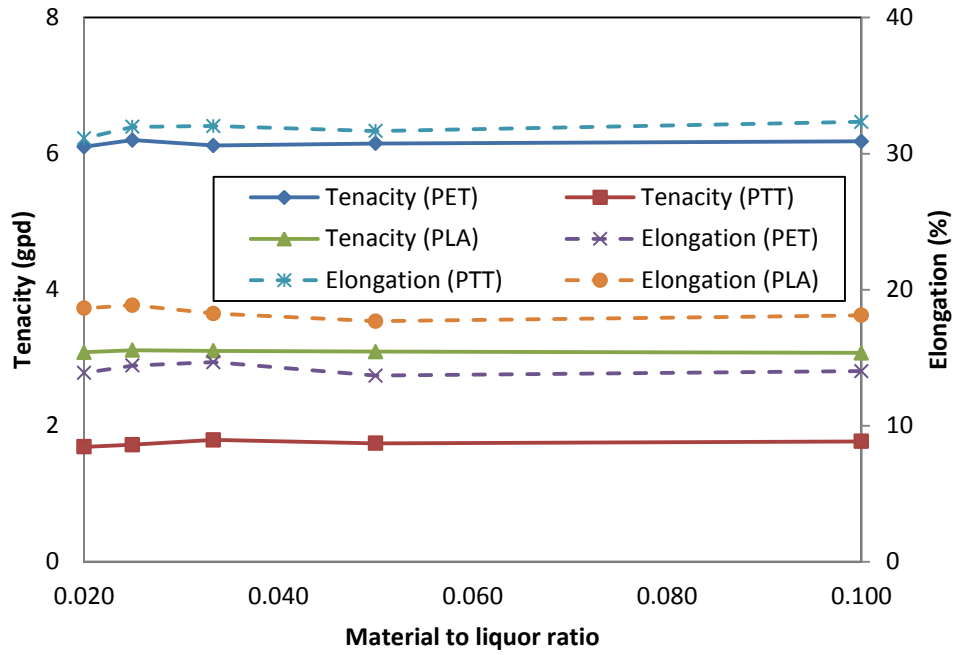


Figure 5.35: Effect of material to liquor ratio on tensile properties for Disperse Yellow

56.

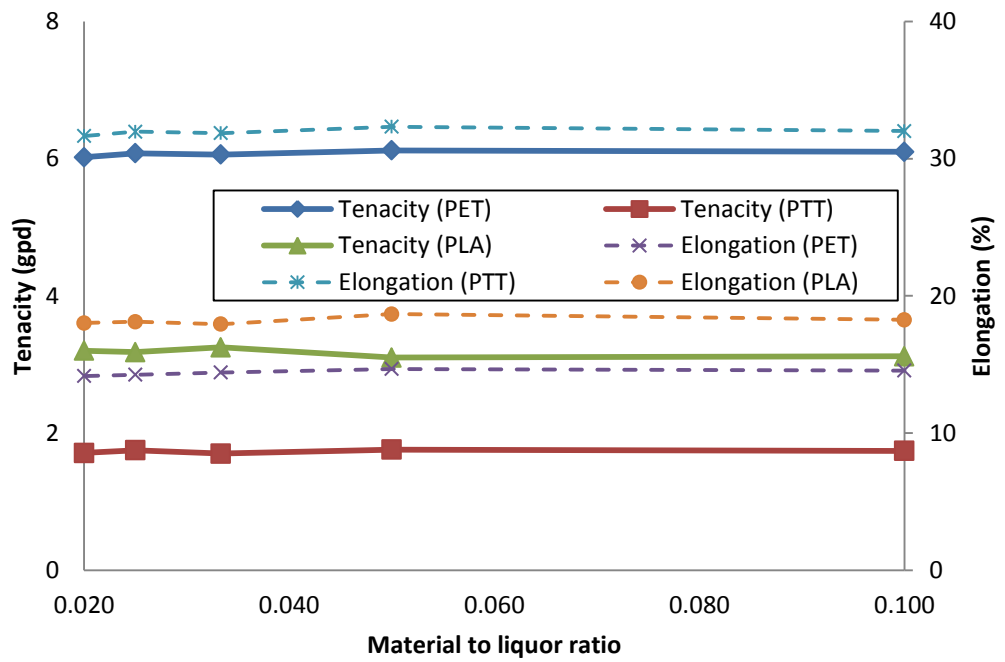


Figure 5.36: Effect of material to liquor ratio on tensile properties for Disperse Blue 79.

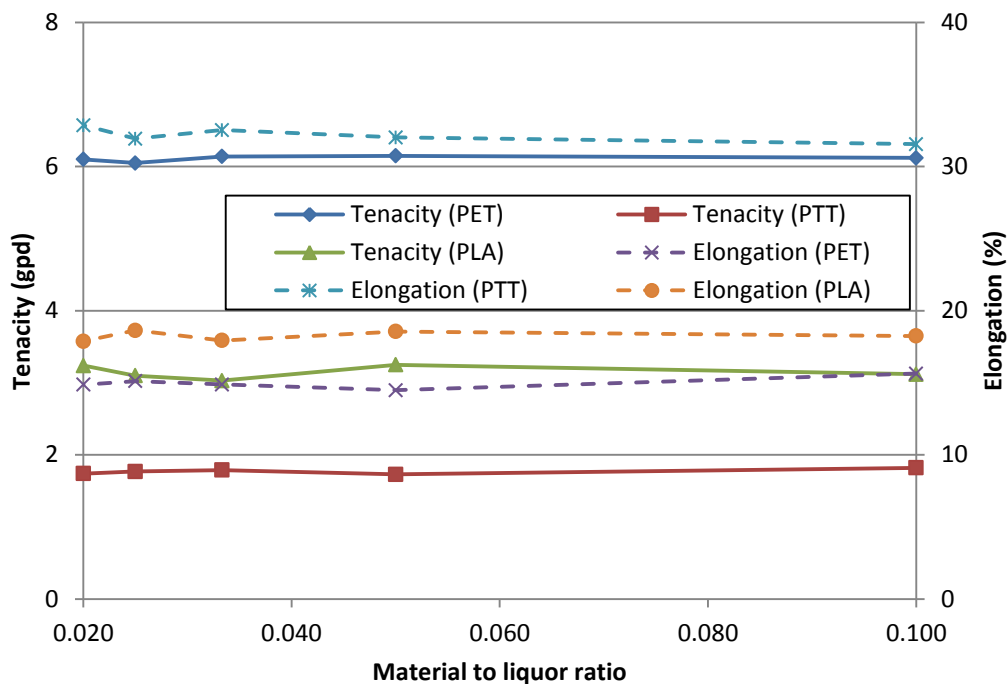


Figure 5.37: Effect of material to liquor ratio on tensile properties for Disperse Red 167.

The graphs depicted that the material to liquor ratio did not have any significant effect on the tensile properties of any of the fibers and with any of the dyes applied. Thus, it was a less significant factor in dyeing of PTT, PLA and PET with disperse dyes as compared to the factors already discussed.

5.2.5 Effect of rate of heating

Three different rates of heating of the dye baths from room temperature to dyeing temperature were chosen for observing their effects on dyed fiber properties. Dyeing were thus carried out at 1^oC/min, 2^oC/min and 3^oC/min, with temperature kept at 110^oC, initial pH of dye bath at 5, time at 30 min and material to liquor ratio at 1:40. The effects of rate of heating on the color strength and wash fastness properties of the three fibers are given in Figures 5.38, 5.39 and 5.40 for Disperse Yellow 56, Disperse Blue 79 and Disperse Red 167 respectively.

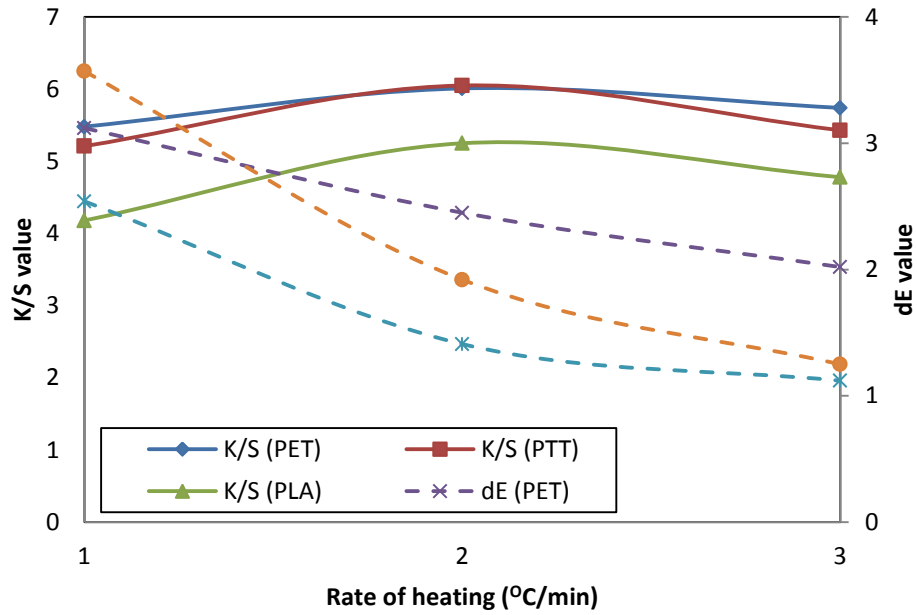


Figure 5.38: Effect of rate of heating on K/S value and dE value for Disperse Yellow 56.

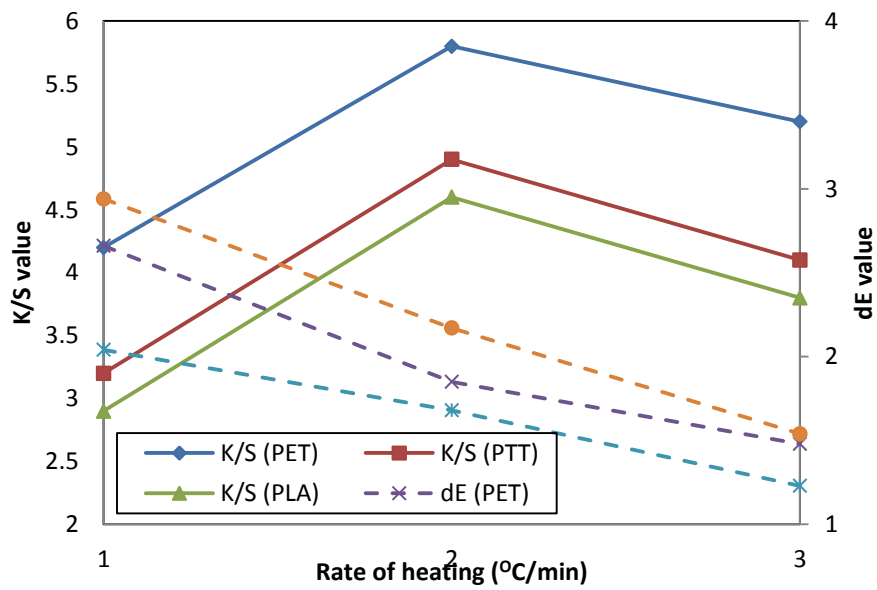


Figure 5.39: Effect of rate of heating on K/S value and dE value for Disperse Blue 79.

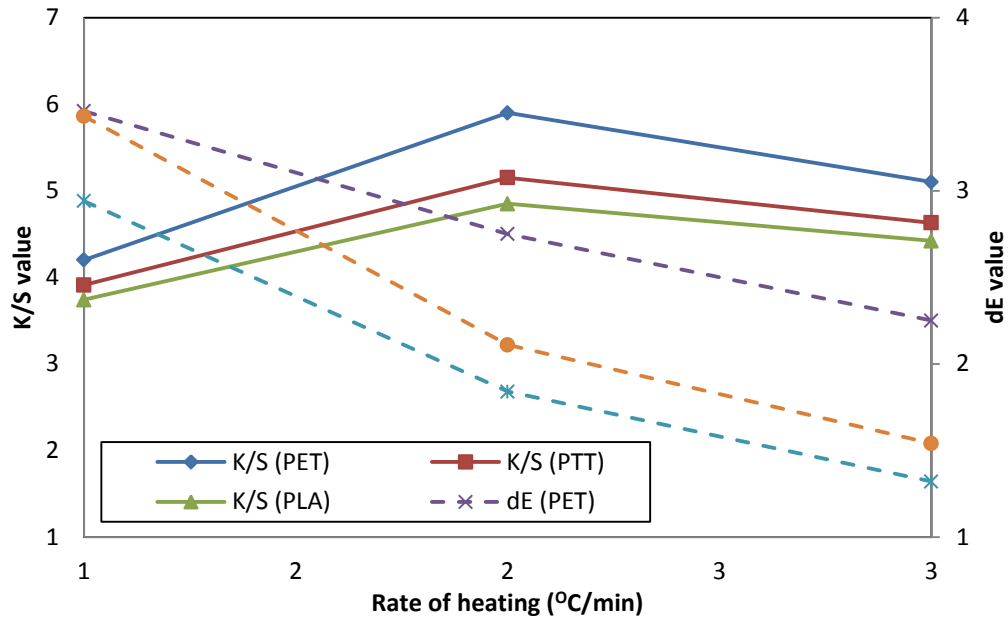


Figure 5.40: Effect of rate of heating on K/S value and dE value for Disperse Red 167.

The graphs indicated that highest K/S values were obtained with the rate of heating of 2^oC/min. The dE values were however lowest at 3^oC/min.

The effects of rate of heating on the tensile properties of the three fibers are exhibited in Figures 5.41, 5.42 and 5.43 for Disperse Yellow 56, Disperse Blue 79 and Disperse Red 167 respectively.

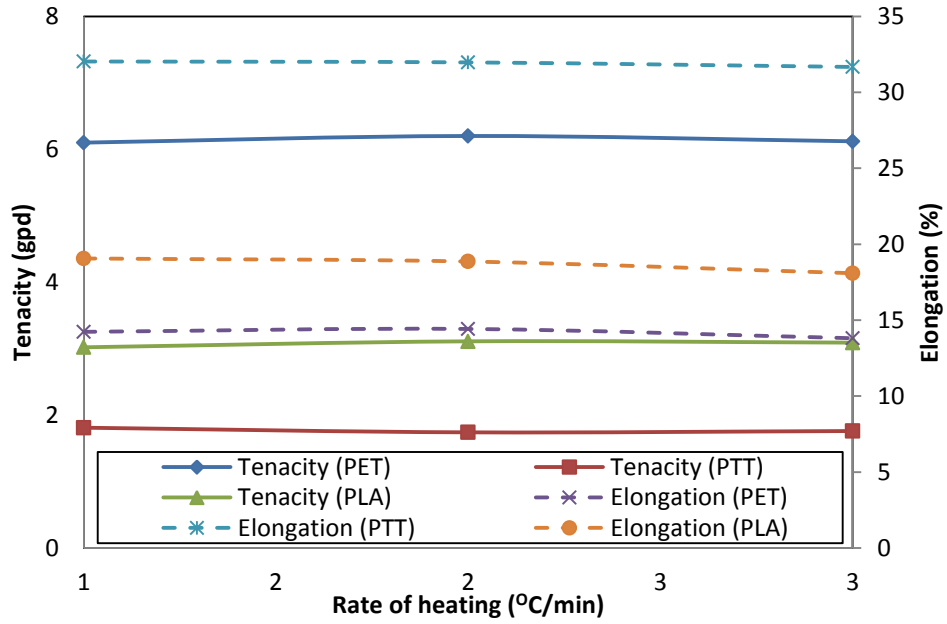


Figure 5.41: Effect of rate of heating on tensile properties for Disperse Yellow 56.

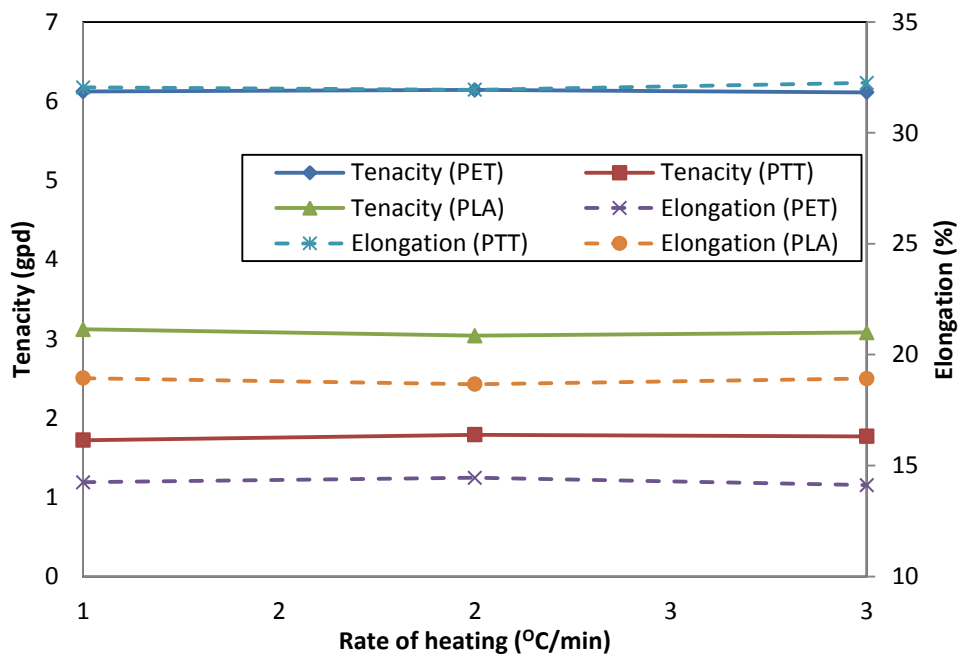


Figure 5.42: Effect of rate of heating on tensile properties for Disperse Blue 79.

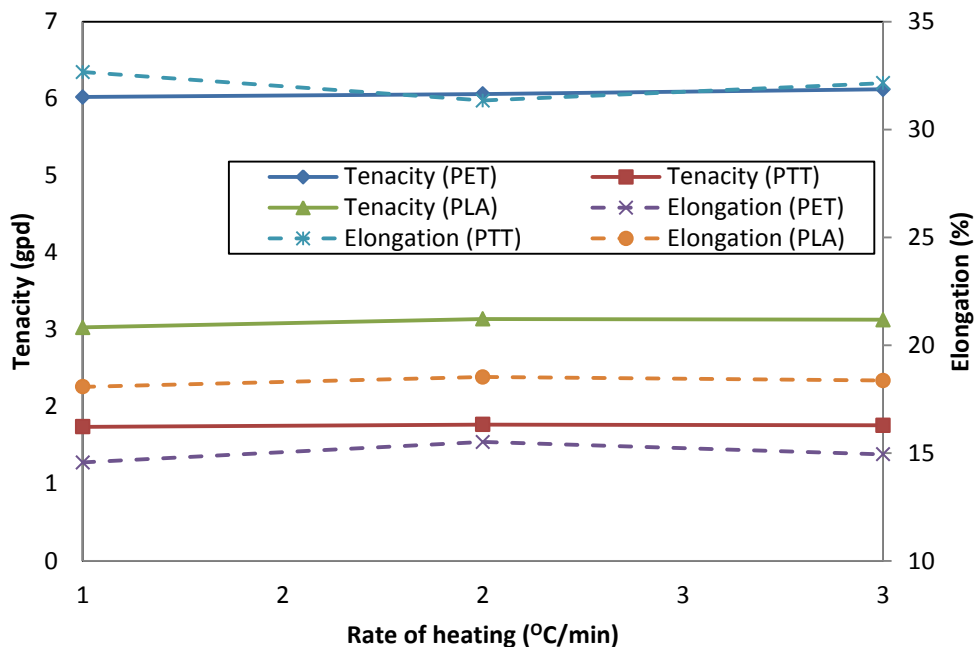


Figure 5.43: Effect of rate of heating on tensile properties for Disperse Red 167.

The rate of heating was found to leave no significant effect on the tensile properties of the dyed fibers. Thus, like material to liquor ratio, this factor was also less significant as compared to temperature, initial pH of the dye bath and time of dyeing in affecting the various properties of PTT, PLA and PET after dyeing with disperse dyes.

5.3 Optimization with disperse dyes

The optimal ranges for various parameters affecting the fiber properties favorably for PTT and PLA after application of disperse dyes could be observed in the above discussions. With these optimal ranges, optimization was done using Response Surface Methodology (RSM) based on Rotatable 2^3 -Factorial Central Composite Design (CCD).

In RSM, three factors were selected that affected the properties of the dyed fibers most significantly. In case of disperse dyes, the effects on dyed fibers were observed for temperature, initial pH of dye bath, time, material to liquor ratio and rate of heating. Using the normal probability plots, the three factors that were most significant in

affecting the color strength of the dyed fibers was identified for each of the three disperse dyes used. With these three factors, optimization was done using RSM. The main effects and the effects of interaction of these factors on fiber properties after dyeing were evaluated. The fiber property that was considered was color strength of the dyed fibers, measured as the K/S value. Optimization was done with PTT and PLA fibers for all of the three disperse dyes chosen for this study, viz. Disperse Yellow 56, Disperse Blue 79 and Disperse Red 167. The results obtained are discussed in the following sections.

Response Surface Methodology (RSM) based on Rotatable 2^3 -Factorial Central Composite Rotatable (2^3 -CCR) Design was employed to establish the relationship between color strength (i.e. the response function) and three of the most significant process variables obtained after screening. Statistica software, version 12, from Statsoft Inc., California, U.S.A., was used for design of experiment, analyses and optimization. A total of 20 experiments, including $2^3=8$ factorial points, 6 axial points and 6 center points, were performed five times each, and the average values of color strength were recorded in each case. The optimum values of the selected process variables were obtained by solving the regression model equations obtained in each case using the software and as per the equation 2.12 as mentioned in chapter 2.

5.3.1 Optimization with Disperse Yellow 56

Screening was done out of the five factors to identify the three most significant ones affecting color strength of PTT and PLA with Disperse Yellow 56. The real values of -1 and +1 levels for the five factors used in the normal probability plots for Disperse Yellow 56 with both PTT and PLA are given in Table 5.2, along with the notations and

units. With the three factors selected, optimization was done for PTT and PLA using RSM, as described in the following sections.

Table 5.2: Factors for normal probability plot of PTT with Disperse Yellow 56.

Factors	Notations	Units	Coded values	
			-1	1
			Real values	
Dyeing temperature	A, 1	°C	100	120
Dyeing time	B, 2	min	15	45
Initial pH	C, 3		5	7
Material to liquor ratio	D, 4		01:20	01:40
Rate of heating	E, 5	°C/min	1	3

Five experiments were carried out under each condition and the average values were used for deriving the normal probability plots in each case. With RSM also, five experiments were done in each run and the average values used for the contour plots.

5.3.1.1 Optimization for PTT

The normal probability plot with Disperse Yellow 56 applied on PTT is shown in Figure 5.44. It could be observed that points A, B and C were distinct outliers on the positive side from the cluster of points in the probability plot. Also, it could be seen that points 1x3 and 1x5 were also outliers with distinct negative effects.

It could thus be observed that the main effects of temperature (A, 1), time (B, 2) and initial pH (C, 3) were the more significant than the others affecting the color strength of PTT with Disperse Yellow 56. Also, the interaction effects between temperature (1) and initial pH (3) as well as temperature (1) and rate of heating (5) were more significant than the other factors and their interactions. The R^2 value of 0.99681 and adjusted R^2

value of 0.99381 indicated that the probability plot obtained was statistically significant with a high goodness of fit. It could thus be inferred that temperature, initial pH and time were the three most significant factors that could be used for optimization using RSM.

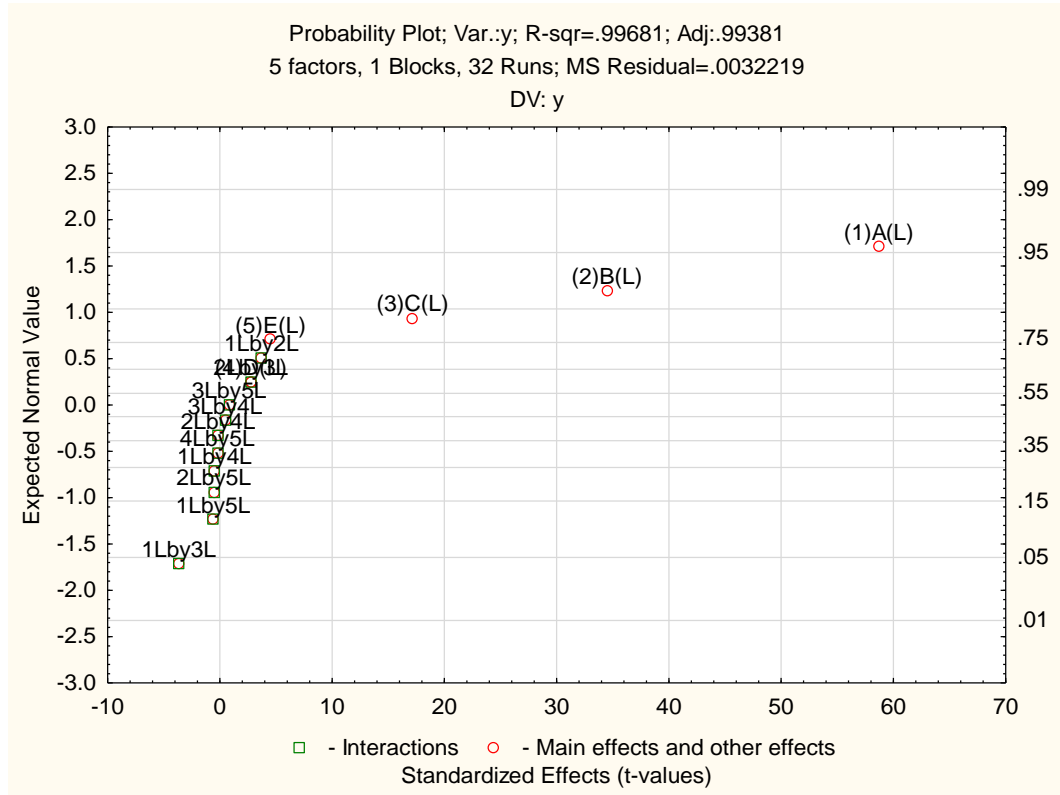


Figure 5.44: Normal probability plot of Disperse Yellow 56 applied on PTT.

With temperature, initial pH of dye bath and time, RSM was done for Disperse Yellow 56 with PTT. The levels of the factors were chosen as in Table 5.3 and the average values used are reported in Table 5.4. The contour plots obtained in the RSM are given in Figures 5.45, 5.46 and 5.47. The analysis of variance (ANOVA) for the factors of response is given in Table 5.5 and the same for the quadratic regression model in Table 5.6.

Table 5.3: Factors for RSM of PTT with Disperse Yellow 56.

Factors	Notations	Coded values				
		$-\alpha(-1.68)$	-1	0	1	$+\alpha(+1.68)$
		Real values				
Dyeing temperature ($^{\circ}\text{C}$)	A	103	110	120	130	137
Initial pH of dye bath	B	4	5	6	7	8
Dyeing time (min)	C	20	30	45	60	70

Table 5.4: Average values of experiments used for RSM.

Runs	Dyeing temperature	Initial pH	Dyeing time	Experimental values
	$^{\circ}\text{C}$		min	K/S
	A	B	C	y
1	-1.00	-1.00	-1.00	4.85
2	-1.00	-1.00	1.00	6.26
3	-1.00	1.00	-1.00	4.49
4	-1.00	1.00	1.00	6.03
5	1.00	-1.00	-1.00	5.26
6	1.00	-1.00	1.00	6.23
7	1.00	1.00	-1.00	4.79
8	1.00	1.00	1.00	5.93
9	-1.68	0.00	0.00	6.12
10	1.68	0.00	0.00	6.4
11	0.00	-1.68	0.00	5.89
12	0.00	1.68	0.00	5.12
13	0.00	0.00	-1.68	3.58
14	0.00	0.00	1.68	6.31
15	0.00	0.00	0.00	6.04
16	0.00	0.00	0.00	6.12
17	0.00	0.00	0.00	5.94
18	0.00	0.00	0.00	6.09
19	0.00	0.00	0.00	6.01
20	0.00	0.00	0.00	5.92

The empirical model equation obtained with the coded variables is as follows:

$$y = 6.02 + 0.08A + 0.07A^2 - 0.19B - 0.20B^2 + 0.71C - 0.39C^2 - 0.02AB - 0.11AC + 0.04BC \quad (5.1)$$

The optimal values were observed as 120°C for temperature, 5.6 for initial pH of dye bath and 58 min for dyeing time approximately. The predicted K/S value under these optimal conditions was 6.37.

It was seen from Table 5.5 that the factors A , B , B^2 , C , C^2 and AC were the most significant factors with p-values less than 0.05. While A and C have a positive effect on y , B , B^2 , C^2 and AC leave a negative effect on the same. Thus, temperature (A), initial pH (B) as well as time (C) had significant effects on K/S value, with the latter two having not only linear but quadratic effects. The interaction term of temperature and time was also found to be significant.

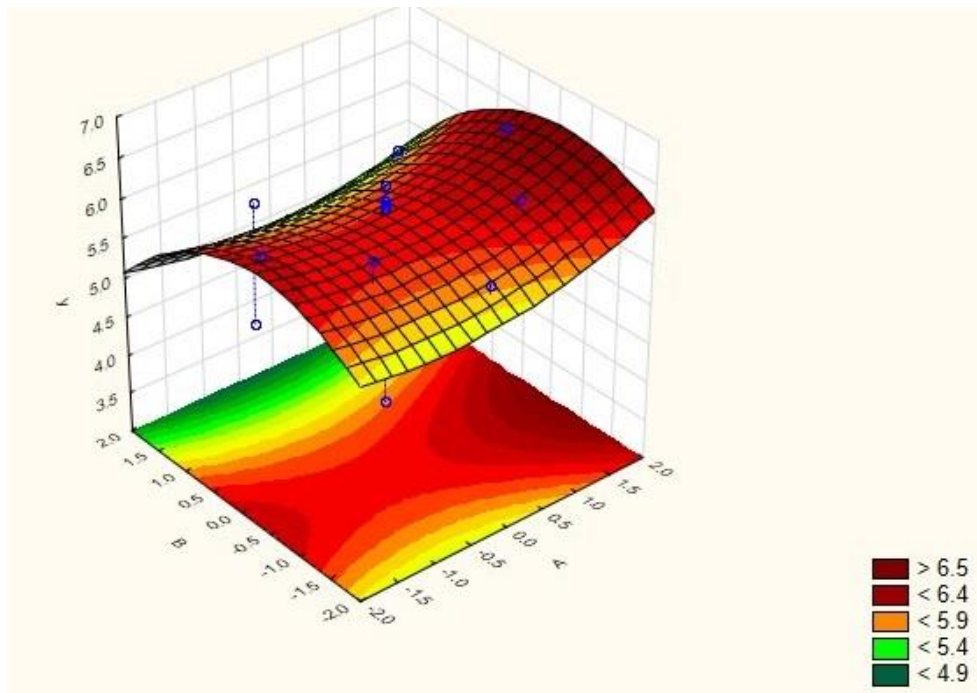


Figure 5.45: Contour plot for K/S value (y) with temperature (A) and initial pH of dye bath (B).

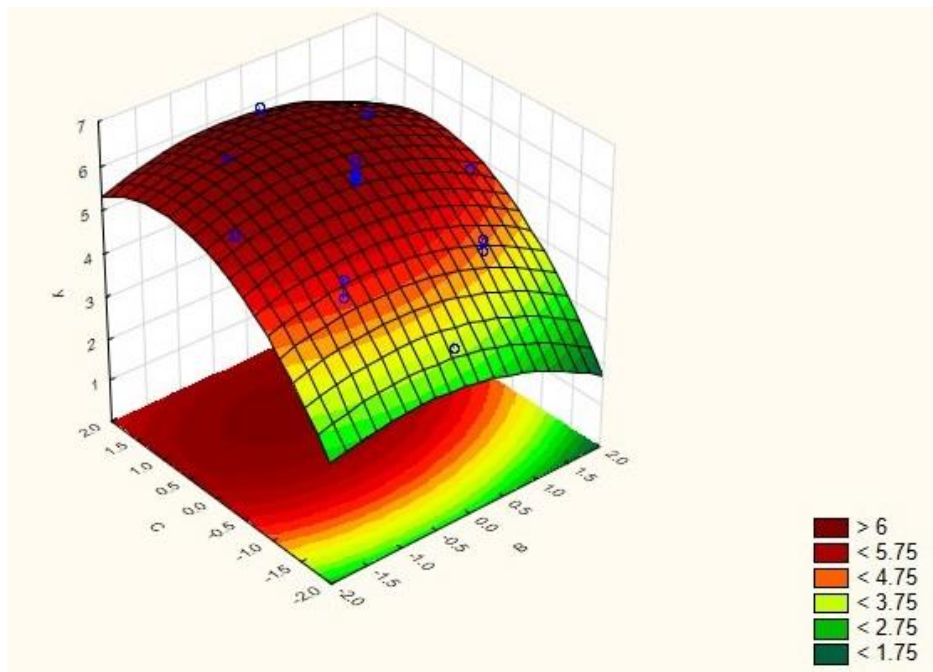


Figure 5.46: Contour plot for K/S value (y) with initial pH of dye bath (B) and time (C).

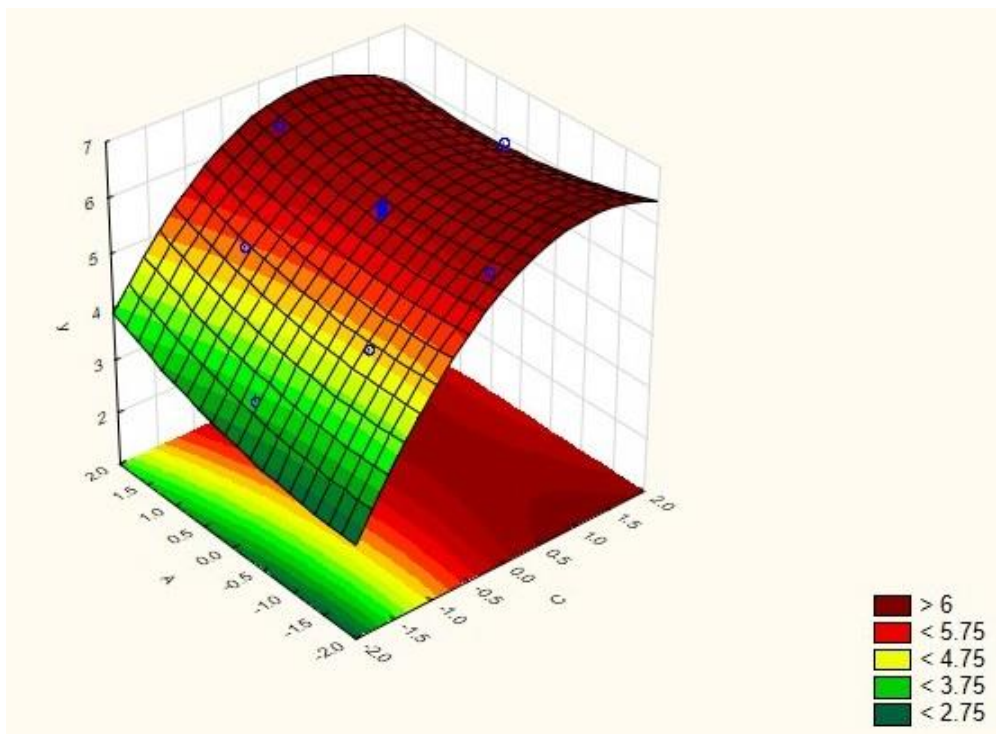


Figure 5.47: Contour plot for K/S value (y) with temperature (A) and time (C).

Table 5.5: Variance analysis (ANOVA) of factors on response.

Factors	Sum of Squares	Degrees of Freedom	Mean Square	F Value	p-Value Prob>F
<i>A</i>	0.08	1.00	0.08	4.97	0.05
<i>A</i> ²	0.07	1.00	0.07	4.54	0.06
<i>B</i>	0.52	1.00	0.52	31.71	0.00
<i>B</i> ²	0.55	1.00	0.55	33.77	0.00
<i>C</i>	6.82	1.00	6.82	419.01	0.00
<i>C</i> ²	2.23	1.00	2.23	136.95	0.00
<i>AxB</i>	0.00	1.00	0.00	0.25	0.63
<i>AxC</i>	0.09	1.00	0.09	5.42	0.04
<i>BxC</i>	0.01	1.00	0.01	0.69	0.43

Table 5.6: Variance analysis (ANOVA) of quadratic regression model.

Source	Sum of Squares	Degrees of Freedom	Mean Square	F Value	p-Value Prob>F
Model	10.34	9	1.15	38.33	0.00
Residual	0.16	10	0.03		
Lack of fit	0.13	5	0.03	4.12	0.07
Pure error	0.03	5	0.01		
Total	10.50	19			

From Table 5.6, it was observed that at 95% confidence level, the quadratic regression model developed was statistically significant with F-value of 38.33 that was much higher than the F-value of the lack of fit (4.12). The R^2 value was found to be 0.98449 indicating that 98.45% of the total variations could be explained by the developed model, and only 1.55% of the variations could not be explained. The adjusted

R^2 value of 0.97054 was reasonably close to the R^2 value, indicating a high goodness of fit for the developed model.

5.3.1.2 Optimization for PLA

The normal probability plot with Disperse Yellow 56 applied on PLA is shown in Figure 5.48. It could be observed that points A, B and C were distinct outliers with positive effects in the probability plot. Also, it could be seen that points 1x2 and 1x3 were also outliers with negative effects.

It could thus be inferred temperature (A, 1), time (B, 2) and initial pH (C, 3) was the most significant factors affecting the color strength of PLA with Disperse Yellow 56. Also, the interaction effects between temperature (1) and time (2) as well as temperature (1) and initial pH (3) were more significant than the other factors and their interactions. The R^2 value of 0.99966 and adjusted R^2 value of 0.99935 indicated that the probability plot obtained was statistically significant with a high goodness of fit.

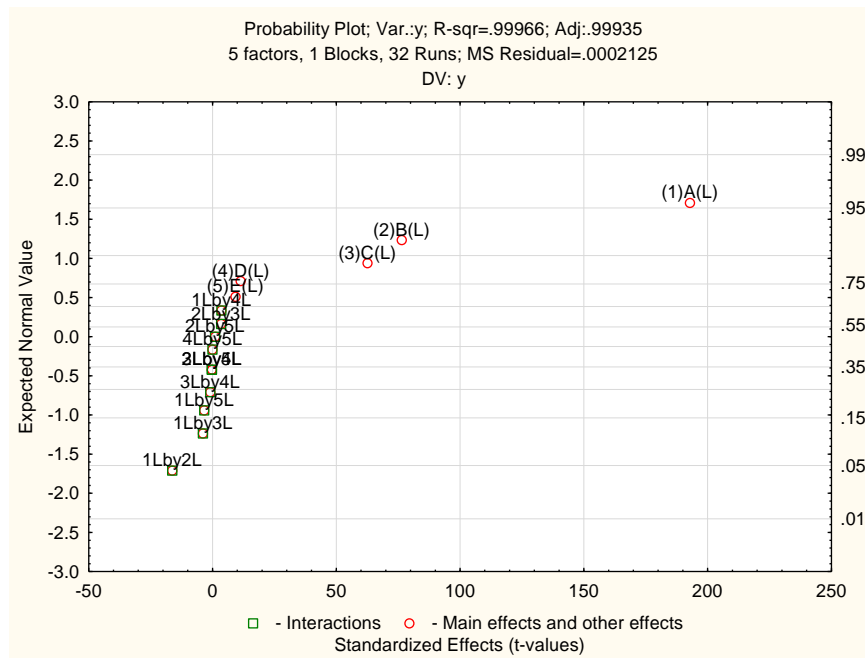


Figure 5.48: Normal probability plot of Disperse Yellow 56 applied on PLA.

Table 5.7: Factors for RSM of PLA with Disperse Yellow 56.

Factors	Notations	Coded values				
		$-\alpha(-1.68)$	-1	0	1	$+\alpha(+1.68)$
		Real values				
Dyeing temperature ($^{\circ}\text{C}$)	A	103	110	120	130	137
Initial pH	B	4	5	6	7	8
Dyeing time (min)	C	5	15	30	45	55

Table 5.8: Average values of experiments used for RSM.

Runs	Dyeing temperature	Initial pH	Dyeing time	Experimental values
	$^{\circ}\text{C}$		min	K/S
	A	B	C	y
1	-1.00	-1.00	-1.00	3.55
2	-1.00	-1.00	1.00	5.48
3	-1.00	1.00	-1.00	3.18
4	-1.00	1.00	1.00	5.24
5	1.00	-1.00	-1.00	4.79
6	1.00	-1.00	1.00	5.68
7	1.00	1.00	-1.00	4.34
8	1.00	1.00	1.00	5.24
9	-1.68	0.00	0.00	4.88
10	1.68	0.00	0.00	6.05
11	0.00	-1.68	0.00	3.79
12	0.00	1.68	0.00	3.02
13	0.00	0.00	-1.68	3.11
14	0.00	0.00	1.68	5.91
15	0.00	0.00	0.00	5.42
16	0.00	0.00	0.00	5.45
17	0.00	0.00	0.00	5.06
18	0.00	0.00	0.00	5.25
19	0.00	0.00	0.00	5.03
20	0.00	0.00	0.00	5.19

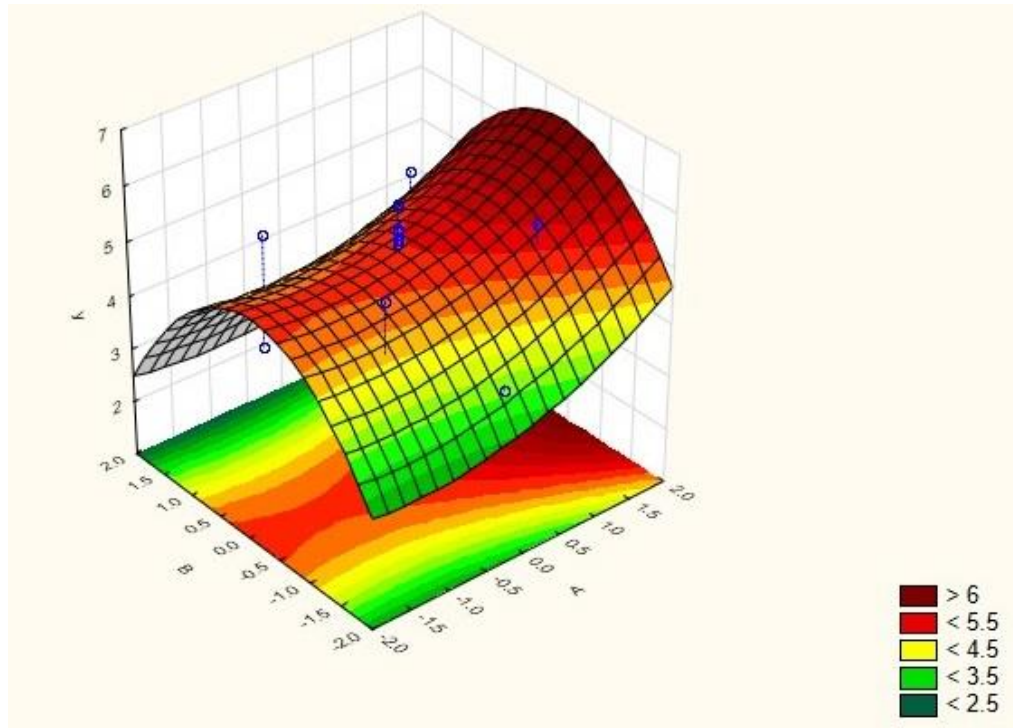


Figure 5.49: Contour plot for K/S value (y) with temperature (A) and initial pH of dye bath (B).

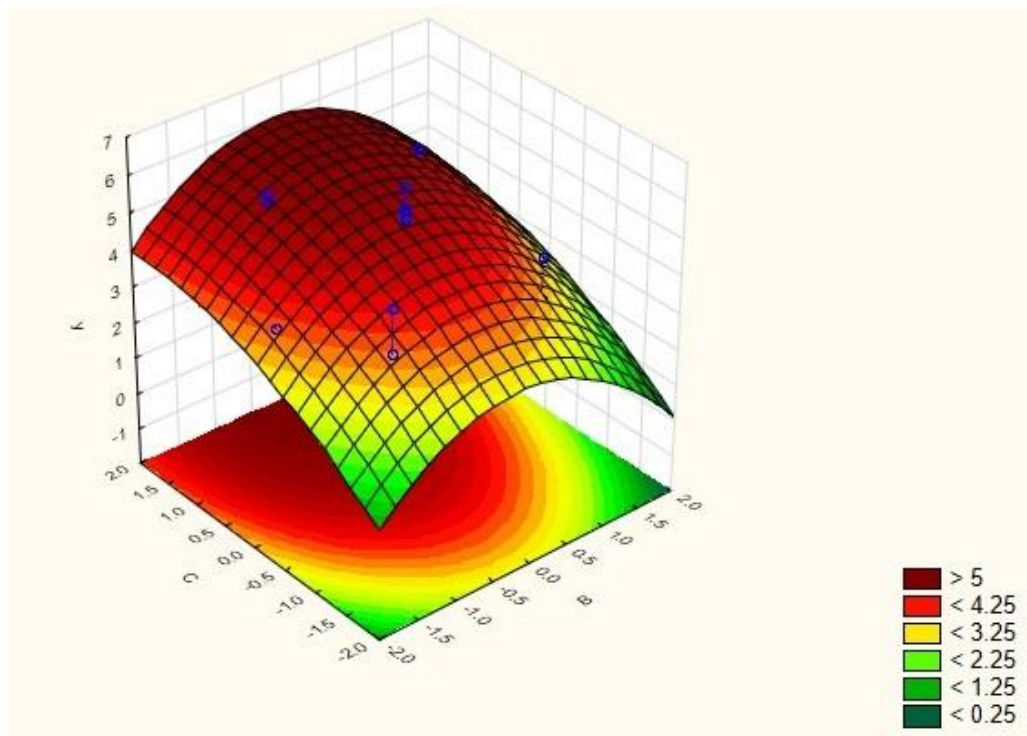


Figure 5.50: Contour plot for K/S value (y) with initial pH of dye bath (B) and time (C).

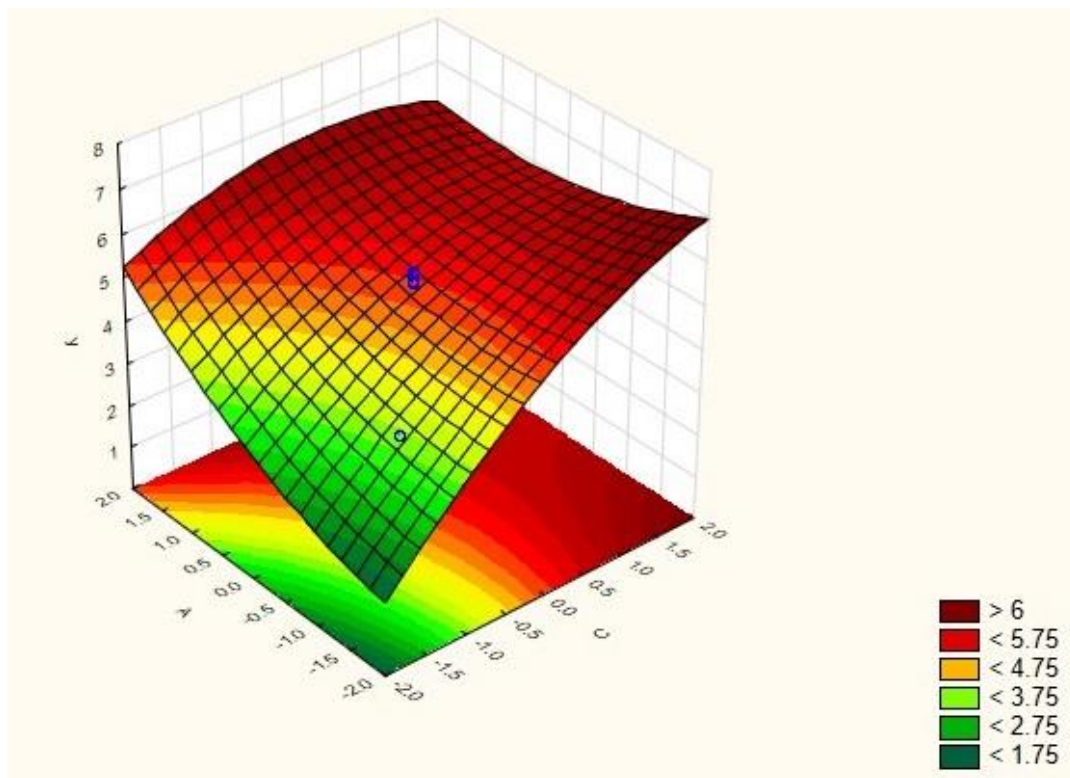


Figure 5.51: Contour plot for K/S value (y) with temperature (A) and time (C).

With temperature, initial pH of dye bath and time, RSM was done for Disperse Yellow 56 with PLA. The levels of the factors were chosen as in Table 5.7 and the average values reported in Table 5.8. The contour plots obtained in the RSM are given in Figures 5.49, 5.50 and 5.51. The analysis of variance (ANOVA) for the factors of response is given in Table 5.9 and the same for the quadratic regression model in Table 5.10.

The empirical model equation obtained with the coded variables is as follows:

$$y = 5.22 + 0.33A + 0.14A^2 - 0.20B - 0.59B^2 + 0.77C - 0.20C^2 - 0.04AB - 0.28AC + 0.02BC \quad (5.2)$$

The optimal values were observed as 124⁰C for temperature, 5.8 for initial pH of dye bath and 55 min for dyeing time approximately. The predicted K/S value under these optimal conditions was 5.94.

It was seen from Table 5.9 that the factors A , A^2 , B , B^2 , C , C^2 and AC were the most significant factors with p-values less than 0.05. While A , A^2 and C have positive effects on y , B , B^2 , C^2 and AC have negative effects on the same. Thus, temperature (A), initial pH (B) as well as time (C) had significant linear as well as quadratic effects on K/S value. The interaction term of temperature and time was also found to be significant.

Table 5.9: Variance analysis (ANOVA) of factors on response.

Factors	Sum of Squares	Degrees of Freedom	Mean Square	F Value	p-Value Prob>F
A	1.53	1.00	1.53	34.32	0.00
A^2	0.28	1.00	0.28	6.33	0.03
B	0.57	1.00	0.57	12.85	0.00
B^2	4.99	1.00	4.99	112.14	0.00
C	8.06	1.00	8.06	180.99	0.00
C^2	0.56	1.00	0.56	12.67	0.01
AxB	0.01	1.00	0.01	0.22	0.65
AxC	0.61	1.00	0.61	13.59	0.00
BxC	0.00	1.00	0.00	0.06	0.82

From Table 5.10, it was observed that at 95% confidence level, the quadratic regression model developed was statistically significant with F-value of 41.11 that was much higher than the F-value of the lack of fit (1.87). The R^2 value was found to be 0.97404 indicating that 97.40% of the total variations could be explained by the

developed model, and only 2.60% of the variations could not be explained. The adjusted R^2 value of 0.95067 was reasonably close to the R^2 value, indicating a high goodness of fit for the developed model.

Table 5.10: Variance analysis (ANOVA) of quadratic regression model.

Source	Sum of Squares	Degrees of Freedom	Mean Square	F Value	p-Value Prob>F
Model	16.69	9	1.85	41.11	0.00
Residual	0.45	10	0.03		
Lack of fit	0.29	5	0.06	1.87	0.26
Pure error	0.16	5	0.03		
Total	17.14	19			

5.3.2 Optimization with Disperse Blue 79

The real values of -1 and +1 levels for the five factors used in the normal probability plots for Disperse Blue 79 with both PTT and PLA were the same as used for Disperse Yellow 56, as mentioned in Table 5.2, along with the notations and units.

5.3.2.1 Optimization for PTT

The normal probability plot with Disperse Blue 79 applied on PTT is shown in Figure 5.52. It could be observed that points A, B and C were distinct outliers with positive effects in the probability plot. Also, it could be seen that points 3x5 was also an outlier on the negative side

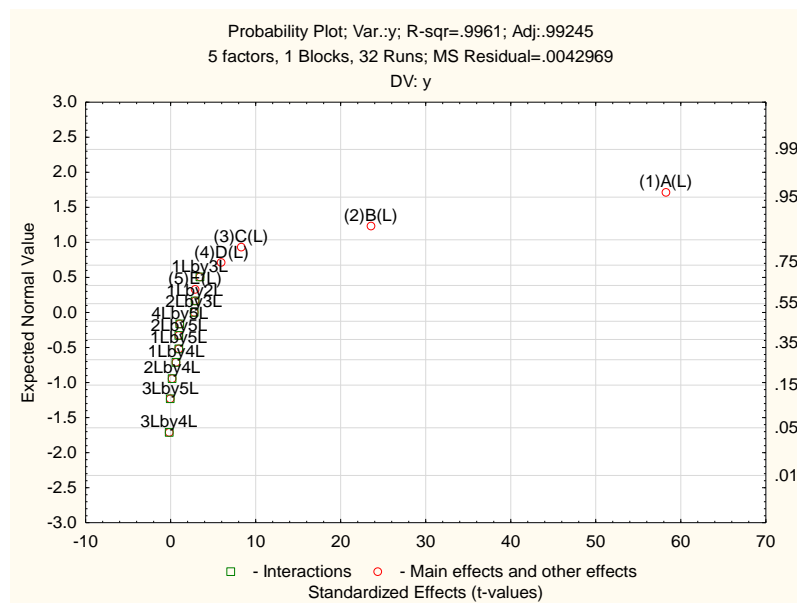


Figure 5.52: Normal probability plot of Disperse Blue 79 applied on PTT.

. It could thus be inferred temperature (A, 1), time (B, 2) and initial pH (C, 3) was the most significant factors affecting the color strength of PTT with Disperse Blue 79. Also, the interaction effects between initial pH (3) and rate of heating was more significant than the other factors and their interactions. The R^2 value of 0.9961 and adjusted R^2 value of 0.99245 indicated that the probability plot obtained was statistically significant with a high goodness of fit.

With temperature, initial pH of dye bath and time, RSM was done for Disperse Blue 79 with PTT. The levels of the factors chosen were the same for Disperse Yellow 56 as given in Table 5.3 and the average values reported in Table 5.11. The contour plots obtained in the RSM are given in Figures 5.53, 5.54 and 5.55. The analysis of variance (ANOVA) for the factors of response is given in Table 5.12 and the same for the quadratic regression model in Table 5.13.

Table 5.11: Average values of experiments used for RSM.

Runs	Dyeing temperature	Initial pH	Dyeing time	Experimental values
	^o C		min	K/S
	A	B	C	y
1	-1.00	-1.00	-1.00	4.15
2	-1.00	-1.00	1.00	5.84
3	-1.00	1.00	-1.00	4.08
4	-1.00	1.00	1.00	5.73
5	1.00	-1.00	-1.00	4.81
6	1.00	-1.00	1.00	5.93
7	1.00	1.00	-1.00	4.37
8	1.00	1.00	1.00	5.52
9	-1.68	0.00	0.00	5.79
10	1.68	0.00	0.00	5.98
11	0.00	-1.68	0.00	5.47
12	0.00	1.68	0.00	4.85
13	0.00	0.00	-1.68	3.14
14	0.00	0.00	1.68	5.92
15	0.00	0.00	0.00	5.64
16	0.00	0.00	0.00	5.79
17	0.00	0.00	0.00	5.49
18	0.00	0.00	0.00	5.75
19	0.00	0.00	0.00	5.61
20	0.00	0.00	0.00	5.53

The empirical model equation obtained with the coded variables is as follows:

$$y = 5.64 + 0.08A + 0.06A^2 - 0.15B - 0.19B^2 + 0.75C - 0.41C^2 - 0.08AB - 0.13AC + 0.001BC \quad (5.3)$$

The optimal values were observed as 120^oC for temperature, 5.6 for initial pH of dye bath and 59 min for dyeing time approximately. The predicted K/S value under these optimal conditions was 6.01.

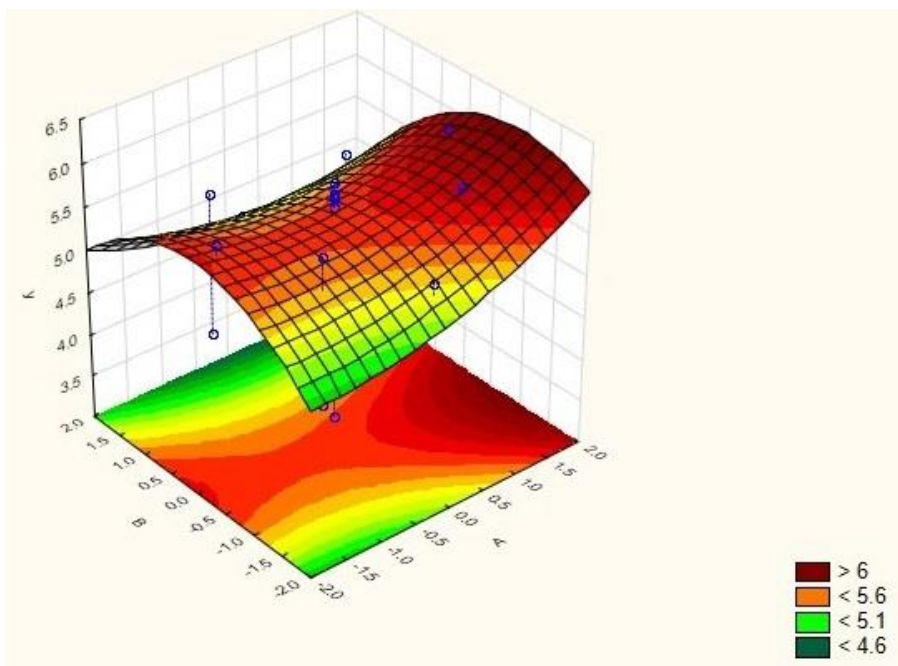


Figure 5.53: Contour plot for K/S value (y) with temperature (A) and initial pH of dye bath (B).

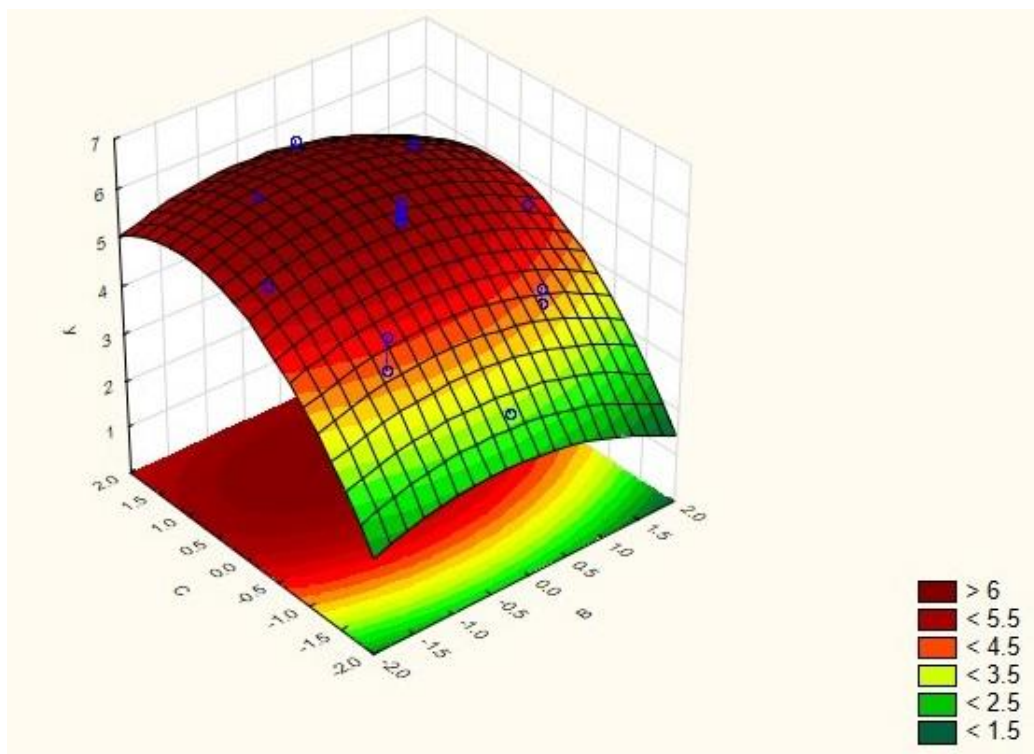


Figure 5.54: Contour plot for K/S value (y) with initial pH of dye bath (B) and time (C).

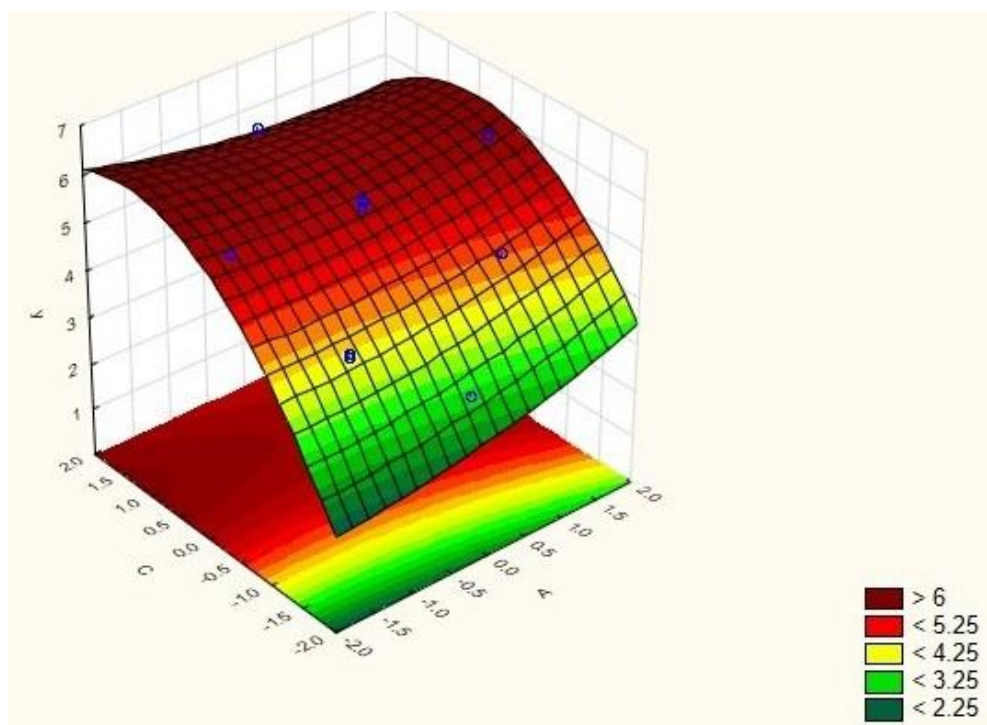


Figure 5.55: Contour plot for K/S value (y) with temperature (A) and time (C).

It was seen from Table 5.12 that the factors A , B , B^2 , C , C^2 and AC were the most significant factors with p -values less than 0.05. While A and C leave positive effects on y , B , B^2 , C^2 and AC have negative effects. Thus, temperature (A), initial pH (B) as well as time (C) had significant linear effects on K/S value, with the latter two also having significant quadratic effects. The interaction term of temperature and time was also found to be significant.

Table 5.12: Variance analysis (ANOVA) of factors on response.

Factors	Sum of Squares	Degrees of Freedom	Mean Square	F Value	p-Value Prob>F
<i>A</i>	0.10	1.00	0.10	5.39	0.04
<i>A</i> ²	0.06	1.00	0.06	3.39	0.10
<i>B</i>	0.31	1.00	0.31	17.52	0.00
<i>B</i> ²	0.53	1.00	0.53	29.39	0.00
<i>C</i>	7.75	1.00	7.75	431.42	0.00
<i>C</i> ²	2.47	1.00	2.47	137.64	0.00
<i>AxB</i>	0.06	1.00	0.06	3.13	0.11
<i>AxC</i>	0.14	1.00	0.14	7.97	0.02
<i>BxC</i>	0.00	1.00	0.00	0.00	0.98

Table 5.13: Variance analysis (ANOVA) of quadratic regression model.

Source	Sum of Squares	Degrees of Freedom	Mean Square	F Value	p-Value Prob>F
Model	11.37	9	1.26	70.00	0.00
Residual	0.18	10	0.02		
Lack of fit	0.11	5	0.02	1.57	0.32
Pure error	0.07	5	0.01		
Total	11.55	19			

From Table 5.13, it was observed that at 95% confidence level, the quadratic regression model developed was statistically significant with F-value of 70.00 that was much higher than the F-value of the lack of fit (1.57). The R^2 value was found to be 0.98445 indicating that 98.45% of the total variations could be explained by the developed model, and only 1.55% of the variations could not be explained. The adjusted

R^2 value of 0.97045 was reasonably close to the R^2 value, indicating a high goodness of fit for the developed model.

5.3.2.2 Optimization for PLA

The normal probability plot with Disperse Blue 79 applied on PTT is shown in Figure 5.56. It could be observed that points A and B were distinct outliers with positive effects in the probability plot. Also, it could be seen that point 2x5 was also an outlier on the negative side.

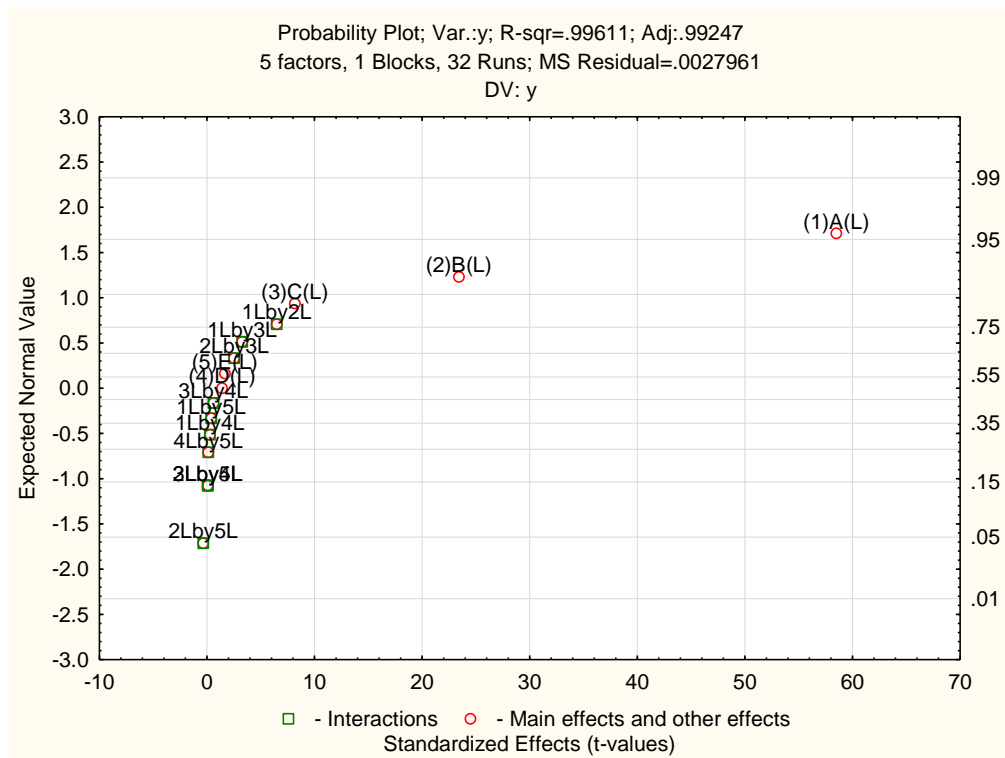


Figure 5.56: Normal probability plot of Disperse Blue 79 applied on PLA.

It could thus be inferred temperature (A, 1) and time (B, 2) was the most significant factors affecting the color strength of PTT with Disperse Blue 79. Also, the interaction effects between time (2) and rate of heating (5) was more significant than the other factors and their interactions. The R^2 value of 0.99611 and adjusted R^2 value of

0.99247 indicated that the probability plot obtained was statistically significant with a high goodness of fit.

Table 5.14: Average values of experiments used for RSM.

Runs	Dyeing temperature	Initial pH	Dyeing time	Experimental values
	$^{\circ}\text{C}$		min	K/S
	A	B	C	y
1	-1.00	-1.00	-1.00	3.65
2	-1.00	-1.00	1.00	5.33
3	-1.00	1.00	-1.00	3.59
4	-1.00	1.00	1.00	5.21
5	1.00	-1.00	-1.00	4.34
6	1.00	-1.00	1.00	5.45
7	1.00	1.00	-1.00	3.88
8	1.00	1.00	1.00	4.99
9	-1.68	0.00	0.00	5.31
10	1.68	0.00	0.00	5.49
11	0.00	-1.68	0.00	4.97
12	0.00	1.68	0.00	4.36
13	0.00	0.00	-1.68	2.65
14	0.00	0.00	1.68	5.43
15	0.00	0.00	0.00	5.15
16	0.00	0.00	0.00	5.32
17	0.00	0.00	0.00	5.01
18	0.00	0.00	0.00	5.28
19	0.00	0.00	0.00	5.16
20	0.00	0.00	0.00	5.07

With temperature, initial pH of dye bath and time, RSM was done for Disperse Blue 79 with PLA. The levels of the factors chosen were the same for Disperse Yellow 56 as given in Table 5.7 and the average values reported in Table 5.14. The contour plots obtained in the RSM are given in Figures 5.57, 5.58 and 5.59. The analysis of variance

(ANOVA) for the factors of response is given in Table 5.15 and the same for the quadratic regression model in Table 5.16.

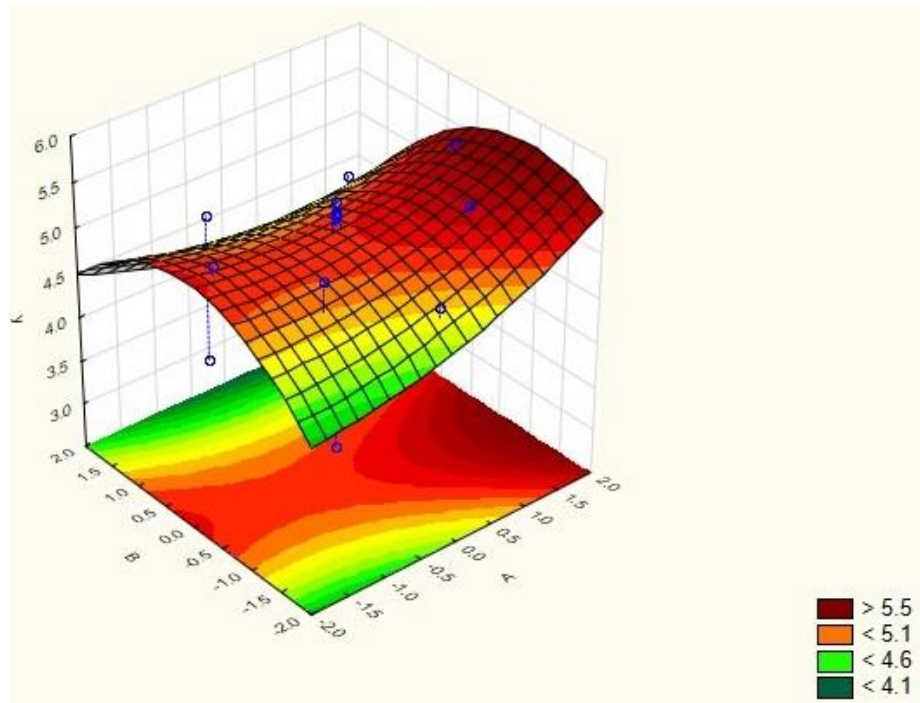


Figure 5.57: Contour plot for K/S value (y) with temperature (A) and initial pH of dye bath (B).

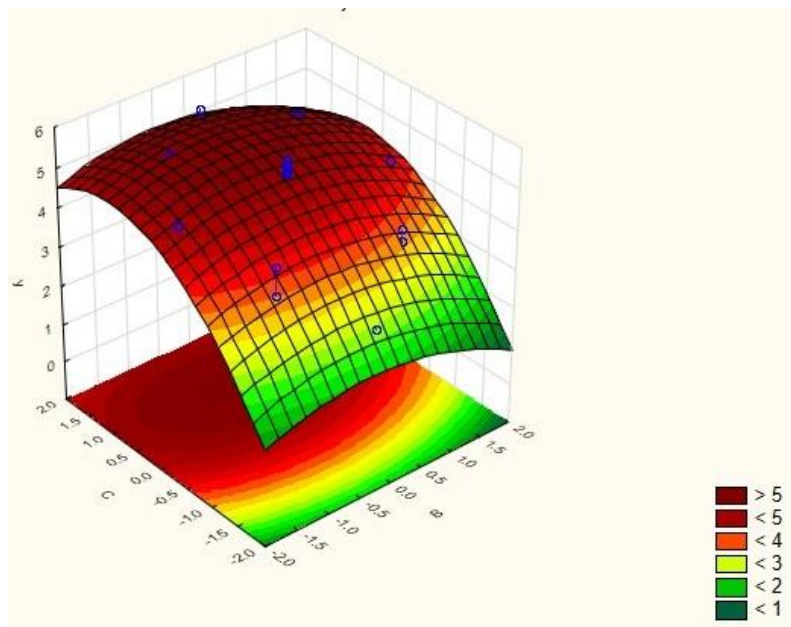


Figure 5.58: Contour plot for K/S value (y) with initial pH of dye bath (B) and time (C).

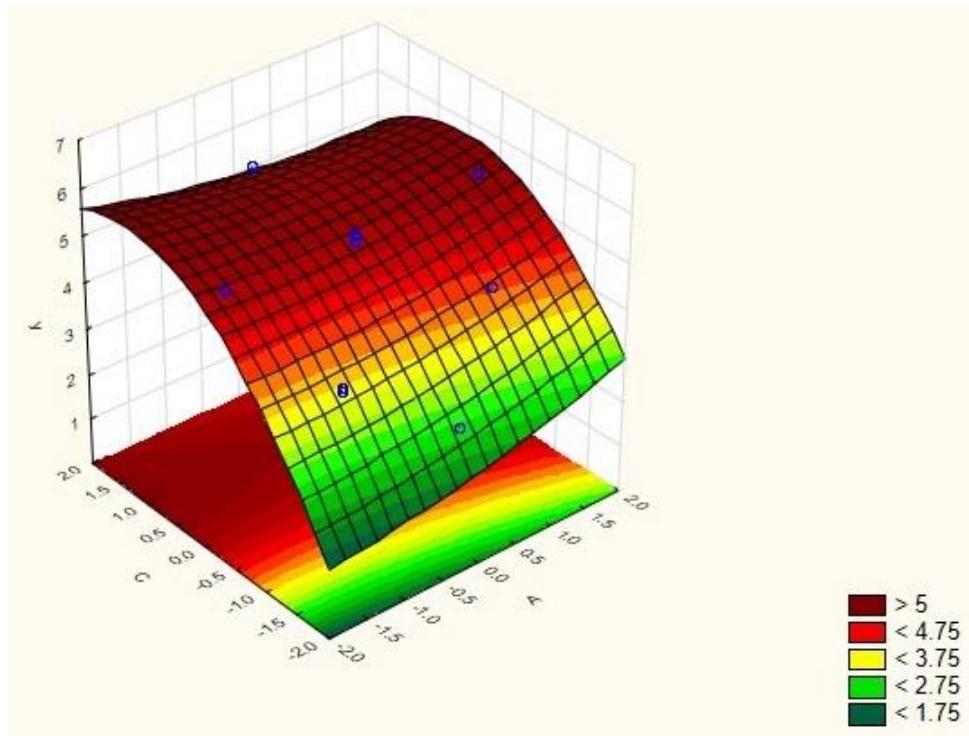


Figure 5.59: Contour plot for K/S value (y) with temperature (A) and time (C).

Table 5.15: Variance analysis (ANOVA) of factors on response.

Factors	Sum of Squares	Degrees of Freedom	Mean Square	F Value	p-Value Prob>F
A	0.10	1.00	0.10	5.26	0.04
A^2	0.05	1.00	0.05	2.50	0.15
B	0.33	1.00	0.33	17.01	0.00
B^2	0.59	1.00	0.59	30.16	0.00
C	7.61	1.00	7.61	391.16	0.00
C^2	2.58	1.00	2.58	132.38	0.00
AxB	0.07	1.00	0.07	3.52	0.09
AxC	0.15	1.00	0.15	7.49	0.02
BxC	0.00	1.00	0.00	0.02	0.88

The empirical model equation obtained with the coded variables is as follows:

$$y = 5.17 + 0.09A + 0.06A^2 - 0.16B - 0.20B^2 + 0.75C - 0.42C^2 - 0.09AB - 0.14AC + 0.007BC \quad (5.4)$$

The optimal values were observed as 120⁰C for temperature, 5.6 for initial pH of dye bath and 43 min for dyeing time approximately. The predicted K/S value under these optimal conditions was 5.53.

It was seen from Table 5.15 that the factors *A*, *B*, *B*², *C*, *C*² and *AC* were the most significant factors with p-values less than 0.05. The factors *A* and *C* had a positive impact on *y* while *B*, *B*², *C*² and *AC* had negative influences. Thus, temperature (*A*), initial pH (*B*) as well as time (*C*) had significant linear effects on K/S value, with the latter two also having significant quadratic effects. The interaction term of temperature and time was also found to be significant.

Table 5.16: Variance analysis (ANOVA) of quadratic regression model.

Source	Sum of Squares	Degrees of Freedom	Mean Square	F Value	p-Value Prob>F
Model	11.40	9	1.27	63.50	0.00
Residual	0.19	10	0.02		
Lack of fit	0.12	5	0.025	1.758	0.275
Pure error	0.07	5	0.014		
Total	11.59	19			

From Table 5.16, it was observed that at 95% confidence level, the quadratic regression model developed was statistically significant with F-value of 63.50 that was much higher than the F-value of the lack of fit (1.758). The R² value was found to be 0.98322 indicating that 98.32% of the total variations could be explained by the

developed model, and only 1.68% of the variations could not be explained. The adjusted R^2 value of 0.96811 was reasonably close to the R^2 value, indicating a high goodness of fit for the developed model.

5.3.3 Optimization with Disperse Red 167

5.3.3.1 Optimization for PTT

The normal probability plot with Disperse Red 167 applied on PTT is shown in Figure 5.60. It could be observed that points A, B and C were distinct outliers with positive effects in the probability plot. Also, it could be seen that point 2x3 was also an outlier on the negative side.

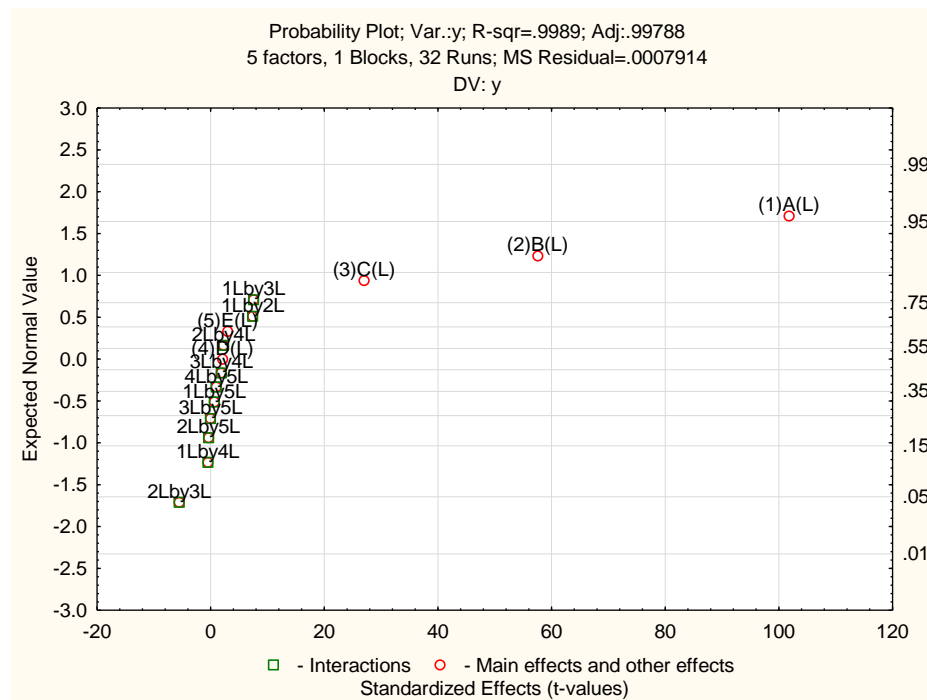


Figure 5.60: Normal probability plot of Disperse Red 167 applied on PTT.

It could thus be inferred temperature (A, 1), time (B, 2) and initial pH (C, 3) was the most significant factors affecting the color strength of PTT with Disperse Red 167. Also, the interaction effects between time (2) and initial pH (3) was more significant than the other factors and their interactions. The R^2 value of 0.9989 and adjusted R^2 value of

0.99788 indicated that the probability plot obtained was statistically significant with a high goodness of fit.

Table 5.17: Average values of experiments used for RSM.

Runs	Dyeing temperature	Initial pH	Dyeing time	Experimental values
	$^{\circ}\text{C}$		min	K/S
	A	B	C	y
1	-1.00	-1.00	-1.00	4.34
2	-1.00	-1.00	1.00	6.01
3	-1.00	1.00	-1.00	4.25
4	-1.00	1.00	1.00	5.91
5	1.00	-1.00	-1.00	4.99
6	1.00	-1.00	1.00	6.15
7	1.00	1.00	-1.00	4.56
8	1.00	1.00	1.00	5.71
9	-1.68	0.00	0.00	5.95
10	1.68	0.00	0.00	6.15
11	0.00	-1.68	0.00	5.63
12	0.00	1.68	0.00	5.04
13	0.00	0.00	-1.68	3.35
14	0.00	0.00	1.68	6.11
15	0.00	0.00	0.00	5.81
16	0.00	0.00	0.00	5.95
17	0.00	0.00	0.00	5.67
18	0.00	0.00	0.00	5.93
19	0.00	0.00	0.00	5.79
20	0.00	0.00	0.00	5.72

With temperature, initial pH of dye bath and time, RSM was done for Disperse Red 167 with PTT. The levels of the factors chosen were the same for Disperse Yellow 56 as given in Table 5.3 and the average values reported in Table 5.17. The contour plots obtained in the RSM are given in Figures 5.61, 5.62 and 5.63. The analysis of variance

(ANOVA) for the factors of response is given in Table 5.18 and the same for the quadratic regression model in Table 5.19.

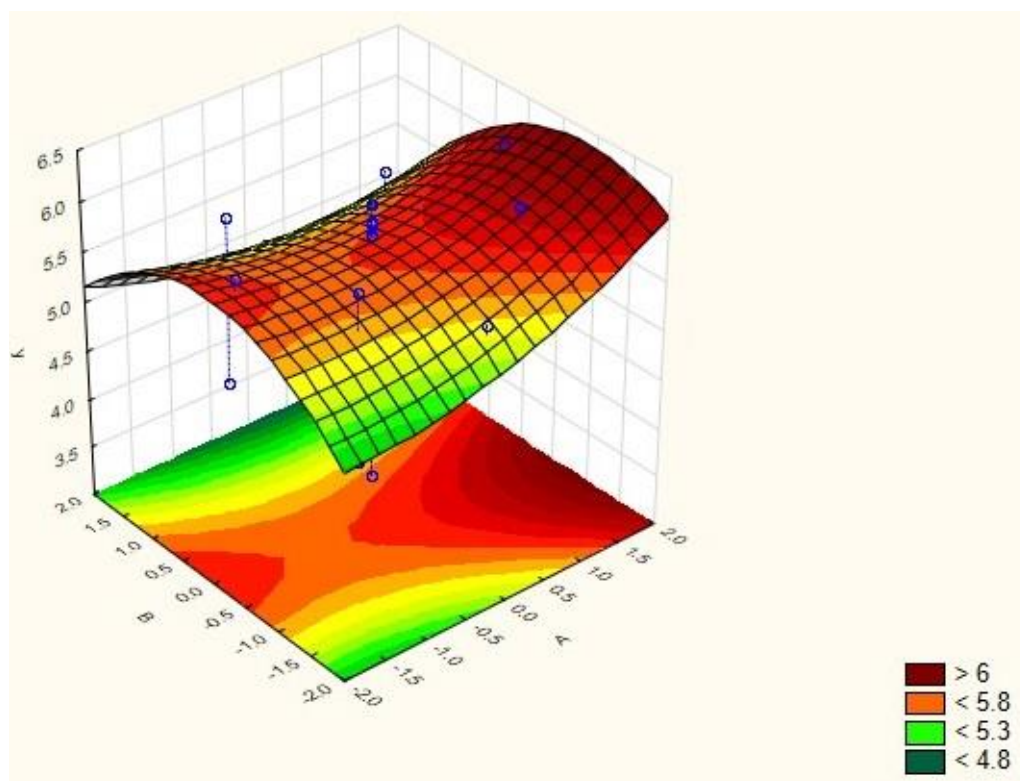


Figure 5.61: Contour plot for K/S value (y) with temperature (A) and initial pH of dye bath (B).

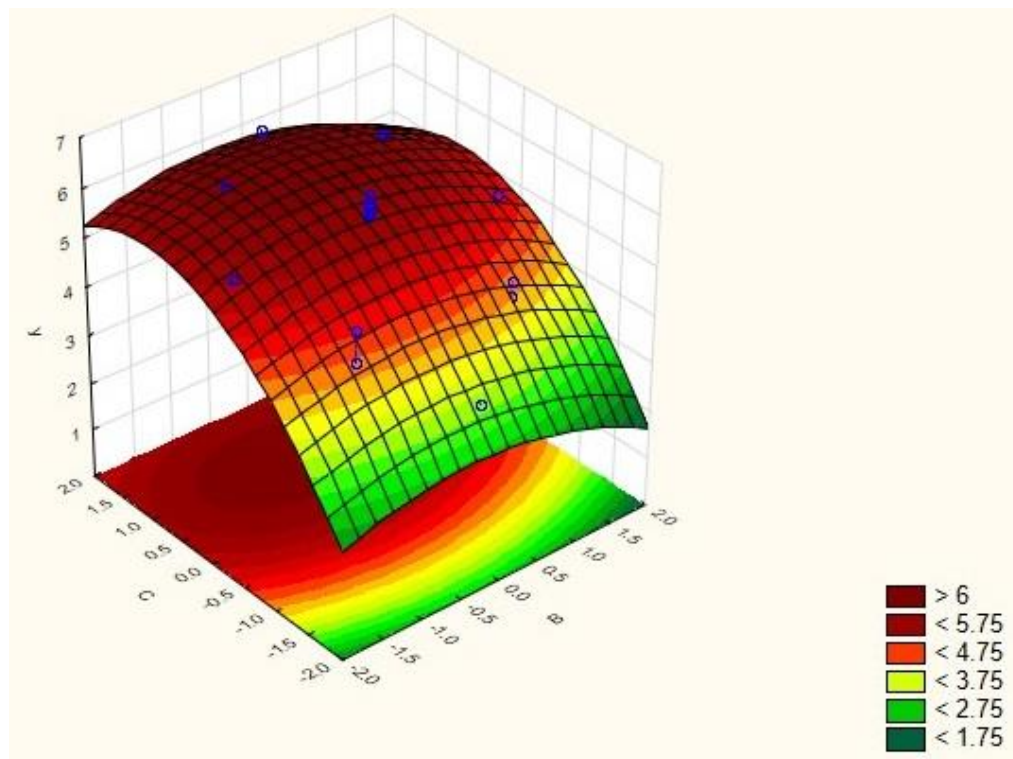


Figure 5.62: Contour plot for K/S value (y) with initial pH of dye bath (B) and time (C).

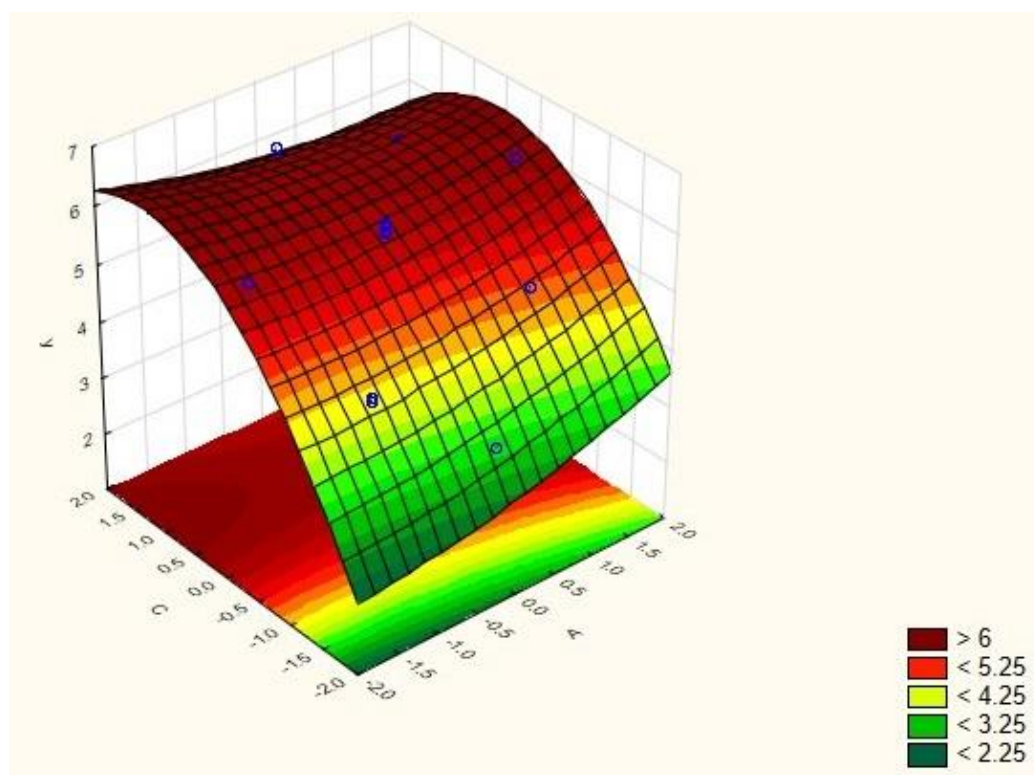


Figure 5.63: Contour plot for K/S value (y) with temperature (A) and time (C).

The empirical model equation obtained with the coded variables is as follows:

$$y = 5.82 + 0.09A + 0.06A^2 - 0.15B - 0.19B^2 + 0.75C - 0.41C^2 - 0.09AB - 0.13AC + 0.003BC \quad (5.5)$$

The optimal values were observed as 120⁰C for temperature, 5.6 for initial pH of dye bath and 59 min for dyeing time approximately. The predicted K/S value under these optimal conditions was 6.19.

It was seen from Table 5.18 that the factors A , B , B^2 , C , C^2 and AC were the most significant factors with p-values less than 0.05. While the factors A and C had positive influences, the others left negative impacts on y . Thus, temperature (A), initial pH (B) as well as time (C) had significant linear effects on K/S value, with the latter two also having significant quadratic effects. The interaction term of temperature and time was also found to be significant.

Table 5.18: Variance analysis (ANOVA) of factors on response.

Factors	Sum of Squares	Degrees of Freedom	Mean Square	F Value	p-Value Prob>F
<i>A</i>	0.11	1.00	0.11	7.13	0.02
<i>A</i> ²	0.06	1.00	0.06	3.54	0.09
<i>B</i>	0.31	1.00	0.31	19.65	0.00
<i>B</i> ²	0.52	1.00	0.52	33.39	0.00
<i>C</i>	7.74	1.00	7.74	493.21	0.00
<i>C</i> ²	2.36	1.00	2.36	150.30	0.00
<i>AxB</i>	0.06	1.00	0.06	3.68	0.08
<i>AxC</i>	0.13	1.00	0.13	8.29	0.02
<i>BxC</i>	0.00	1.00	0.00	0.00	0.96

Table 5.19: Variance analysis (ANOVA) of quadratic regression model.

Source	Sum of Squares	Degrees of Freedom	Mean Square	F Value	p-Value Prob>F
Model	11.24	9	1.25	83.26	0.00
Residual	0.15	10	0.015		
Lack of fit	0.09	5	0.019	1.528	0.327
Pure error	0.06	5	0.012		
Total	11.39	19			

From Table 5.19, it was observed that at 95% confidence level, the quadratic regression model developed was statistically significant with F-value of 83.26 that was much higher than the F-value of the lack of fit (1.528). The R^2 value was found to be 0.98622 indicating that 98.62% of the total variations could be explained by the developed model, and only 1.38% of the variations could not be explained. The adjusted

R^2 value of 0.97382 was reasonably close to the R^2 value, indicating a high goodness of fit for the developed model.

5.3.3.2 Optimization for PLA

The normal probability plot with Disperse Red 167 applied on PLA is shown in Figure 5.64. It could be observed that points A, B and C were distinct outliers with positive effects in the probability plot. Also, it could be seen that point 2x3 was also an outlier on the negative side.

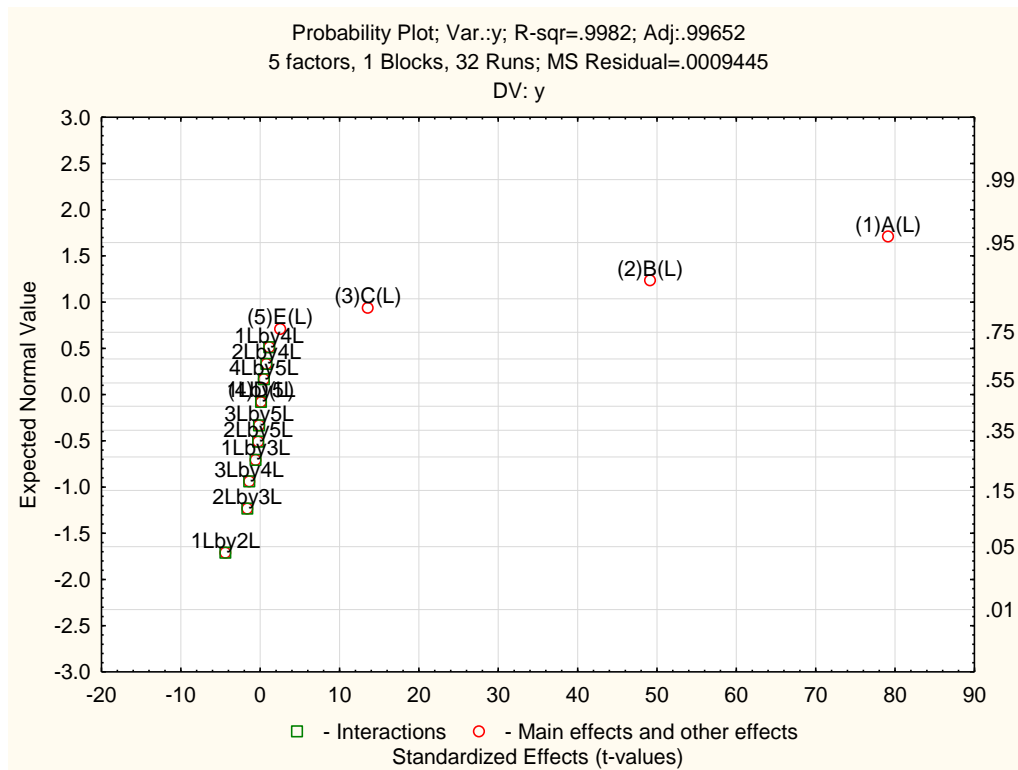


Figure 5.64: Normal probability plot of Disperse Red 167 applied on PLA.

It could thus be inferred temperature (A, 1), time (B, 2) and initial pH (C, 3) was the most significant factors affecting the color strength of PTT with Disperse Red 167. Also, the interaction effects between time (2) and initial pH (3) was more significant than the other factors and their interactions. The R^2 value of 0.9989 and adjusted R^2 value of

0.99788 indicated that the probability plot obtained was statistically significant with a high goodness of fit.

With temperature, initial pH of dye bath and time, RSM was done for Disperse Red 167 with PLA. The levels of the factors chosen were the same for Disperse Yellow 56 as given in Table 5.7 and the average values reported in Table 5.20. The contour plots obtained in the RSM are given in Figures 5.65, 5.66 and 5.67. The analysis of variance (ANOVA) for the factors of response is given in Table 5.21 and the same for the quadratic regression model in Table 5.22.

Table 5.20: Average values of experiments used for RSM.

Runs	Dyeing temperature	Initial pH	Dyeing time	Experimental values
	^o C		min	K/S
	A	B	C	y
1	-1.00	-1.00	-1.00	4.34
2	-1.00	-1.00	1.00	6.01
3	-1.00	1.00	-1.00	4.25
4	-1.00	1.00	1.00	5.91
5	1.00	-1.00	-1.00	4.99
6	1.00	-1.00	1.00	6.15
7	1.00	1.00	-1.00	4.56
8	1.00	1.00	1.00	5.71
9	-1.68	0.00	0.00	5.95
10	1.68	0.00	0.00	6.15
11	0.00	-1.68	0.00	5.63
12	0.00	1.68	0.00	5.04
13	0.00	0.00	-1.68	3.35
14	0.00	0.00	1.68	6.11
15	0.00	0.00	0.00	5.81
16	0.00	0.00	0.00	5.95
17	0.00	0.00	0.00	5.67
18	0.00	0.00	0.00	5.93
19	0.00	0.00	0.00	5.79
20	0.00	0.00	0.00	5.72

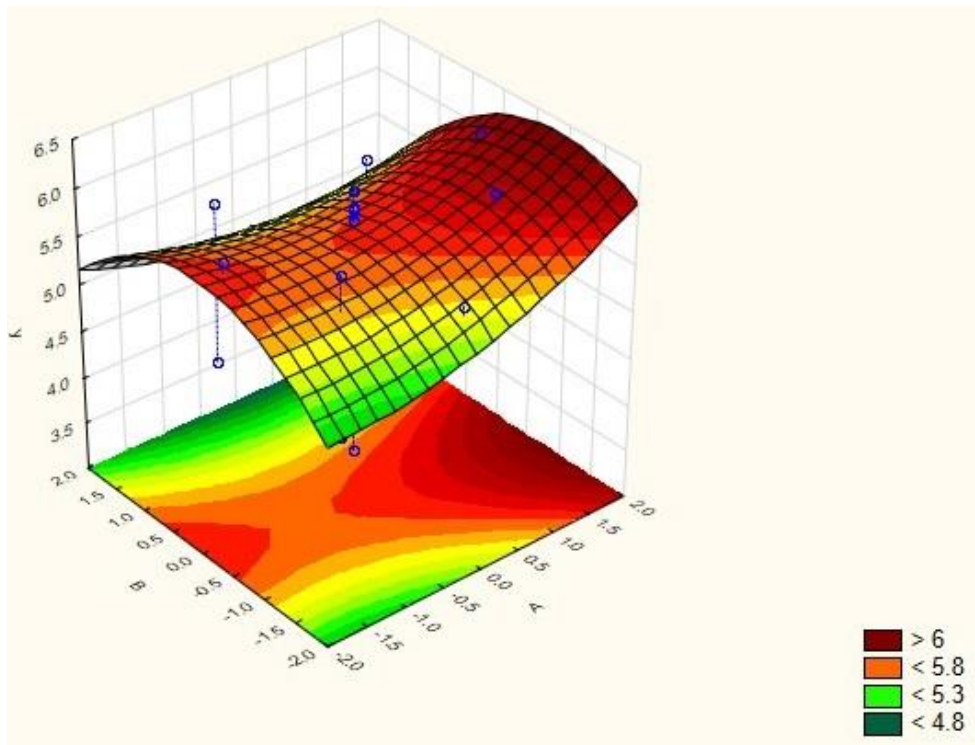


Figure 5.65: Contour plot for K/S value (y) with temperature (A) and initial pH of dye bath (B).

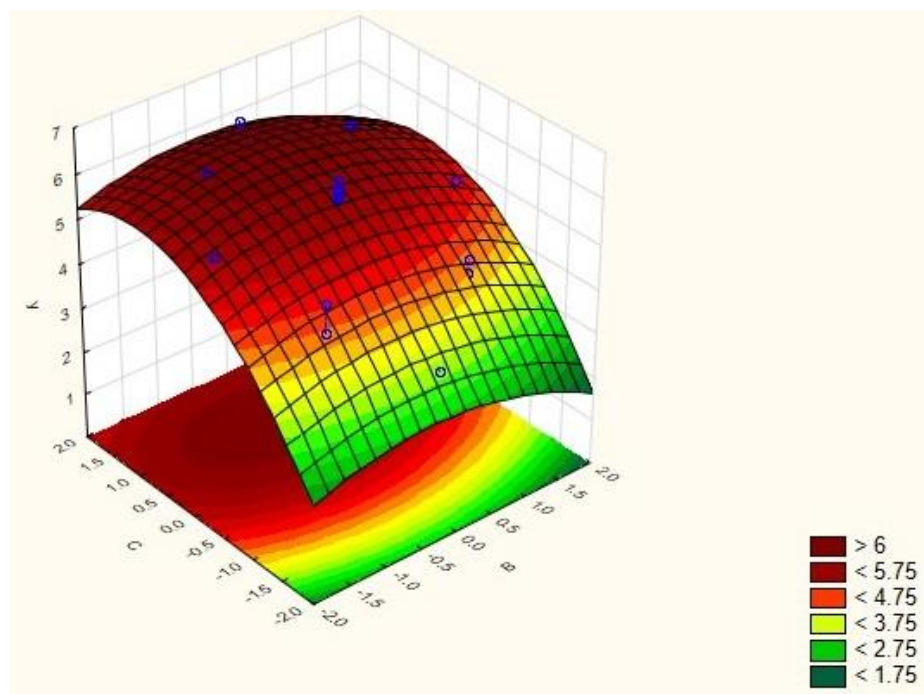


Figure 5.66: Contour plot for K/S value (y) with initial pH of dye bath (B) and time (C).

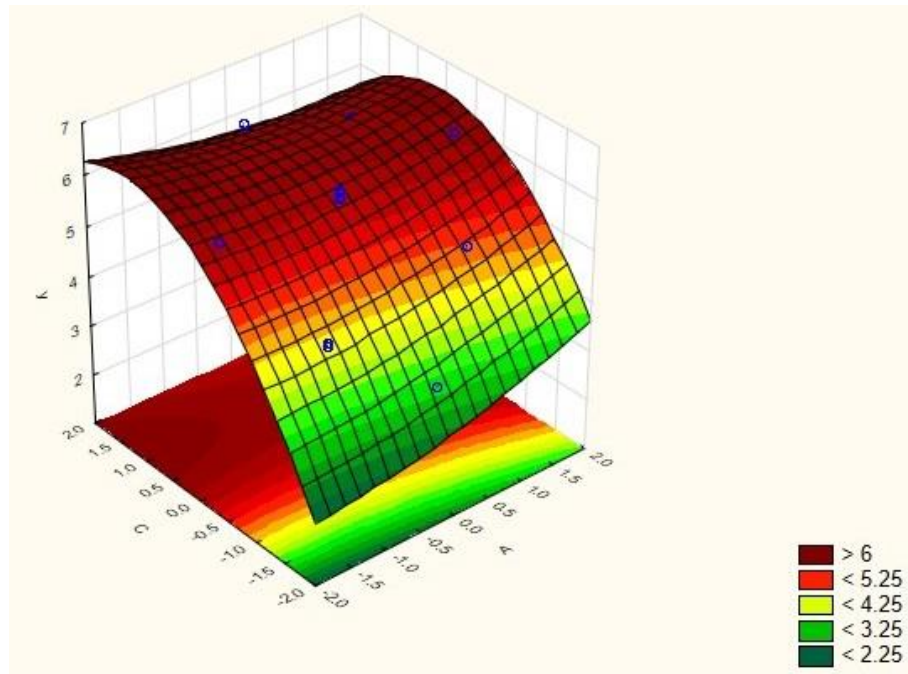


Figure 5.67: Contour plot for K/S value (y) with temperature (A) and time (C).

The empirical model equation obtained with the coded variables is as follows:

$$y = 5.34 + 0.09A + 0.05A^2 - 0.15B - 0.20B^2 + 0.75C - 0.42C^2 - 0.096AB - 0.13AC + 0.009BC \quad (5.6)$$

The optimal values were observed as 120°C for temperature, 5.6 for initial pH of dye bath and 43 min for dyeing time approximately. The predicted K/S value under these optimal conditions was 5.71.

It was seen from Table 5.21 that the factors A , B , B^2 , C , C^2 and AC were the most significant factors with p-values less than 0.05. The factors A and C had positive impacts on y while B , B^2 , C^2 and AC left negative impacts. Thus, temperature (A), initial pH (B) as well as time (C) had significant linear effects on K/S value, with the latter two also having significant quadratic effects. The interaction term of temperature and time was also found to be significant.

Table 5.21: Variance analysis (ANOVA) of factors on response.

Factors	Sum of Squares	Degrees of Freedom	Mean Square	F Value	p-Value Prob>F
<i>A</i>	0.105	1	0.105	5.127	0.047
<i>A</i> ²	0.043	1	0.043	2.111	0.177
<i>B</i>	0.304	1	0.304	14.859	0.003
<i>B</i> ²	0.596	1	0.596	29.188	0.000
<i>C</i>	7.677	1	7.677	375.842	0.000
<i>C</i> ²	2.595	1	2.595	127.061	0.000
<i>AxB</i>	0.074	1	0.074	3.629	0.086
<i>AxC</i>	0.133	1	0.133	6.493	0.029
<i>BxC</i>	0.001	1	0.001	0.030	0.866

Table 5.22: Variance analysis (ANOVA) of quadratic regression model.

Source	Sum of Squares	Degrees of Freedom	Mean Square	F Value	p-Value Prob>F
Model	11.448	9	1.272	62.276	0.00
Residual	0.204	10	0.020		
Lack of fit	0.134	5	0.027	1.893	0.250
Pure error	0.071	5	0.014		
Total	11.652	19			

From Table 5.22, it was observed that at 95% confidence level, the quadratic regression model developed was statistically significant with F-value of 62.276 that was much higher than the F-value of the lack of fit (1.893). The R^2 value was found to be 0.98247 indicating that 98.25% of the total variations could be explained by the developed model, and only 1.75% of the variations could not be explained. The adjusted

R^2 value of 0.9667 was reasonably close to the R^2 value, indicating a high goodness of fit for the developed model.

5.3 Summary

From the results observed for the effects of different parameters, it could be concluded that the range of temperature of 110°C to 130°C was found to be optimal for dyeing of PTT, PLA and PET with disperse dyes. Above 130°C, the K/S values increased and the wash fastness was also better but the tensile properties decreased significantly. The initial pH was found to be optimal in the range of 5-6 for PTT and PLA and 3-4 for PET.

For PLA, the optimal range of dyeing time was found to be 15-45 min which was different from PTT and PET. For these two fibers, the optimal range was 30-60 min. In case of PLA, the fall in tensile properties was much sharper at temperatures beyond 45 min, and hence, the optimal range was lower than the other two fibers.

The material to liquor ratio was found to be optimal from 1:20 to 1:40 for all the fibers whereas in case of rate of heating, 2 °C/min gave the best results. However, it could also be observed that these two factors did not have any significant effects on the tensile properties of the dyed fibers. Thus, they were less significant factors than temperature, initial pH of dye bath and time of dyeing in dyeing of PTT, PLA and PET with disperse dyes.

With optimization of disperse dyes applied on PTT and PLA, the following observations could be made:

- (i) In case of dyeing with disperse dyes, it was observed that temperature, initial pH of the dye bath as well as dyeing time were the three most significant

factors out of the five chosen. The material to liquor ratio and rate of heating were less significant as factors affecting the color strength of PTT and PLA, as suggested by the normal probability plots developed in each case. This was also in agreement to the observations made while evaluating the effects of various parameters on dyeing of these fibers with disperse dyes. It was observed therein that both these factors had little or no significant effects on the tensile properties of the fibers, while temperature, initial pH and time left significant impacts. The high values of R^2 in case of each of the normal probability plots as well as their close proximity to the adjusted R^2 values indicated a high accuracy of prediction and a high probability of reproducibility for them.

- (ii) It was observed that with disperse dyes, optimal values for the significant factors affecting the color strength for PTT were temperature of 120^oC, initial pH of 5.6 and time of 58-59 min. The color strength predicted by the model equations derived was 6.37 with Disperse Yellow 56, 6.01 with Disperse Blue 79 and 6.20 with Disperse Red 167. The optimal values for the significant factors affecting color strength for PLA were temperature of 124^oC, initial pH of the dye bath of 5.8 and time of 55 min with Disperse Yellow 56; and temperature of 120^oC, initial pH of the dye bath of 5.6 and time of 43 min with both Disperse Blue 79 and Disperse Red 167. The K/S values predicted at the optimal levels of dyeing using the model equations derived were 5.94 with Disperse Yellow 56, 5.53 with Disperse Blue 79 and 5.71 with Disperse Red 167.

- (iii) The observed values of optimal temperatures for PTT and PLA were higher than reported in literature (100-110°C). This was due to the reason that in this study, no auxiliary chemicals were used in dyeing other than acetic acid. No dispersing, sequestering or other agents were applied that assist in dyeing. Without such assistance, the dyeing temperature was higher than as reported in the studies where these auxiliary chemicals were used. The optimal ranges for pH was same as reported (5-6), while that for dyeing time was again on a slightly higher side. It was also due to lack of assisting chemicals because of which proper penetration of dyes took longer time. However, the optimal conditions achieved were much lower as compared to the conventional dyeing conditions of PET with disperse dyes that require 130°C, pH 3-4 and 60 min along with polluting and harmful auxiliaries. This study therefore presented satisfactory dyeing processes for PTT and PLA with disperse dyes without the use of any auxiliary chemicals except for acetic acid, with optimal values for temperature and time lower than PET. Hence, the dyeing processes described here were more ecofriendly than with PET for disperse dyes.
- (iv) While the linear effects of temperature and time were found to have positive impacts on the color strength of the dyed fibers, the quadratic effects of initial pH and time left negative effects on the same. Also, negative effects were observed on the color strength for the linear term of initial pH as well as the interaction term of temperature and time. These trends were similar in case of both PTT and PLA and with all of the three dyes used. The similarity in the trend indicated the accuracy of the model equations and their predictions.

- (v) For the model equations derived with both PTT and PLA, the R^2 values were found to be very high, indicating that a majority of the total variations predicted by them in the processes of dyeing could be explained by the respective models. The close proximity of the adjusted R^2 value to those of R^2 in these cases also signified a good fit of the derived model equations. Thus, the models developed were robust in nature with a high probability of reproducibility for the fibers and dyes used.

Chapter 6

**Application of Natural
Dyes**

In the first section of this chapter, natural dyes were applied to the fibers. In the first part, three natural dyes, viz. Lac, Catechu and Myrobalan, were applied to PTT, PLA and PET. The effects of temperature, initial pH of the dye bath, time and material to liquor ratio were evaluated on the color strength and tensile properties. The color strength was measured as the K/S value while tenacity (gpd) and elongation (%) were used to evaluate the tensile properties. The results with PTT and PLA were compared to that of PET dyed with the same dyes under similar conditions.

In the second section of this chapter, the three natural dyes chosen are applied in combination among themselves as well as with another natural dye, Pomegranate, as a biomordant. Thus, Lac was applied to the fibers in combination with Catechu, Myrobalan and Pomegranate, all of which have biomordanting properties. Catechu was also applied in combination with Myrobalan and Pomegranate while another combination of Myrobalan and Pomegranate was also used.

In these applications, the biomordant was applied using three different techniques of mordanting, viz. pre-mordanting, meta-mordanting and post-mordanting, and the results compared. Two fibers, PTT and PLA, were dyed in these cases. From the results obtained, the most suitable mordanting technique was identified.

In the third section in this chapter, the color strength of PTT, PLA and PET were compared for the three chosen natural dyes, along with biomordants against the application of three inorganic mordants. This comparison was aimed at finding out whether the K/S values obtained by application of the chosen natural dyes on these fibers were satisfactory as compared to the colors achieved with inorganic mordants. Thus, PTT, PLA and PET were dyed with Lac using the biomordants Catechu, Myrobalan and

Pomegranate, and with inorganic mordants as well. The inorganic mordants used were alum or aluminium potassium sulphate $[\text{AlK}(\text{SO}_4)_2 \cdot 12\text{H}_2\text{O}]$, ferrous sulfate ($\text{FeSO}_4 \cdot 7\text{H}_2\text{O}$) and stannous chloride ($\text{SnCl}_2 \cdot 5\text{H}_2\text{O}$). The three fibers were also dyed with Catechu as the natural dye using Myrobalan and Pomegranate as biomordants, and with inorganic mordants as mentioned above. The fibers were also dyed with Myrobalan as the natural dye using Pomegranate as biomordant and with the three inorganic mordants as above. The K/S values of the fibers were compared for each of the natural dyes used with biomordants and inorganic mordants.

6.1 Materials and methods

6.1.1 Materials

The three fibers used, viz. PTT, PLA and PET, were the same as mentioned in the section 5.1.1. The acetic acid used in solution (10% v/v), alum or aluminium potassium sulphate $[\text{AlK}(\text{SO}_4)_2 \cdot 12\text{H}_2\text{O}]$, ferrous sulfate ($\text{FeSO}_4 \cdot 7\text{H}_2\text{O}$) and stannous chloride ($\text{SnCl}_2 \cdot 5\text{H}_2\text{O}$) were obtained as laboratory grade reagents.

6.1.2 Dyes

Three natural dyes were used in this section of the study. They were Lac, Catechu and Myrobalan. The structures of the main components and other details for Lac are given in section 2.2.2.1; those for Catechu are provided in section 2.2.2.2; and the same for Myrobalan are given in section 2.2.2.3. Besides these three, another natural dye, Pomegranate, was used as a biomordant in this study. The structural details of its main components and other details are provided in the earlier section 2.2.2.4. All of these four natural dyes were obtained in powder form from Sky Morn Exports Ltd., NOIDA, India.

6.1.3 Equipment

The dyeing apparatus was Superlab High Temperature and High Pressure dyeing equipment of laboratory scale, the same as mentioned in the section 5.1.3.1 earlier. The launder-o-meter used and the AATCC test method followed for evaluation of the wash fastness properties were also the same as in the earlier section 5.1.3.2. Crocking fastness was evaluated using the same instrument as in the section 5.1.3.3. The AATCC test method followed is also mentioned therein. The spectrophotometer used for the purpose of spectral analyses is the same as in the earlier section 5.1.3.4.

6.1.4 Methods

6.1.4.1 Dyeing

For each dyeing experiment, 1 g of fiber was taken. Stock solutions of 10% strength were prepared for each of the natural dyes by taking 10 g of dye in 100 ml of distilled water. 1 ml of the stock solution was introduced to the dye baths and the total volume made to the required amount based on the material to liquor ratio chosen. Thus, all fibers were dyed with 10% of the natural dyes. Other additions for biomordants and inorganic mordants were made after this, which are described in detail later on. Finally, acetic acid solution (10% v/v) was added to the dye baths after all other additions were made in order to achieve the level of initial pH as required.

The dye baths after preparation were introduced into the HTHP apparatus at room temperature. The temperature was gradually raised to the required level of dyeing temperature as has been determined for the experiment. The rate of heating was kept at 2^oC/min. Dyeing was carried out for the required amount of time after which the dye bath was drained and the samples collected. The dyed fibers were washed with distilled

water followed by an acid wash with acetic acid solution (10% v/v). Finally, they were washed again with distilled water and dried in air for at least 8 hours.

In case of use of biomordants, stock solutions of the selected biomordant was prepared in the similar way and added to the dye baths. In case of meta-mordaning, these additions were made after adding from the stock solution of the natural dye. In case of pre-mordanting, the fibers were first dyed with the biomordant at predetermined dyeing temperature and for the required amount of time. The dyed fibers were then washed with distilled water, acid and again distilled water, and dried in air. These samples were later used for application of the chosen natural dyes in a similar manner as described above. For post-mordanting, the fibers were dyed with the chosen natural dye first, which were washed and dried. The dried fibers were again treated with biomordant in the dye baths, washed and finally dried for measurements.

In case of inorganic mordants, the amount required was measured in a weighing scale and added directly to the dye baths. After these additions were made, the total volume was made to the required amount by addition of distilled water, based on the material to liquor ratio. Here also, the inorganic mordants were added to the dye bath along with the natural dye in case of meta-mordanting. In case of pre-mordanting, the treatment of the fibers with inorganic mordants was done prior to application of the natural dyes. The treated fibers were washed, dried and used for further dyeing with natural dyes. For post-mordanting, the fibers were first dyed with the natural dyes, washed and dried. They were then treated with the chosen inorganic mordants, washed and dried again before preparing for the measurements. The dyeing cycle followed for the

natural dyes and biomordants were the same as followed for the disperse dyes, the schematic diagram of which is given in Figure 5.7.

6.1.4.2 Measurement of color, wash fastness and tensile properties

For measurement of color strength, wash fastness and tensile properties, the steps as well as instruments mentioned in the earlier sections 5.1.4.2, 5.1.4.3 and 5.1.4.4 were followed respectively. In case of wash fastness evaluation, the dE values were however not measured in this chapter. Instead, the samples after the test were evaluated using the AATCC grey scales for color change as well as color staining. The AATCC test method followed was however the same as mentioned in the section 5.1.4.3. For measuring the tensile properties, the ASTM test methods were also the same as mentioned in the section 5.1.4.4.

6.1.4.3 Measurement of perspiration fastness

The perspiration fastness was measured following the AATCC 15-2002 standard method. The AATCC perspiration tester was used for the purpose, as given in Figure 6.1. The samples after the test were evaluated using the AATCC grey scales for color change as well as color staining.



Figure 6.1: AATCC Perspiration Tester [114].

6.1.4.4 Measurement of fastness to acids and alkalis

For evaluating the fastness to acids and alkalis, the AATCC 6-2001 method was followed. The changes in color of the dyed fiber samples after treatment with acids as well as alkalis were evaluated.

6.1.4.5 Measurement of hydrogen peroxide bleaching fastness

For evaluation of fastness to hydrogen peroxide bleaching, the standard method of AATCC 101-2004 was followed. The change in color of the dyed samples as well as color stain on cotton fabrics was reported.

6.2 Results and Discussions

The effects of temperature, initial pH of dye bath, dyeing time and material to liquor ratio on color strength and tensile properties of dyed PTT, PLA and PET were evaluated with disperse dyes in the following sections. The color strength was measured as K/S values while for tensile properties, the tenacity was measured in grams per denier (gpd) and the elongation at break as percentage (%) of the initial length of the dyed fibers. The CIE $L^*a^*b^*$, C^* and h° values of PTT and PLA fibers dyed with the three natural dyes are given in Table 6.1. They were representative samples dyed at 120°C with initial pH of 5, dyeing time of 30 min and material to liquor ratio at 1:40.

Table 6.1: CIE L*a*b* values of PTT and PLA fibers with three natural dyes.

Fiber	Dye	L*	a*	b*	C*	h°	Figure no.
PTT	Lac	47.44	10.26	5.64	11.70	28.79	5.1
	Catechu	46.23	13.92	16.28	21.42	49.47	5.2
	Myrobalan	63.36	10.13	12.91	16.41	51.88	5.3
PLA	Lac	42.90	11.61	6.33	13.22	28.60	5.4
	Catechu	41.32	14.77	16.00	21.78	47.28	5.5
	Myrobalan	60.18	1.56	12.77	12.86	83.02	5.6

6.2.1 Effect of various parameters on color strength and tensile properties

The effects of temperature, initial pH value, dyeing time and material to liquor ratio on the color strength and tensile properties of PTT, PLA and PET are discussed in the following sections. Each experiment was carried out five times and the average values reported.

6.2.1.1 Effect of temperature

In chapter 5, under section 5.2.1, we have seen that with disperse dyes, the K/S value of PTT, PLA and PET increases steadily with temperature. It was also observed that the tensile properties decreased steadily. Thus, there was a need felt to strike the right balance between color strength and tensile properties.

From chapter 4, we know that the suitable range of temperature for dyeing of PTT and PLA are 80-120°C and 90-145°C respectively. But the effect of temperature on the properties of these fibers with the three selected natural dyes are not known to us, and it needs to be investigated if they follow the same trend as that with the disperse dyes.

In this study, dyeing was carried out for PTT, PLA and PET with Lac, Catechu and Myrobalan at five different temperatures of 90 °C, 100 °C, 110 °C, 120 °C and

130°C. The other factors were kept at constant levels, viz. initial pH of 5 in the dye bath, time of 30 min and material to liquor ratio of 1:30. The effect of temperature on K/S value is depicted in Figures 6.2, 6.3 and 6.4 for Lac, Catechu and Myrobalan respectively.

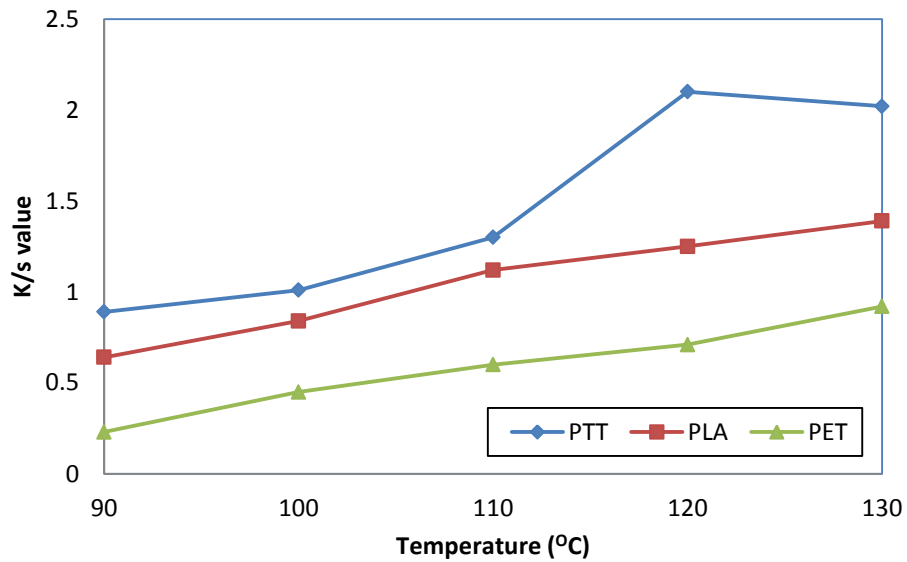


Figure 6.2: Effect of temperature on K/S value for Lac.

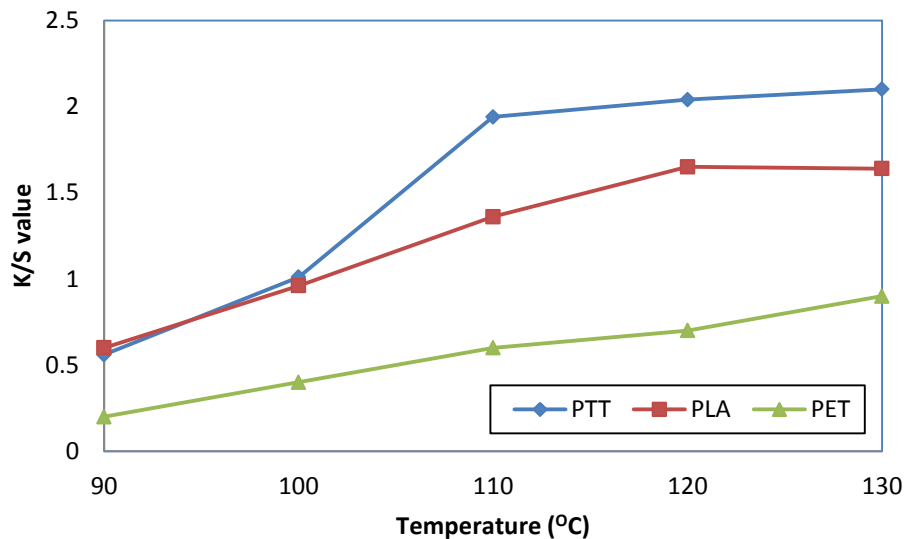


Figure 6.3: Effect of temperature on K/S value for Catechu.

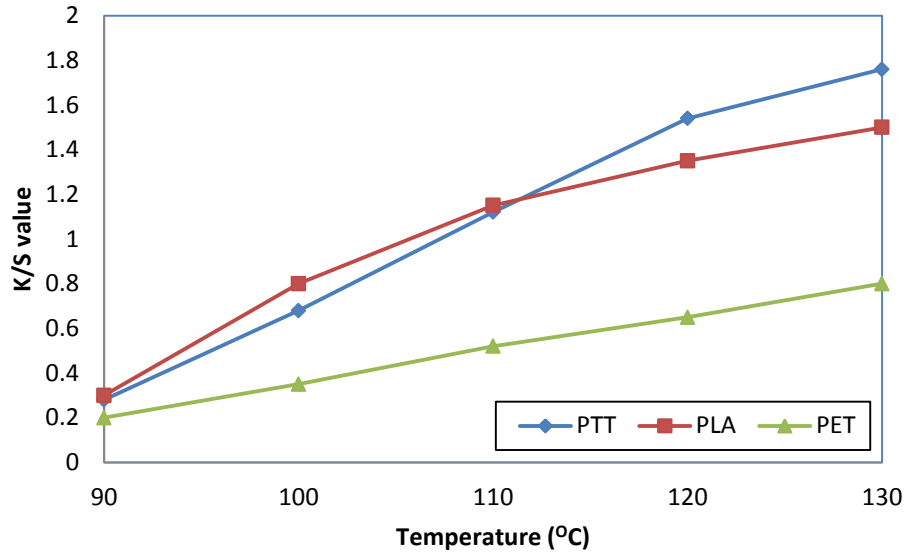


Figure 6.4: Effect of temperature on K/S value for Myrobalan.

It could be observed that with temperature, the K/S value increased for all of the three fibers. The increase was more marked for PTT in the range of 110-120°C. It also exhibited the highest K/S value among the fibers for all of the three dyes. Interestingly, the K/S value obtained with PET was the lowest in all cases.

The effect of temperature on the tensile properties of the dyed fibers is shown in Figures 6.5, 6.6 and 6.7 for Lac, Catechu and Myrobalan respectively. The tenacity (gpd) is shown along the primary axis while the elongation (%) at break along the secondary axis.

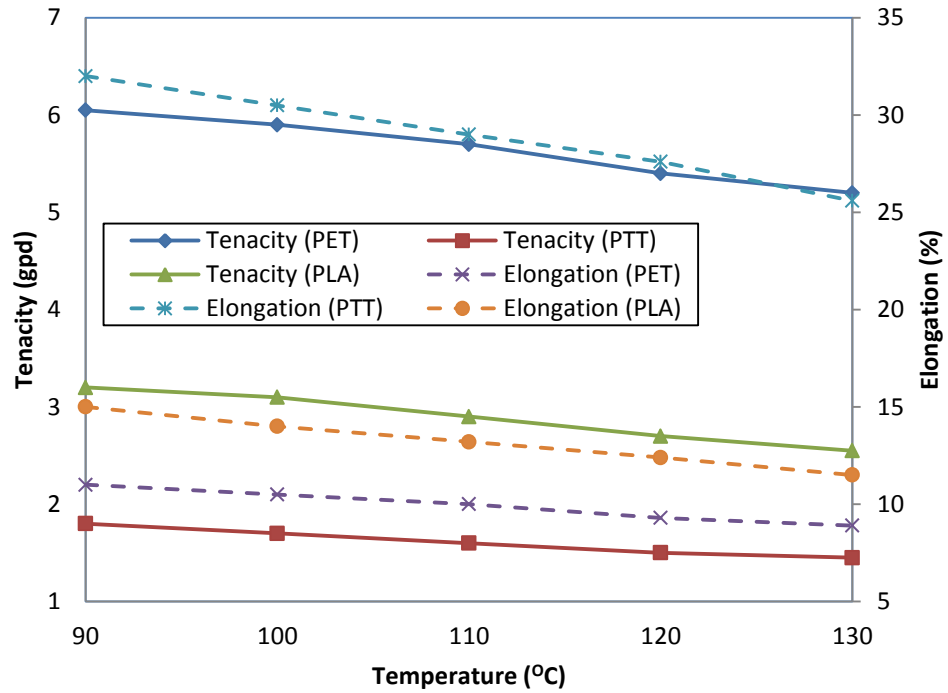


Figure 6.5: Effect of temperature on tensile properties for Lac.

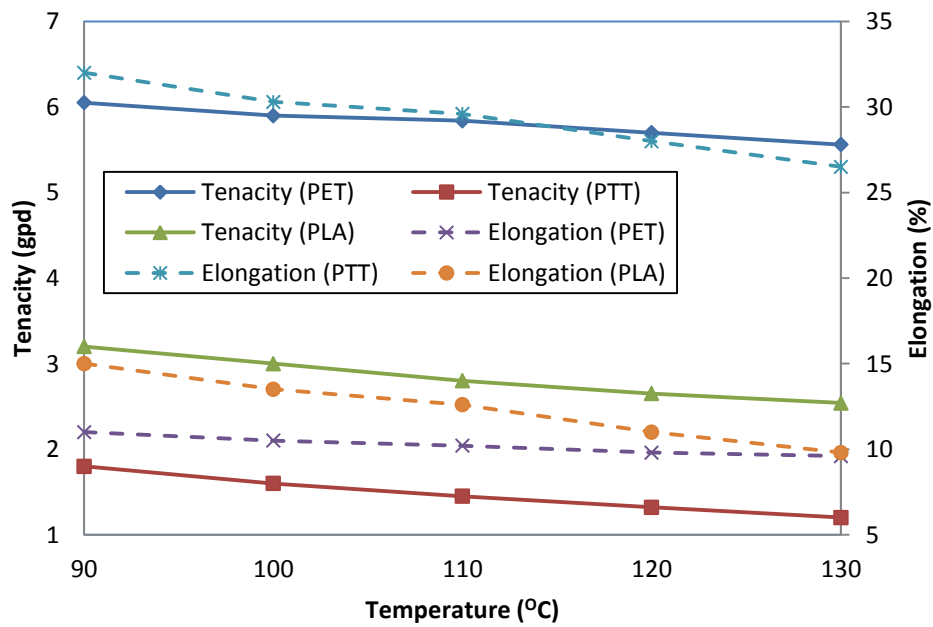


Figure 6.6: Effect of temperature on tensile properties for Catechu.

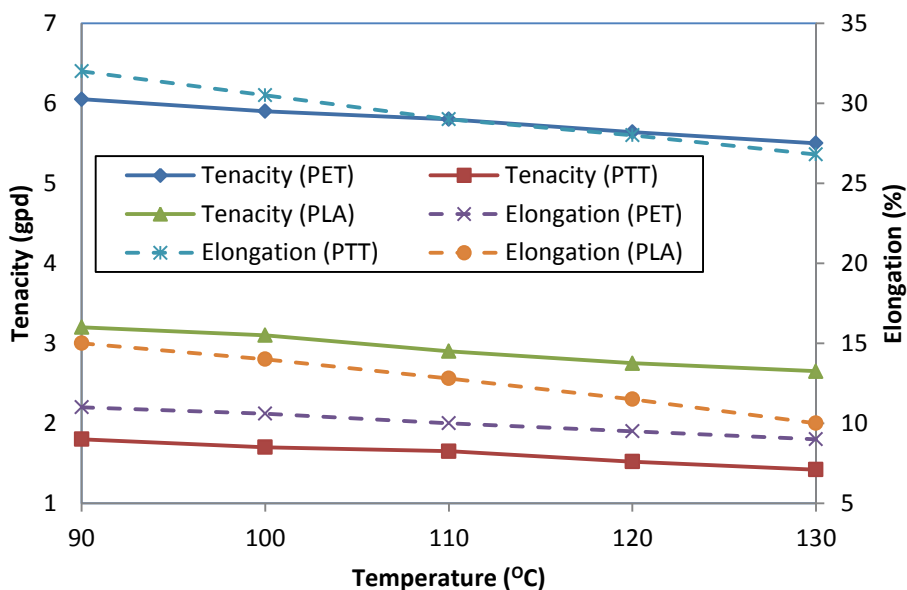


Figure 6.7: Effect of temperature on tensile properties for Myrobalan.

From the results of tensile properties, it could be observed that the tenacity of all the fibers were lowered with temperature. The elongation also decreased, indicating a fall in the tensile properties. The rate of fall was found to be similar for all the three fibers and in case of all of the dyes used. The tenacity was found to be highest for PET and the elongation highest for PTT.

The fall in the tensile properties was a result of thermal degradation of the fiber polymers due to reduction in the degree of polymerization with temperature. Dyeing at high temperatures also caused reduction in the crystallinity percentage of the fibers, thereby damaging the tensile properties further. The trend was similar for all of the fibers due to the fact that they generically belong to the similar class and hence have common polymer properties.

6.2.1.2 Effect of initial pH of the dye bath

Dyeing experiments were carried out at five different levels of initial pH of the dye bath, which were 3, 4, 5, 6 and 7. During these experiments, temperature was kept at 110°C, time at 30 min and material to liquor ratio at 1:30. The effect of initial pH of the dye bath on the K/S value for all the three fibers is given in Figures 6.8, 6.9 and 6.10 for Lac, Catechu and Myrobalan respectively.

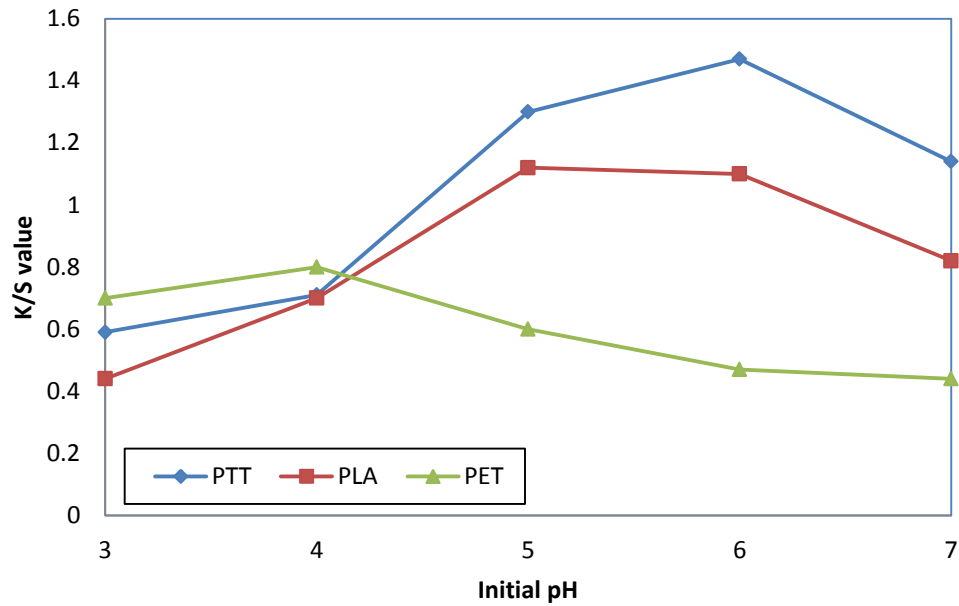


Figure 6.8: Effect of initial pH of dye bath on K/S value for Lac.

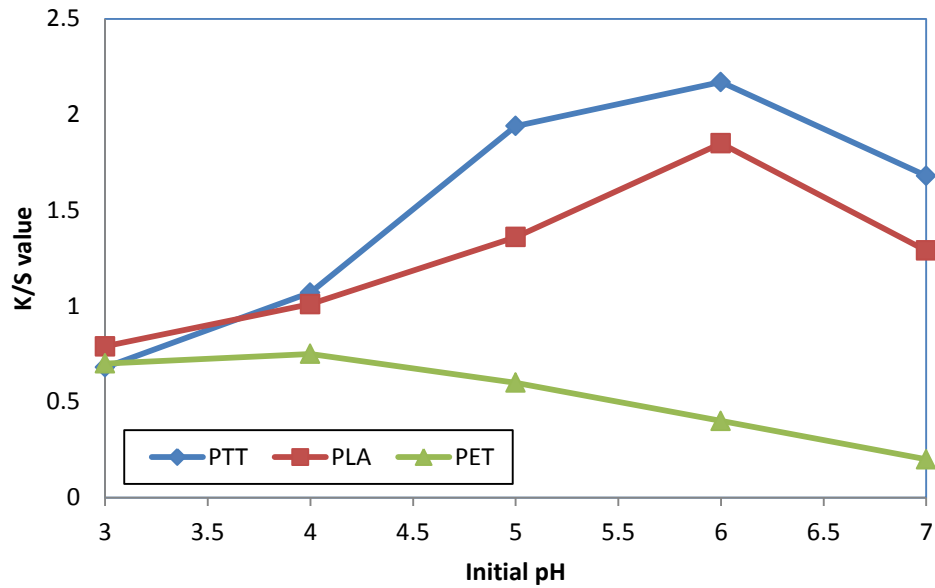


Figure 6.9: Effect of initial pH of dye bath on K/S value for Catechu.

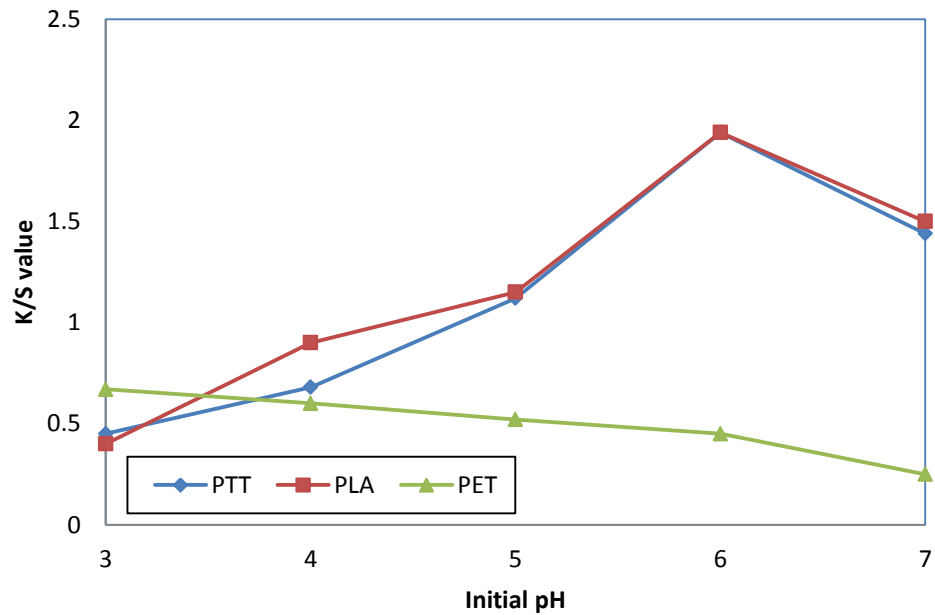


Figure 6.10: Effect of initial pH of dye bath on K/S value for Myrobalan.

It could be seen from the results that the K/S value for PTT and PLA reached higher values at pH 5-6 and decreased on both sides of this pH range with the chosen dyes. The K/S values for PTT were higher than PLA in all cases except for Myrobalan

where they were very close to each other. For PET, the K/S value was found to decrease steadily above pH 4. Also, the values were inferior to PTT and PLA at all pH levels.

The effect of initial pH of the dye bath on the tensile properties of the three fibers is given in Figures 6.11, 6.12 and 6.13 for Lac, Catechu and Myrobalan respectively. The tenacity (gpd) is shown along the primary axis while the elongation (%) at break along the secondary axis.

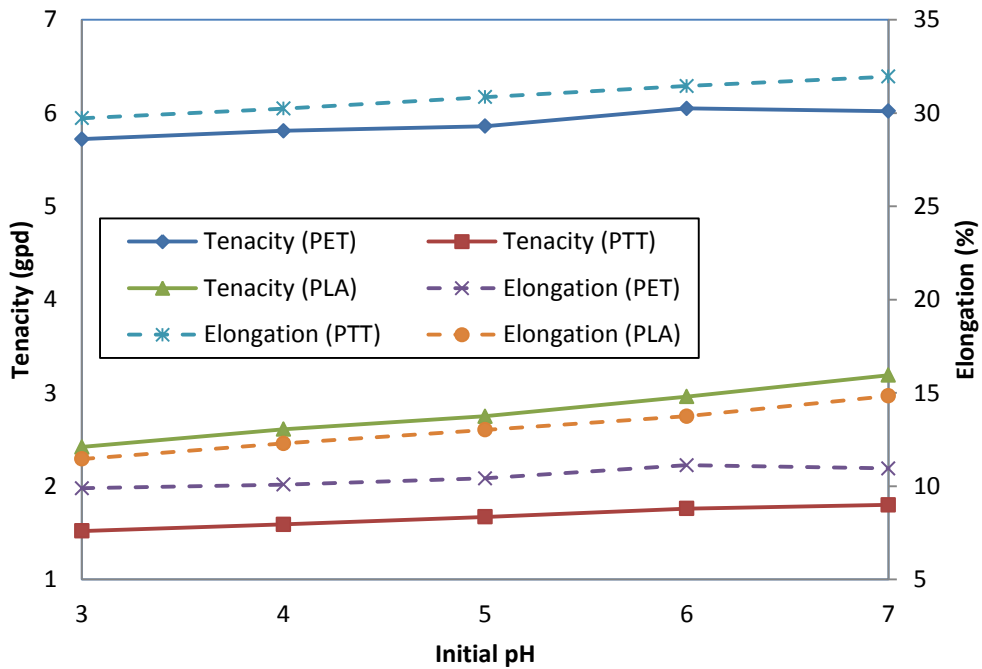


Figure 6.11: Effect of initial pH of dye bath on tensile properties of Lac.

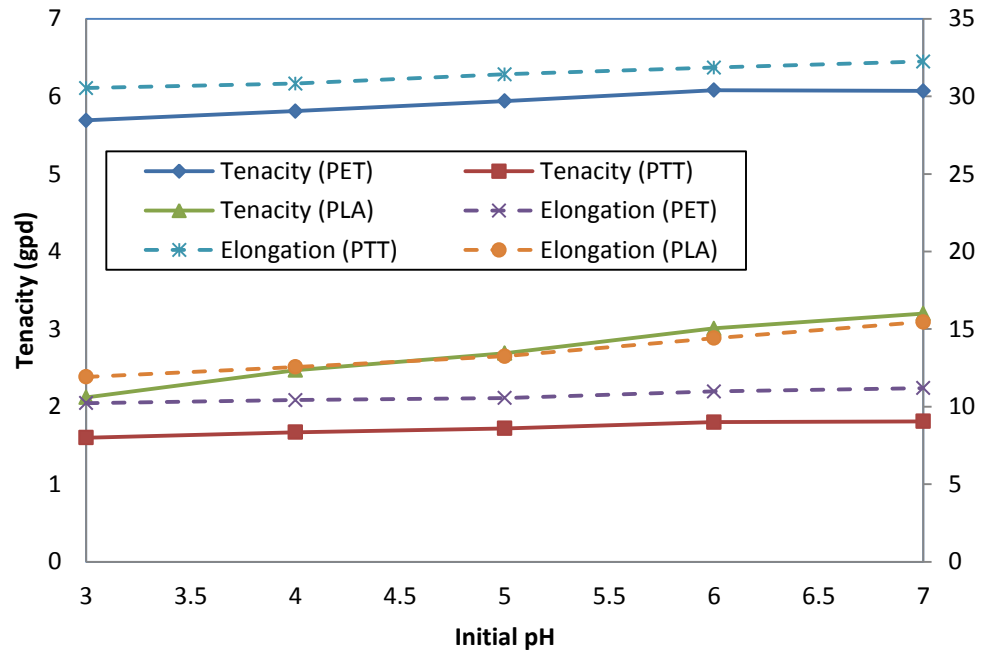


Figure 6.12: Effect of initial pH of dye bath on tensile properties of Catechu.

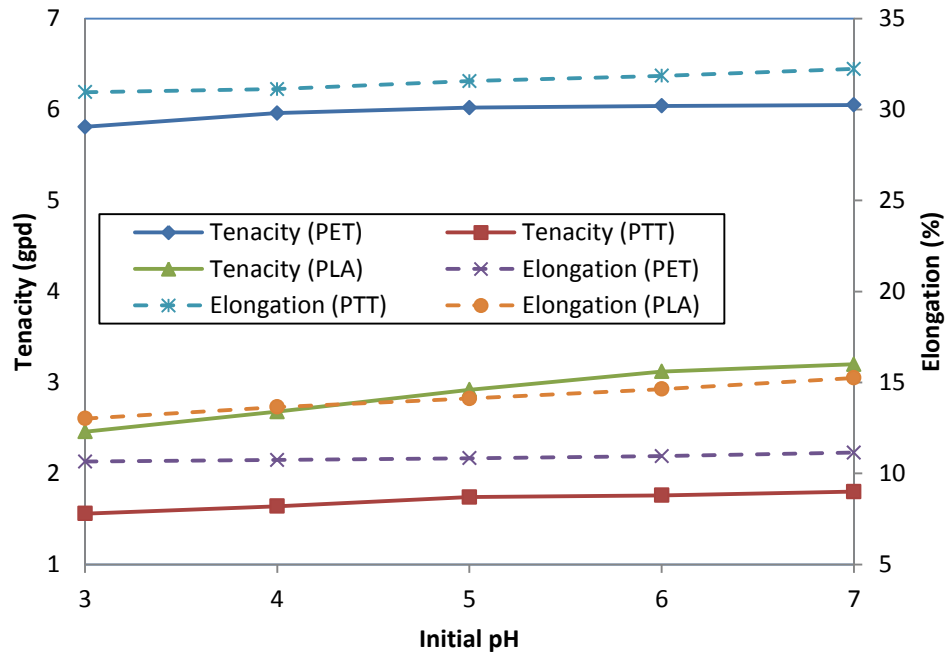


Figure 6.13: Effect of initial pH of dye bath on tensile properties of Myrobalan.

The tensile properties in case of all the fibers were found to decrease towards the range of acidic pH. The tenacity as well as elongation reduced with lowering of the pH

and the fall became slightly sharper below pH of 5. The ideal pH for dyeing of PET has been reported at 3-4. But it has also been found that PET loses strength considerably after dyeing, which may be due to many factors including the pH. It can thus be concluded from the results that acidic pH left a detrimental effect on the tensile properties of the fibers, and pH near to the neutral range (5-7) showed lesser fall in tenacity and elongation.

6.2.1.3 Effect of time

Experiments were performed to see the effect on dyeing time on the fiber properties as well. So, five different levels of dyeing time were identified, viz. 15 min, 30 min, 45 min, 60 min and 75 min, for dyeing of the fibers. The temperature was kept at 110°C, the initial pH of the dye bath at 5 and the material to liquor ratio at 1:30, in all cases. The results for K/S values of the three fibers are given in Figures 6.14, 6.15 and 6.16 for Lac, Catechu and Myrobalan respectively.

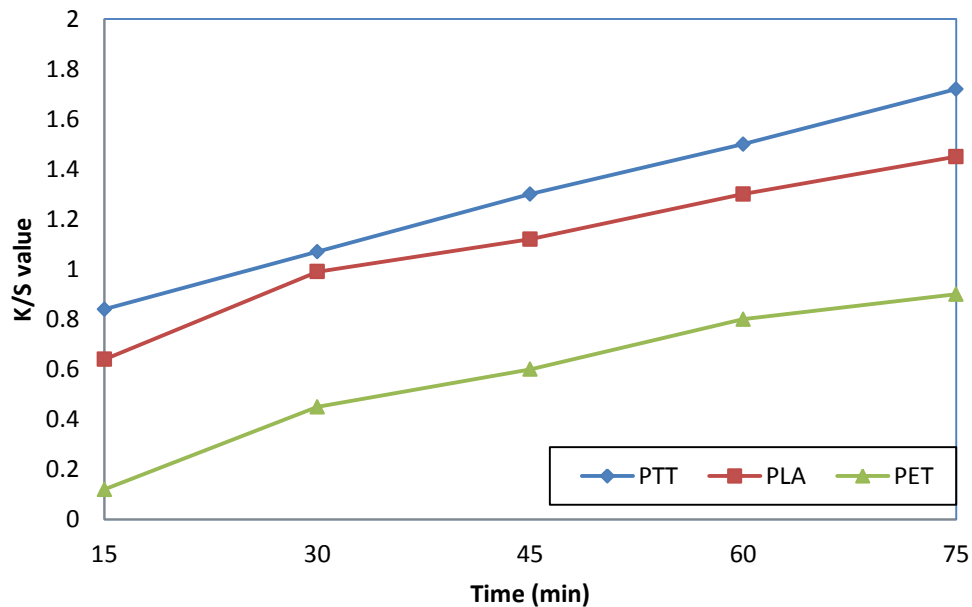


Figure 6.14: Effect of time on K/S value for Lac.

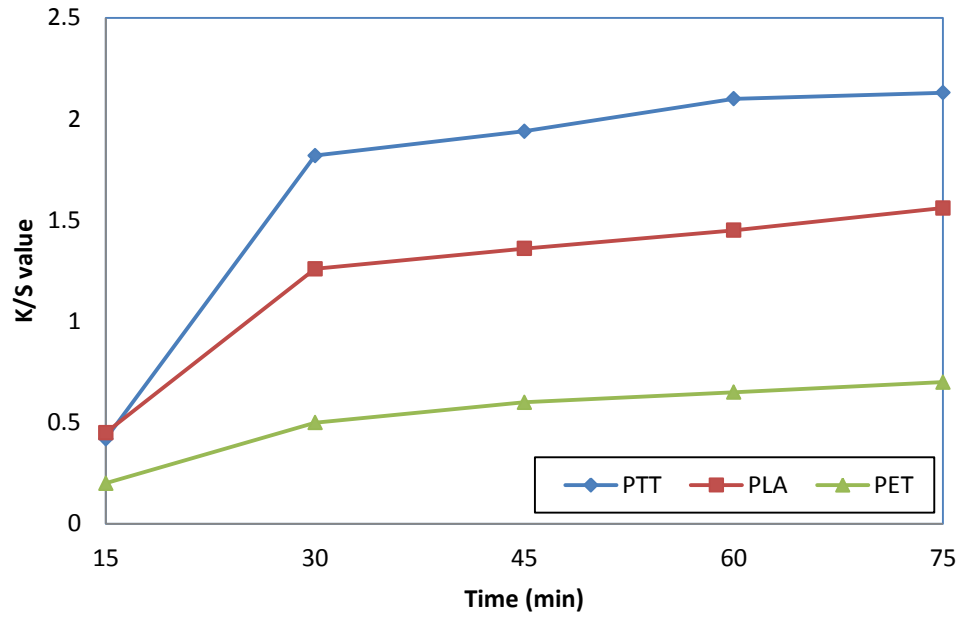


Figure 6.15: Effect of time on K/S value for Catechu.

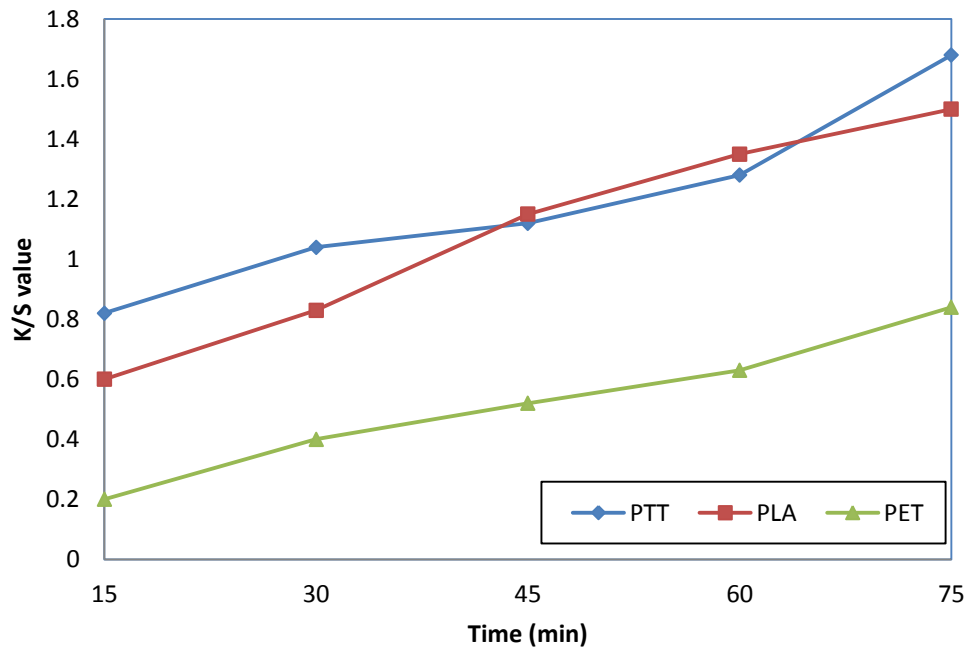


Figure 6.16: Effect of time on K/S value for Myrobalan.

With Lac and Myrobalan, the K/S for all the fibers increased steadily with time, indicating a positive effect of temperature in case of these two dyes. The effect was

similar even for Catechu where the increase in K/S value was sharp at the initial stage but flattened for all three fibers beyond 30 min. PTT exhibited highest K/S values and PET the lowest.

The effect of dyeing time on the tensile properties of the three fibers is given in Figures 6.17, 6.18 and 6.19 for Lac, Catechu and Myrobalan respectively. The tenacity (gpd) is shown along the primary axis while the elongation (%) at break along the secondary axis.

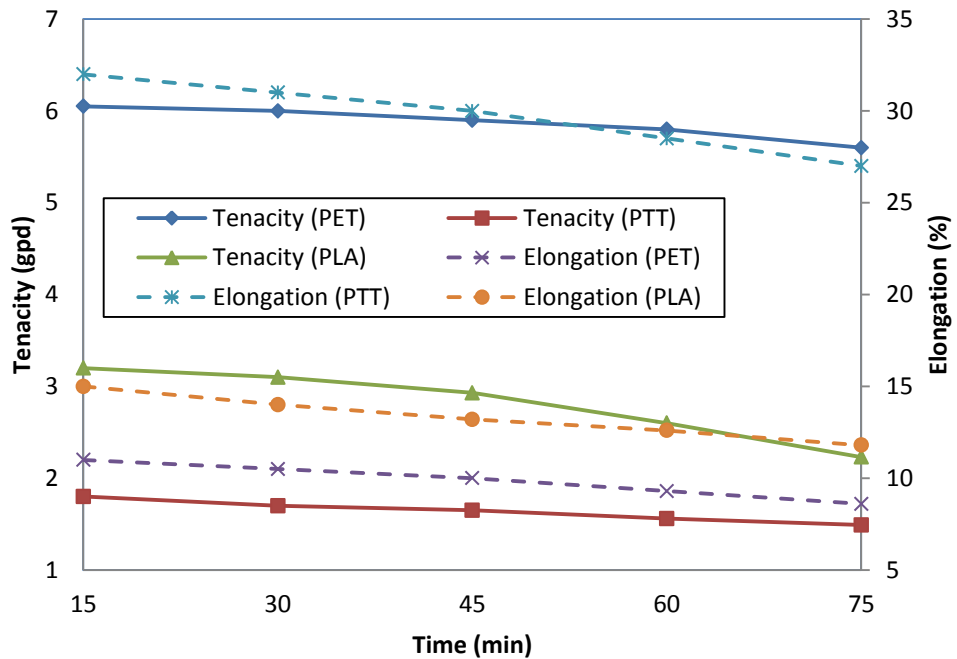


Figure 6.17: Effect of time on tensile properties for Lac.

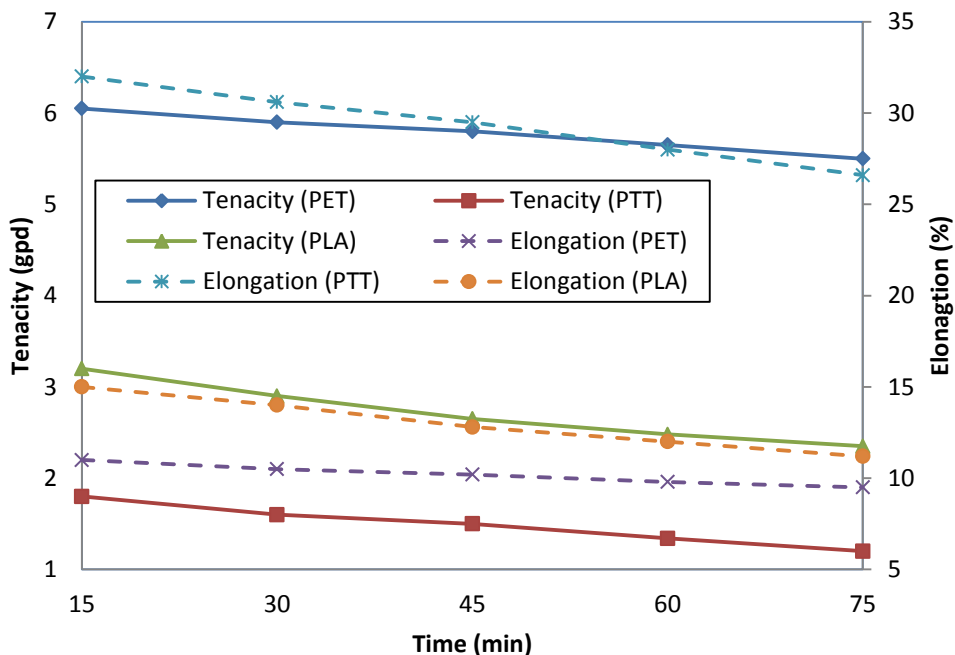


Figure 6.18: Effect of time on tensile properties for Catechu.

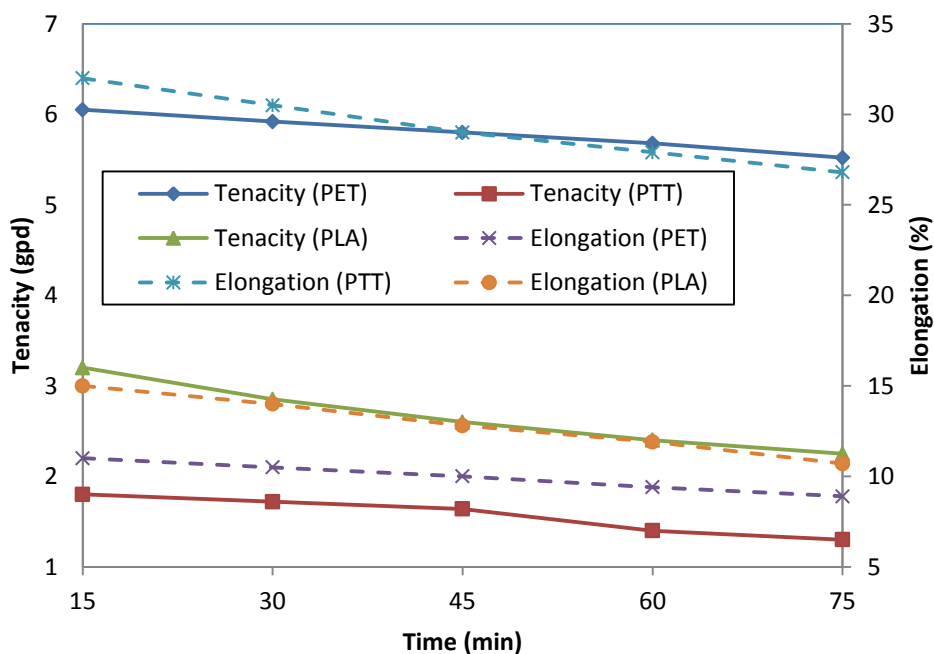


Figure 6.19: Effect of time on tensile properties for Myrobalan.

From the results, it could be seen that the tenacity and elongation of the fibers decreased considerably with time. The decrease beyond 45 min was very high, especially

for PLA. It is known that PLA is very much susceptible to hydrolysis. Thus, exposure to elevated temperatures for such longer duration proves to be detrimental for the fiber. For the other fibers too, there was a considerable decrease in the tensile properties with time, although the rate of decrease was lesser than that of PLA. Thus, duration of dyeing up to 45 min was found to be preferable for the three fibers in case of all the three dyes used.

6.2.1.4 Effect of material to liquor ratio

In order to assess the effect of material to liquor ratio on the properties of the dyed fibers, dyeing experiments were carried out at five different ratios of material to liquor, which were 1:10 (=0.10), 1:20 (0.05), 1:30 (0.033), 1:40 (0.025) and 1:50 (0.02). During these experiments, temperature was kept at 110°C, initial pH of the dye bath at 5 and time at 30 min. The effect of material to liquor ratio on the K/S value of three dyed fibers are depicted in Figures 6.20, 6.21 and 6.22 for Lac, Catechu and Myrobalan respectively.

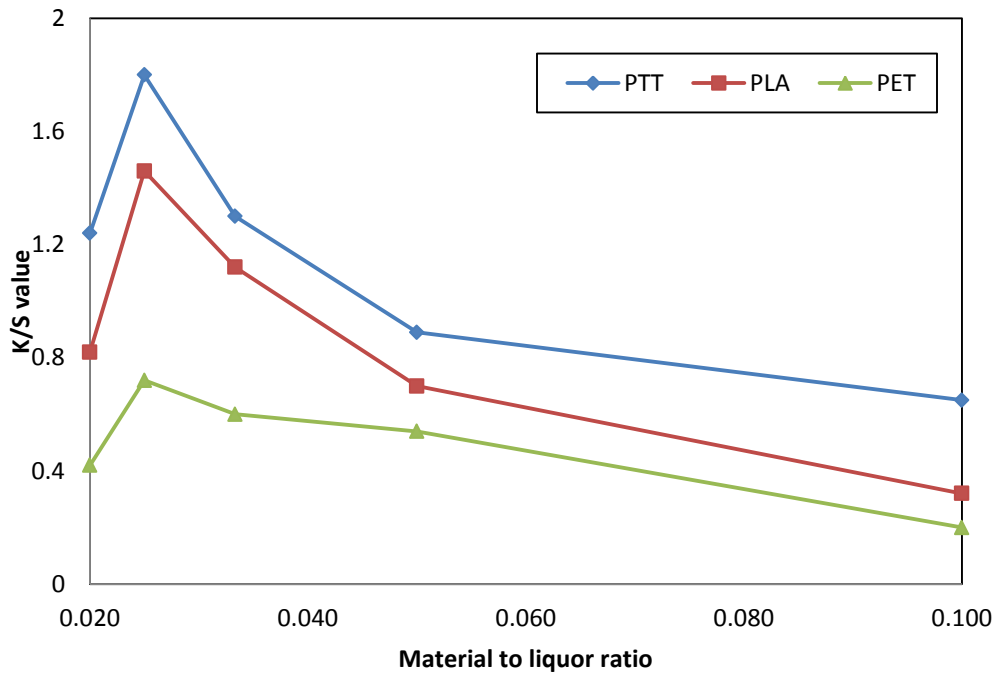


Figure 6.20; Effect of material to liquor ratio on K/S value for Lac.

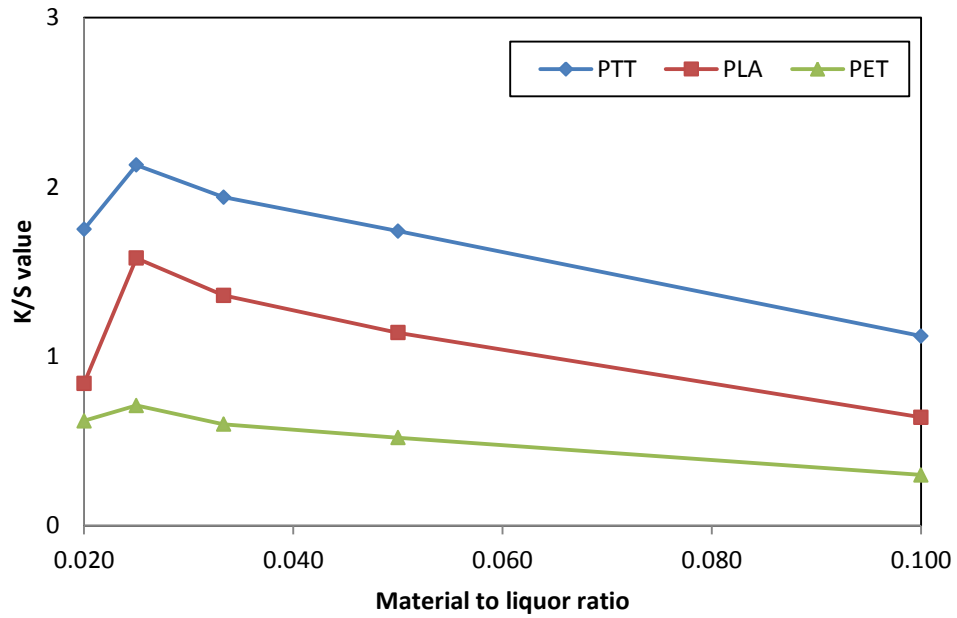


Figure 6.21; Effect of material to liquor ratio on K/S value for Catechu.

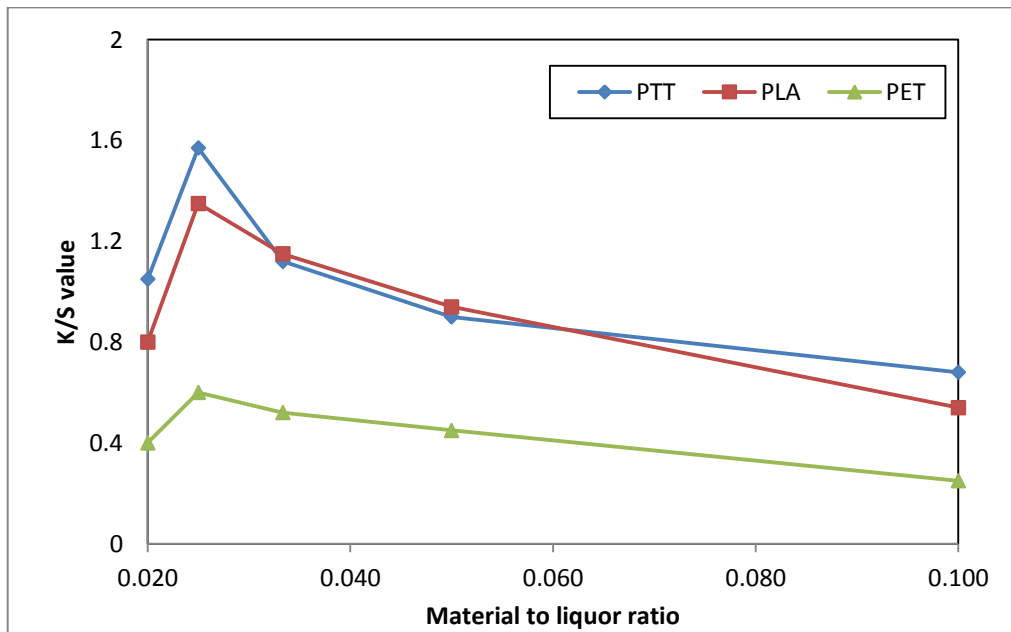


Figure 6.22; Effect of material to liquor ratio on K/S value for Myrobalan.

With material to liquor ratio, it was observed that the K/S value was highest for all the fibers at the ratio of 1:40 and decreased with increase in the ratio. Beyond this, the K/S value was found to reduce in case of all the dyes. It could thus be inferred that with

high volume of liquor at 1:50, it was difficult for the dyes to penetrate the fibers. This may be due to a decrease in the dye concentration in solution that reduced the rate of diffusion of the dye inside the fiber.

The effect of material to liquor ratio on the tensile properties of the dyed fibers are exhibited in Figures 6.23, 6.24 and 6.25 for Lac, Catechu and Myrobalan respectively. The tenacity (gpd) is depicted along the primary axis while the elongation (%) along the secondary axis.

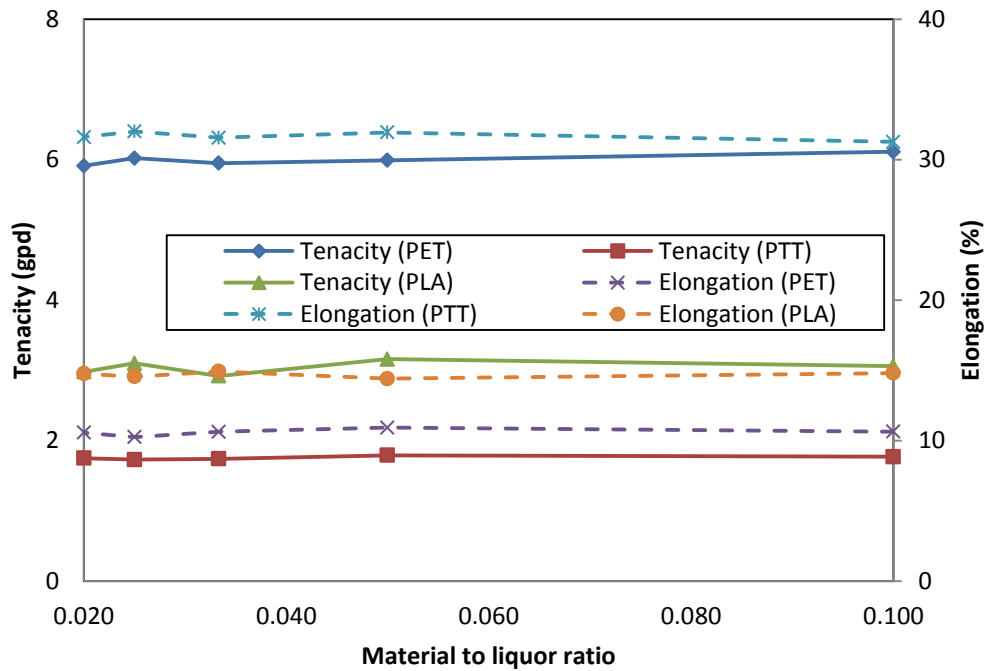


Figure 6.23: Effect of material to liquor ratio on tensile properties for Lac.

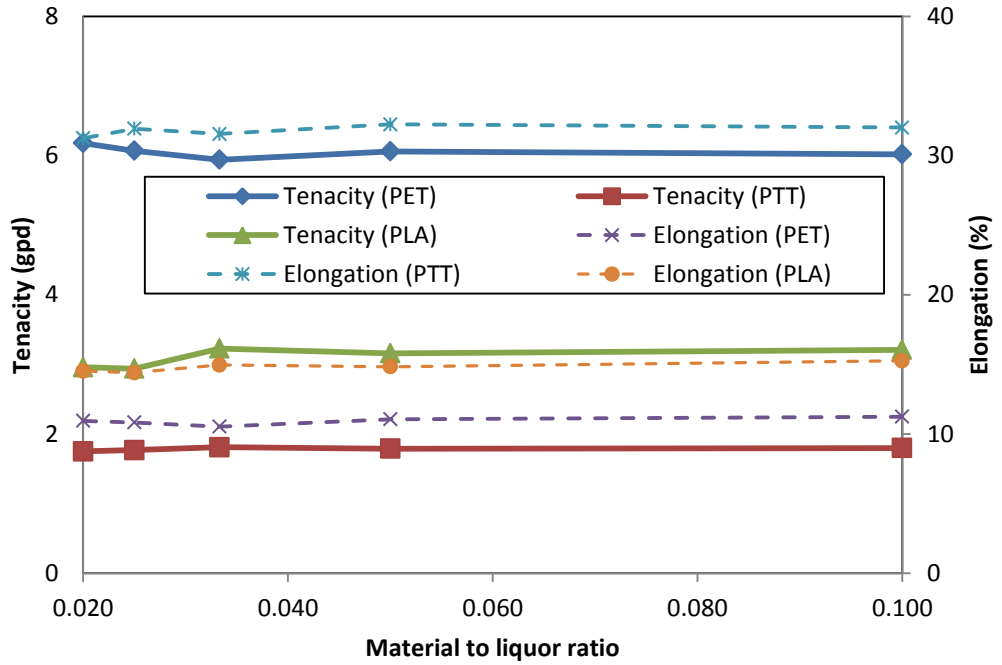


Figure 6.24: Effect of material to liquor ratio on tensile properties for Catechu.

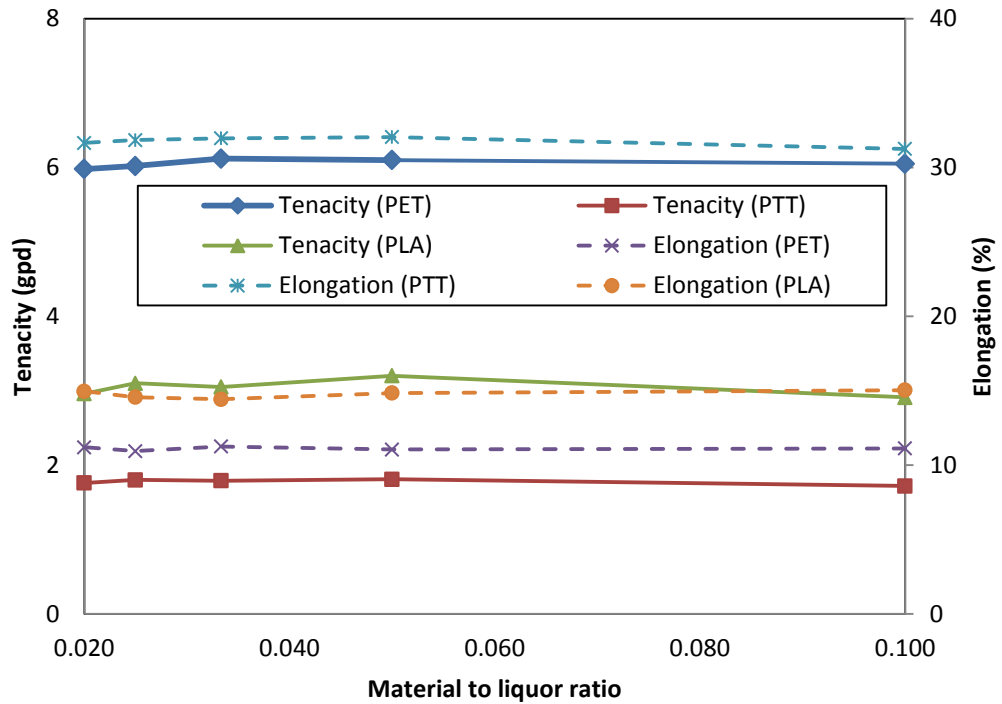


Figure 6.25: Effect of material to liquor ratio on tensile properties for Myrobalan.

Interestingly, no significant effect of material to liquor ratio could be observed on the tensile properties of the fibers. Thus, the material to liquor ratio solely affected the dyeing properties like dye uptake that eventually reflected in the K/S values, but left no significant effect on the tensile properties. Since dyeing is a process that affects the tensile properties of the fibers as well, hence the material to liquor ratio was a less significant factor in dyeing of PTT, PLA and PET with the three chosen natural dyes.

6.2.2 Evaluation of fastness properties

The wash fastness, perspiration fastness and fastness to acids, alkalis and hydrogen peroxide bleaching were evaluated for PTT and PLA fibers dyed with the natural dyes, Lac, Catechu and Myrobalan. The legends for the tables with the results of fastness properties are given in Table 6.2 and the results of evaluation of the various fastness properties for PTT and PLA are shown in Tables 6.3 to 6.5.

Table 6.2: Legend for Tables 6.3 to 6.5.

Symbol	Full name
CC	Color change
CS	Color stain
W	Wool
A	Acrylic
P	Polyester (PET)
N	Nylon
C	Cotton
T	Cellulose triacetate

Table 6.3: Results for wash fastness for PTT and PLA with natural dyes.

Fiber	Dye	Wash fastness						
		CC	CS					
			W	A	P	N	C	T
PTT	Lac	3-4	3-4	5	5	3-4	3	3-4
	Catechu	4	4	5	5	4	3-4	4
	Myrobalan	4	4	5	5	4	3-4	3-4
PLA	Lac	3	3-4	5	5	3-4	3	3-4
	Catechu	4	4	5	5	4	3-4	4
	Myrobalan	3-4	4	5	5	4	3-4	3-4

Table 6.4: Results for perspiration fastness for PTT and PLA with natural dyes.

Fiber	Dye	Perspiration fastness						
		CC	CS					
			W	A	P	N	C	T
PTT	Lac	3-4	3-4	5	5	3-4	3	3-4
	Catechu	4	4	5	5	4	3-4	4
	Myrobalan	4	4	5	5	4	3-4	3-4
PLA	Lac	3	3-4	5	5	3-4	3	3-4
	Catechu	4	4	5	5	4	3-4	4
	Myrobalan	3-4	4	5	5	4	3-4	3-4

Table 6.5: Results for fastness to acids, alkalis and hydrogen peroxide for PTT and PLA with natural dyes.

Fiber	Dye	Fastness to acids	Fastness to alkalis	Fastness to Hydrogen peroxide bleaching	
		CC	CC	CC	CS
	Lac	3-4	3	3-4	3-4
PTT	Catechu	4	3-4	4	3-4
	Myrobalan	4	3-4	4	3-4
	Lac	3-4	3	3-4	3
PLA	Catechu	4	3-4	4	3-4
	Myrobalan	4	3	4	3-4

The results depicted that for Catechu, the fastness properties achieved were superior as compared to Lac and Myrobalan. The results with Myrobalan were better than that with Lac. This was due to the presence of tannins in higher amount in Catechu that helped in better attachment of the dye with the fiber. For the same reason, the results with Myrobalan were better than with Lac that had almost no tannin content in it.

With PLA, the fastness properties were inferior to that with PTT, indicating the tendency of hydrolysis of the fiber during treatment at elevated temperatures with water, which released a considerable amount of dye.

6.2.3 Evaluation of FT-IR spectra after dyeing with natural dyes and biomordants

In order to find out the nature of chemical bonding of the fibers with the natural dyes and biomordants, Fourier Transform Infrared (FTIR) spectra were obtained for both PTT and PLA fibers with the natural dyes. The FT-IR spectra obtained with Lac, Catechu and Myrobalan for PTT fibers are given in Figures 6.26, 6.27 and 6.28 respectively.

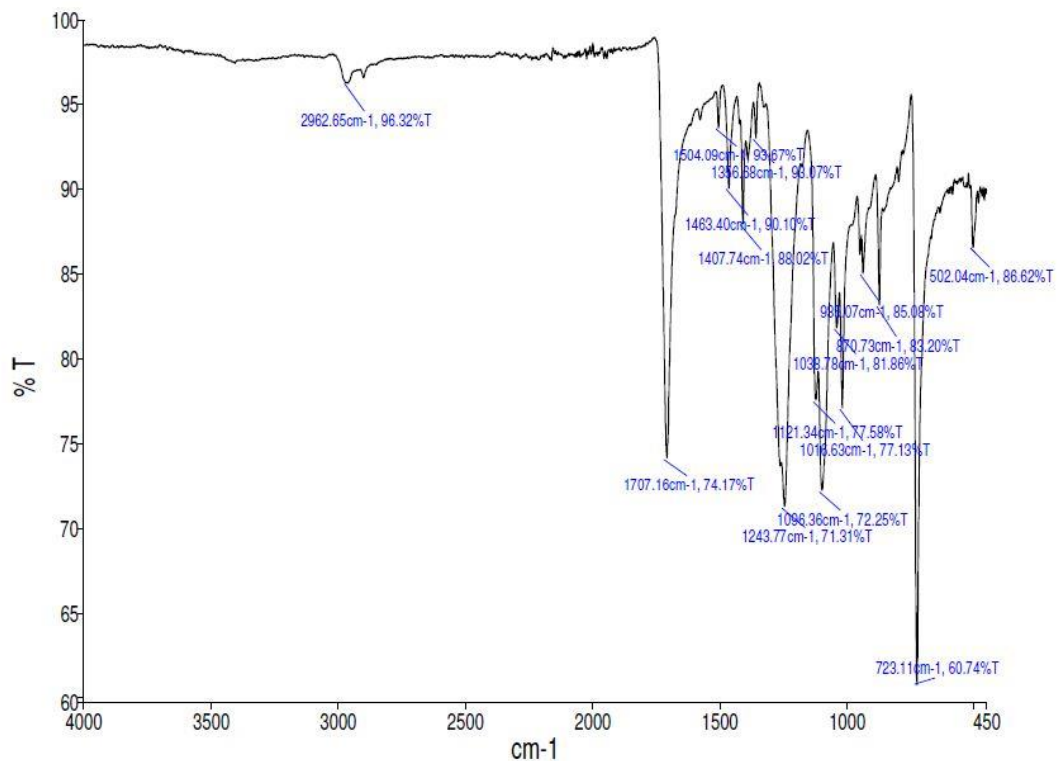


Figure 6.26: FT-IR spectrum for PTT dyed with Lac.

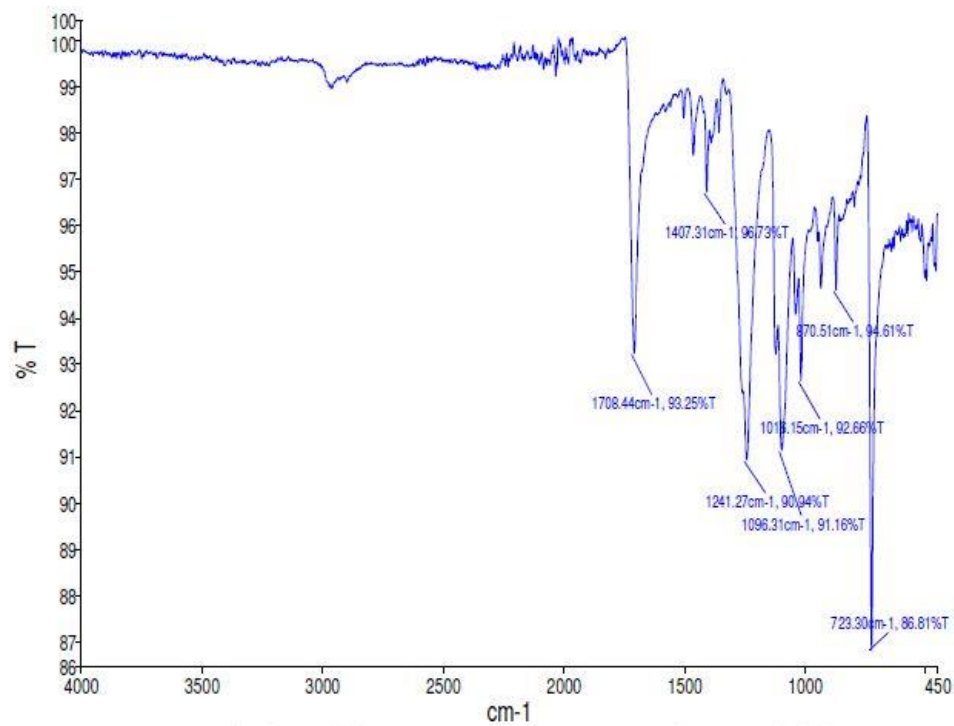


Figure 6.27: FT-IR spectrum for PTT dyed with Catechu.

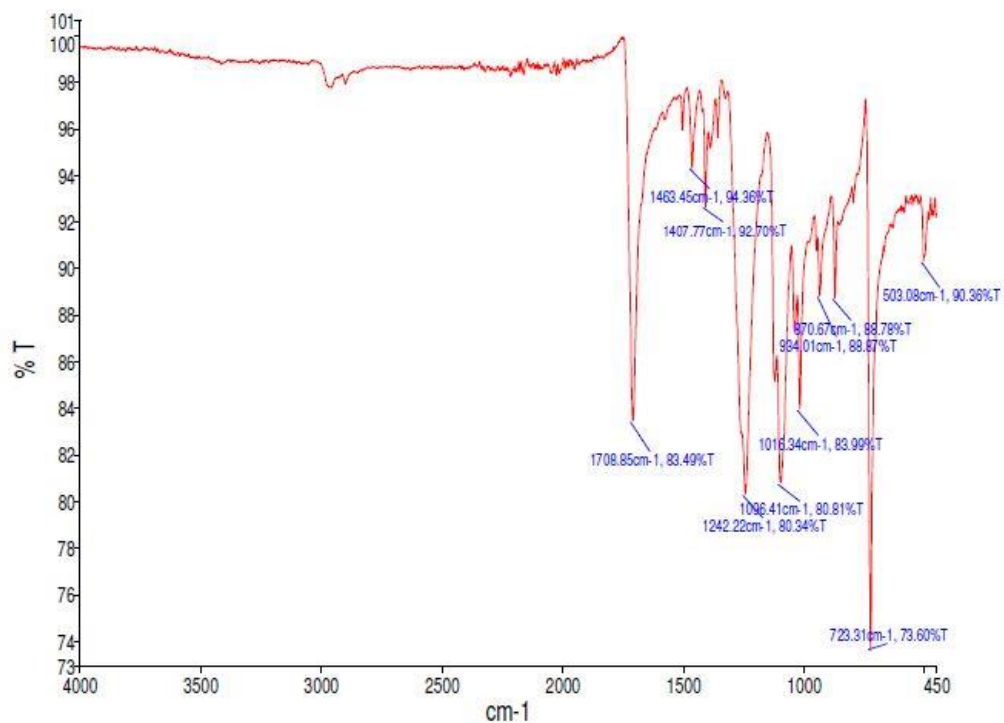


Figure 6.28: FT-IR spectrum for PTT dyed with Myrobalan.

When the FTIR spectra for PTT fibers dyed with natural dyes were compared to that of undyed fiber as in Figure 4.5, no significant changes in the spectra could be observed. The FT-IR spectra of PLA fibers were also similar to that of the undyed fiber as in Figure 4.6, with no significant change in the peaks were observed. This indicated that there was no chemical bonding formed during dyeing between either PTT or PLA with any of the natural dyes. Thus, the dyeing mechanism was similar to that of disperse dyes applied to PET, where the dyes entered the fiber by mere physical penetration.

6.2.4 Evaluation of adsorption isotherms

In order to further substantiate the findings of the FTIR spectra, the adsorption isotherms of PTT, PLA and PET with the natural dyes Lac, Catechu and Myrobalan, were evaluated. The isotherms for fibers dyed with Lac, Catechu and Myrobalan are shown in Figures 6.29, 6.30 and 6.31 respectively.

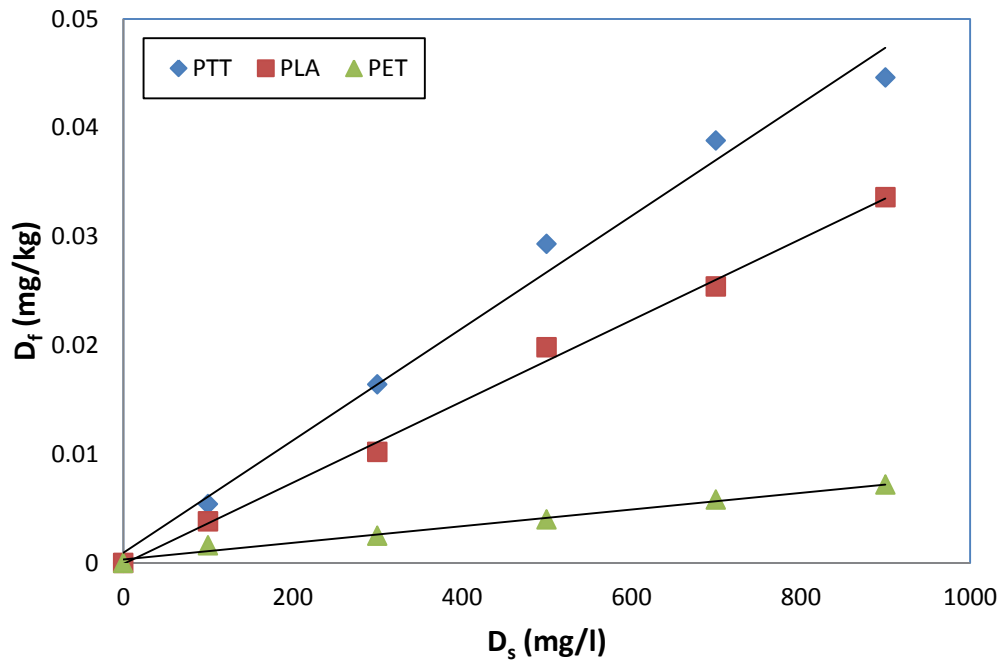


Figure 6.29: Adsorption isotherm of fibers dyed with Lac.

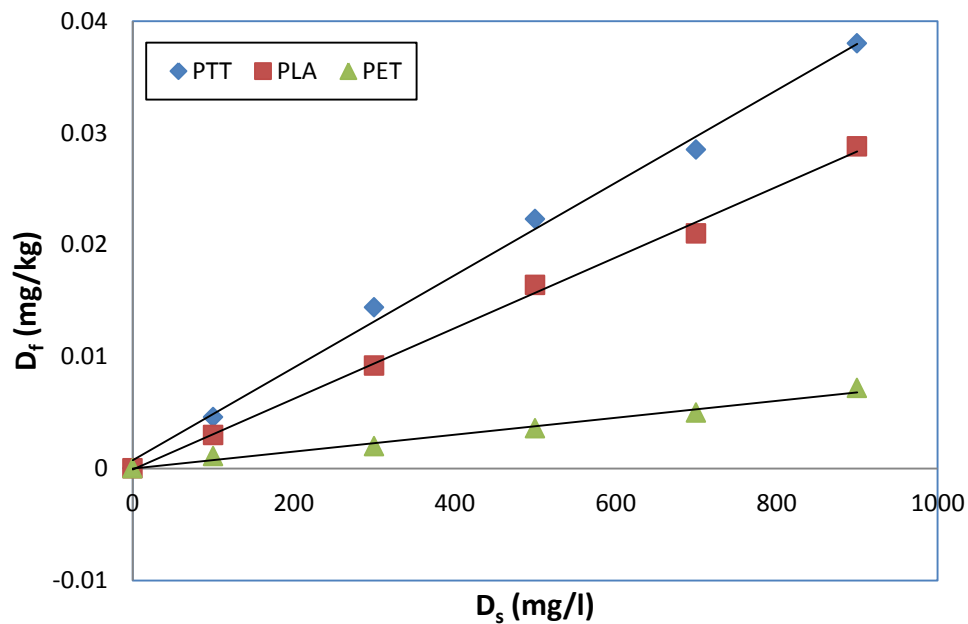


Figure 6.30: Adsorption isotherm of fibers dyed with Catechu.

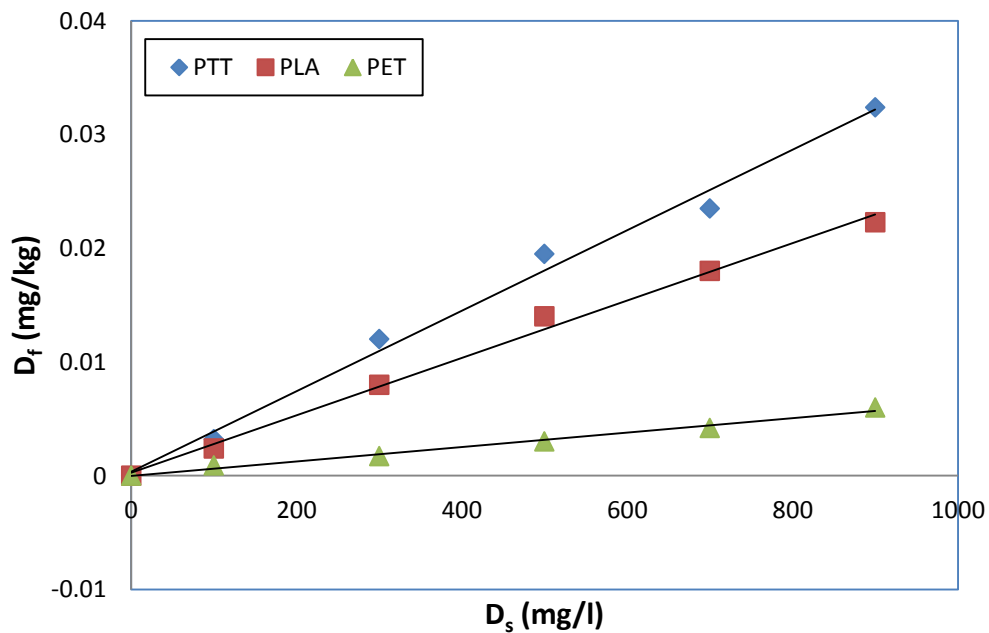


Figure 6.31: Adsorption isotherm of fibers dyed with Myrobalan.

It could be observed that the isotherms were linear in nature for all the fibers. The values for correlation coefficient (R^2 values) were also high indicating a good fit of the

linear models for the points obtained. The linearity of the adsorption isotherms obtained indicated that the adsorption of the selected natural dyes followed the Nernst adsorption isotherm model in case of all the fibers, as given in equation 2.9 [113]. It is well known that this model is followed when dyeing PET with disperse dyes. This model also indicated that there is no chemical bonding between the dye and the fiber, and dyeing occurred as a result of physical penetration of the dye molecules inside the fibers [113].

It could thus be inferred that in case of the selected natural dyes too, there was no chemical bonding that took place during dyeing of PTT, PLA or PET. Physical penetration was the only means of attachment between these fibers and the natural dyes. The observations were in sync with the findings of the FT-IR spectra for PTT and PLA, in which there were no indications of chemical bonding between the selected natural dyes and the fibers.

It could also be observed from the slope of the adsorption isotherms that the rate of dye uptake was higher in case of PTT than the other two fibers. For PET, the rate was found to be the lowest in case of all the three natural dyes selected. These observations were in concordance with the results observed while discussing the effects of various factors on the color strength of the three fibers, in which the K/S values of PTT with these natural dyes were the highest and those for PET the lowest in all the cases.

6.2.5 Pre-mordanting, meta-mordanting and post-mordanting with biomordants

In the application of natural dyes, mordants are often used. The mordants have the function of helping in binding the dyes strongly with the fibers. This improves the fastness properties of the natural dyes. Traditionally, biomordants have been used in the application of natural dyes, but later on, they were replaced by inorganic mordants. The

inorganic mordants were salts of iron, copper, aluminium, tin, chromium, etc. these salts could help in achieving better properties than the biomordants and in less time. Also, the inorganic mordants were available readily and in large quantities as compared to the biomordants which had to be extracted with difficulty, and were still available in limited quantities only.

In the present study, an objective was to assess the use of biomordants in the dyeing of PTT and PLA with natural dyes. The dyes chosen were Lac, Catechu and Myrobalan, while the biomordants selected were Catechu, Myrobalan and Pomegranate. Dyeing experiments were carried out with various combinations of one of these natural dyes and one of the biomordants for PTT and PLA. The fibers were thus dyed in combinations of Lac and Catechu (biomordant), and Myrobalan (biomordant), and Lac and Pomegranate (biomordant). Fibers were also dyed with Catechu and Myrobalan (biomordant), Catechu and Pomegranate (Biomordant) and Myrobalan and Pomegranate (biomordant).

6.2.5.1 Identification of suitable mordanting technique

In mordanting, there are three techniques that can be resorted to, as has been discussed earlier in section 1.3.1.2. In order to identify the technique of mordanting that would suit the combinations of dye and biomordant as mentioned above, PTT and PLA were dyed in pre-mordanting, meta-mordanting and post-mordanting techniques. The K/S values of the dyed fibers were then compared.

In pre-mordanting, the fiber was first treated with the biomordant at 120^oC with initial pH of the dye bath at 6 and material to liquor ratio of 1:40 and for 30 min. The treated fiber was then washed with distilled water, acetic acid solution (10% v/v) and

again with distilled water. The treated fiber sample was then dried in air, followed by dyeing with the chosen natural dye under the same conditions as above, viz. temperature of 120°C, initial pH of the dye bath of 6, time of 30 min and material to liquor ratio of 1:40.

In meta-mordanting, the natural dye and the biomordant selected were applied to the fibers the same dye bath, with the dyeing conditions, viz. temperature, initial pH of dye bath, time and material to liquor ratio, identical to pre-mordanting. In post-mordanting, the fiber was first dyed with the natural dye selected, washed and dried in air, followed by treatment with the selected biomordant. The dyeing conditions were again kept identical to pre-mordanting and meta-mordanting both during dyeing and treatment with biomordant.

In case of each of the natural dye-biomordant combination used here, a fiber sample each for PTT and PLA was also dyed with no biomordant used, and the K/S values of the dyed sample compared to the ones with biomordanting. The results for all of the six combinations of natural dyes and biomordants applied on PTT and PLA are depicted in Figures 6.32-6.37.

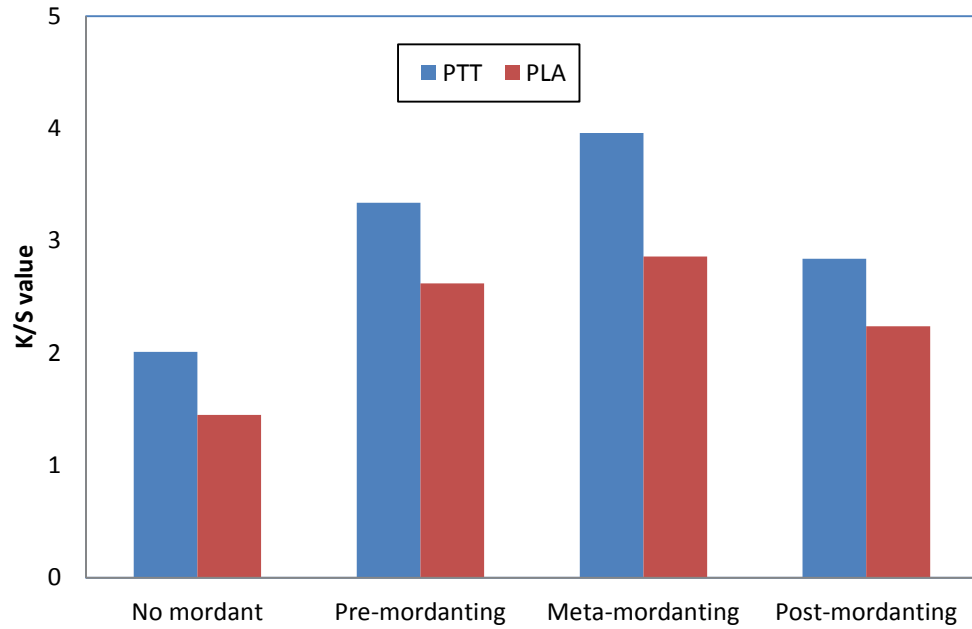


Figure 6.32: K/S values with Lac and Catechu (biomordant).

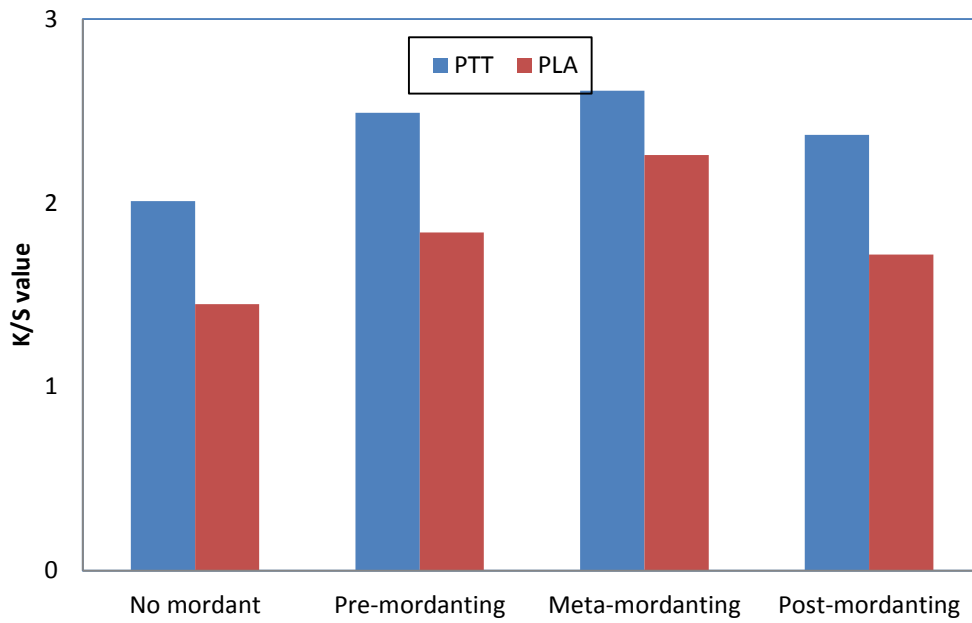


Figure 6.33: K/S values with Lac and Myrobalan (biomordant).

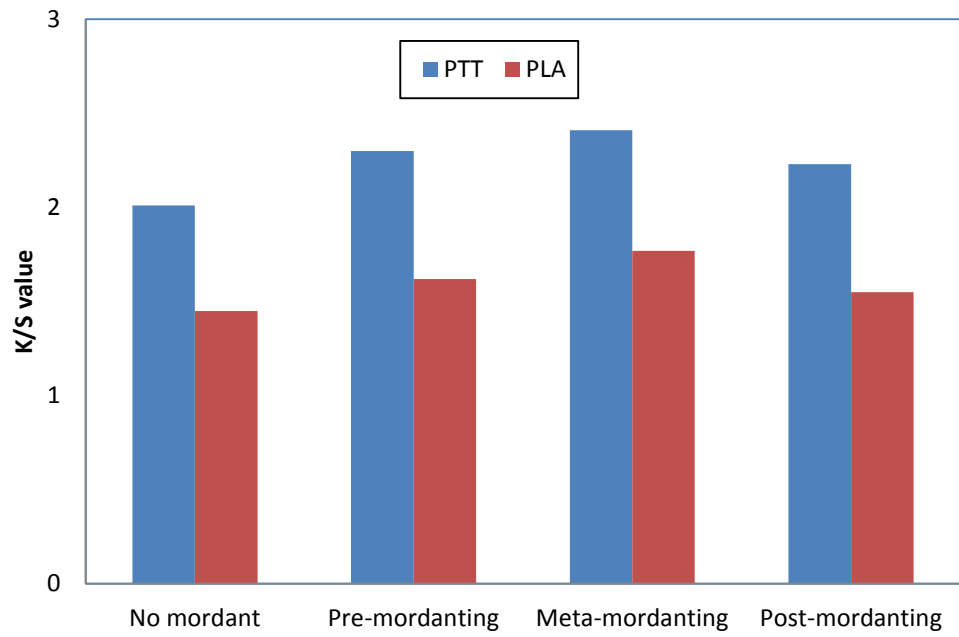


Figure 6.34: K/S values with Lac and Pomegranate (biomordant).

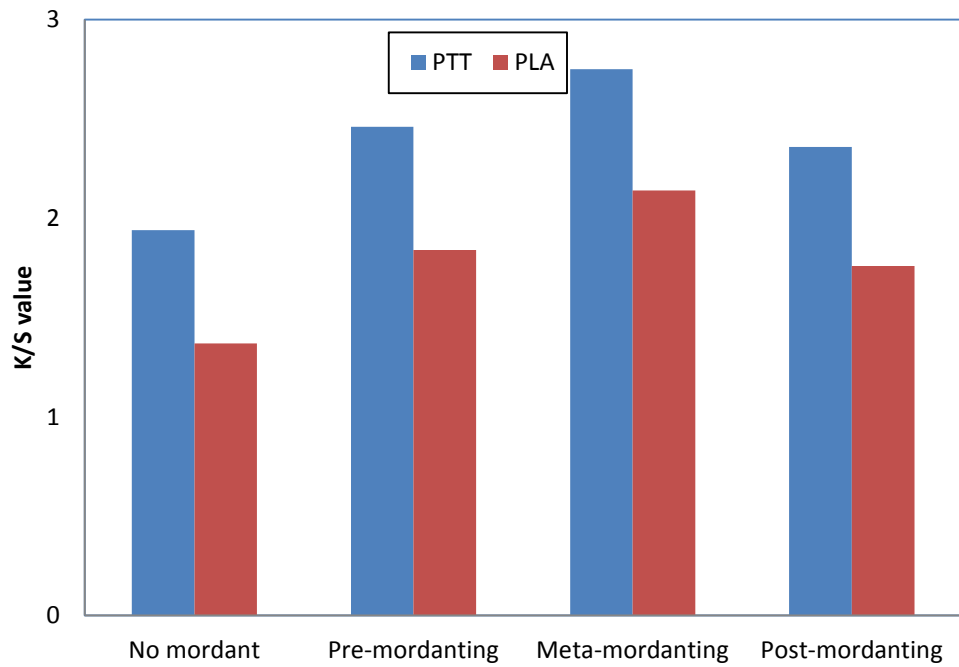


Figure 6.35: K/S values with Catechu and Myrobalan (biomordant).

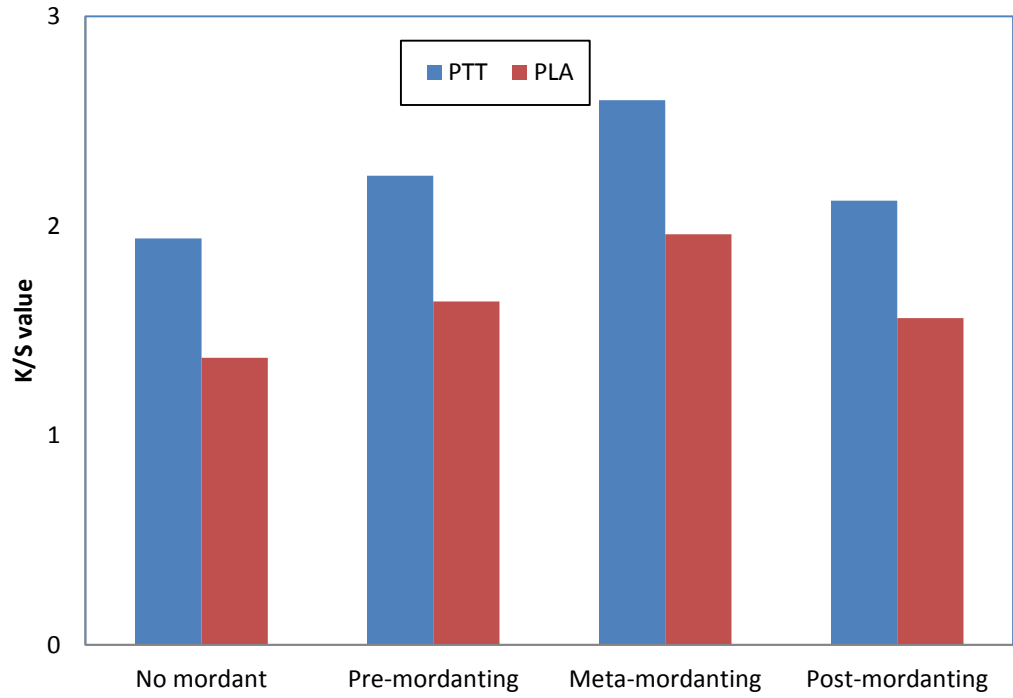


Figure 6.36: K/S values with Catechu and Pomegranate (biomordant).

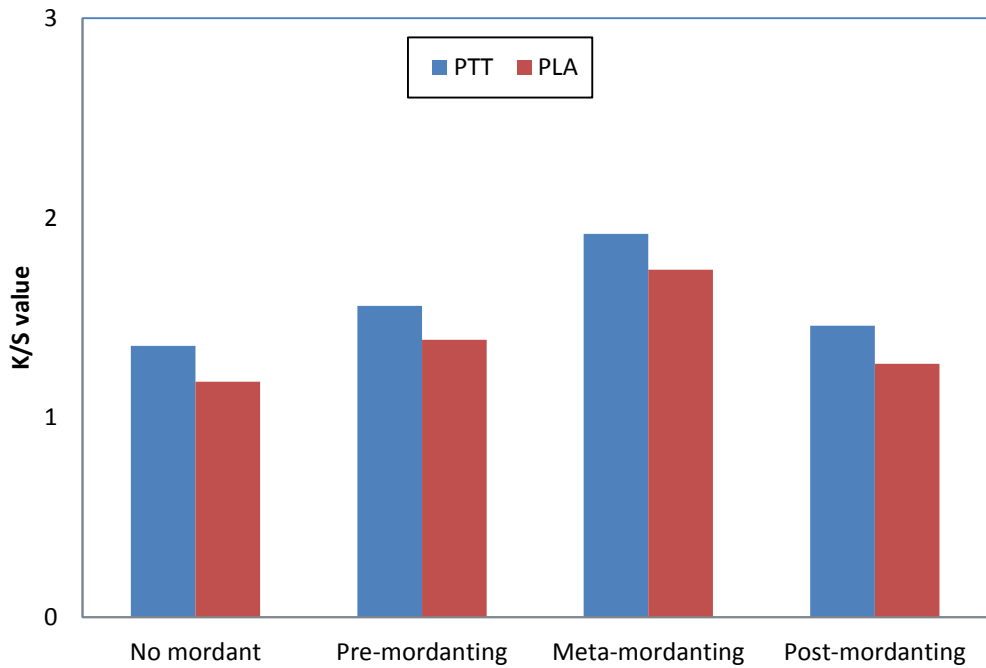


Figure 6.37: K/S values with Myrobalan and Pomegranate (biomordant).

The results with all of the combinations of natural dyes and biomordants for PTT fiber indicated that the color strength increased when biomordants were applied in dyeing. The K/S values were higher than when no mordant was applied for all the cases. However, a considerable increase in K/S value was observed with the meta-mordanting technique, where the dye and the biomordant were applied simultaneously in the same dye bath. The same trend was observed in case of PLA too with all of the dyes. With pre-mordanting, the increase in K/S value was lesser than with meta-mordanting in case of both the fibers. Also, the increase in K/S value with post-mordanting was not substantial in any of the cases.

6.2.5.2 Evaluation of fastness properties

The wash fastness, perspiration fastness, and fastness to acids, alkalis and hydrogen peroxide bleaching were also evaluated for the fibers dyed using the three natural dyes and biomordants with all the three techniques of mordanting, as above. The legend for the tables with results of the fastness properties are given in Table 6.6 and the results for PTT and PLA fibers for the various fastness properties evaluated are shown in Tables 6.7 to 6.12.

Table 6.7: Legend for Tables 6.7 and 6.12.

Symbol	Full name
CC	Color change
CS	Color stain
W	Wool
A	Acrylic
P	Polyester (PET)
N	Nylon
C	Cotton
T	Cellulose triacetate

Table 6.7: Results for wash fastness of PTT for pre-, meta- and post-mordanting.

Dye	Biomordant	Technique	Wash fastness						
			CC	CS					
				W	A	P	N	C	T
Lac	Catechu	Pre-	4-5	4-5	5	5	4-5	4	4
		Meta-	4-5	4-5	5	5	4-5	4	4-5
		Post-	4	4	5	5	4-5	4	4
Lac	Myrobalan	Pre-	4	4-5	5	5	4-5	4	4
		Meta-	4-5	4-5	5	5	4-5	4	4-5
		Post-	4	4	5	5	4	3-4	4
Lac	Pomegranate	Pre-	4	4	5	5	4	4	4
		Meta-	4-5	4-5	5	5	4-5	4	4-5
		Post-	4	4	5	5	4	3-4	4
Catechu	Myrobalan	Pre-	4-5	4	5	5	4-5	4	4
		Meta-	4-5	4-5	5	5	4-5	4	4-5
		Post-	4	4	5	5	4	4	4
Catechu	Pomegranate	Pre-	4	4-5	5	5	4	4	4
		Meta-	4	4-5	5	5	4-5	4	4-5
		Post-	3-4	4	5	5	4	3-4	3-4
Myrobalan	Pomegranate	Pre-	4	4	5	5	4	4	4
		Meta-	4-5	4-5	5	5	4-5	4	4-5
		Post-	3-4	4	5	5	4	3-4	3-4

Table 6.8: Results for wash fastness of PLA for pre-, meta- and post-mordanting.

Dye	Biomordant	Technique	Wash fastness						
			CC	CS					
				W	A	P	N	C	T
Lac	Catechu	Pre-	4	4	5	5	4	4	4-5
		Meta-	4-5	4-5	5	5	4-5	4	4-5
		Post-	4	4	5	5	4	4	4
Lac	Myrobalan	Pre-	4	4	5	5	4	4	4
		Meta-	4-5	4-5	5	5	4-5	4	4-5
		Post-	4	4	5	5	4	3-4	4
Lac	Pomegranate	Pre-	4	4	5	5	4	4	3-4
		Meta-	4-5	4-5	5	5	4-5	4	4
		Post-	3-4	3-4	5	5	4	3-4	3-4
Catechu	Myrobalan	Pre-	4	4	5	5	4	4	4
		Meta-	4-5	4-5	5	5	4-5	4	4-5
		Post-	4	4	5	5	4	4	4
Catechu	Pomegranate	Pre-	4	4-5	5	5	4	4	4
		Meta-	4-5	4-5	5	5	4-5	4	4-5
		Post-	4	4	5	5	4	3-4	3-4
Myrobalan	Pomegranate	Pre-	4	3-4	5	5	4	4	4
		Meta-	4-5	4-5	5	5	4-5	4	4-5
		Post-	3-4	3-4	5	5	3-4	3-4	3-4

Table 6.9: Results for perspiration fastness of PTT for pre-, meta- and post-mordanting.

Dye	Biomordant	Technique	Perspiration Fastness						
			CC	CS					
				W	A	P	N	C	T
Lac	Catechu	Pre-	4-5	4	5	5	4	4	4
		Meta-	4-5	4-5	5	5	4-5	4	4-5
		Post-	4	4	5	5	4	4	4
Lac	Myrobalan	Pre-	4	4	5	5	4	4	4
		Meta-	4-5	4-5	5	5	4-5	4	4-5
		Post-	4	4	5	5	4	3-4	4
Lac	Pomegranate	Pre-	4	4	5	5	4	4	4
		Meta-	4-5	4-5	5	5	4-5	4	4
		Post-	4	4	5	5	4	3-4	4
Catechu	Myrobalan	Pre-	4-5	4	5	5	4	4	4
		Meta-	4-5	4-5	5	5	4-5	4	4-5
		Post-	4	4	5	5	4	4	4
Catechu	Pomegranate	Pre-	4	4	5	5	4	4	4
		Meta-	4-5	4-5	5	5	4-5	4	4-5
		Post-	4	3-4	5	5	3-4	3-4	4
Myrobalan	Pomegranate	Pre-	4	4	5	5	4	3-4	4
		Meta-	4	4-5	5	5	4-5	4	4-5
		Post-	3-4	3-4	5	5	3-4	3-4	3-4

Table 6.10: Results for perspiration fastness of PLA for pre-, meta- and post-mordanting.

Dye	Biomordant	Technique	Wash fastness						
			CC	CS					
				W	A	P	N	C	T
Lac	Catechu	Pre-	4	4	5	5	4	4	4
		Meta-	4-5	4-5	5	5	4-5	4	4-5
		Post-	4	4	5	5	4	4	4
Lac	Myrobalan	Pre-	4	4	5	5	4	4	4
		Meta-	4-5	4-5	5	5	4-5	4	4-5
		Post-	4	4	5	5	4	4	4
Lac	Pomegranate	Pre-	4	4	5	5	4	4	4
		Meta-	4-5	4-5	5	5	4-5	4	4-5
		Post-	3-4	3-4	5	5	3-4	3-4	3-4
Catechu	Myrobalan	Pre-	4	4	5	5	4	4	4
		Meta-	4-5	4-5	5	5	4-5	4	4-5
		Post-	4	4	5	5	4	4	4
Catechu	Pomegranate	Pre-	4	4	5	5	4	4	4
		Meta-	4-5	4-5	5	5	4-5	4	4-5
		Post-	4	3-4	5	5	3-4	3-4	3-4
Myrobalan	Pomegranate	Pre-	4	4	5	5	4	3-4	4
		Meta-	4-5	4-5	5	5	4-5	4	4-5
		Post-	3-4	3-4	5	5	3-4	3-4	3-4

Table 6.11: Results for fastness to acids, alkalis and hydrogen peroxide bleaching of PTT
for pre-, meta- and post-mordanting.

Dye	Biomordant	Technique	Fastness to acids	Fastness to alkalis	Fastness to Hydrogen peroxide bleaching	
			CC	CC	CC	CS
Lac	Catechu	Pre-	4-5	4	4	4
		Meta-	4-5	4	4	4-5
		Post-	4	3-4	3-4	4
Lac	Myrobalan	Pre-	4	3-4	4	4
		Meta-	4-5	4	4	4
		Post-	4	3-4	3-4	4
Lac	Pomegranate	Pre-	4	3-4	3-4	4
		Meta-	4-5	3-4	4	4
		Post-	4	3-4	3-4	3-4
Catechu	Myrobalan	Pre-	4	3-4	4	4
		Meta-	4-5	4	4	4
		Post-	4	3-4	3-4	4
Catechu	Pomegranate	Pre-	4	3-4	4	4
		Meta-	4-5	4	4	4
		Post-	3-4	3	3-4	3-4
Myrobalan	Pomegranate	Pre-	4	3-4	3-4	3-4
		Meta-	4-5	3-4	4	4
		Post-	3-4	3	3-4	3-4

Table 6.12: Results for fastness to acids, alkalis and hydrogen peroxide bleaching of PLA for pre-, meta- and post-mordanting.

Dye	Biomordant	Technique	Fastness to acids	Fastness to alkalis	Fastness to Hydrogen peroxide bleaching	
			CC	CC	CC	CS
Lac	Catechu	Pre-	4	4	4	4
		Meta-	4-5	4	4-5	4-5
		Post-	4	3-4	4	4
Lac	Myrobalan	Pre-	4	3-4	4	4
		Meta-	4-5	4	4	4-5
		Post-	4	3-4	3-4	4
Lac	Pomegranate	Pre-	4	3-4	3-4	4
		Meta-	4-5	4	4	4
		Post-	3-4	3-4	3-4	3-4
Catechu	Myrobalan	Pre-	4	3-4	3-4	4
		Meta-	4-5	4	4	4
		Post-	3-4	3-4	3-4	3-4
Catechu	Pomegranate	Pre-	4	3-4	3-4	3-4
		Meta-	4	4	4	4
		Post-	3-4	3	3-4	3-4
Myrobalan	Pomegranate	Pre-	4	3-4	3-4	3-4
		Meta-	4	4	4	4
		Post-	3-4	3	3-4	3-4

It could be observed with pre- and post-mordanting, the values were better than samples without any mordant. However, the superior values could be observed in case of meta-mordanting in all the cases. Also, the fastness properties with pre-mordanting were better than post-mordanting. It could thus be concluded that meta-mordanting was the most suitable technique for the use of the biomordants used here with the selected natural dyes for PTT and PLA.

6.2.5.3 Measurement of color values of meta-mordanted samples

The CIE L*a*b*, C* and h° values of some representative samples of PTT and PLA fibers dyed with the six different combinations of natural dyes and biomordants, as discussed above, are given in Table 6.13. In all the cases, meta-mordanting technique was used while using the biomordants. They were dyed at 120°C with initial pH of 5, dyeing time of 30 min, material to liquor ratio at 1:40 and mordant concentration of 9% owf..

Table 6.13: CIE L*a*b* values of PTT and PLA fibers with three natural dyes and biomordants.

Fiber	Dye	Biomordant	L*	a*	b*	C*	h°
PTT	Lac	Catechu	50.80	12.86	9.07	15.74	35.20
	Lac	Myrobalan	45.59	8.35	3.49	9.06	22.70
	Lac	Pomegranate	46.09	10.08	7.43	12.52	36.42
	Catechu	Myrobalan	52.86	9.26	11.89	15.07	52.07
	Catechu	Pomegranate	61.04	7.32	13.65	15.49	61.81
	Myrobalan	Pomegranate	60.87	2.81	13.82	14.11	78.51
PLA	Lac	Catechu	48.94	13.73	12.18	18.35	41.57
	Lac	Myrobalan	50.53	9.38	8.03	12.35	40.55
	Lac	Pomegranate	49.32	6.64	7.86	10.29	49.81
	Catechu	Myrobalan	58.89	11.56	15.83	19.60	53.87
	Catechu	Pomegranate	55.82	4.70	10.56	11.56	66.01
	Myrobalan	Pomegranate	65.86	1.37	13.64	13.71	84.27

6.2.6 Comparison of color strength with inorganic mordants

In order to find out whether the use of biomordant in application of natural dyes on PTT and PLA was justified, it was felt that there was a need to compare the color strength obtained using biomordants with that achieved using inorganic mordants. Thus, PTT and PLA were dyed with biomordants as well as inorganic mordants using the selected natural dyes, and the K/S values obtained compared. The dyes chosen in this case were also Lac, Catechu and Myrobalan. The biomordants selected were Catechu, Myrobalan and Pomegranate. The inorganic mordants used were alum or aluminium potassium sulphate [$\text{AlK}(\text{SO}_4)_2 \cdot 12\text{H}_2\text{O}$], ferrous sulfate ($\text{FeSO}_4 \cdot 7\text{H}_2\text{O}$) and stannous chloride ($\text{SnCl}_2 \cdot 5\text{H}_2\text{O}$).

In case of dyeing with Lac, the biomordants used were Catechu, Myrobalan and Pomegranate. While dyeing with Catechu, Myrobalan and Pomegranate were used as biomordants. With Myrobalan used as the natural dye, Catechu and Pomegranate were used as biomordants. The mordanting technique used was meta-mordanting, as observed in the section 6.2.5. Since in this case, the natural dye and the biomordant were applied to the fibers in the same bath, the values for Myrobalan-Catechu combination were the same when either of them was used as the natural dye and the other as the biomordant. These readings are shown in both cases where Myrobalan and Catechu were used as the natural dye respectively.

With the above fiber samples dyed, the effects of temperature, initial pH of the dye bath, time of dyeing, material to liquor ratio as well as mordant concentration, expressed as the percentage on weight of the fiber (% owf), were evaluated. Dyeing was carried out not only for PTT and PLA but also PET for comparison of the color strength

achieved. Also, in case of each of the natural dyes, one fiber sample was also dyed without using any biomordant or inorganic mordant while observing the effects of temperature, initial pH of dye bath, time and material to liquor ratio. For assessing the effect of mordant concentration, this could not be done. In each case, five experiments were carried out and the average values reported in the tables given in the Appendix.

The effects of various factors on the dyed fibers are discussed in the following sections. The coding used for the samples and their descriptions are given in Table 6.14.

Table 6.14: Coding used for dyed fiber samples.

Code	Natural dye	Mordant	Figure no. for PTT	Figure no. for PLA
Lac	Lac	No mordant	6.38 (a)	6.41 (a)
Lac+Cat	Lac	Catechu	6.38 (b)	6.41 (b)
Lac+Myr	Lac	Myrobalan	6.38 (c)	6.41 (c)
Lac+Pom	Lac	Pomegranate	6.38 (d)	6.41 (d)
Lac+Al	Lac	Alum	6.38 (e)	6.41 (e)
Lac+Fe	Lac	Ferrous sulfate	6.38 (f)	6.41 (f)
Lac+Sn	Lac	Stannous chloride	6.38 (g)	6.41 (g)
Cat	Catechu	No mordant	6.39 (a)	6.42 (a)
Cat+Myr	Catechu	Myrobalan	6.39 (b)	6.42 (b)
Cat+Pom	Catechu	Pomegranate	6.39 (c)	6.42 (c)
Cat+Al	Catechu	Alum	6.39 (d)	6.42 (d)
Cat+Fe	Catechu	Ferrous sulfate	6.39 (e)	6.42 (e)
Cat+Sn	Catechu	Stannous chloride	6.39 (f)	6.42 (f)
Myr	Myrobalan	No mordant	6.40 (a)	6.43 (a)
Myr+Cat	Myrobalan	Catechu	6.40 (b)	6.43 (b)
Myr+Pom	Myrobalan	Pomegranate	6.40 (c)	6.43 (c)
Myr+Al	Myrobalan	Alum	6.40 (d)	6.43 (d)
Myr+Fe	Myrobalan	Ferrous sulfate	6.40 (e)	6.43 (e)
Myr+Sn	Myrobalan	Stannous chloride	6.40 (f)	6.43 (f)

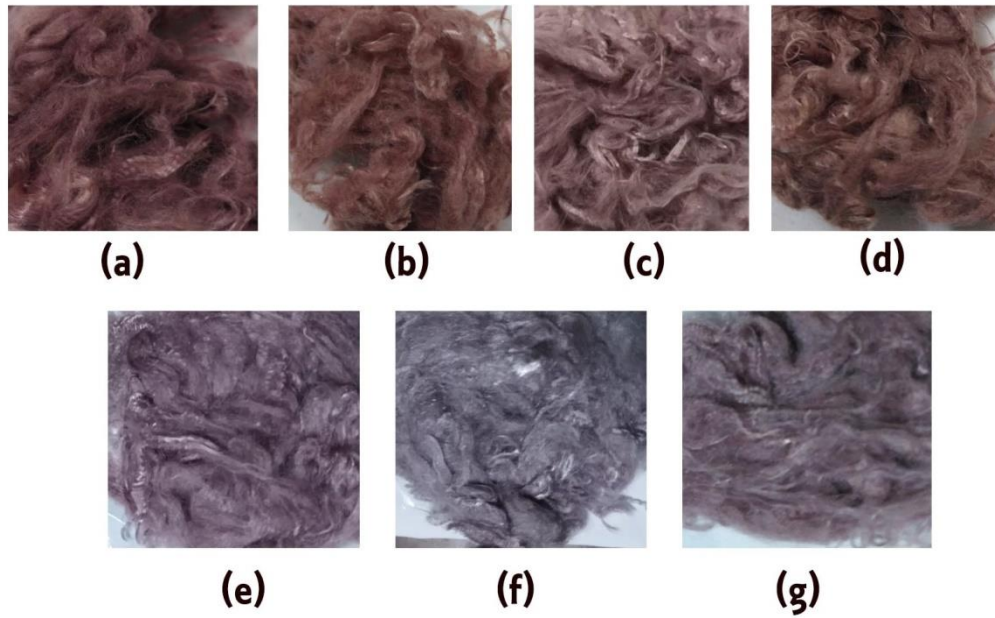


Figure 6.38: Shades of PTT with Lac using different mordants.

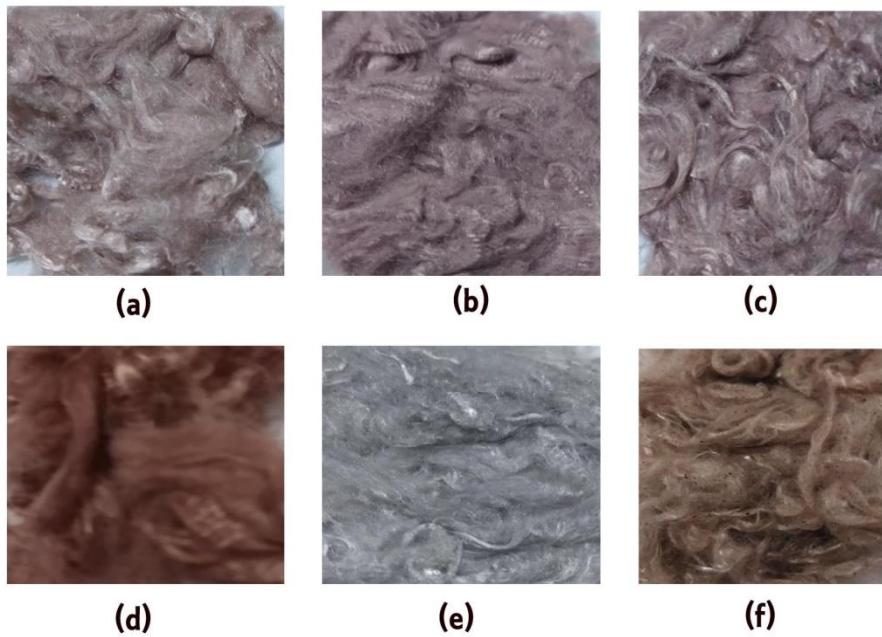


Figure 6.39: Shades of PTT with Catechu using different mordants.

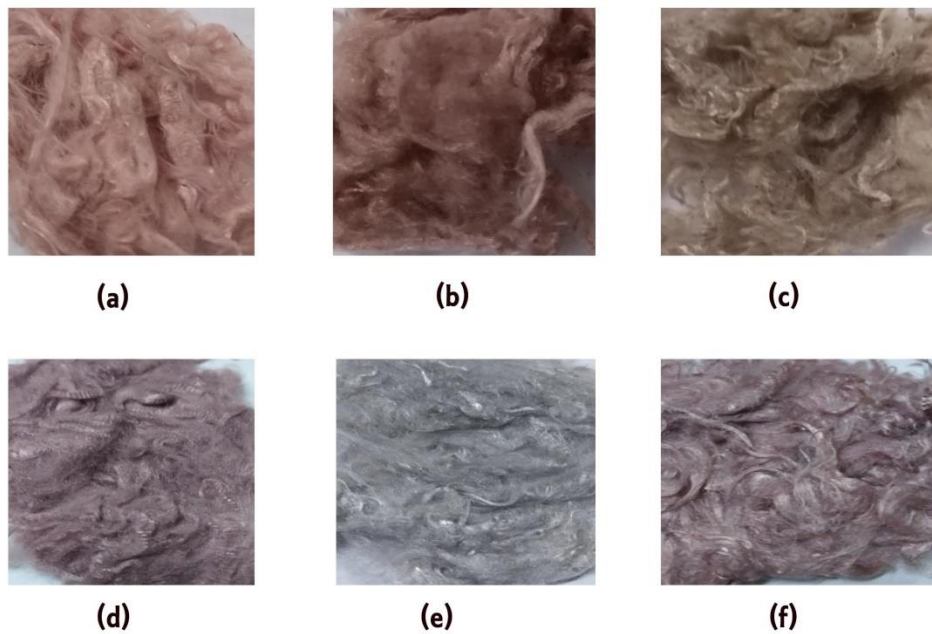


Figure 6.40: Shades of PTT with Myrobalan using different mordants.



Figure 6.41: Shades of PLA with Lac using different mordants.

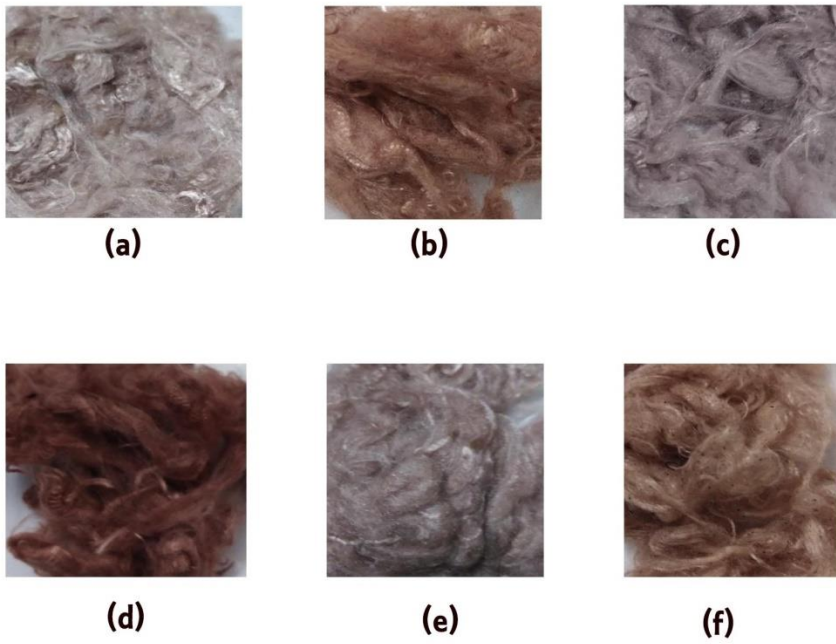


Figure 6.42: Shades of PLA with Catechu using different mordants.

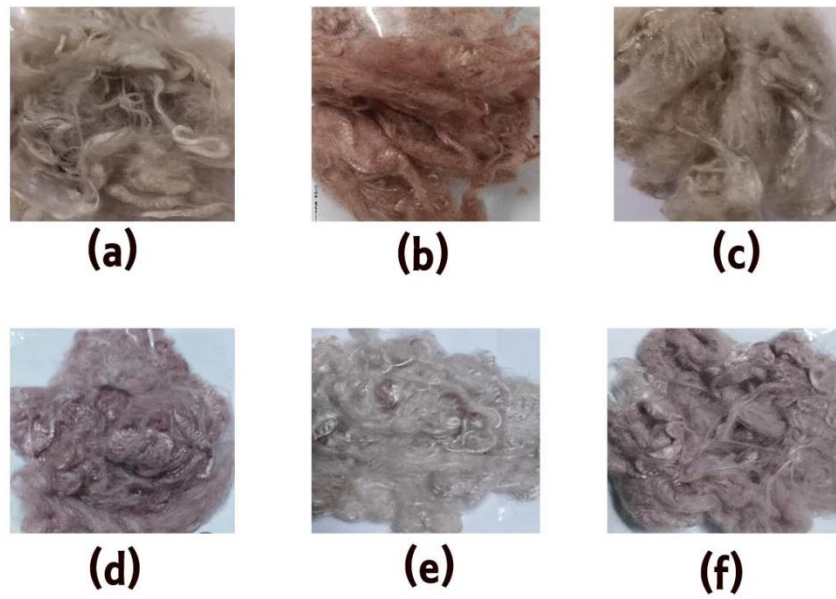


Figure 6.43: Shades of PLA with Myrobalan using different mordants.

6.2.6.1 Effect of temperature

In order to assess the effect of temperature on the K/S values of PTT, PLA and PET, dyeing experiments were carried out at 90°C, 100°C, 110°C, 120°C and 130°C, keeping other factors constant at their middle levels, as subsequently used in further experiments. Thus, the initial pH of the dye bath was kept at 5, time at 45 min, material to liquor ratio at 1:30 and mordant concentration at 9 % owf. The results for the three fibers with Lac used as the natural dye are shown in Figures 6.44, 6.45 and 6.46.

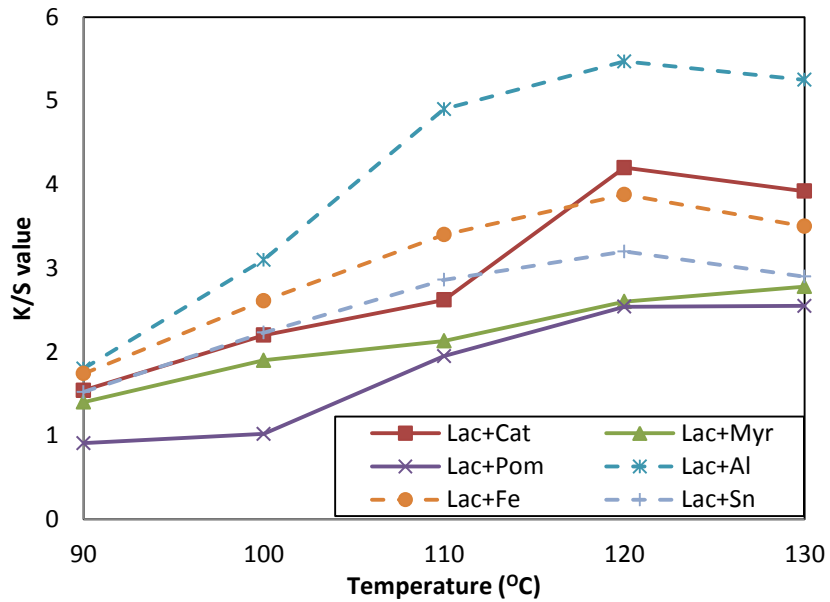


Figure 6.44: Effect of temperature on K/S value of PTT with Lac.

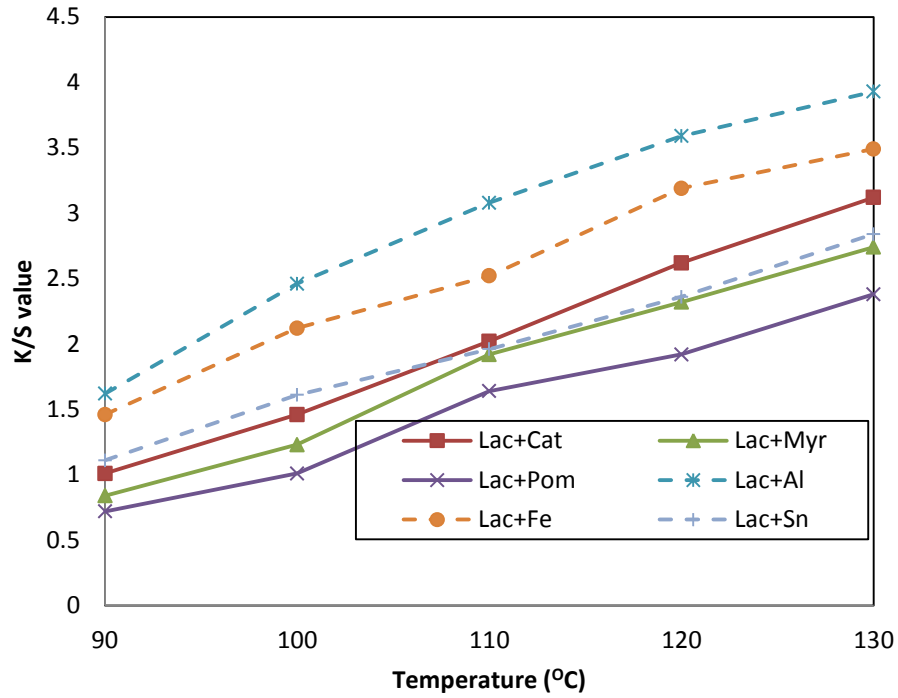


Figure 6.45: Effect of temperature on K/S value of PLA with Lac.

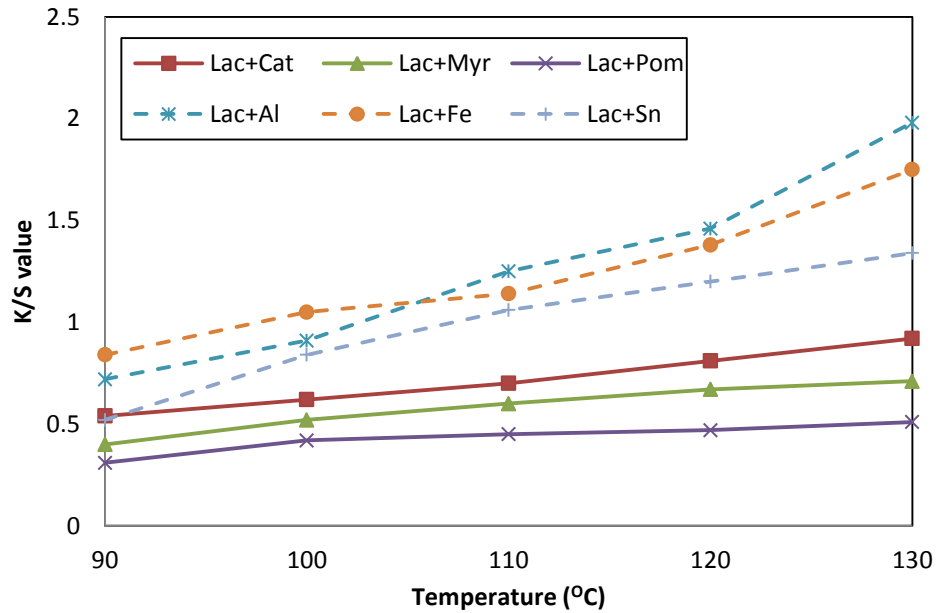


Figure 6.46: Effect of temperature on K/S value of PET with Lac.

The results for the three fibers with Catechu used as the natural dye are shown in Figures 6.47, 6.48 and 6.49 for PTT, PLA and PET respectively.

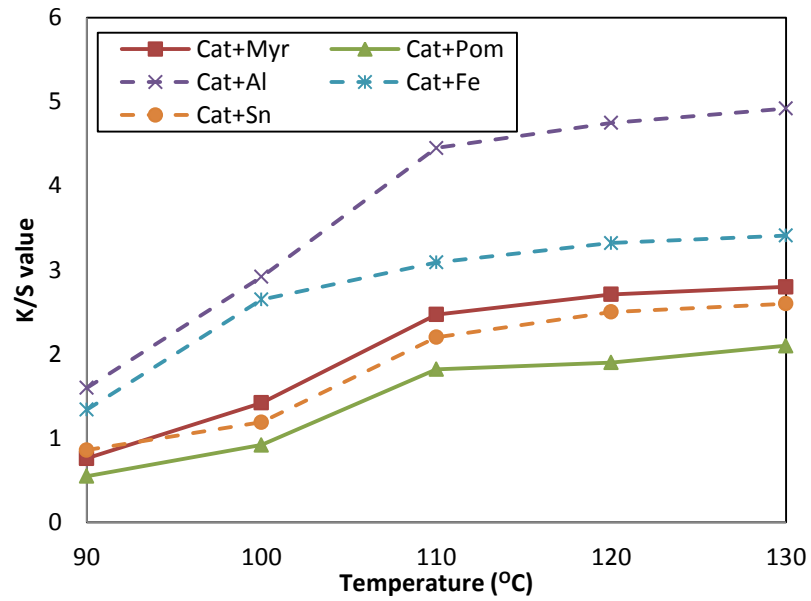


Figure 6.47: Effect of temperature on K/S value of PTT with Catechu.

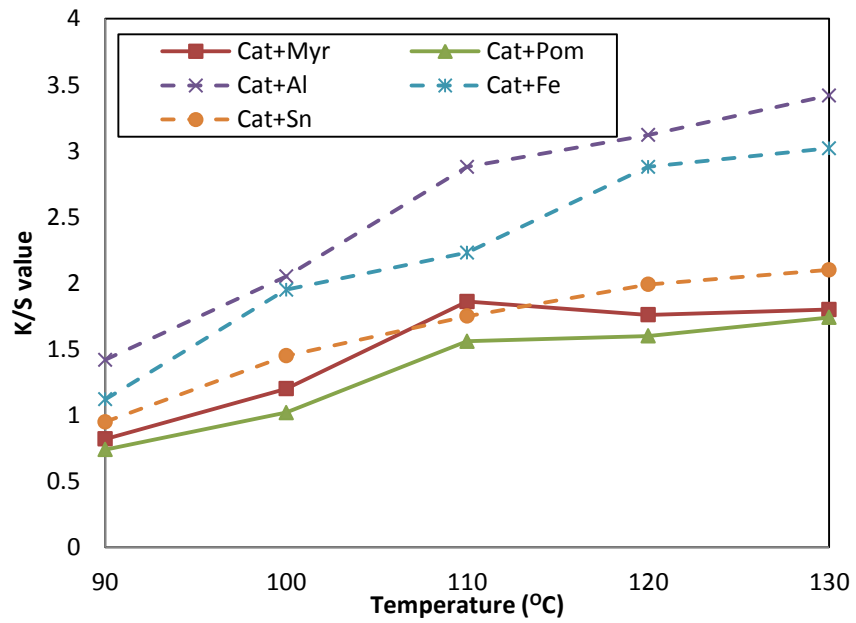


Figure 6.48: Effect of temperature on K/S value of PLA with Catechu.

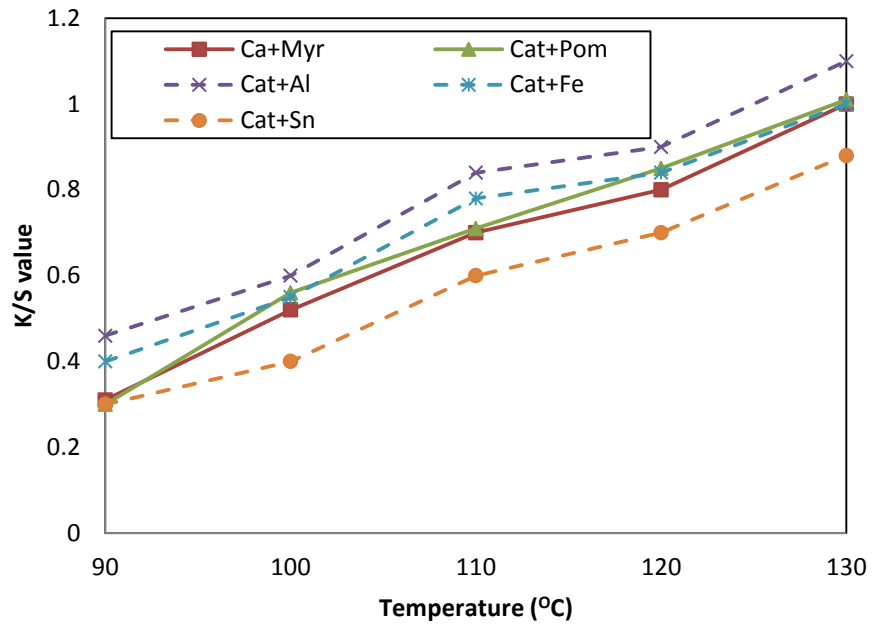


Figure 6.49: Effect of temperature on K/S value of PET with Catechu.

The results for the three fibers with Myrobalan used as the natural dye are shown in Figures 6.50, 6.51 and 6.52 for PTT, PLA and PET respectively.

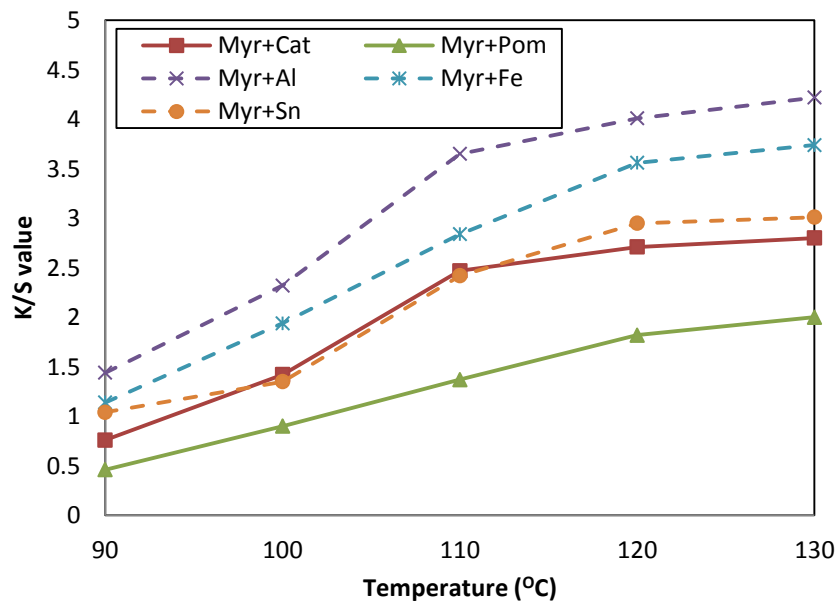


Figure 6.50: Effect of temperature on K/S value of PTT with Myrobalan.

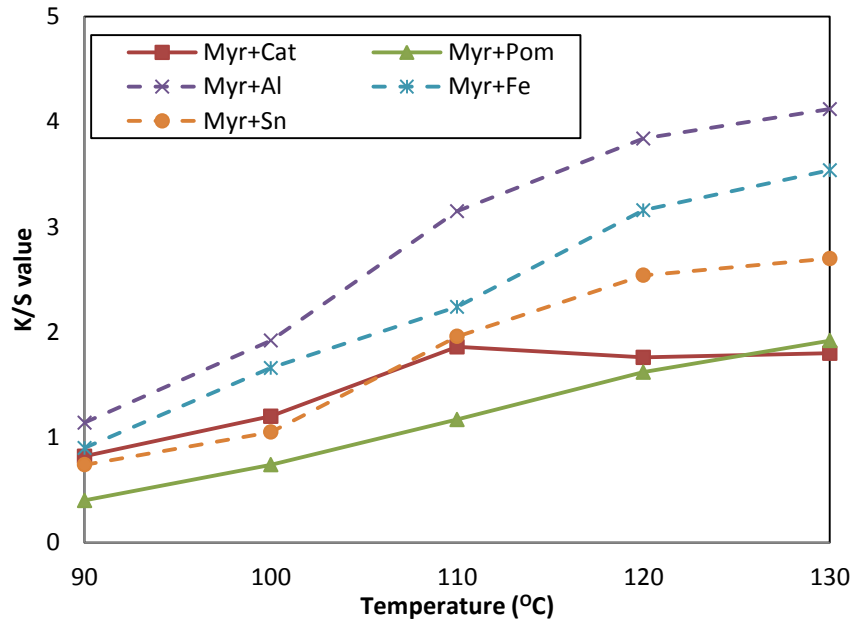


Figure 6.51: Effect of temperature on K/S value of PLA with Myrobalan.

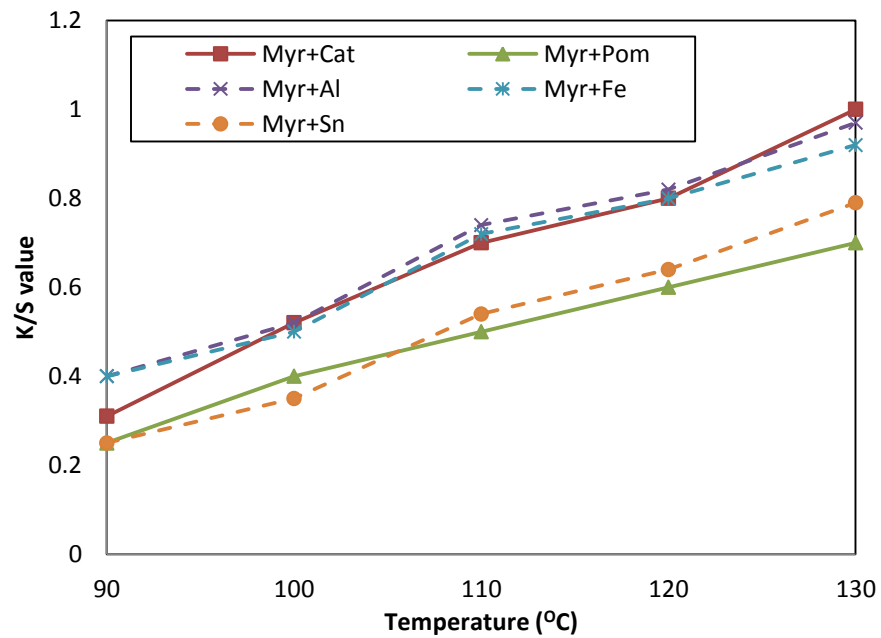


Figure 6.52: Effect of temperature on K/S value of PET with Myrobalan.

The results indicated that with rise in temperature, the K/S value increased for the fibers with all combinations of mordants and for all the dyes employed. The increase was

however found to be less sharp at temperatures above 110^oC for PTT and PLA. In case of PET, the increase was similar across all the levels of temperatures applied. This indicated that for PET, higher temperature was required for dyeing than for PTT and PLA. Also, the K/S values obtained with PET was inferior in all cases than PTT and PLA.

It could also be seen that with Catechu as a biomordant for Lac and with Catechu-Myrobalan combination, the K/S values obtained were very close to those with stannous chloride for PTT and PLA. The values with alum and ferrous sulfate were higher in all cases than the biomordants. In case of PET also, the K/S values were less with the biomordants.

It could thus be inferred that Catechu had the potential to exhibit similar K/S values as stannous chloride, an inorganic mordant, when used in application of the natural dyes, Lac and Myrobalan, on PTT and PLA. It could thus replace some of the inorganic mordants in dyeing of selected natural dyes for these fibers.

6.2.6.2 Effect of initial pH of the dye bath

For evaluation of the effect of initial pH of the dye bath on the K/S value of the dyed fibers, experiments were carried out at five different levels of initial pH of the dye bath, viz. 3, 4, 5, 6 and 7. The dyeing temperature was kept at 110^oC, time at 45 min, material to liquor ratio at 1:30 and mordant concentration at 9% owf. The results obtained for PTT, PLA and PET with Lac as the natural dye are given in Figures 6.53, 6.54 and 6.55.

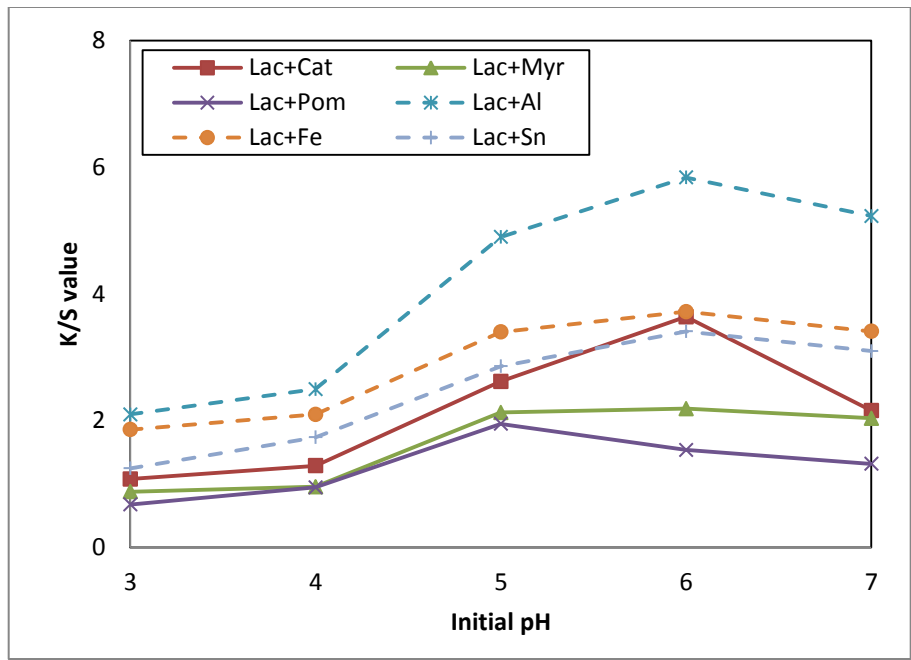


Figure 6.53: Effect of initial pH of dye bath on K/S value of PTT with Lac.

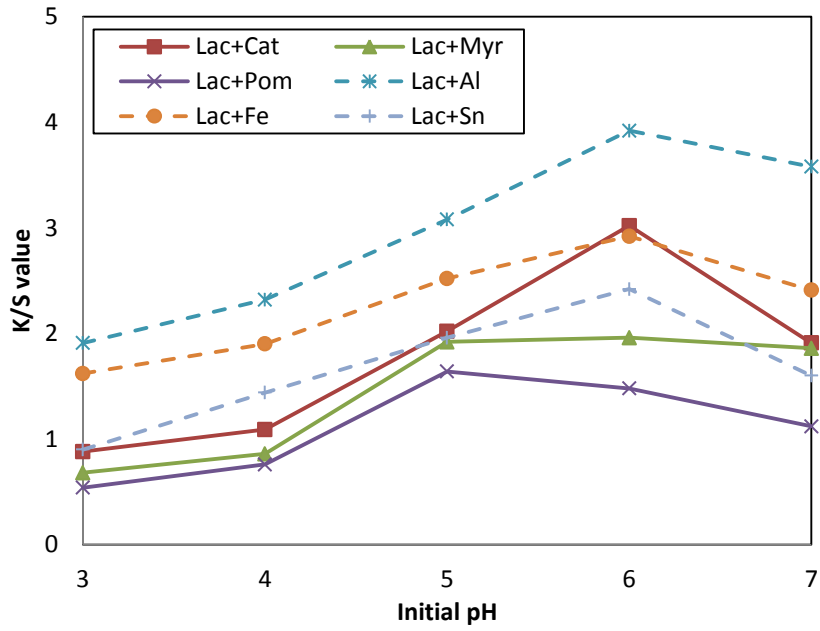


Figure 6.54: Effect of initial pH of dye bath on K/S value of PLA with Lac.

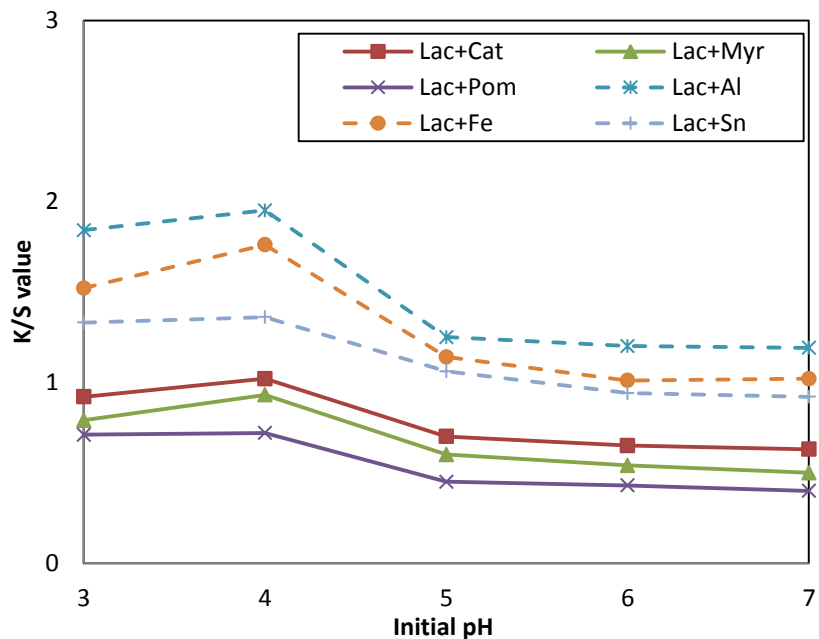


Figure 6.55: Effect of initial pH of dye bath on K/S value of PET with Lac.

The results obtained with Catechu as the natural dye are given in Figures 6.56, 6.57 and 6.58 respectively for PTT, PLA and PET.

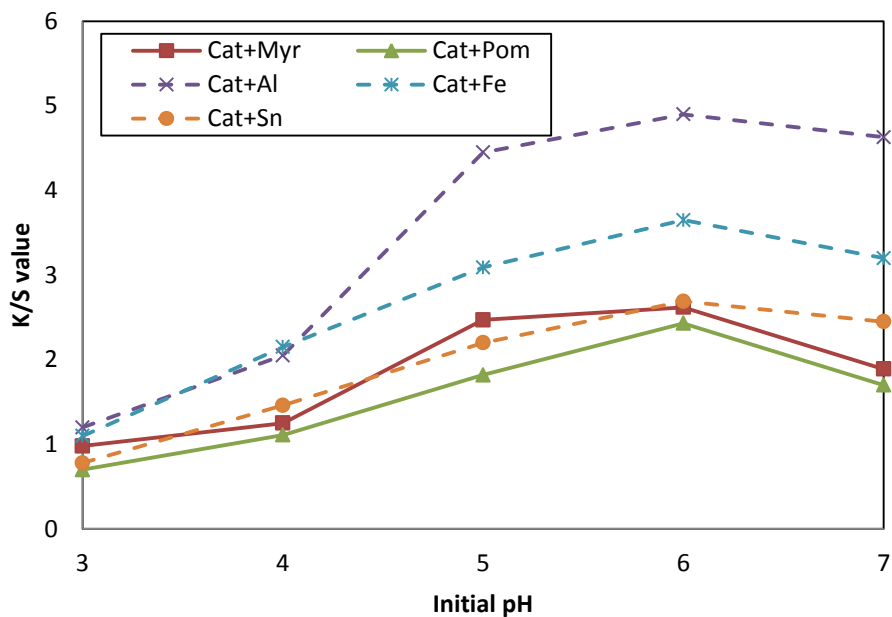


Figure 6.56: Effect of initial pH of dye bath on K/S value of PTT with Catechu.

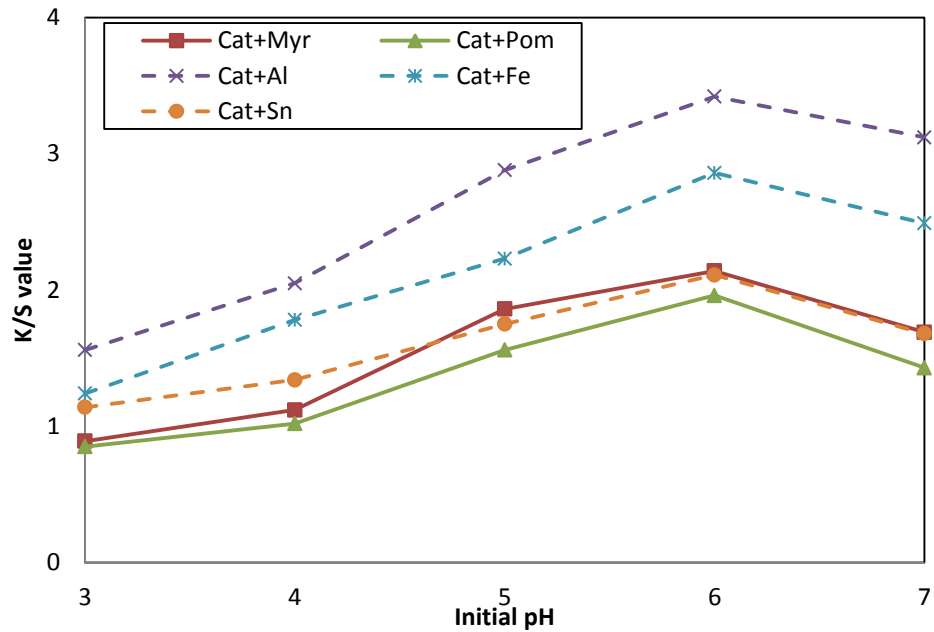


Figure 6.57: Effect of initial pH of dye bath on K/S value of PLA with Catechu.

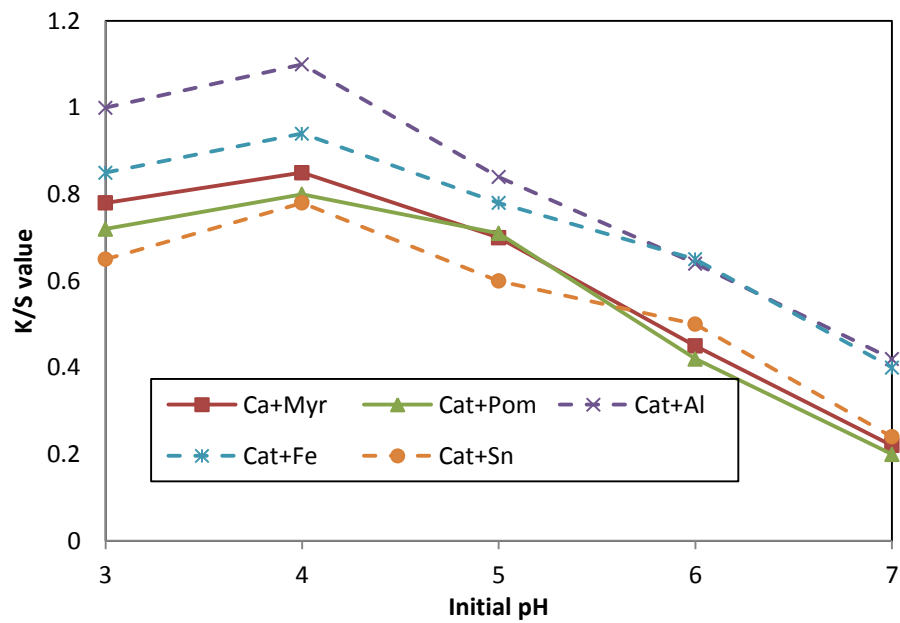


Figure 6.58: Effect of initial pH of dye bath on K/S value of PET with Catechu.

The results obtained for PTT, PLA and PET with Myrobalan as the natural dye are given in Figures 6.59, 6.60 and 6.61 respectively.

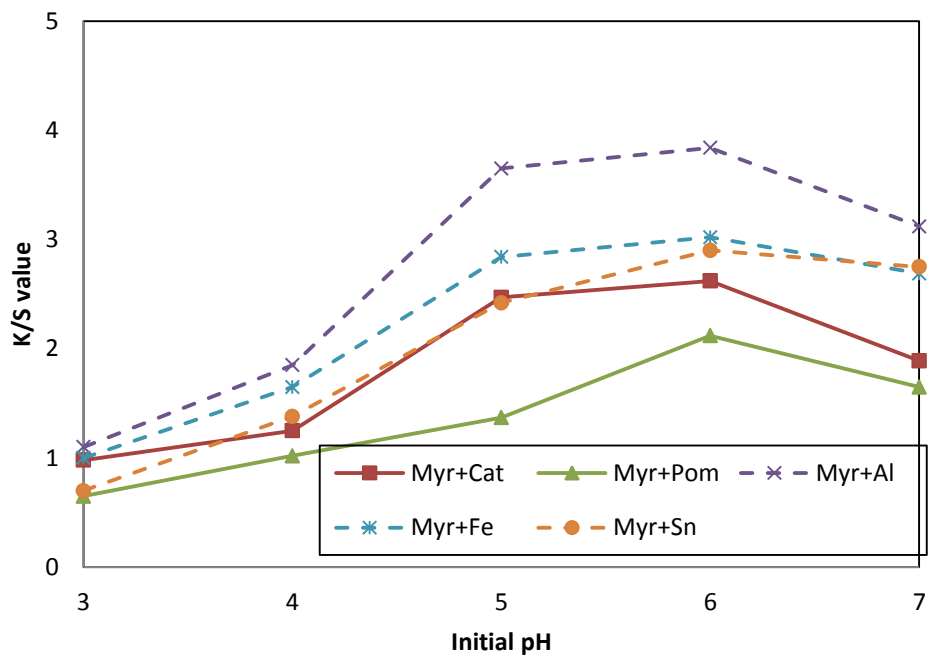


Figure 6.59: Effect of initial pH on K/S value of PTT with Myrobalan.

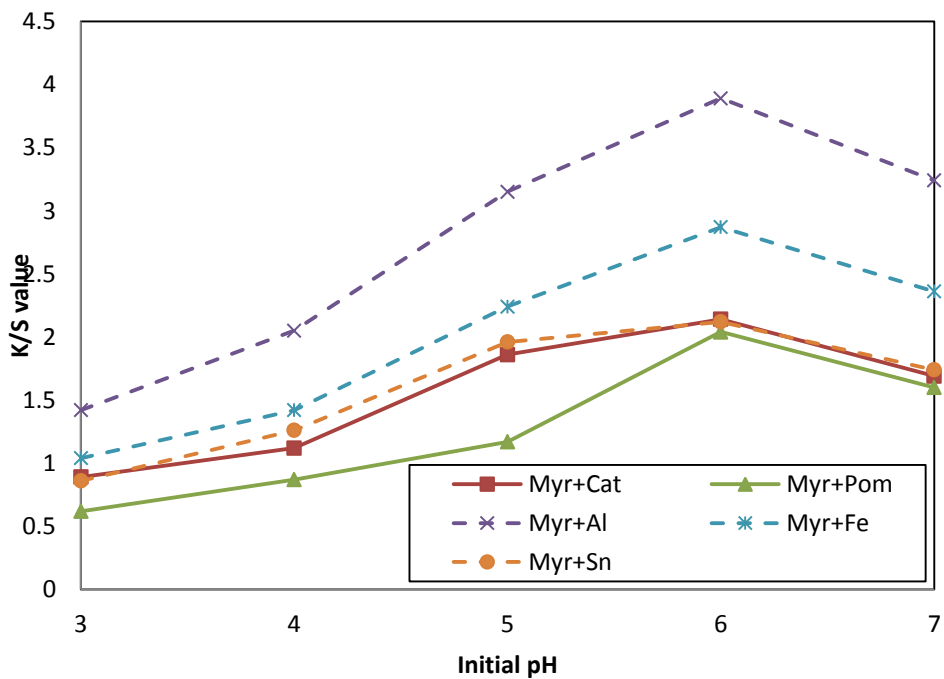


Figure 6.60: Effect of initial pH on K/S value of PLA with Myrobalan.

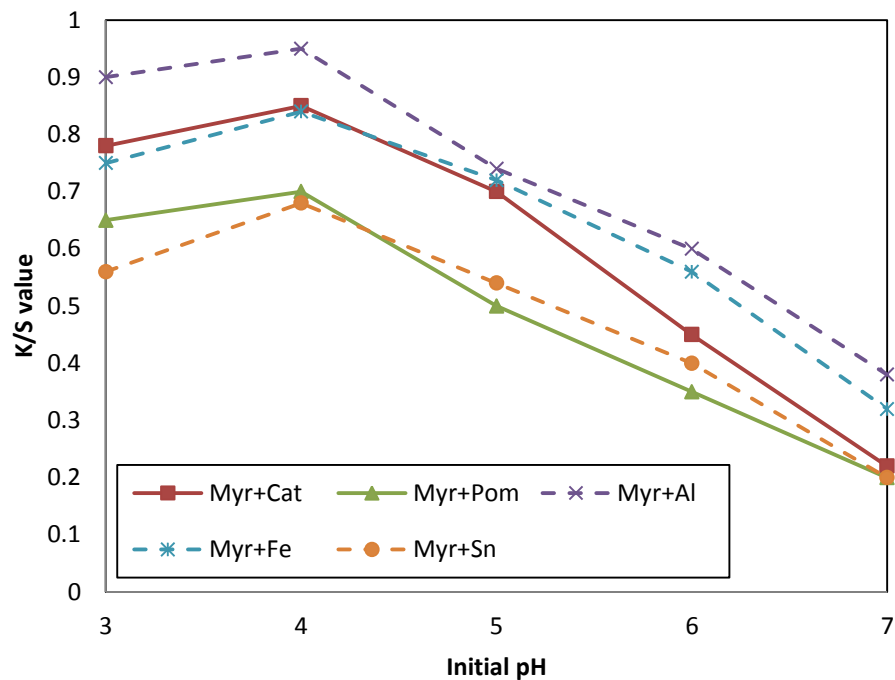


Figure 6.61: Effect of initial pH on K/S value of PET with Myrobalan.

The best results of K/S value with PTT and PLA were seen at the pH range of 5-6 in case of all the combinations of natural dyes and mordants. This was similar to the earlier observations with disperse dyes as discussed in chapter 5, and with natural dyes as discussed earlier in this chapter. With PET too, the observations were similar to those discussed earlier in case of disperse and natural dyes. The higher K/S values in its case were observed at pH range of 3-4.

It was also observed that the K/S values obtained with Lac using Catechu as biomordant, and with the combination of Myrobalan and Catechu, for PTT and PLA were in close proximity to the values obtained when stannous chloride was used. However, the K/S values with alum and ferrous sulfate were distinctly higher than with all of the biomordants. The close proximity of the values with Lac-Catechu and Myrobalan-Catechu combinations as against stannous chloride indicated that the some biomordants

could help in achieving the color strength that was comparable to and even higher in some cases than a few of the inorganic mordants. In case of PET, the values obtained with all the biomordants were inferior to those with inorganic mordants.

6.2.6.3 Effect of time

In order to assess the effect of dyeing time on the K/S value of PTT, PLA and PET, experiments were carried out at five different levels of 15 min, 30 min, 45 min, 60 min and 75 min. The dyeing temperature was kept at 110°C, initial pH of dye bath at 5, material to liquor ratio at 1:30 and mordant concentration at 9% owf. The graphs obtained with Lac as the selected natural dye are depicted in Figures 6.62, 6.63 and 6.64 for PTT, PLA and PET respectively.

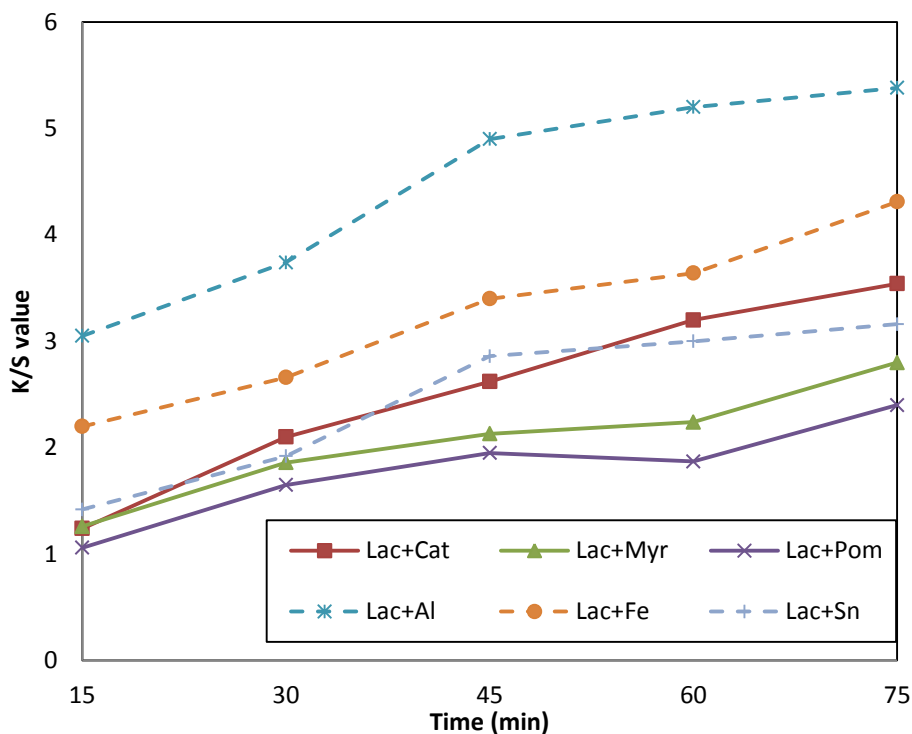


Figure 6.62: Effect of time on K/S value of PTT with Lac.

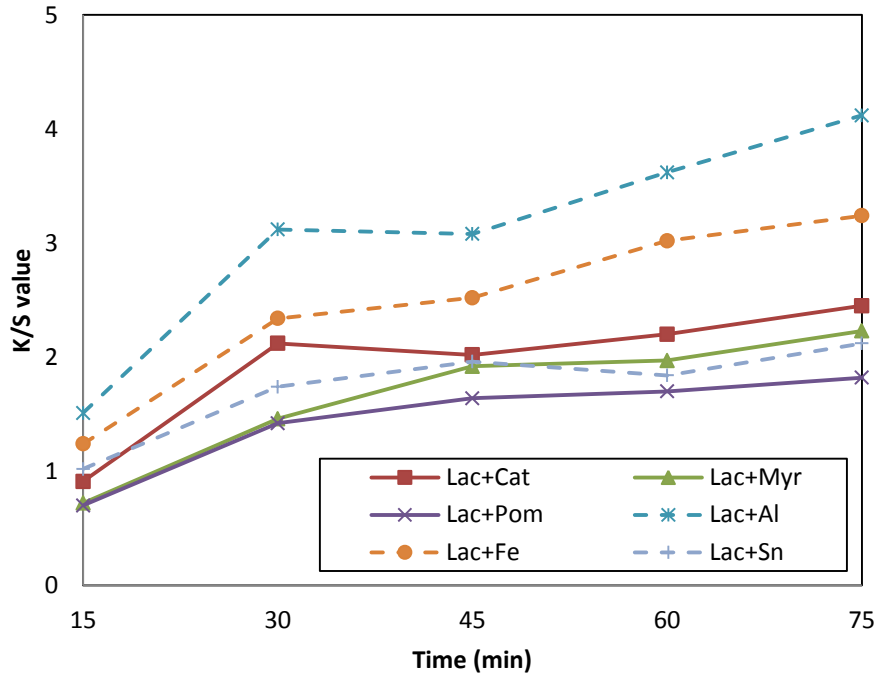


Figure 6.63: Effect of time on K/S value of PLA with Lac.

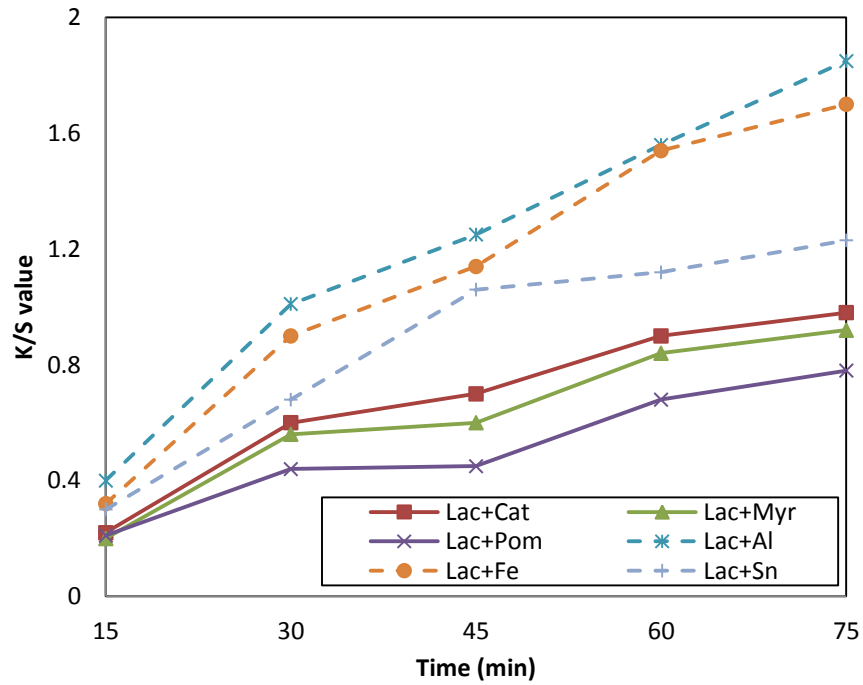


Figure 6.64: Effect of time on K/S value of PET with Lac.

The results obtained with Catechu as the natural dye applied to PTT, PLA and PET are exhibited in Figures 6.65, 6.66 and 6.67 respectively.

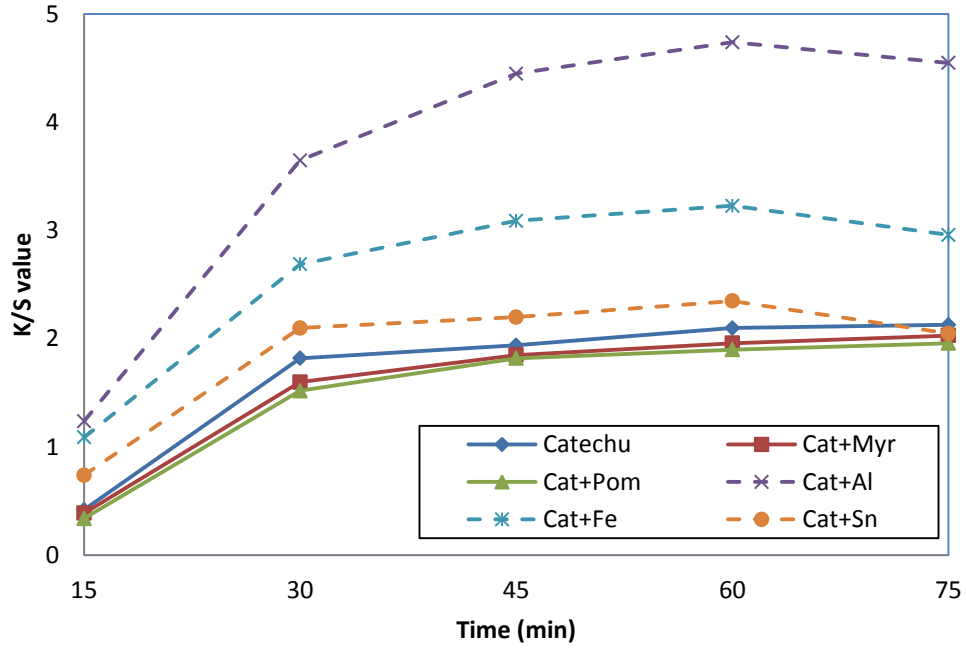


Figure 6.65: Effect of time on K/S value of PTT with Catechu.

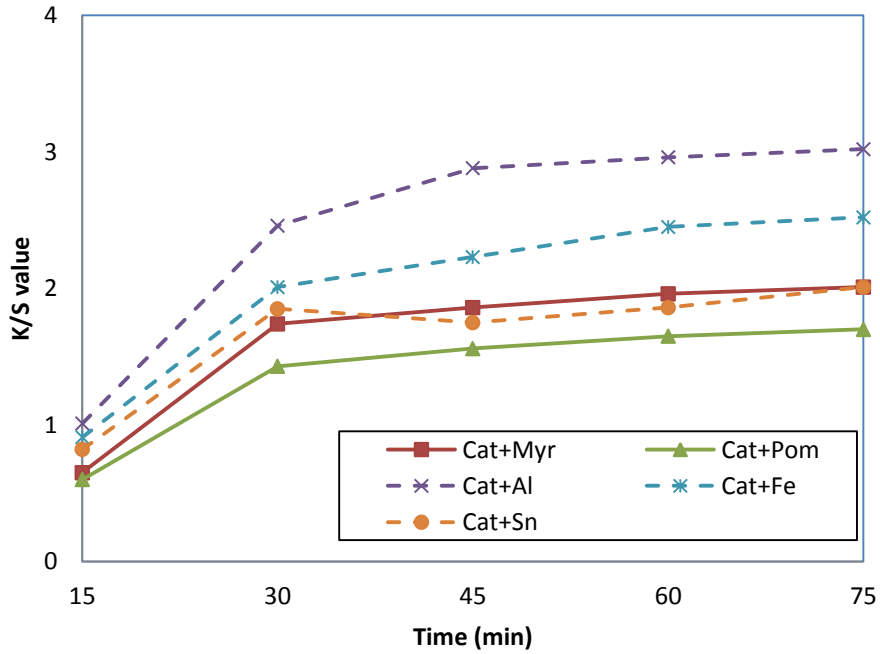


Figure 6.66: Effect of time on K/S value of PLA with Catechu.

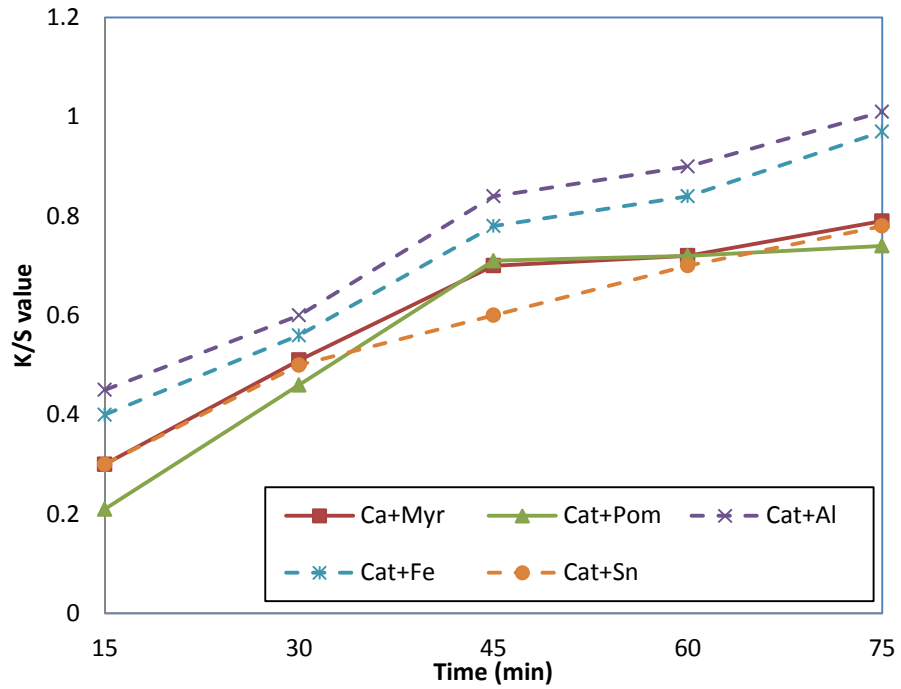


Figure 6.67: Effect of time on K/S value of PET with Catechu.

The results obtained for PTT, PLA and PET with Myrobalan as the natural dye are exhibited in Figures 6.68, 6.69 and 6.70 respectively.

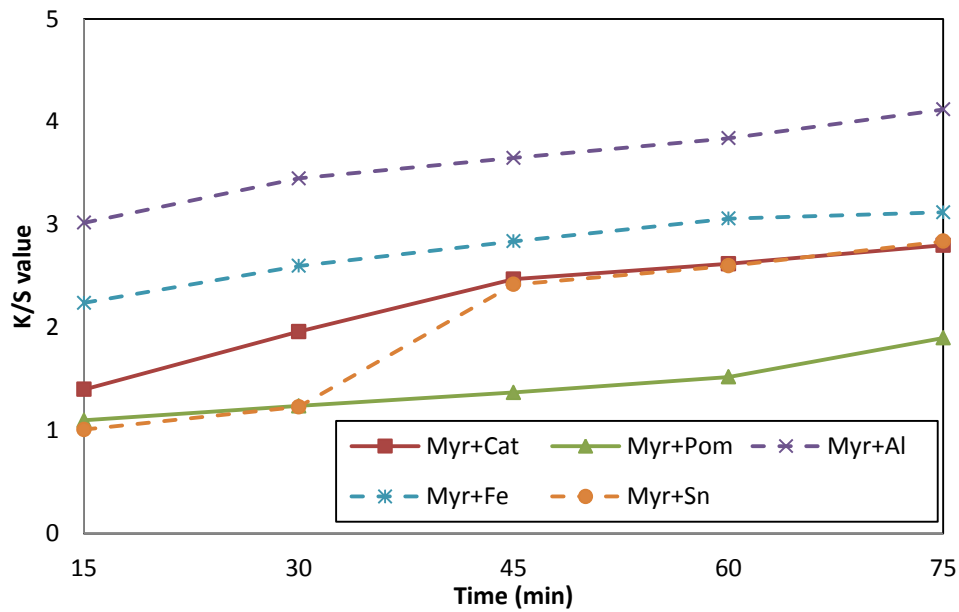


Figure 6.68: Effect of time on K/S value of PTT with Myrobalan.

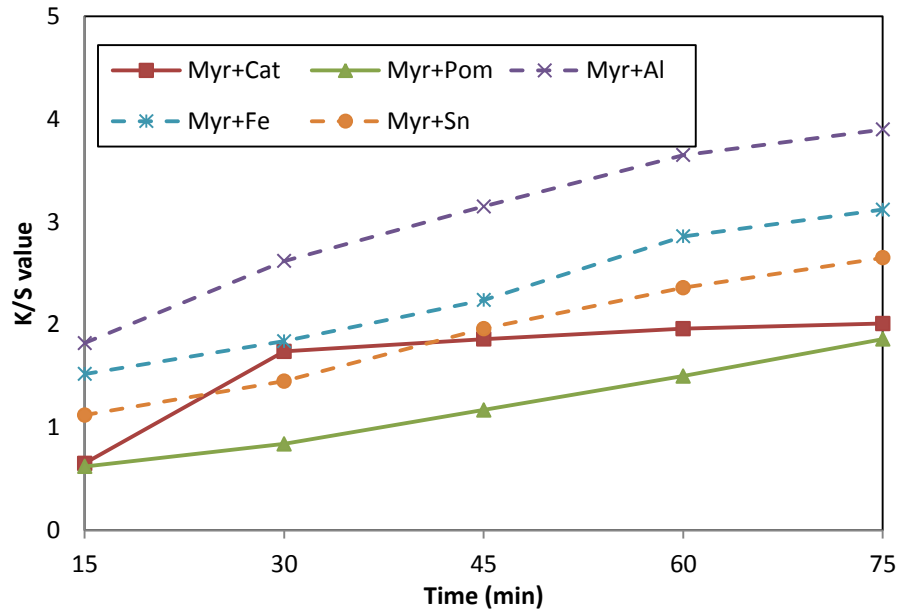


Figure 6.69: Effect of time on K/S value of PLA with Myrobalan

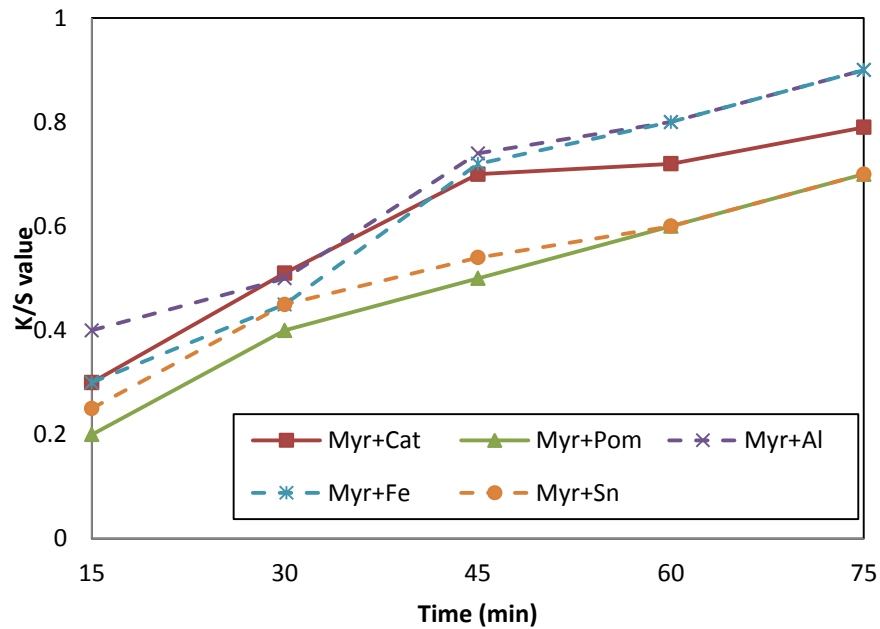


Figure 6.70: Effect of time on K/S value of PET with Myrobalan

The K/S values were found to increase with time for all the fibers. The steepness of increment was found to fall for PTT and PLA above 45 min but it continued in the similar

manner as the initial stages for PET beyond this level. The K/S values with alum and ferrous sulfate were higher than all of the biomordants used for all the fibers.

It was observed from these results that Catechu as a biomordant offered higher K/S values when applied with Lac and Myrobalan for PTT and PLA fibers, as compared to stannous chloride used as the mordant. Even in case of PET, in some cases, the K/S values with Catechu were higher than with stannous chloride. The observations were similar to those in case of effects of temperature and initial pH. Thus, Catechu was observed to have the potential to replace some of the inorganic mordants like stannous chloride in dyeing of PTT and PLA with Lac and Myrobalan.

6.2.6.4 Effect of material to liquor ratio

To observe the effect of material to liquor ratio on the properties of the dyed fibers, PTT, PLA and PET were dyed at five different ratios of the material to liquor. They were 1:10, 1:20, 1:30, 1:40 and 1:50. The dyeing temperature was kept at 110°C, initial pH of dye bath at 5, time at 45 min and mordant concentration at 9% owf. The results obtained are given in Figures 6.71, 6.72 and 6.73 for PTT, PLA and PET respectively with Lac as the natural dye.

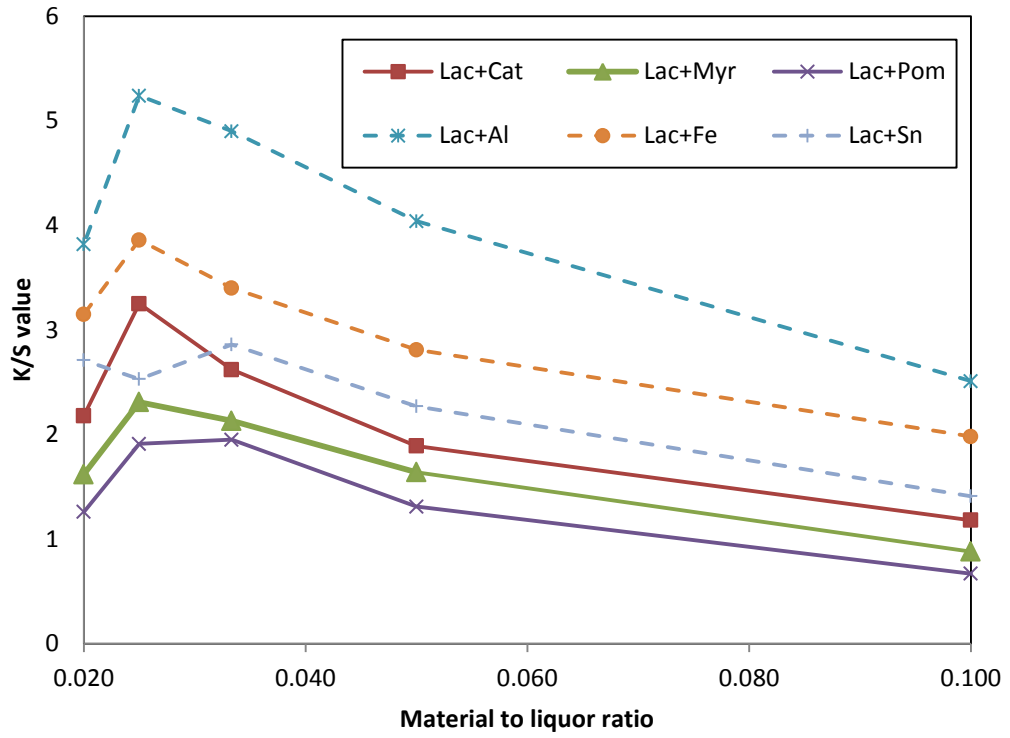


Figure 6.71: Effect of material to liquor ratio on K/S value of PTT with Lac.

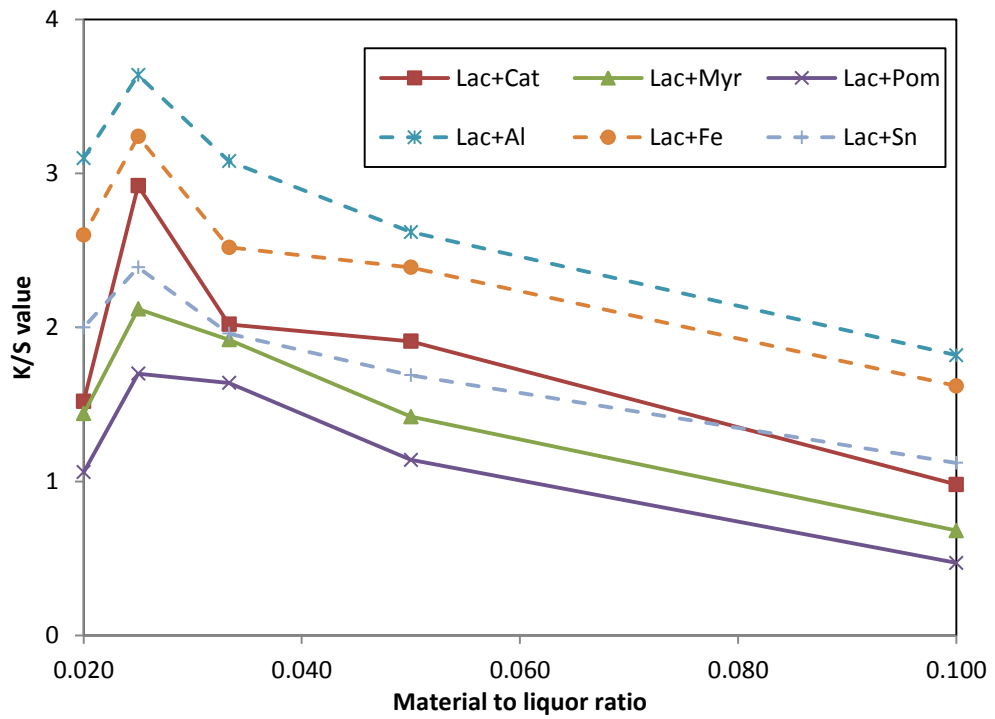


Figure 6.72: Effect of material to liquor ratio on K/S value of PLA with Lac.

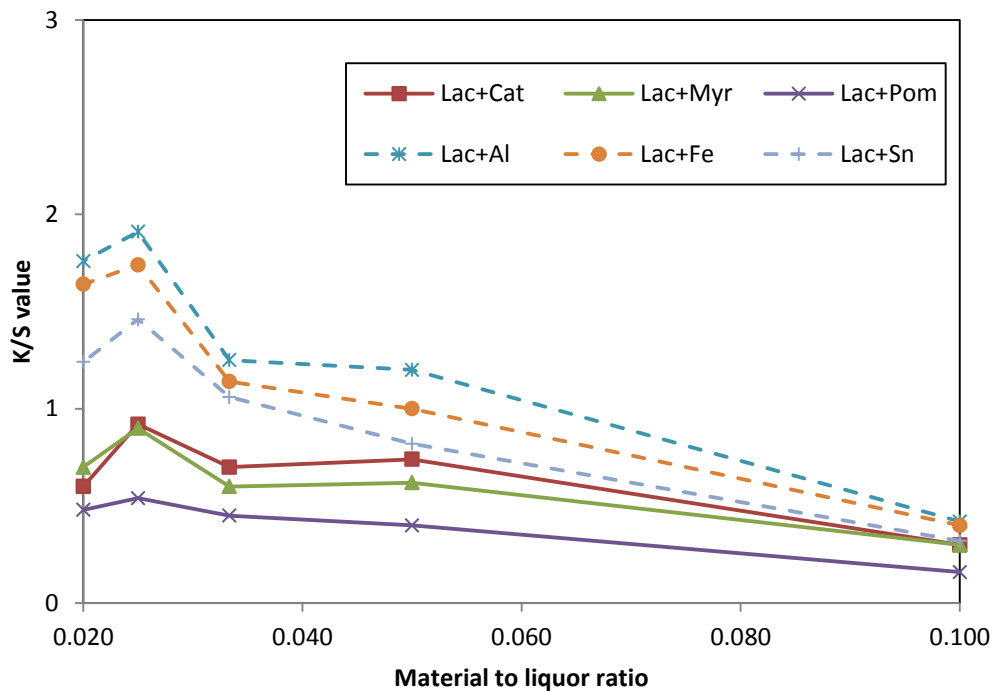


Figure 6.73: Effect of material to liquor ratio on K/S value of PET with Lac.

The graphs obtained with Catechu as the natural dye for PTT, PLA and PET are depicted in Figures 6.74, 6.75 and 6.76 respectively.

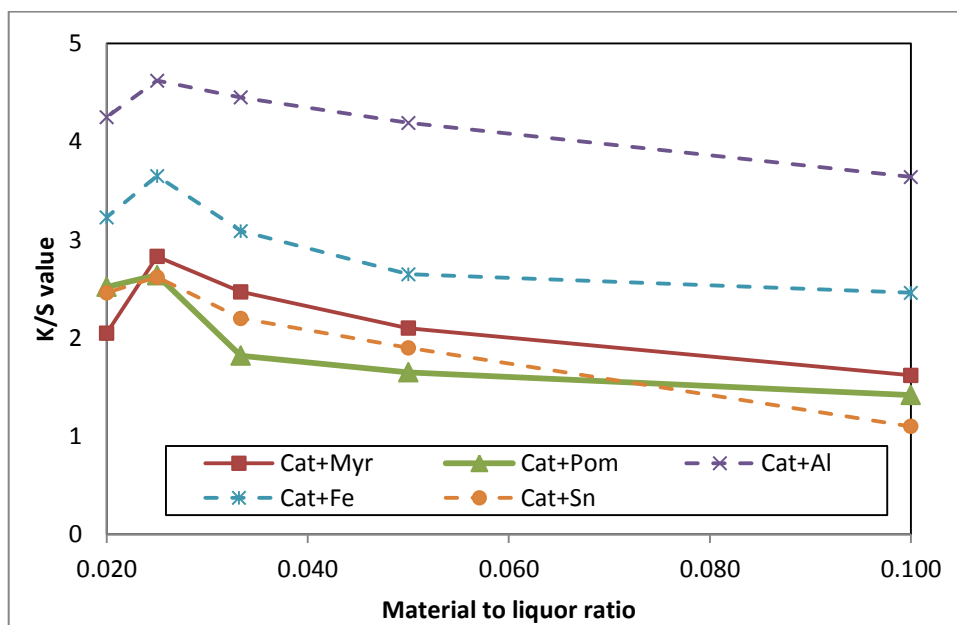


Figure 6.74: Effect of material to liquor ratio for PTT with Catechu.

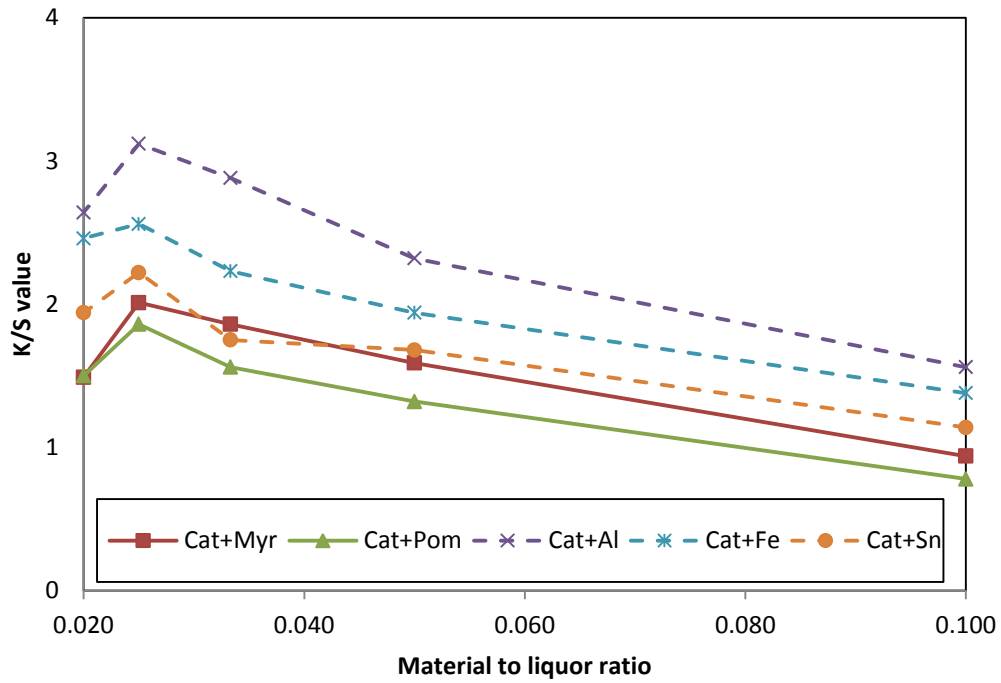


Figure 6.75: Effect of material to liquor ratio for PLA with Catechu.

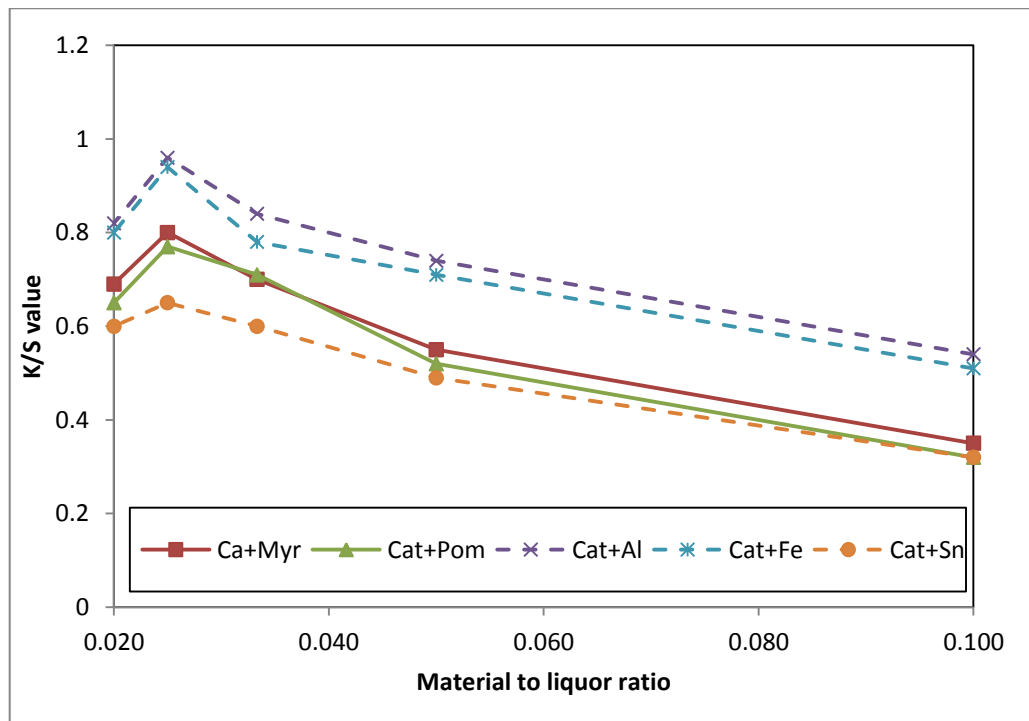


Figure 6.76: Effect of material to liquor ratio for PET with Catechu.

The results obtained for PTT, PLA and PET dyed with Myrobalan are given in Figures 6.77, 6.78 and 6.79 respectively.

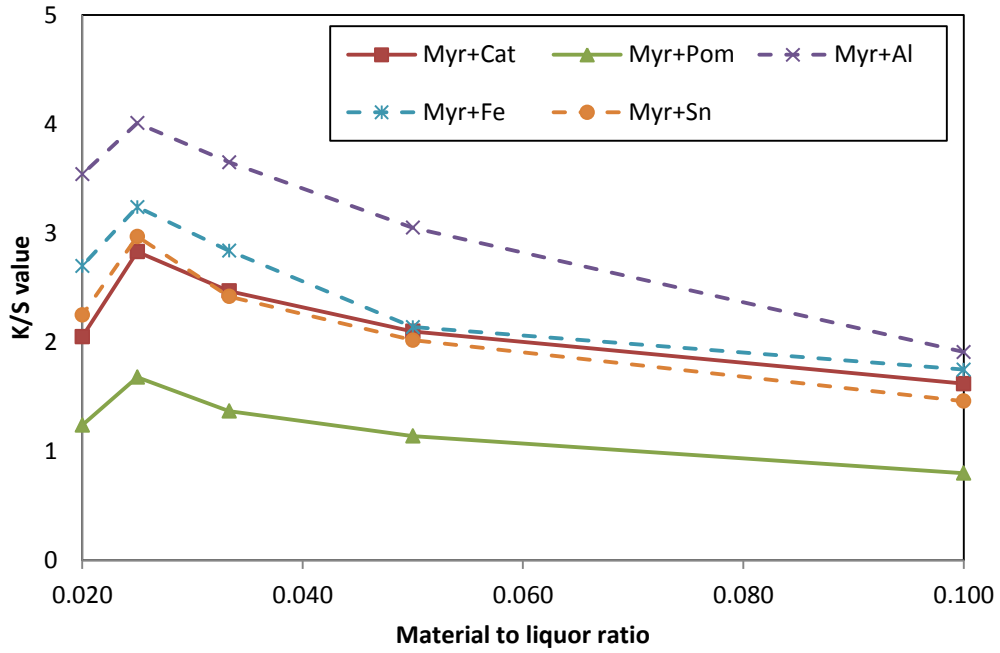


Figure 6.77: Effect of material to liquor ratio for PTT with Myrobalan.

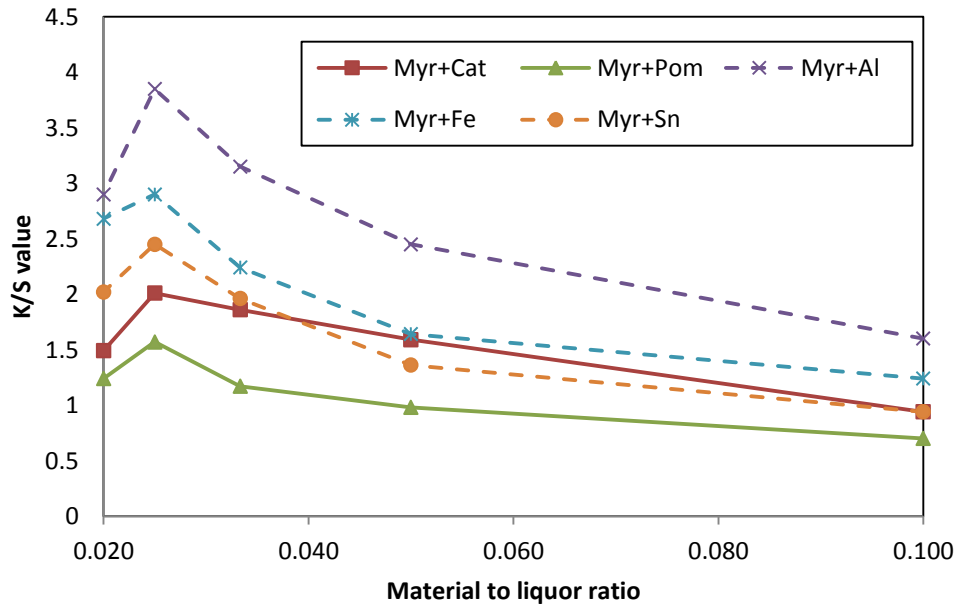


Figure 6.78: Effect of material to liquor ratio for PLA with Myrobalan.

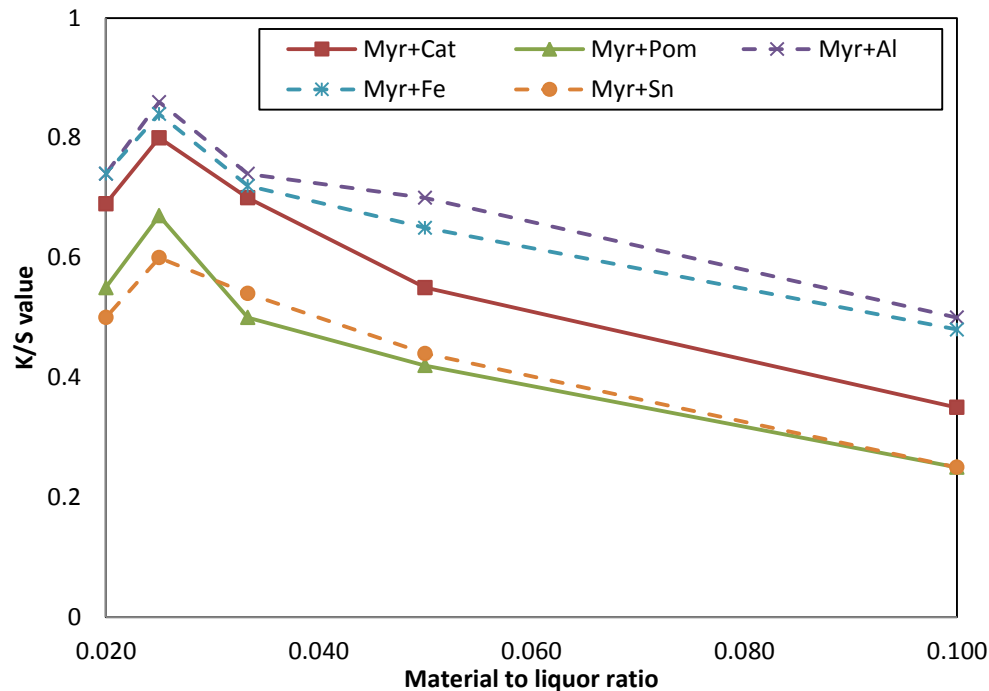


Figure 6.79: Effect of material to liquor ratio for PET with Myrobalan.

The results indicated that the K/S value increased initially up to the ratio of 1:40 beyond which it tended to decrease. This observation was the same with all the fibers and was similar to the observations with regard to disperse dyes and natural dyes made in chapter 5 and in the earlier part of this chapter respectively. It could thus be inferred that with material to liquor ratio above 1:40, the concentration of the dye in solution decreased so much that the rate of diffusion of the dyes into the fiber was affected.

It could also be observed that the K/S values for PTT and PLA with Catechu as a biomordant was higher in some cases and in very close proximity in the other cases with stannous chloride. The values with alum and ferrous sulfate in these cases too were much higher than any of the biomordants used. In case of PET also, Catechu was found to give substantially higher K/S values than stannous chloride with Myrobalan. The results

indicated that Catechu as a biomordant could outperform some of the inorganic mordants like stannous chloride in the application of Lac and Myrobalan on PTT and PLA.

6.2.6.5 Effect of mordant concentration

In order to find out the effect of mordant concentration on the K/S value of the three chosen fibers, they were dyed with five different concentrations of the mordants used, which were 3, 6, 9, 12 and 15 % owf. The dyeing temperature was kept at 110°C, initial pH of the dye bath at 5, time at 45 min and material to liquor ratio of 1:30. The results for PTT, PLA and PET with Lac as the natural dye are depicted in Figures 6.80, 6.81 and 6.82 respectively.

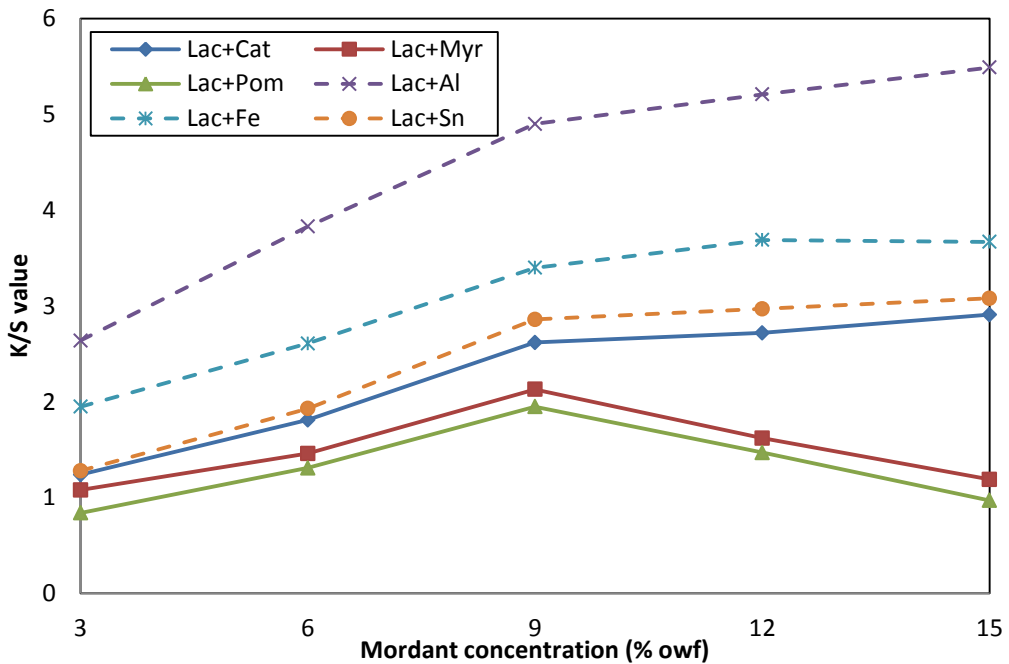


Figure 6.80: Effect of mordant concentration on K/S value of PTT with Lac.

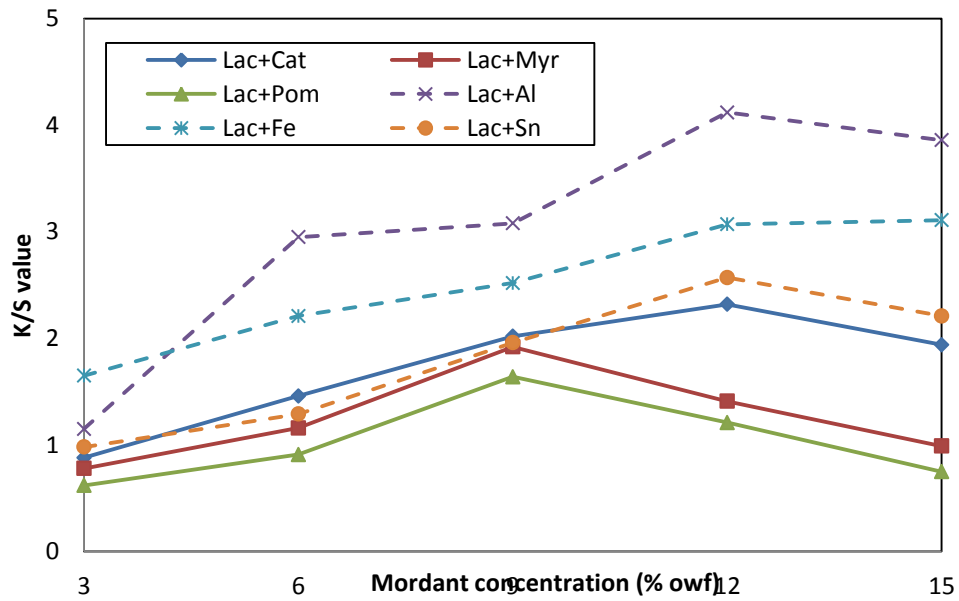


Figure 6.81: Effect of mordant concentration on K/S value of PLA with Lac.

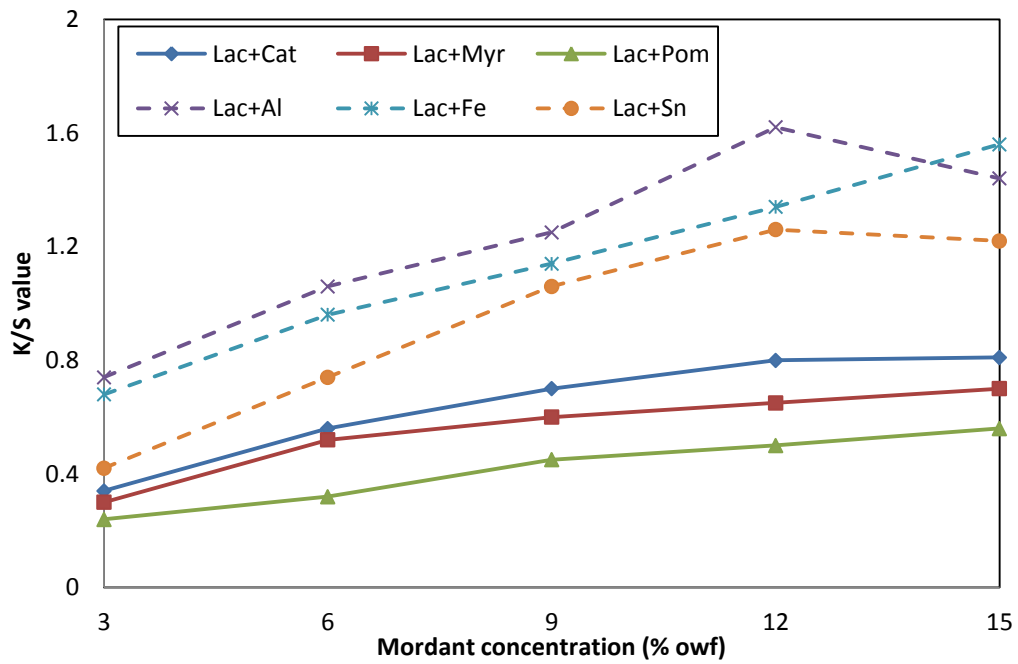


Figure 6.82: Effect of mordant concentration on K/S value of PET with Lac.

The results obtained for the three fibers with Catechu as the natural dye are given in Figures 6.83, 6.84 and 6.85 for PTT, PLA and PET respectively.

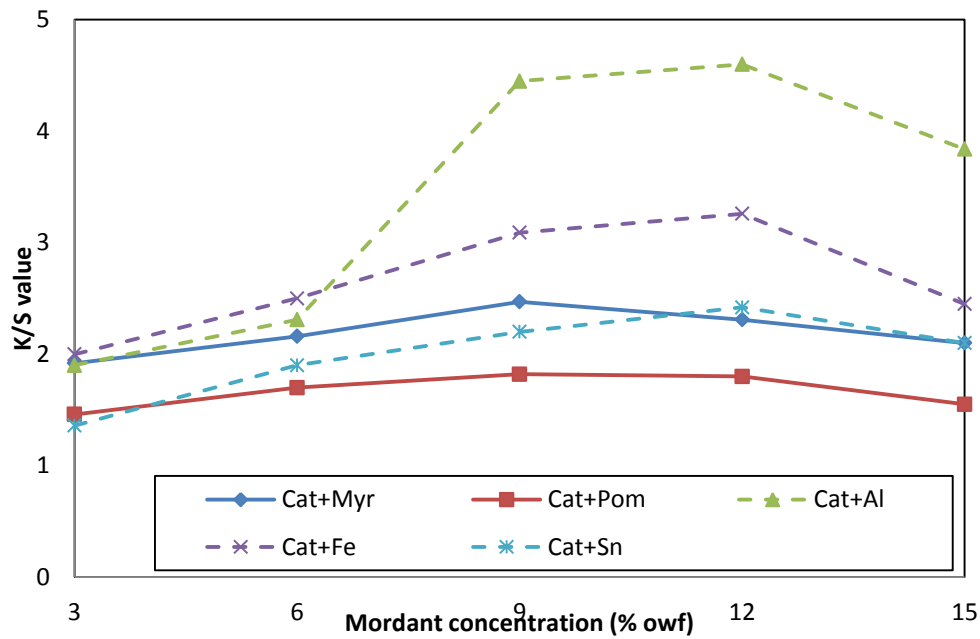


Figure 6.83: Effect of mordant concentration on K/S value of PTT with Catechu.

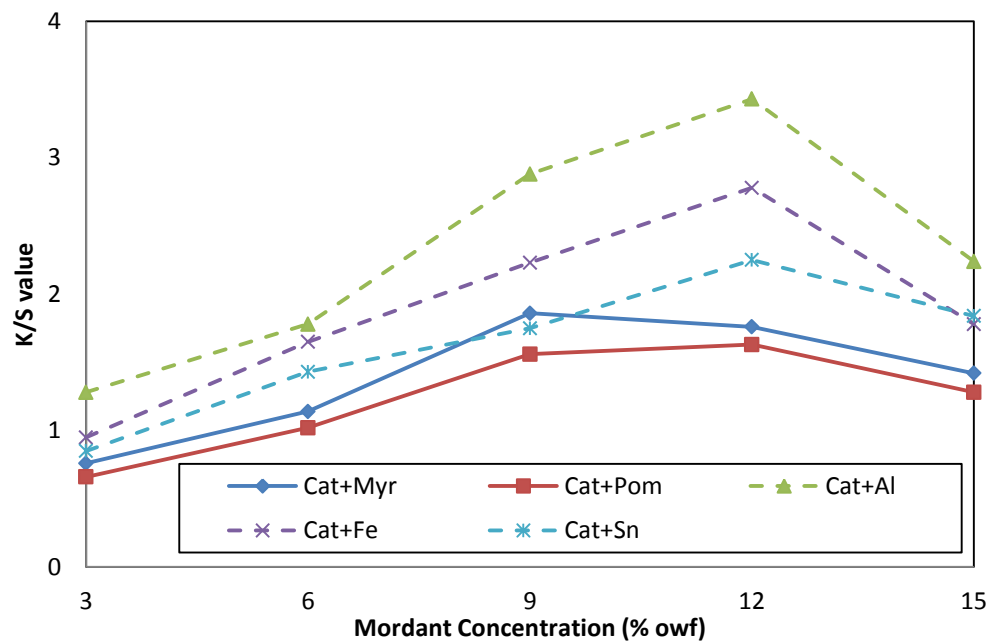


Figure 6.84: Effect of mordant concentration on K/S value of PLA with Catechu.

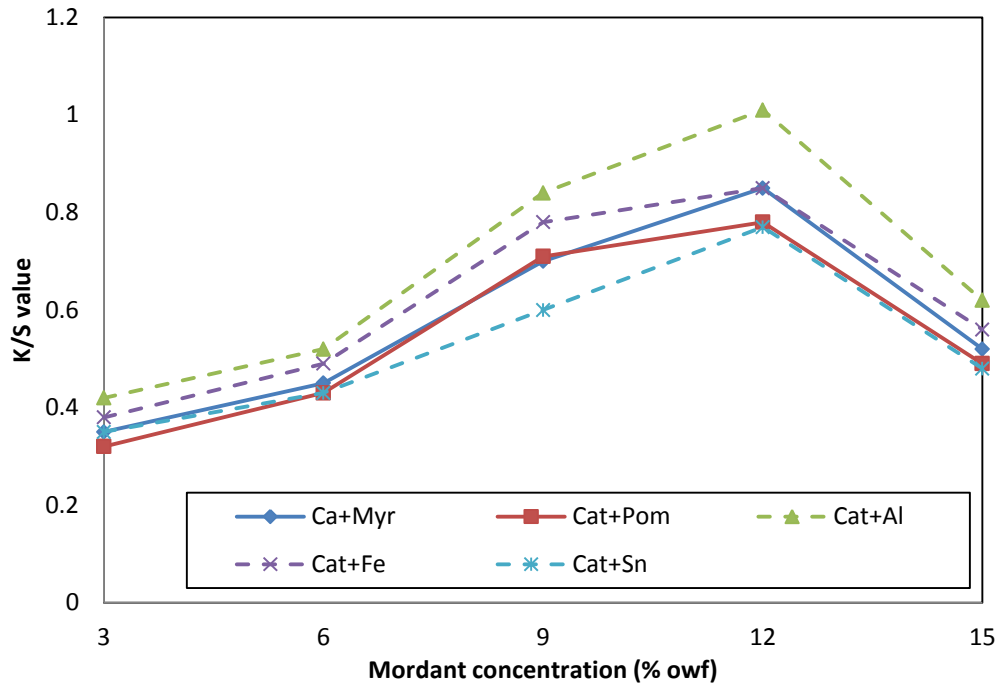


Figure 6.85: Effect of mordant concentration on K/S value of PET with Catechu.

The effect of mordant concentration on the K/S values of PTT, PLA and PET fibers dyed with Myrobalan are depicted in Figures 6.86, 6.87 and 6.88 respectively.

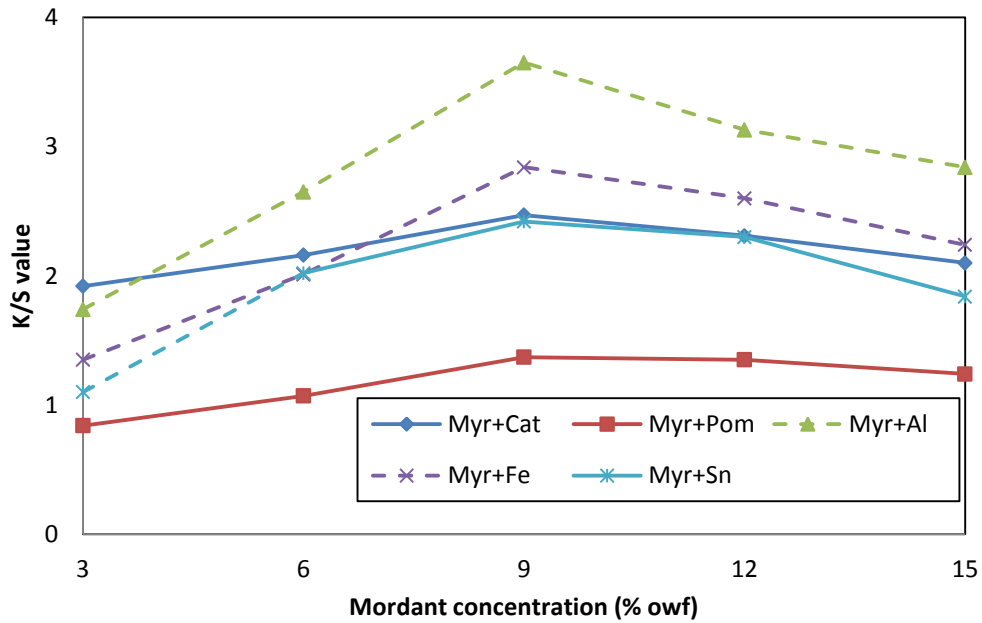


Figure 6.86: Effect of mordant concentration on K/S value of PTT with Myrobalan.

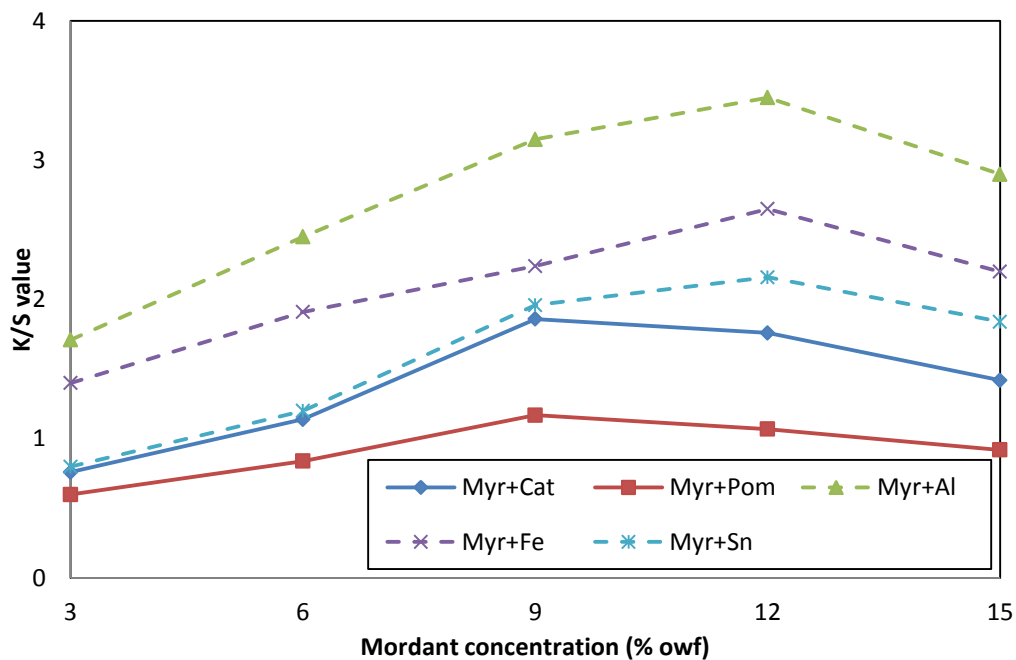


Figure 6.87: Effect of mordant concentration on K/S value of PLA with Myrobalan.

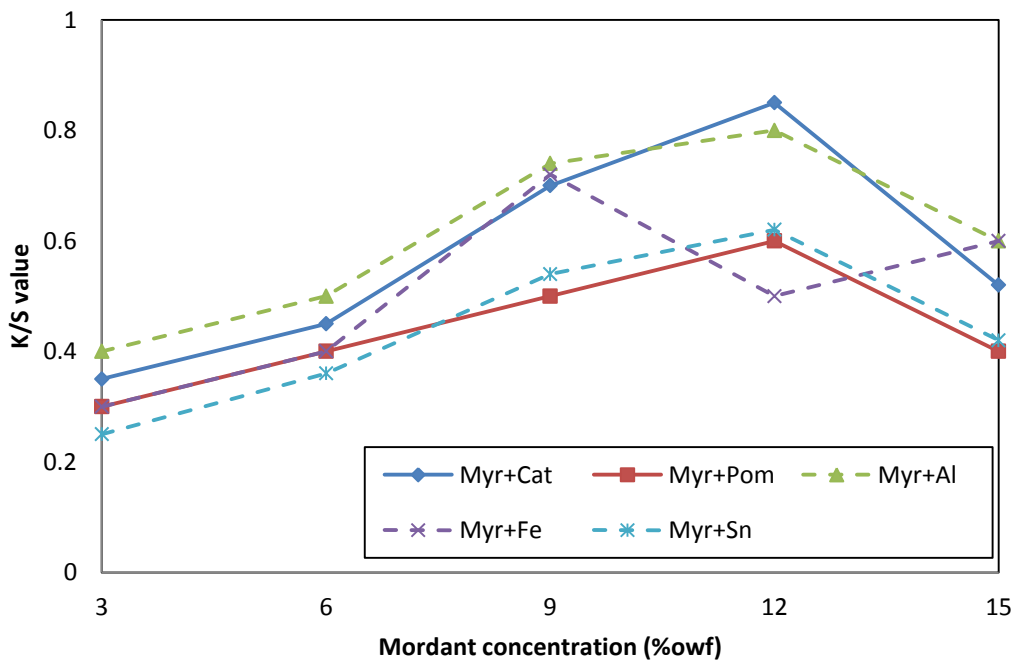


Figure 6.88: Effect of mordant concentration on K/S value of PET with Myrobalan.

In most cases, it was observed that the K/S value decreased above the mordant concentration of 12 % owf. In case of application of Lac on PTT, he K/S value was found

o increase even beyond this range, although the steepness of the increment was lower than the initial stages. In case of Myrobalan applied to PTT with Catechu as biomordant, the lowering of the K/S value was observed at above mordant concentration of 9% owf.

In case of dyeing of PTT and PLA, the K/S values with Catechu as biomordant were found to be very close to those achieved with stannous chloride. The values with alum and ferrous sulfate were higher than the biomordants in all cases. The proximity of the results with Catechu as biomordant to stannous chloride was again similar to the observations made earlier in evaluating the effects of other four factors on the color strength. This once again reiterated that Catechu as a biomordant could potentially replace some of the inorganic mordants like stannous chloride when used with Lac and Myrobalan to dye PTT and PLA. Interestingly, the K/S values obtained for PET with both Catechu-Myrobalan and Catechu-Pomegranate combinations were also higher than those obtained with stannous chloride.

6.3 Summary

The findings of the experiments with natural dyes are as follows:

- (i) Considering both color strength and tensile properties, the optimal range of temperature for dyeing PTT and PLA fibers was identified as 110-120^oC. At temperatures lower than this range, the K/S value was substantially reduced; at higher temperatures above this range, the tenacity and elongation was lowered to a substantial extent.
- (ii) The color strength of PTT and PLA were found to be satisfactory at pH 5-6. The tensile properties were also found to be satisfactory for the two fibers at

this pH range, below which it decreased largely. For PET, the optimal pH range was 3-4.

- (iii) Although color strength increased with time for the three fibers, the tensile properties decreased sharply too. The optimal dyeing time was found to be 30-45 min. Above this duration, the strength of the fibers were considerably lost, with PLA showing a very sharp decline. Below this time duration for dyeing, the color strength was below satisfactory.
- (iv) For material to liquor ratio, the optimal range was observed at 1:30-1:40. The color strength decreased both above and below this range. The correlation between material to liquor ratio and tensile properties of the dyed fibers were found to be insignificant.
- (v) The FTIR spectra of dyed PTT and PLA fibers revealed no significant changes in the peaks as compared to that of the undyed fibers. It could thus be concluded that the dyes did not form any chemical bonding with PTT and PLA while dyeing them. The adsorption isotherms with the three natural dyes for PTT and PLA were found to resemble the Nernst adsorption isotherm model. The dyes thus penetrated the fibers physically.
- (vi) The color strength of the fibers was found to increase with the application of biomordants. Out of the three techniques of mordanting, the results were most favorable with meta-mordanting. The results with pre-mordanting were however better than post-mordanting.
- (vii) When biomordants were compared with inorganic mordants, it was observed that for all the three fibers, the color strength with alum and ferrous sulfate

was far superior than the biomordants. Among the inorganic mordants, higher color strength achieved followed the sequence alum> ferrous sulfate> stannous chloride.

- (viii) Among the biomordants, higher color strength was observed to follow the sequence Catechu> Myrobalan> Pomegranate. With Catechu, the results were very encouraging, as the color strength obtained was in close proximity to those with one of the inorganic mordants, stannous chloride. In some cases, the color strength with Catechu for PTT and PLA were even higher than that with stannous chloride. Even with PET, the results for Catechu used with Myrobalan and Pomegranate were found to be comparable to the color strength achieved with stannous chloride. Thus, the possibility of Catechu replacing stannous chloride in dyeing of PTT and PLA with the chosen natural dyes was found to be substantial.

Chapter 7

Optimization with Natural Dyes and Biomordants

In chapters 5 and 6, the effects of various parameters on the different properties of PTT and PLA fibers have been discussed. While chapter 5 dealt with disperse dyes, the application of natural dyes and biomordants were discussed in chapter 6. From these studies, the optimal ranges for various parameters affecting the fiber properties favorably for PTT and PLA after application of these dyes could be noted. With these optimal ranges, optimization was done using Response Surface Methodology (RSM) based on Rotatable 2^3 -Factorial Central Composite Design (CCD).

In RSM, three factors were selected that affected the properties of the dyed fibers most significantly. However, in chapters 5 and 6, more than three factors have been considered to study the various effects. Hence, a statistical method was executed identify the three most significant factors from among them. The method of normal probability plots were employed in order to find out the main effects and the effects of interaction of these factors on fiber properties after dyeing. The fiber property that was considered in these plots to study these effects was color strength of the dyed fibers, measured as the K/S value.

Optimization was also done for PTT and PLA with the natural dyes Lac, Catechu and Myrobalan. For both the fibers, it was performed using Lac as the natural dye with Catechu, Myrobalan and Pomegranate as the biomordants respectively. It was also performed for the natural dye Catechu with Myrobalan and Pomegranate as the biomordants. When Myrobalan was used as the natural dye, Pomegranate was used as the biomordant and optimization executed. The results obtained are discussed in the following sections of this chapter.

Response Surface Methodology (RSM) based on Rotatable 2^3 -Factorial Central Composite Rotatable (2^3 -CCR) Design was employed to establish the relationship between color strength (i.e. the response function) and three of the most significant process variables obtained after screening. Statistica software, version 12, from Statsoft Inc., California, U.S.A., was used for design of experiment, analyses and optimization. A total of 20 experiments, including $2^3=8$ factorial points, 6 axial points and 6 center points, were performed five times each, and the average values of color strength were recorded in each case. The optimum values of the selected process variables were obtained by solving the regression model equations obtained in each case using the software and as per the equation 2.12 as mentioned in chapter 2.

7.1 Optimization with natural dyes and biomordants

When the PTT and PLA fibers were dyed with natural dyes along with application of biomordants, the effects were observed on dyed fibers for temperature, initial pH of dye bath, time, material to liquor ratio and mordant concentration as has been reported in chapter 6. Using the normal probability plots, the three factors among these that were most significant in affecting the color strength of the dyed fibers was identified for each of the combinations of natural dyes and biomordants. In all cases, the natural dyes and biomordants were applied through the meta-mordanting technique, i.e. the natural dye and biomordant selected were applied to the fibers in the dye bath simultaneously. Optimization was done using RSM with these three factors in case of each of the combinations used.

7.1.1 Optimization with Lac using Catechu as biomordant

The real values of -1 and +1 levels for the five factors used in the normal probability plots for dyeing of PTT and PLA with Lac using Catechu as biomordant are given in Tables 7.1 and 7.2 respectively, along with the notations and units.

Table 7.1: Factors for normal probability plot of PTT with Lac using Catechu as biomordant.

Factors	Notations	Coded values		
			-1	1
			- α (-1.68)	1
			Real values	
Dyeing temperature	A	$^{\circ}\text{C}$	100	120
Dyeing time	B	min	30	60
Initial pH	C		5	7
Material to liquor ratio	D		1:20	1:40
Mordant concentration	E	% owf	9	15

Table 7.2: Factors for normal probability plot of PLA with Lac using Catechu as biomordant.

Factors	Notations	Units	Coded values	
			-1	1
			Real values	
Dyeing temperature	A	$^{\circ}\text{C}$	100	120
Dyeing time	B	min	15	45
Initial pH	C		5	7
Material to liquor ratio	D		1:20	1:40
Mordant concentration	E	% owf	9	15

7.1.1.1 Optimization for PTT

The normal probability plot with Lac applied on PTT using Catechu as biomordant is shown in Figure 7.1. It could be observed that points A, B, C and D were distinct outliers with positive effects in the probability plot. Also, it could be seen that point 1x3 was also an outlier on the negative side.

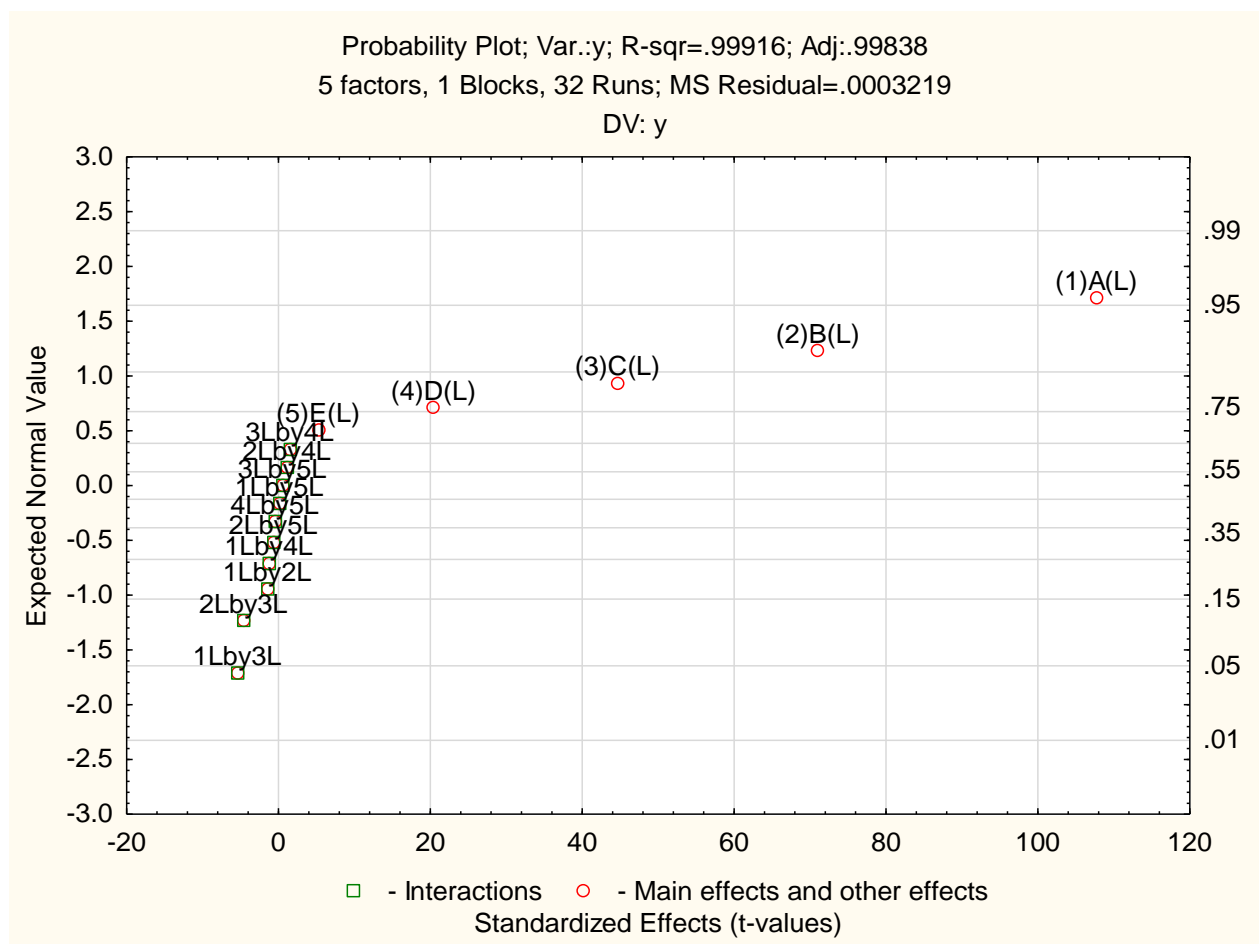


Figure 7.1: Normal probability plot of Lac applied on PTT using Catechu as biomordant.

It could thus be inferred temperature (A, 1), time (B, 2), initial pH of the dye bath (C, 3) and material to liquor ratio (D, 4) were the most significant factors affecting the color strength of PTT with Lac using Catechu as biomordant. Also, the interaction effect of temperature (1) and initial pH (3) were more significant than the other factors and their

interactions. The R^2 value of 0.99916 and adjusted R^2 value of 0.99838 indicated that the probability plot obtained was statistically significant with a high goodness of fit.

Table 7.3: Factors for RSM of PTT with Lac using Catechu as biomordant.

Factors	Notations	Coded values				
		$-\alpha(-1.68)$	-1	0	1	$+\alpha(+1.68)$
		Real values				
Dyeing temperature ($^{\circ}\text{C}$)	A	93	100	110	120	127
Initial pH	B	4	5	6	7	8
Dyeing time (min)	C	20	30	45	60	70

With temperature, initial pH of dye bath and time, RSM was done for Lac with PTT using Catechu as biomordant. The levels of the factors chosen for this combination of natural dye and biomordant are given in Table 7.3. Five experiments were done in each run and the average values reported in Table 7.4. The contour plots obtained in the RSM are given in Figures 7.2-7.4. The analysis of variance (ANOVA) for the factors of response is given in Table 7.5 and the same for the quadratic regression model in Table 7.6.

The empirical model equation obtained with the coded variables is as follows:

$$y = 3.498 + 0.246A - 0.291A^2 + 0.134B - 0.245B^2 + 0.229C - 0.296C^2 + 0.019AB + 0.006AC + 0.014BC \quad (7.1)$$

The optimal values were observed as 114°C for temperature, 6.3 for initial pH of dye bath and 51 min for dyeing time approximately. The predicted K/S value under these optimal conditions was 3.62.

Table 7.4: Average values of experiments used for RSM.

Runs	Dyeing temperature	Initial pH	Dyeing time	Experimental values
	^o C		min	K/S
	A	B	C	y
1	-1.00	-1.00	-1.00	2.03
2	-1.00	-1.00	1.00	2.41
3	-1.00	1.00	-1.00	2.21
4	-1.00	1.00	1.00	2.72
5	1.00	-1.00	-1.00	2.48
6	1.00	-1.00	1.00	2.96
7	1.00	1.00	-1.00	2.81
8	1.00	1.00	1.00	3.27
9	-1.68	0.00	0.00	2.39
10	1.68	0.00	0.00	3.11
11	0.00	-1.68	0.00	2.67
12	0.00	1.68	0.00	3.09
13	0.00	0.00	-1.68	2.35
14	0.00	0.00	1.68	3.12
15	0.00	0.00	0.00	3.49
16	0.00	0.00	0.00	3.47
17	0.00	0.00	0.00	3.42
18	0.00	0.00	0.00	3.55
19	0.00	0.00	0.00	3.52
20	0.00	0.00	0.00	3.51

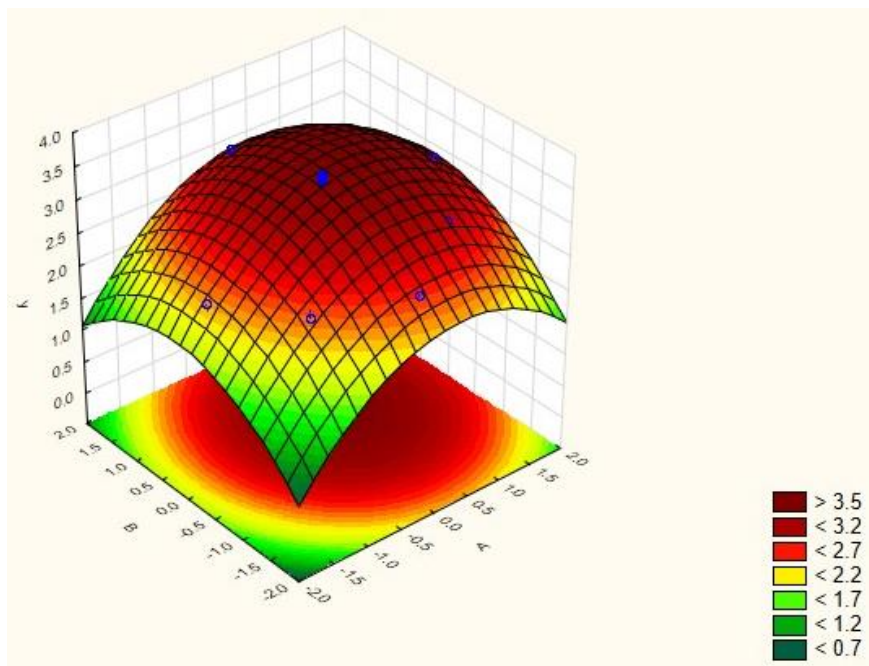


Figure 7.2: Contour plot for K/S value (y) with temperature (A) and initial pH of dye bath (B).

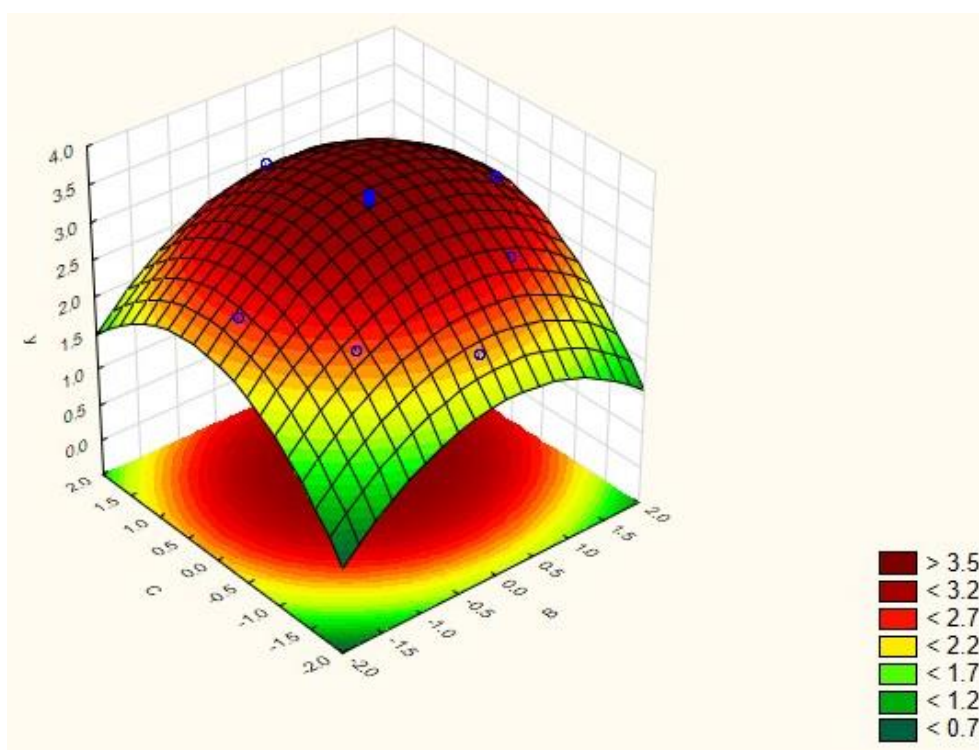


Figure 7.3: Contour plot for K/S value (y) with initial pH of dye bath (B) and time (C).

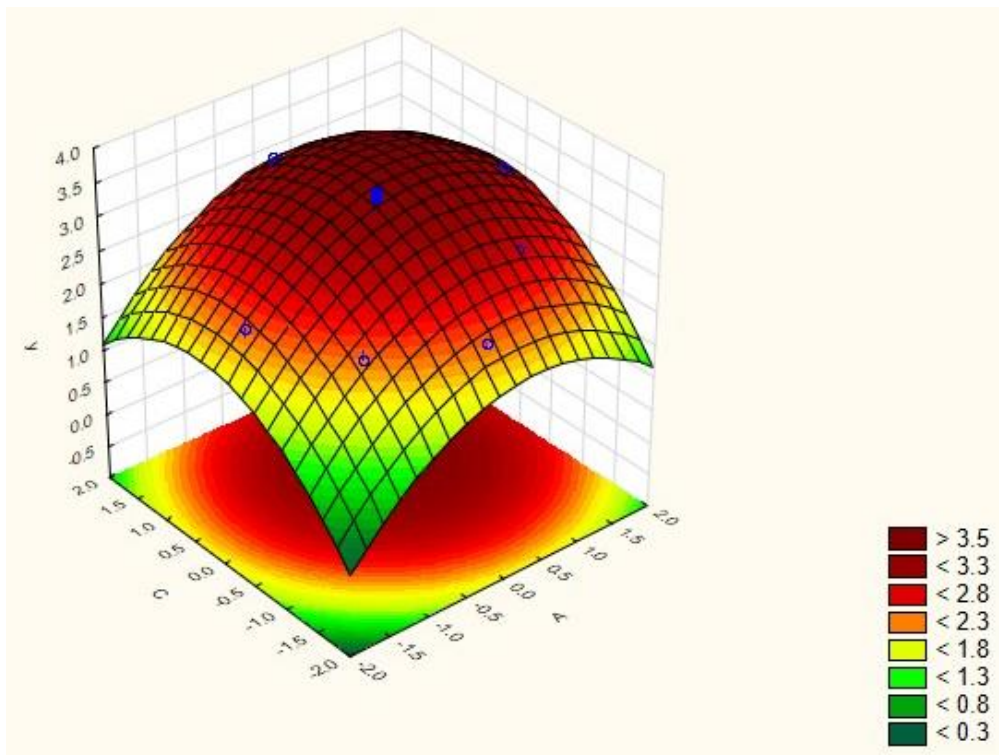


Figure 7.4: Contour plot for K/S value (y) with temperature (A) and time (C).

Table 7.5: Variance analysis (ANOVA) of factors on response.

Factors	Sum of Squares	Degrees of Freedom	Mean Square	F Value	p-Value Prob>F
<i>A</i>	0.827	1	0.827	101.651	0.000
<i>A</i> ²	1.222	1	1.222	150.140	0.000
<i>B</i>	0.247	1	0.247	30.347	0.000
<i>B</i> ²	0.866	1	0.866	106.479	0.000
<i>C</i>	0.715	1	0.715	87.881	0.000
<i>C</i> ²	1.267	1	1.267	155.659	0.000
<i>AxB</i>	0.003	1	0.003	0.346	0.570
<i>AxC</i>	0.000	1	0.000	0.038	0.849
<i>BxC</i>	0.002	1	0.002	0.186	0.676

Table 7.6: Variance analysis (ANOVA) of quadratic regression model.

Source	Sum of Squares	Degrees of Freedom	Mean Square	F Value	p-Value Prob>F
Model	4.5988	9	0.5109	62.799	0.00
Residual	0.0814	10	0.0081		
Lack of fit	0.0712	5	0.01425	7.0296	0.3
Pure error	0.0101	5	0.00203		
Total	4.6802	19			

It was seen from Table 7.5 that the factors A , A^2 , B , B^2 , C and C^2 were the most significant factors with p-values less than 0.05. Thus, temperature (A), initial pH (B) as well as time (C) had significant linear as well as quadratic effects on K/S value.

From Table 7.6, it was observed that at 95% confidence level, the quadratic regression model developed was statistically significant with F-value of 62.799 that was much higher than the F-value of the lack of fit (7.0296). The R^2 value was found to be 0.98261 indicating that 98.26% of the total variations could be explained by the developed model, and 1.74% of the variations could not be explained. The adjusted R^2 value of 0.96697 was reasonably close to the R^2 value, indicating a high goodness of fit for the developed model.

7.1.1.2 Optimization for PLA

The normal probability plot with Lac applied on PLA using Catechu as biomordant is shown in Figure 7.5. It could be observed that points A, B and C were distinct outliers with positive effects in the probability plot. Also, it could be seen that point 1x2 was also an outlier on the negative side.

It could thus be inferred temperature (A , 1), time (B , 2) and initial pH of the dye bath (C , 3) were the most significant factors affecting the color strength of PLA with Lac using Catechu as biomordant. Also, the interaction effect of temperature (1) and time (2)

were more significant than the other factors and their interactions. The R^2 value of 0.99968 and adjusted R^2 value of 0.99938 indicated that the probability plot obtained was statistically significant with a high goodness of fit.

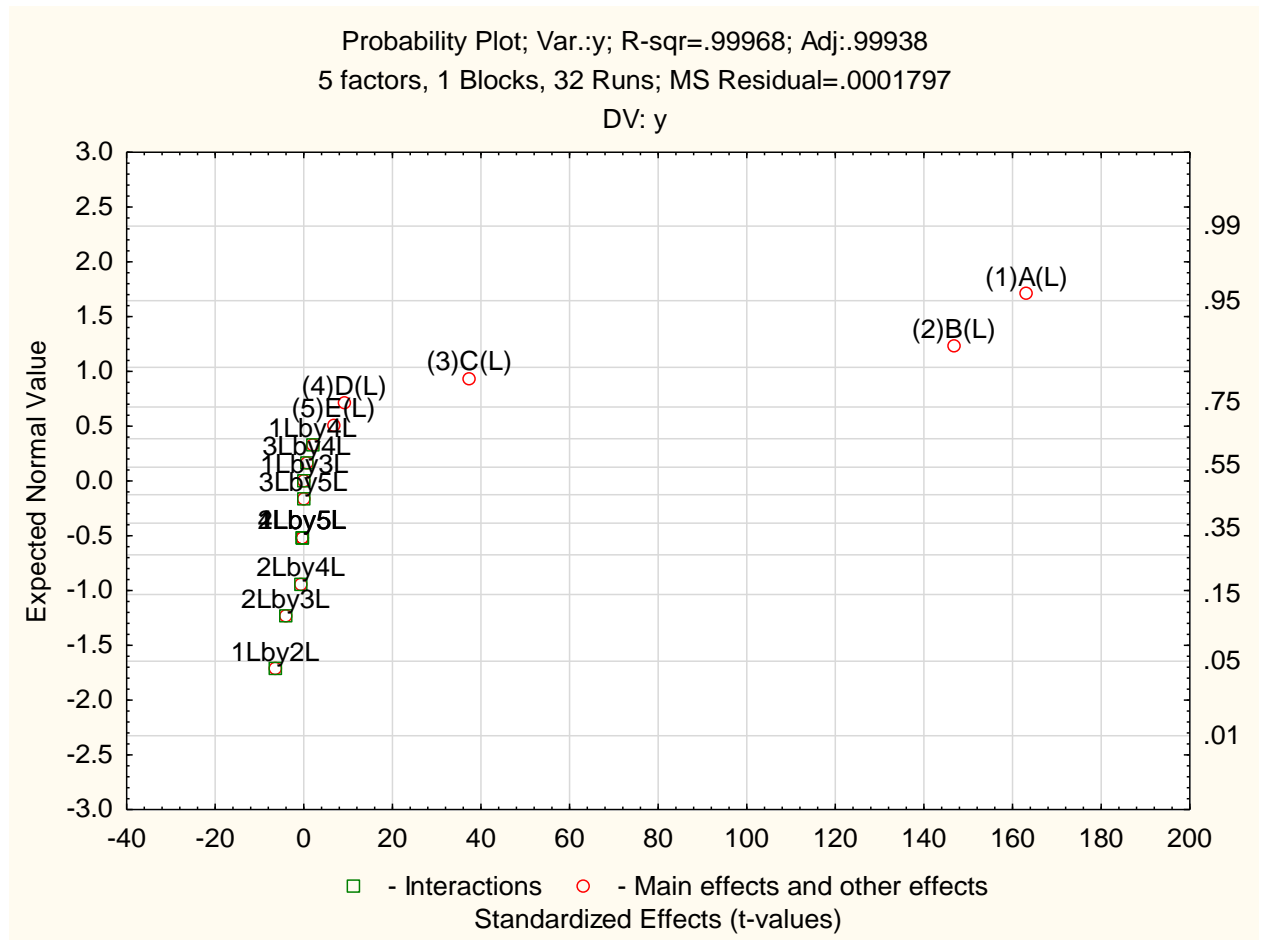


Figure 7.5: Normal probability plot of Lac applied on PLA using Catechu as biomordant.

Table 7.7: Factors for RSM of PLA with Lac using Catechu as biomordant.

Factors	Notations	Coded values				
		$-\alpha(-1.68)$	-1	0	1	$+\alpha(+1.68)$
Real values						
Dyeing temperature ($^{\circ}\text{C}$)	A	93	100	110	120	127
Initial pH	B	4	5	6	7	8
Dyeing time (min)	C	5	15	30	45	55

Table 7.8: Average values of experiments used for RSM.

Runs	Dyeing temperature	Initial pH	Dyeing time	Experimental values
	$^{\circ}\text{C}$		min	K/S
	A	B	C	y
1	-1.00	-1.00	-1.00	1.22
2	-1.00	-1.00	1.00	1.72
3	-1.00	1.00	-1.00	1.84
4	-1.00	1.00	1.00	2.23
5	1.00	-1.00	-1.00	2.06
6	1.00	-1.00	1.00	2.42
7	1.00	1.00	-1.00	2.55
8	1.00	1.00	1.00	2.63
9	-1.68	0.00	0.00	1.82
10	1.68	0.00	0.00	2.96
11	0.00	-1.68	0.00	1.81
12	0.00	1.68	0.00	2.28
13	0.00	0.00	-1.68	1.62
14	0.00	0.00	1.68	2.25
15	0.00	0.00	0.00	3
16	0.00	0.00	0.00	2.9
17	0.00	0.00	0.00	2.94
18	0.00	0.00	0.00	2.92
19	0.00	0.00	0.00	2.89
20	0.00	0.00	0.00	2.96

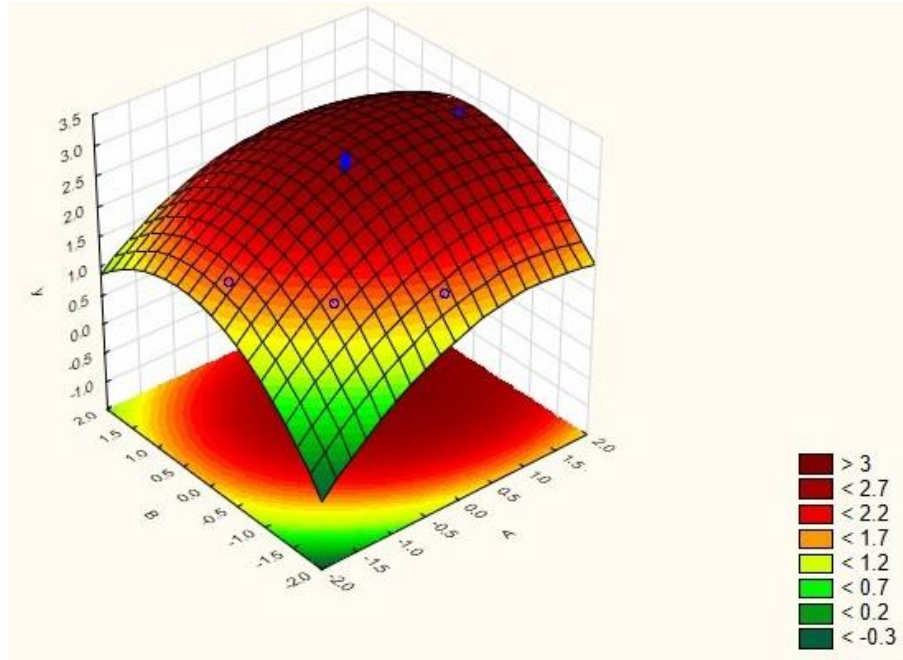


Figure 7.6: Contour plot for K/S value (y) with temperature (A) and initial pH of dye bath

(B).

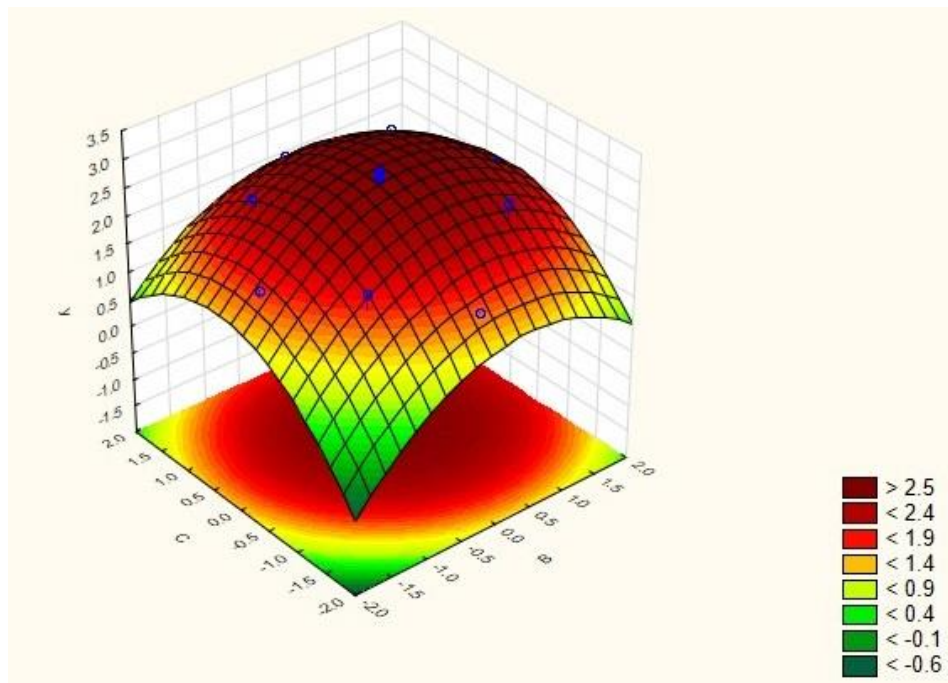


Figure 7.7: Contour plot for K/S value (y) with initial pH of dye bath (B) and time (C).

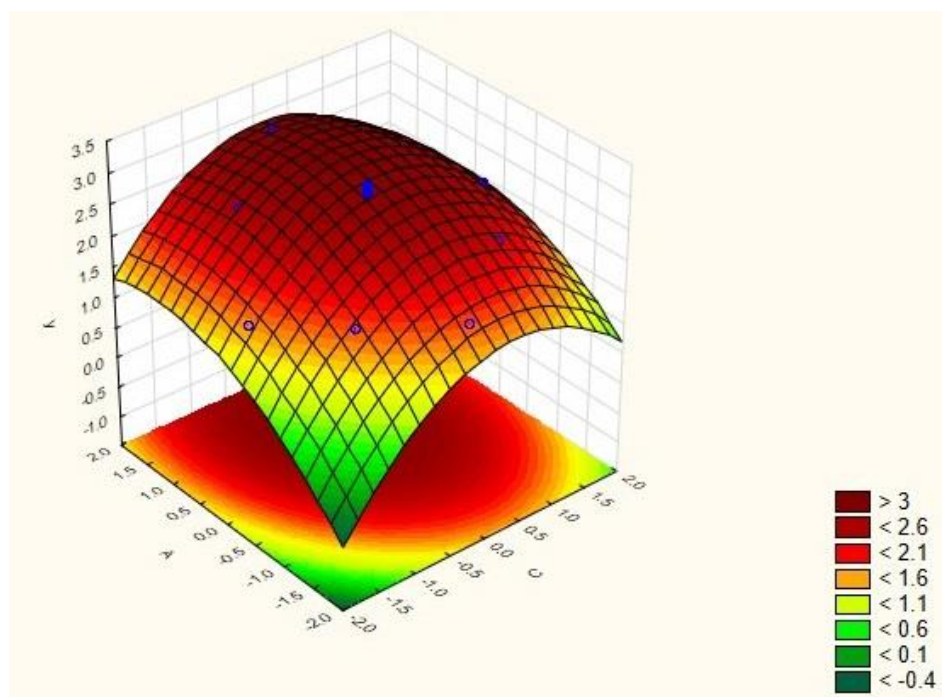


Figure 7.8: Contour plot for K/S value (y) with temperature (A) and time (C).

With temperature, initial pH of dye bath and time, RSM was done for Lac with PLA using Catechu as biomordant. The levels of the factors chosen for this combination of natural dye and biomordant are given in Table 7.7.

Five experiments were done in each run and the average values reported in Table 7.8. The contour plots obtained in the RSM are given in Figures 7.6-7.8. The analysis of variance (ANOVA) for the factors of response is given in Table 7.9 and the same for the quadratic regression model in Table 7.10.

The empirical model equation obtained with the coded variables is as follows:

$$y = 2.935 + 0.334A - 0.191A^2 + 0.192B - 0.313B^2 + 0.175C - 0.352C^2 - 0.054AB - 0.056AC - 0.049BC \quad (7.2)$$

The optimal values were observed as 118⁰C for temperature, 6.2 for initial pH of dye bath and 33 min for dyeing time approximately. The predicted K/S value under these optimal conditions was 3.11.

It was seen from Table 7.9 that the factors A , A^2 , B , B^2 , C , C^2 , AB and AC were the most significant factors with p-values less than 0.05. Thus, temperature (A), initial pH (B) as well as time (C) had significant linear as well as quadratic effects on K/S value. Besides, the interaction effects between temperature and initial pH as well as temperature and time were found to have significant effects on the K/S value.

From Table 7.10, it was observed that at 95% confidence level, the quadratic regression model developed was statistically significant with F-value of 156.775 that was much higher than the F-value of the lack of fit (3.8122). The R^2 value was found to be 0.99296 indicating that 99.30% of the total variations could be explained by the developed model, and 0.70% of the variations could not be explained. The adjusted R^2 value of 0.98663 was reasonably close to the R^2 value, indicating a high goodness of fit for the developed model.

Table 7.9: Variance analysis (ANOVA) of factors on response.

Factors	Sum of Squares	Degrees of Freedom	Mean Square	F Value	p-Value Prob>F
A	1.527	1	1.527	380.123	0.000
A^2	0.524	1	0.524	130.359	0.000
B	0.503	1	0.503	125.131	0.000
B^2	1.408	1	1.408	350.525	0.000
C	0.418	1	0.418	104.050	0.000
C^2	1.781	1	1.781	443.161	0.000
AxB	0.023	1	0.023	5.752	0.037
AxC	0.025	1	0.025	6.299	0.031
BxC	0.019	1	0.019	4.732	0.055

Table 7.10: Variance analysis (ANOVA) of quadratic regression model.

Source	Sum of Squares	Degrees of Freedom	Mean Square	F Value	p-Value Prob>F
Model	5.6696	9	0.6299	156.775	0.00
Residual	0.0402	10	0.0040		
Lack of fit	0.0318	5	0.00637	3.8122	0.08
Pure error	0.0084	5	0.00167		
Total	5.7098	19			

7.1.2 Optimization with Lac using Myrobalan as biomordant

The real values of -1 and +1 levels for the five factors used in the normal probability plots for dyeing with Lac using Myrobalan as biomordant were the same when Lac was applied using Catechu as biomordant, as given in Tables 7.1 and 7.2 for PTT and PLA respectively, along with the notations and units.

7.1.2.1 Optimization for PTT

The normal probability plot with Lac applied on PTT using Myrobalan as biomordant is shown in Figure 7.9. It could be observed that points A, B and C were distinct outliers with positive effects in the probability plot. Also, it could be seen that point 1x2 was also an outlier on the negative side.

It could thus be inferred temperature (A, 1), time (B, 2) and initial pH of the dye bath (C, 3) were the most significant factors affecting the color strength of PTT with Lac using Myrobalan as biomordant. Also, the interaction effect of temperature (1) and time (2) were more significant than the other factors and their interactions. The R^2 value of 0.99811 and adjusted R^2 value of 0.99633 indicated that the probability plot obtained was statistically significant with a high goodness of fit.

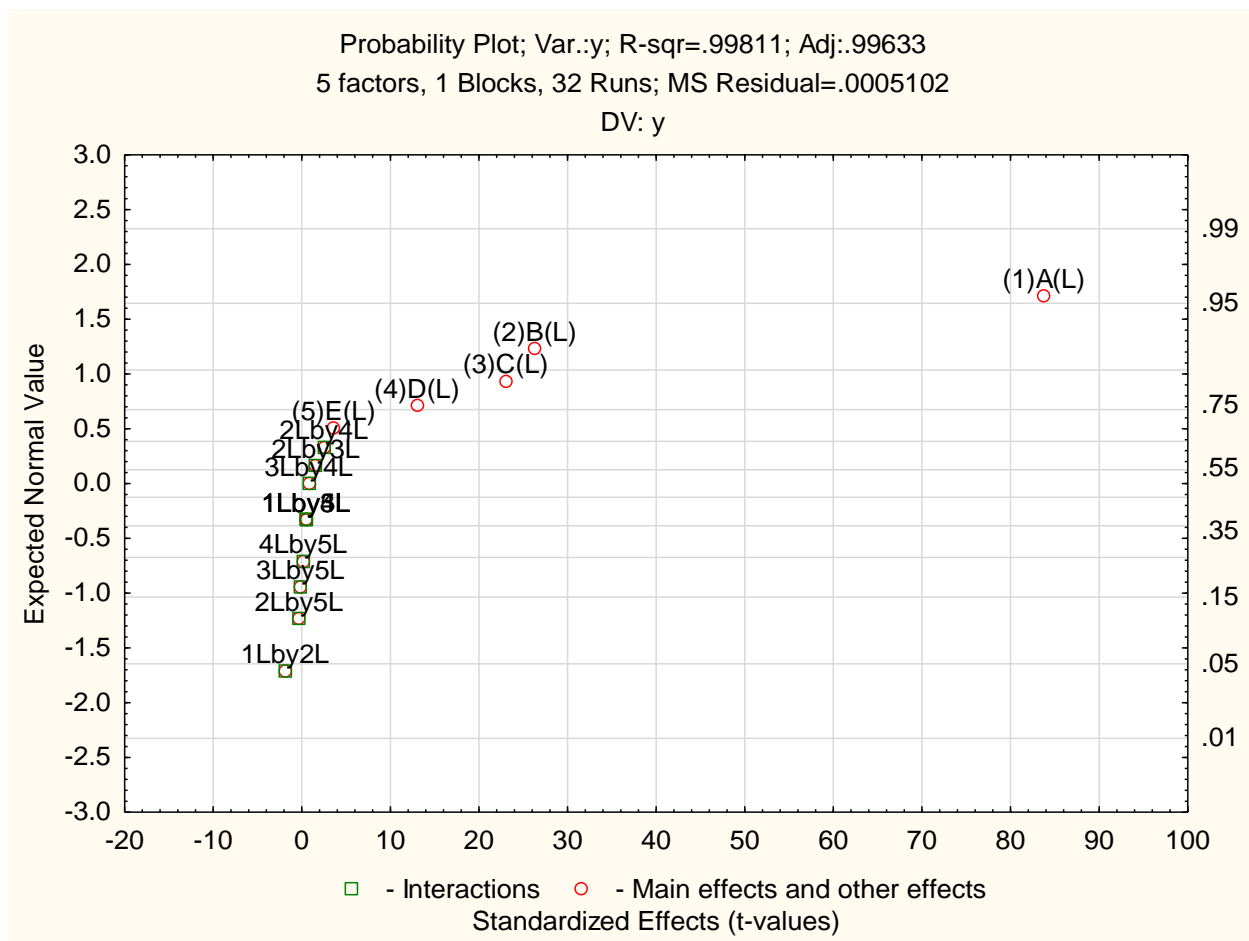


Figure 7.9: Normal probability plot of Lac applied on PTT using Myrobalan as biomordant.

With temperature, initial pH of dye bath and time, RSM was done for Lac with PTT using Myrobalan as biomordant. The levels of the factors chosen for this combination of natural dye and biomordant were the same when Lac was applied with Catechu as biomordant, as given in Table 7.3. Five experiments were done in each run and the average values reported in Table 7.11. The contour plots obtained in the RSM are given in Figures 7.10-7.12. The analysis of variance (ANOVA) for the factors of response is given in Table 7.12 and the same for the quadratic regression model in Table 7.13.

Table 7.11: Average values of experiments used for RSM.

Runs	Dyeing temperature	Initial pH	Dyeing time	Experimental values
	$^{\circ}\text{C}$		min	K/S
	A	B	C	y
1	-1.00	-1.00	-1.00	1.95
2	-1.00	-1.00	1.00	2.29
3	-1.00	1.00	-1.00	2.15
4	-1.00	1.00	1.00	2.42
5	1.00	-1.00	-1.00	2.37
6	1.00	-1.00	1.00	2.54
7	1.00	1.00	-1.00	2.48
8	1.00	1.00	1.00	2.49
9	-1.68	0.00	0.00	2.07
10	1.68	0.00	0.00	2.51
11	0.00	-1.68	0.00	2.44
12	0.00	1.68	0.00	2.59
13	0.00	0.00	-1.68	2.18
14	0.00	0.00	1.68	2.52
15	0.00	0.00	0.00	2.63
16	0.00	0.00	0.00	2.74
17	0.00	0.00	0.00	2.67
18	0.00	0.00	0.00	2.6
19	0.00	0.00	0.00	2.68
20	0.00	0.00	0.00	2.71

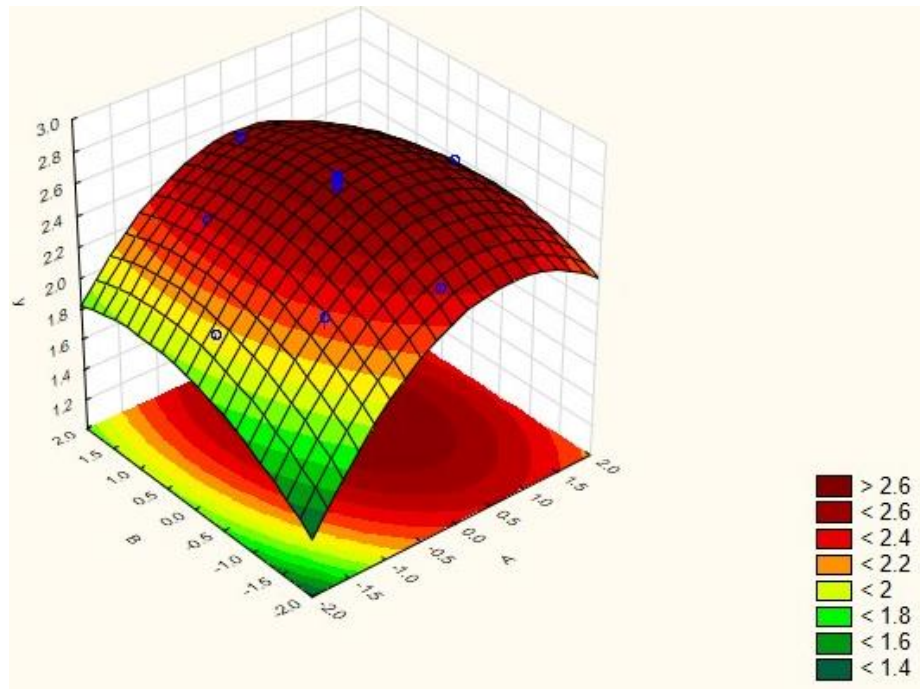


Figure 7.10: Contour plot for K/S value (y) with temperature (A) and initial pH of dye bath (B).

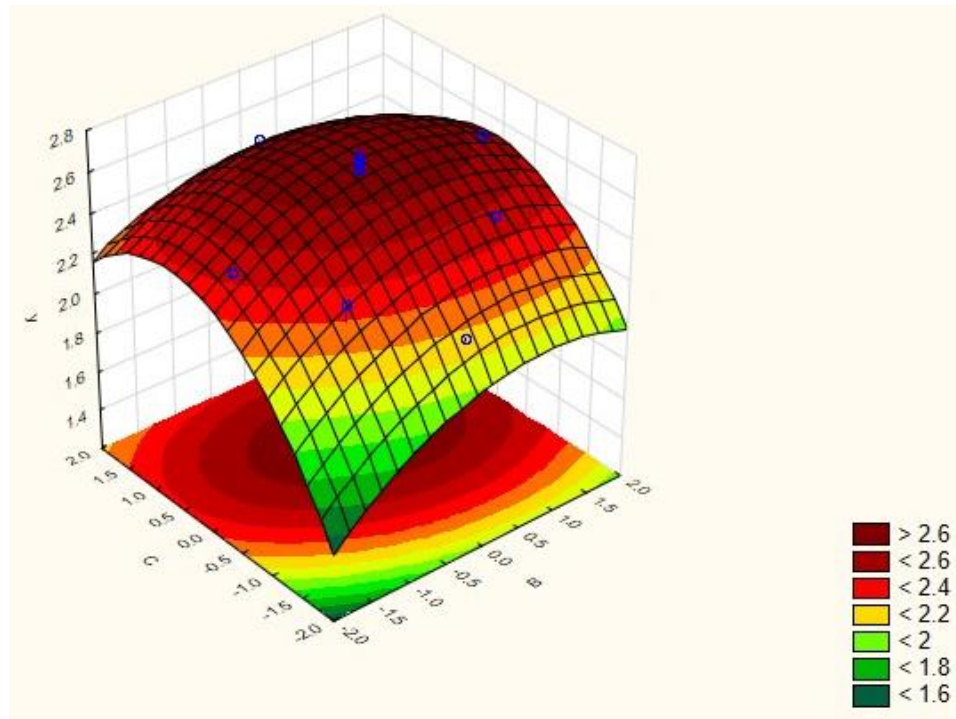


Figure 7.11: Contour plot for K/S value (y) with initial pH of dye bath (B) and time (C).

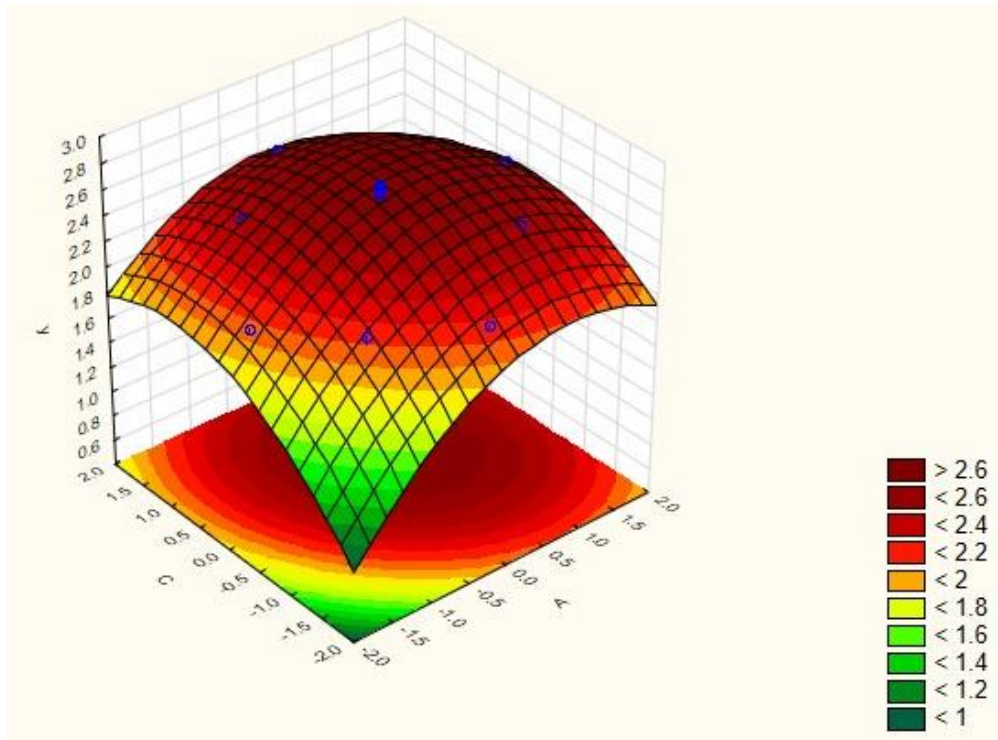


Figure 7.12: Contour plot for K/S value (y) with temperature (A) and time (C).

The empirical model equation obtained with the coded variables is as follows:

$$y = 2.673 + 0.133A - 0.142A^2 + 0.047B - 0.062B^2 + 0.099C - 0.12C^2 - 0.034AB - 0.054AC - 0.029BC \quad (7.3)$$

The optimal values were observed as 114°C for temperature, 6.2 for initial pH of dye bath and 50 min for dyeing time approximately. The predicted K/S value under these optimal conditions was 2.72.

It was seen from Table 7.12 that the factors A , A^2 , B , B^2 , C , C^2 , AB and AC were the most significant factors with p -values less than 0.05. Thus, temperature (A), initial pH (B) as well as time (C) had significant linear as well as quadratic effects on K/S value. Besides, the interaction effects between temperature and initial pH as well as temperature and time were found to have significant effects on the K/S value.

From Table 7.13, it was observed that at 95% confidence level, the quadratic regression model developed was statistically significant with F-value of 58.918 that was much higher than the F-value of the lack of fit (0.3254). The R^2 value was found to be 0.98149 indicating that 98.15% of the total variations could be explained by the developed model, and 1.65% of the variations could not be explained. The adjusted R^2 value of 0.96483 was reasonably close to the R^2 value, indicating a high goodness of fit for the developed model.

Table 7.12: Variance analysis (ANOVA) of factors on response.

Factors	Sum of Squares	Degrees of Freedom	Mean Square	F Value	p-Value Prob>F
<i>A</i>	0.240	1	0.240	138.336	0.000
<i>A</i> ²	0.289	1	0.289	166.534	0.000
<i>B</i>	0.030	1	0.030	17.419	0.002
<i>B</i> ²	0.055	1	0.055	31.954	0.000
<i>C</i>	0.136	1	0.136	78.310	0.000
<i>C</i> ²	0.209	1	0.209	120.361	0.000
<i>AxB</i>	0.009	1	0.009	5.255	0.045
<i>AxC</i>	0.023	1	0.023	13.328	0.004
<i>BxC</i>	0.007	1	0.007	3.813	0.079

Table 7.13: Variance analysis (ANOVA) of quadratic regression model.

Source	Sum of Squares	Degrees of Freedom	Mean Square	F Value	p-Value Prob>F
Model	0.9195	9	0.1022	58.918	0.00
Residual	0.0173	10	0.0017		
Lack of fit	0.0043	5	0.00085	0.3254	0.88
Pure error	0.0131	5	0.00262		
Total	0.9369	19			

7.1.2.2 Optimization for PLA

The normal probability plot with Lac applied on PLA using Myrobalan as biomordant is shown in Figure 7.13. It could be observed that points A, B and C were distinct outliers with positive effects in the probability plot. Also, it could be seen that point 1x4 was also an outlier on the negative side.

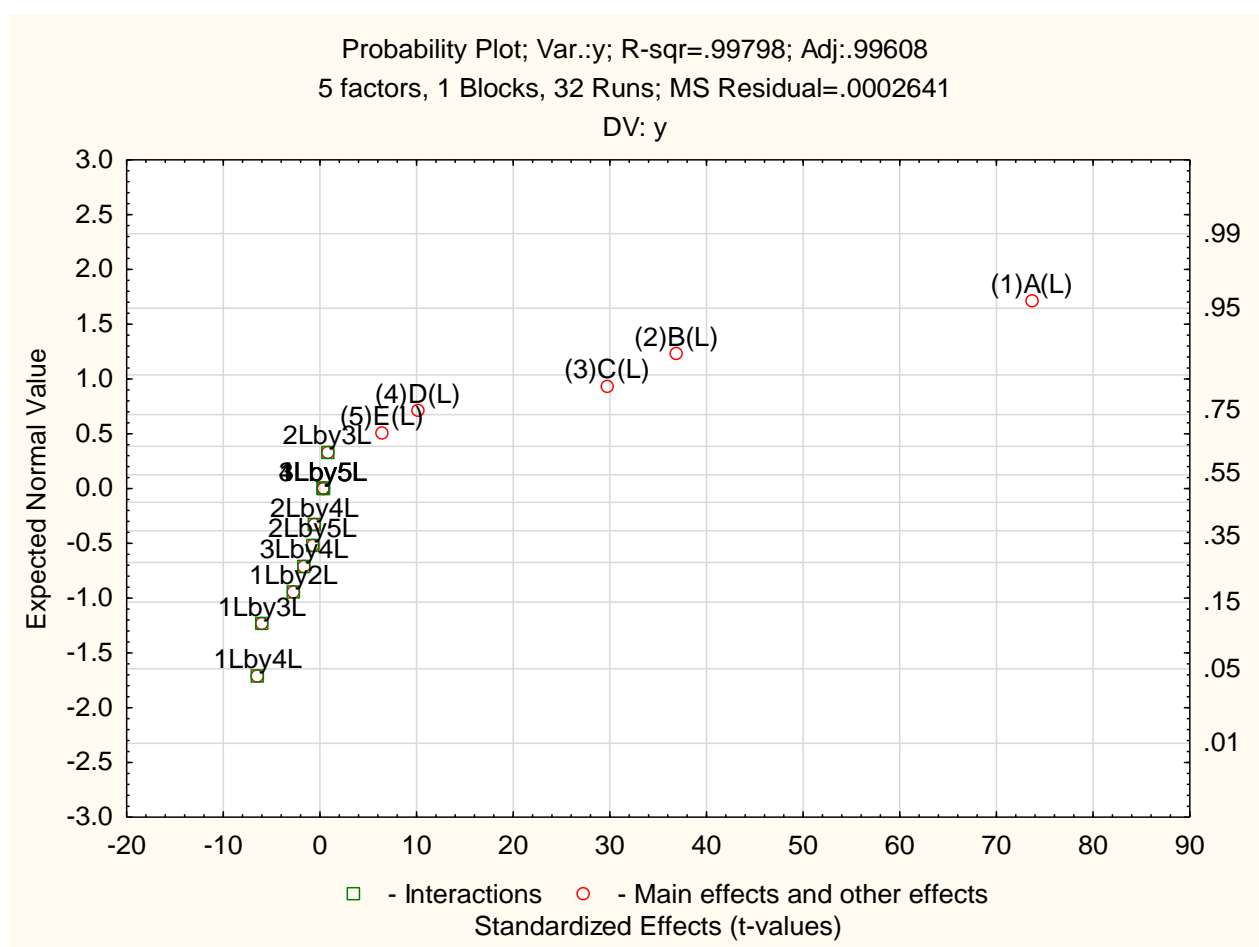


Figure 7.13: Normal probability plot of Lac applied on PLA using Myrobalan as biomordant.

It could thus be inferred temperature (A, 1), time (B, 2) and initial pH of the dye bath (C, 3) were the most significant factors affecting the color strength of PLA with Lac using Myrobalan as biomordant. Also, the interaction effect of temperature (1) and material to liquor ratio (4) were more significant than the other factors and their

interactions. The R^2 value of 0.99798 and adjusted R^2 value of 0.99608 indicated that the probability plot obtained was statistically significant with a high goodness of fit.

With temperature, initial pH of dye bath and time, RSM was done for Lac with PLA using Myrobalan as biomordant. The levels of the factors chosen for this combination of natural dye and biomordant were the same when Lac was applied with Catechu as biomordant, as given in Table 7.7. Five experiments were done in each run and the average values reported in Table 7.14. The contour plots obtained in the RSM are given in Figures 7.14-7.16. The analysis of variance (ANOVA) for the factors of response is given in Table 7.15 and the same for the quadratic regression model in Table 7.16.

The empirical model equation obtained with the coded variables is as follows:

$$y = 2.398 + 0.227A - 0.206A^2 + 0.107B - 0.121B^2 + 0.160C - 0.149C^2 - 0.106AB - 0.111AC - 0.059BC \quad (7.4)$$

The optimal values were observed as 114^oC for temperature, 6.2 for initial pH of dye bath and 35 min for dyeing time approximately. The predicted K/S value under these optimal conditions was 2.48.

It was seen from Table 7.15 that the factors A , A^2 , B , B^2 , C , C^2 , AB and AC were the most significant factors with p-values less than 0.05. Thus, temperature (A), initial pH (B) as well as time (C) had significant linear as well as quadratic effects on K/S value. Besides, the interaction effects between temperature and initial pH as well as temperature and time were found to have significant effects on the K/S value.

Table 7.14: Average values of experiments used for RSM.

Runs	Dyeing temperature	Initial pH	Dyeing time	Experimental values
	°C		min	K/S
	A	B	C	y
1	-1.00	-1.00	-1.00	1.05
2	-1.00	-1.00	1.00	1.77
3	-1.00	1.00	-1.00	1.68
4	-1.00	1.00	1.00	2.07
5	1.00	-1.00	-1.00	2.01
6	1.00	-1.00	1.00	2.19
7	1.00	1.00	-1.00	2.12
8	1.00	1.00	1.00	2.16
9	-1.68	0.00	0.00	1.52
10	1.68	0.00	0.00	2.23
11	0.00	-1.68	0.00	1.98
12	0.00	1.68	0.00	2.25
13	0.00	0.00	-1.68	1.78
14	0.00	0.00	1.68	2.29
15	0.00	0.00	0.00	2.32
16	0.00	0.00	0.00	2.44
17	0.00	0.00	0.00	2.36
18	0.00	0.00	0.00	2.41
19	0.00	0.00	0.00	2.45
20	0.00	0.00	0.00	2.39

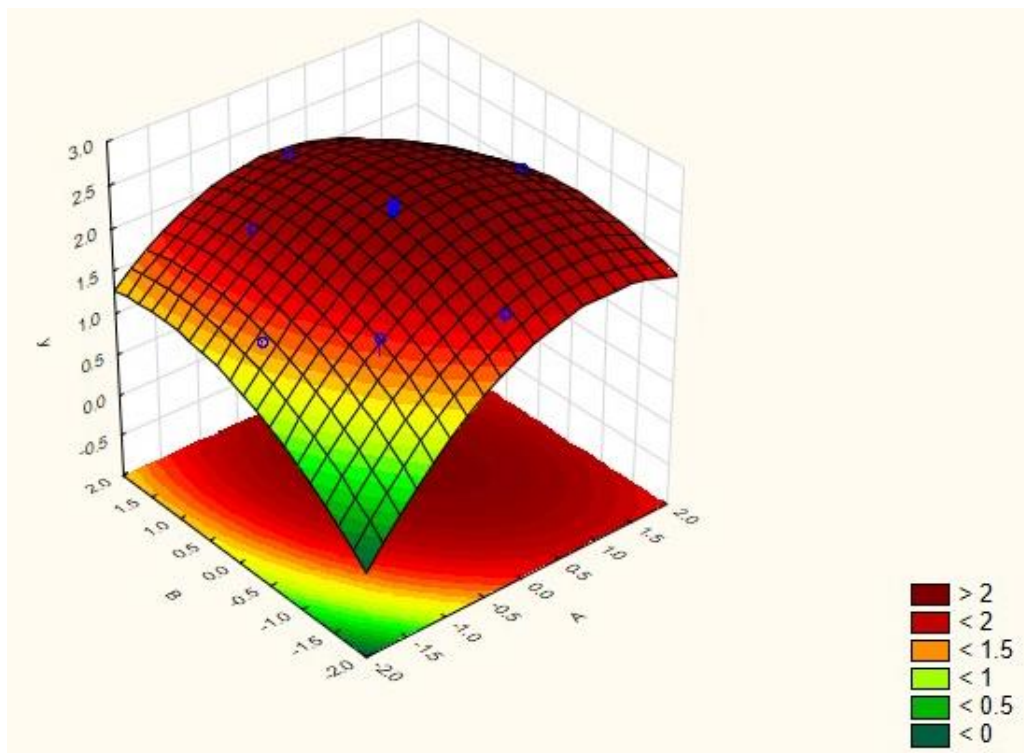


Figure 7.14: Contour plot for K/S value (y) with temperature (A) and initial pH of dye bath (B).

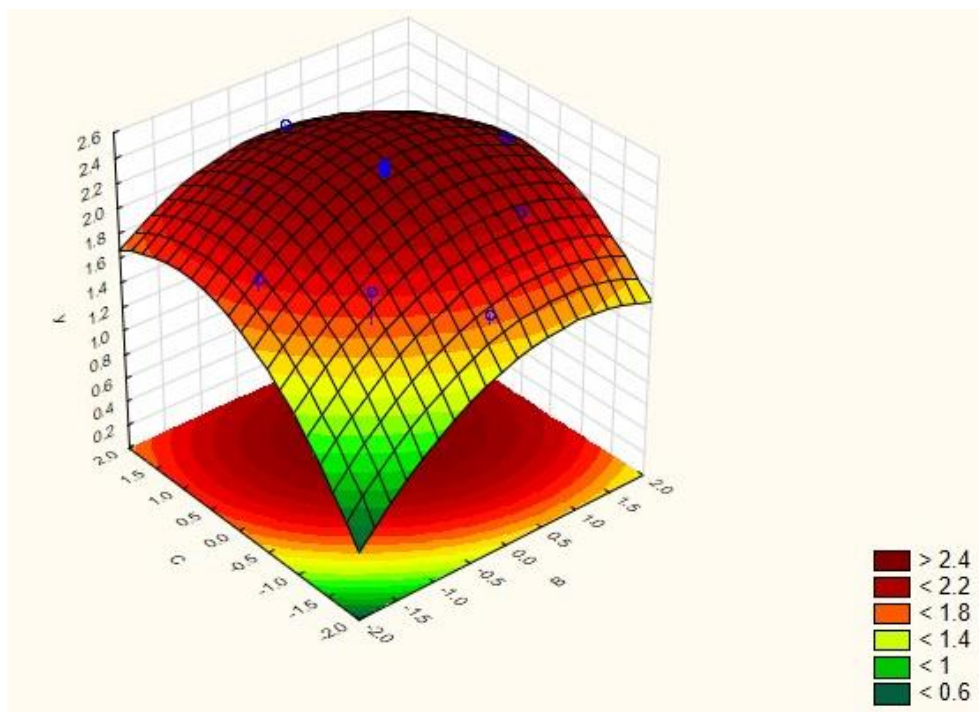


Figure 7.15: Contour plot for K/S value (y) with initial pH of dye bath (B) and time (C).

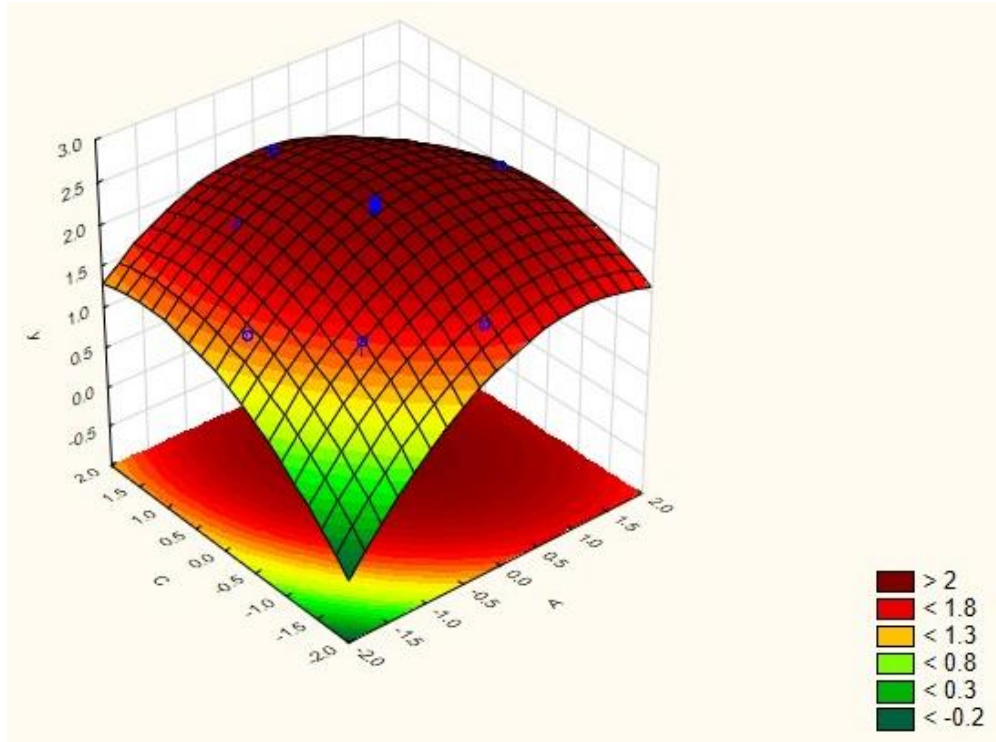


Figure 7.16: Contour plot for K/S value (y) with temperature (A) and time (C).

Table 7.15: Variance analysis (ANOVA) of factors on response.

Factors	Sum of Squares	Degrees of Freedom	Mean Square	F Value	p-Value Prob>F
A	0.706	1	0.706	115.264	0.000
A^2	0.610	1	0.610	99.636	0.000
B	0.157	1	0.157	25.643	0.000
B^2	0.211	1	0.211	34.393	0.000
C	0.350	1	0.350	57.255	0.000
C^2	0.321	1	0.321	52.374	0.000
AxB	0.090	1	0.090	14.755	0.003
AxC	0.099	1	0.099	16.176	0.002
BxC	0.028	1	0.028	4.511	0.060

Table 7.16: Variance analysis (ANOVA) of quadratic regression model.

Source	Sum of Squares	Degrees of Freedom	Mean Square	F Value	p-Value Prob>F
Model	2.3966	9	0.2663	43.505	0.00
Residual	0.0612	10	0.0061		
Lack of fit	0.0491	5	0.00981	4.0378	0.08
Pure error	0.0122	5	0.00243		
Total	2.4579	19			

.From Table 7.16, it was observed that at 95% confidence level, the quadratic regression model developed was statistically significant with F-value of 43.505 that was much higher than the F-value of the lack of fit (4.0378). The R^2 value was found to be 0.9751 indicating that 97.51% of the total variations could be explained by the developed model, and 2.495% of the variations could not be explained. The adjusted R^2 value of 0.95268 was reasonably close to the R^2 value, indicating a high goodness of fit for the developed model.

7.1.3 Optimization with Lac using Pomegranate as biomordant

The real values of -1 and +1 levels for the five factors used in the normal probability plots for dyeing with Lac using Pomegranate as biomordant were the same when Lac was applied using Catechu as biomordant, as given in Tables 7.1 and 7.2 for PTT and PLA respectively, along with the notations and units.

7.1.3.1 Optimization for PTT

The normal probability plot with Lac applied on PTT using Pomegranate as biomordant is shown in Figure 7.17. It could be observed that points A, B and C were distinct outliers with positive effects in the probability plot. Also, it could be seen that points 1x2 and 1x3 were also outliers on the negative side.

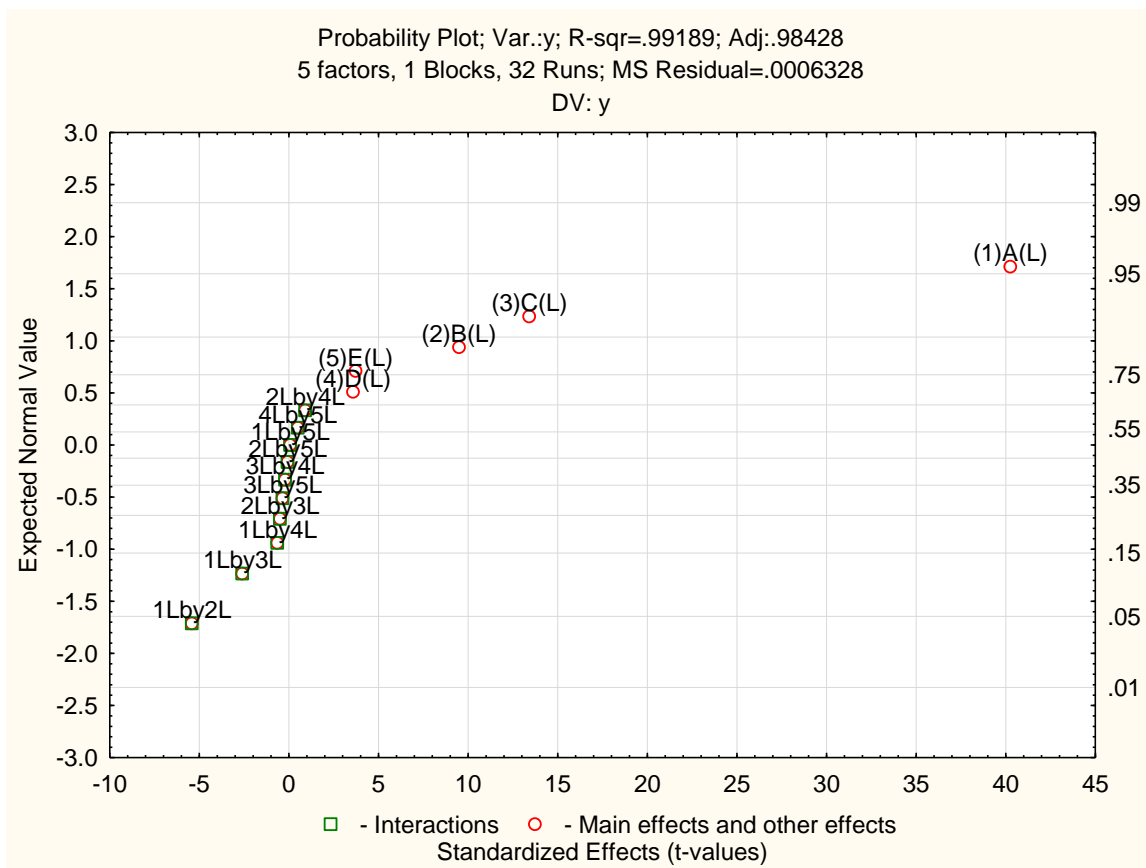


Figure 7.17: Normal probability plot of Lac applied on PTT using Pomegranate as biomordant.

It could thus be inferred temperature (A, 1), time (B, 2) and initial pH of the dye bath (C, 3) were the most significant factors affecting the color strength of PTT with Lac using Pomegranate as biomordant. Also, the interaction effects between temperature (1) and time (2) as well as temperature (1) and initial pH (3) were more significant than the other factors and their interactions. The R^2 value of 0.99189 and adjusted R^2 value of 0.98428 indicated that the probability plot obtained was statistically significant with a high goodness of fit.

With temperature, initial pH of dye bath and time, RSM was done for Lac with PTT using Pomegranate as biomordant. The levels of the factors chosen for this

combination of natural dye and biomordant were the same when Lac was applied with Catechu as biomordant, as given in Table 7.3. Five experiments were done in each run and the average values reported in Table 7.17. The contour plots obtained in the RSM are given in Figures 7.18-7.20. The analysis of variance (ANOVA) for the factors of response is given in Table 7.18 and the same for the quadratic regression model in Table 7.19.

The empirical model equation obtained with the coded variables is as follows:

$$y = 2.115 + 0.197A - 0.218A^2 + 0.103B - 0.109B^2 + 0.165C - 0.148C^2 - 0.081AB - 0.094AC - 0.034BC \quad (7.5)$$

The optimal values were observed as 113⁰C for temperature, 6.3 for initial pH of dye bath and 51 min for dyeing time approximately. The predicted K/S value under these optimal conditions was 2.196.

It was seen from Table 7.18 that the factors A , A^2 , B , B^2 , C , C^2 , AB and AC were the most significant factors with p-values less than 0.05. Thus, temperature (A), initial pH (B) as well as time (C) had significant linear as well as quadratic effects on K/S value. Besides, the interaction effects between temperature and initial pH as well as temperature and time were found to have significant effects on the K/S value.

Table 7.17: Average values of experiments used for RSM.

Runs	Dyeing temperature	Initial pH	Dyeing time	Experimental values
	°C		min	K/S
	A	B	C	y
1	-1.00	-1.00	-1.00	0.91
2	-1.00	-1.00	1.00	1.53
3	-1.00	1.00	-1.00	1.41
4	-1.00	1.00	1.00	1.78
5	1.00	-1.00	-1.00	1.69
6	1.00	-1.00	1.00	1.82
7	1.00	1.00	-1.00	1.75
8	1.00	1.00	1.00	1.86
9	-1.68	0.00	0.00	1.21
10	1.68	0.00	0.00	1.92
11	0.00	-1.68	0.00	1.71
12	0.00	1.68	0.00	2.04
13	0.00	0.00	-1.68	1.46
14	0.00	0.00	1.68	2.07
15	0.00	0.00	0.00	2.09
16	0.00	0.00	0.00	2.11
17	0.00	0.00	0.00	2.17
18	0.00	0.00	0.00	2.13
19	0.00	0.00	0.00	2.05
20	0.00	0.00	0.00	2.12

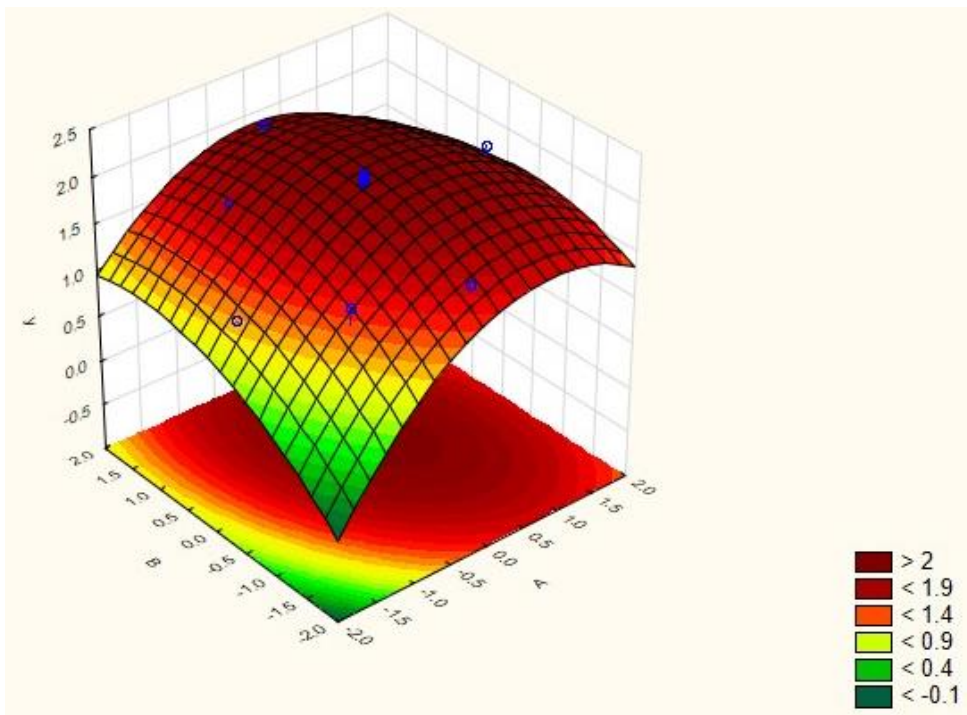


Figure 7.18: Contour plot for K/S value (y) with temperature (A) and initial pH of dye bath (B).

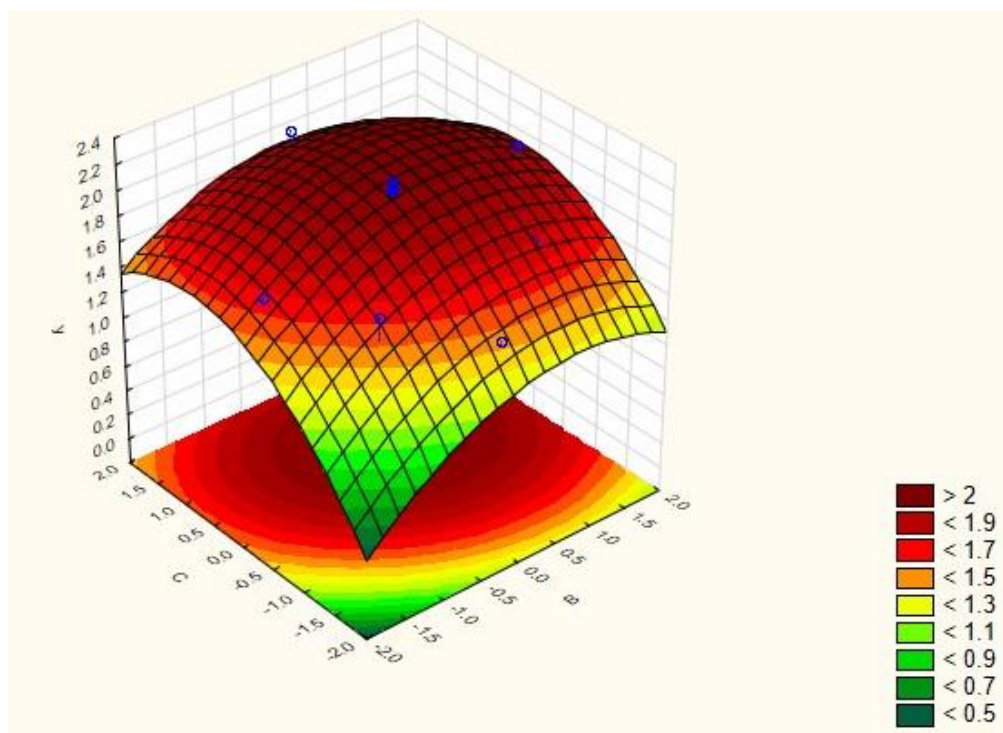


Figure 7.19: Contour plot for K/S value (y) with initial pH of dye bath (B) and time (C).

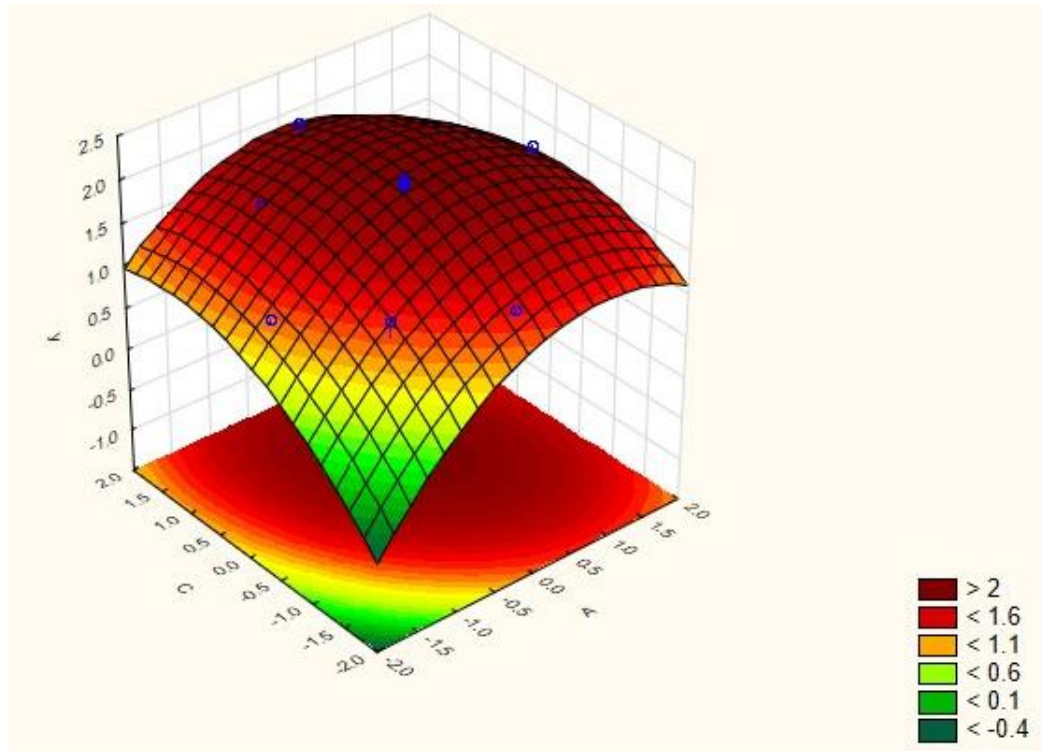


Figure 7.20: Contour plot for K/S value (y) with temperature (A) and time (C).

Table 7.18: Variance analysis (ANOVA) of factors on response.

Factors	Sum of Squares	Degrees of Freedom	Mean Square	F Value	p-Value Prob>F
A	0.528	1	0.528	82.096	0.000
A^2	0.687	1	0.687	106.841	0.000
B	0.145	1	0.145	22.495	0.001
B^2	0.170	1	0.170	26.480	0.000
C	0.373	1	0.373	57.992	0.000
C^2	0.314	1	0.314	48.828	0.000
AxB	0.053	1	0.053	8.219	0.017
AxC	0.070	1	0.070	10.942	0.008
BxC	0.009	1	0.009	1.418	0.261

Table 7.19: Variance analysis (ANOVA) of quadratic regression model.

Source	Sum of Squares	Degrees of Freedom	Mean Square	F Value	p-Value Prob>F
Model	2.1780	9	0.242	37.661	0.00
Residual	0.0643	10	0.0064		
Lack of fit	0.0562	5	0.01123	6.9493	0.3
Pure error	0.0081	5	0.00162		
Total	2.2423	19			

From Table 7.19, it was observed that at 95% confidence level, the quadratic regression model developed was statistically significant with F-value of 37.661 that was much higher than the F-value of the lack of fit (6.9493). The R^2 value was found to be 0.97134 indicating that 97.13% of the total variations could be explained by the developed model, and 2.87% of the variations could not be explained. The adjusted R^2 value of 0.94555 was reasonably close to the R^2 value, indicating a high goodness of fit for the developed model.

7.1.3.2 Optimization for PLA

The normal probability plot with Lac applied on PLA using Pomegranate as biomordant is shown in Figure 7.21. It could be observed that points A, B and C were distinct outliers with positive effects in the probability plot. Also, it could be seen that point 2x3 was also an outlier on the negative side.

It could thus be inferred temperature (A, 1), time (B, 2) and initial pH of the dye bath (C, 3) were the most significant factors affecting the color strength of PLA with Lac using Pomegranate as biomordant. Also, the interaction effect between time (2) and initial pH (3) was more significant than the other factors and their interactions. The R^2 value of 0.99904 and adjusted R^2 value of 0.99814 indicated that the probability plot obtained was statistically significant with a high goodness of fit.

With temperature, initial pH of dye bath and time, RSM was done for Lac with PLA using Pomegranate as biomordant. The levels of the factors chosen for this combination of natural dye and biomordant were the same when Lac was applied with Catechu as biomordant, as given in Table 7.7. Five experiments were done in each run and the average values reported in Table 7.20. The contour plots obtained in the RSM are given in Figures 7.22-7.24. The analysis of variance (ANOVA) for the factors of response is given in Table 7.21 and the same for the quadratic regression model in Table 7.22.

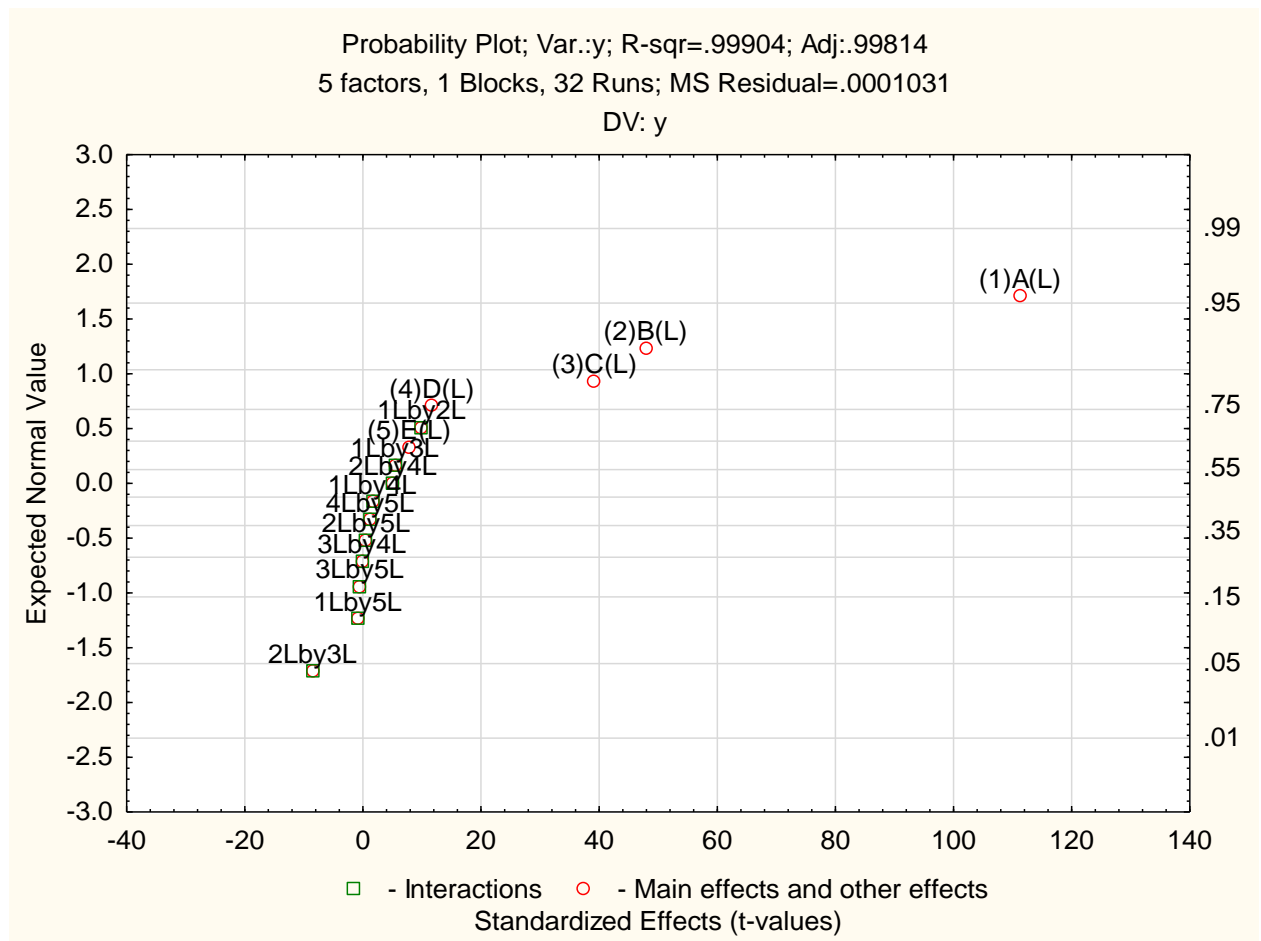


Figure 7.21: Normal probability plot of Lac applied on PLA using Myrobalan as biomordant.

The empirical model equation obtained with the coded variables is as follows:

$$y = 1.916 + 0.208A - 0.235A^2 + 0.101B - 0.115B^2 + 0.169C - 0.159C^2 - 0.086AB - 0.094AC - 0.066BC \quad (7.6)$$

The optimal values were observed as 113⁰C for temperature, 6.2 for initial pH of dye bath and 36 min for dyeing time approximately. The predicted K/S value under these optimal conditions was 1.994.

It was seen from Table 7.21 that the factors A , A^2 , B , B^2 , C , C^2 , AB , AC and BC were the most significant factors with p-values less than 0.05. Thus, temperature (A), initial pH (B) as well as time (C) had significant linear as well as quadratic effects on K/S value. Besides, the interaction effects among temperature, initial pH as well as time were found to have significant effects on the K/S value.

From Table 7.22, it was observed that at 95% confidence level, the quadratic regression model developed was statistically significant with F-value of 71.304 that was much higher than the F-value of the lack of fit (3.9096). The R^2 value was found to be 0.98466 indicating that 98.47% of the total variations could be explained by the developed model, and 1.53% of the variations could not be explained. The adjusted R^2 value of 0.97085 was reasonably close to the R^2 value, indicating a high goodness of fit for the developed model.

Table 7.20: Average values of experiments used for RSM.

Runs	Dyeing temperature	Initial pH	Dyeing time	Experimental values
	^o C		min	K/S
	A	B	C	y
1	-1.00	-1.00	-1.00	0.64
2	-1.00	-1.00	1.00	1.32
3	-1.00	1.00	-1.00	1.18
4	-1.00	1.00	1.00	1.54
5	1.00	-1.00	-1.00	1.43
6	1.00	-1.00	1.00	1.68
7	1.00	1.00	-1.00	1.57
8	1.00	1.00	1.00	1.61
9	-1.68	0.00	0.00	0.94
10	1.68	0.00	0.00	1.67
11	0.00	-1.68	0.00	1.48
12	0.00	1.68	0.00	1.81
13	0.00	0.00	-1.68	1.23
14	0.00	0.00	1.68	1.81
15	0.00	0.00	0.00	1.85
16	0.00	0.00	0.00	1.91
17	0.00	0.00	0.00	1.93
18	0.00	0.00	0.00	1.96
19	0.00	0.00	0.00	1.94
20	0.00	0.00	0.00	1.89

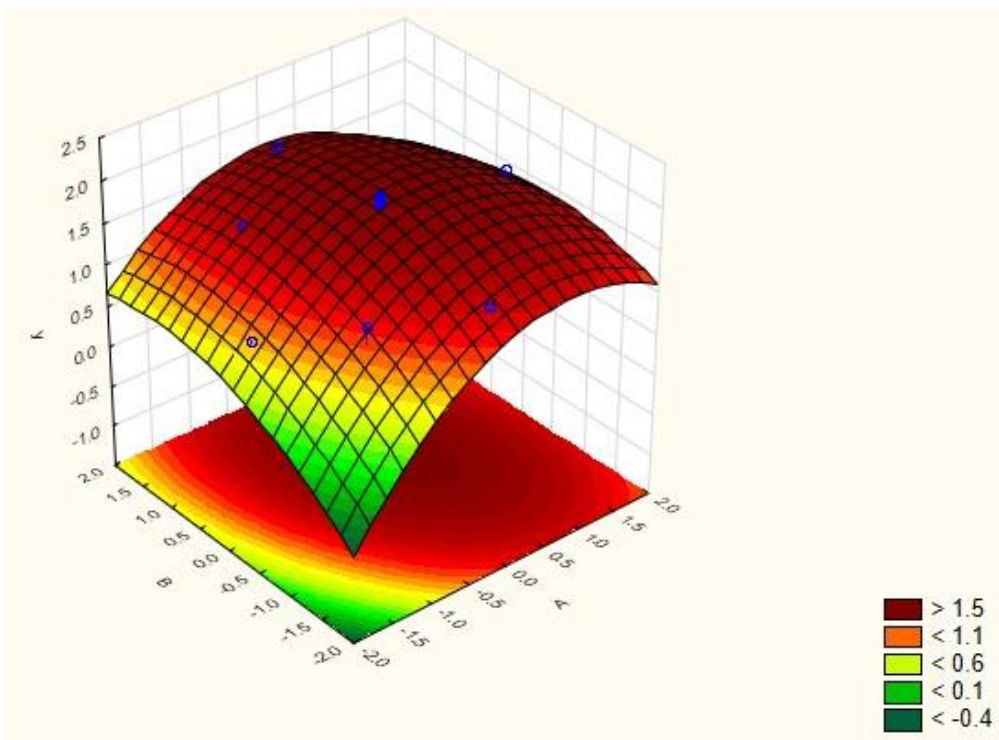


Figure 7.22: Contour plot for K/S value (y) with temperature (A) and initial pH of dye bath (B).

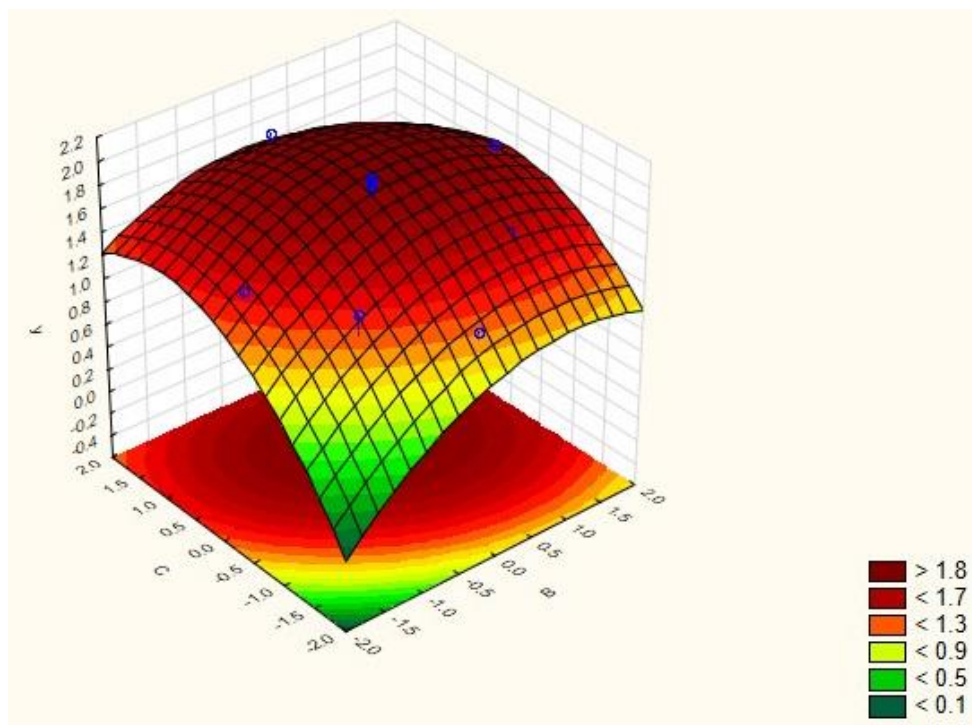


Figure 7.23: Contour plot for K/S value (y) with initial pH of dye bath (B) and time (C).

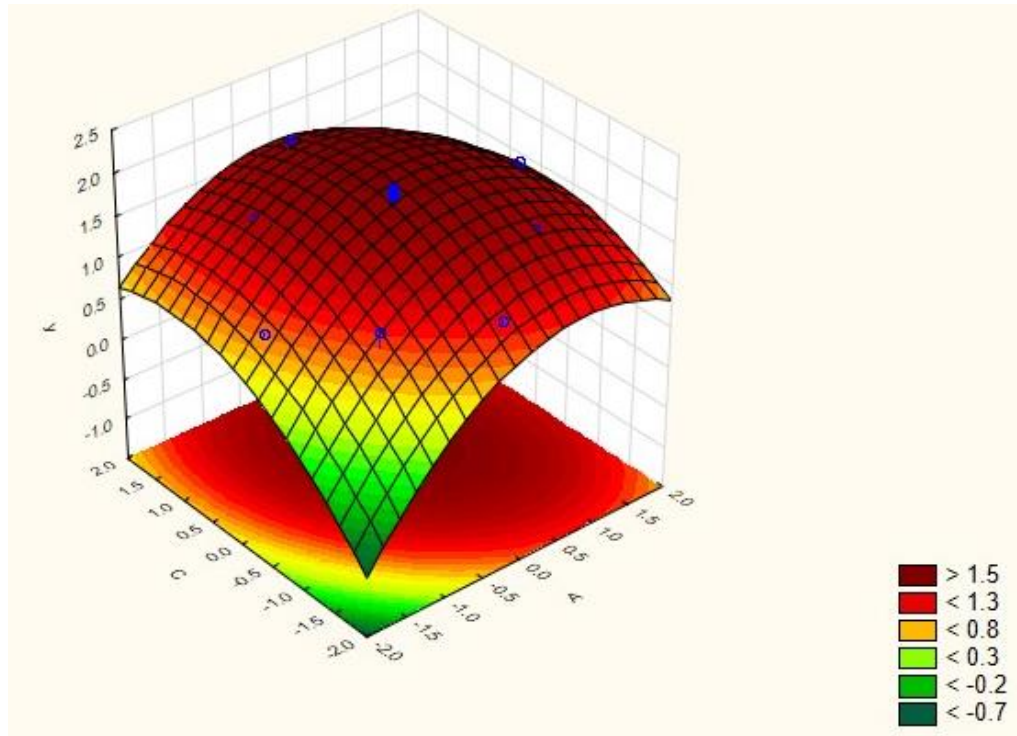


Figure 7.24: Contour plot for K/S value (y) with temperature (A) and time (C).

Table 7.21: Variance analysis (ANOVA) of factors on response.

Factors	Sum of Squares	Degrees of Freedom	Mean Square	F Value	p-Value Prob>F
A	0.590	1	0.590	155.300	0.000
A^2	0.794	1	0.794	209.114	0.000
B	0.140	1	0.140	36.994	0.000
B^2	0.189	1	0.189	49.771	0.000
C	0.389	1	0.389	102.504	0.000
C^2	0.363	1	0.363	95.602	0.000
AxB	0.060	1	0.060	15.675	0.003
AxC	0.070	1	0.070	18.519	0.002
BxC	0.035	1	0.035	9.248	0.012

Table 7.22: Variance analysis (ANOVA) of quadratic regression model.

Source	Sum of Squares	Degrees of Freedom	Mean Square	F Value	p-Value Prob>F
Model	2.4365	9	0.2707	71.304	0.00
Residual	0.0380	10	0.0038		
Lack of fit	0.0302	5	0.00605	3.9096	0.08
Pure error	0.0077	5	0.00155		
Total	2.4745	19			

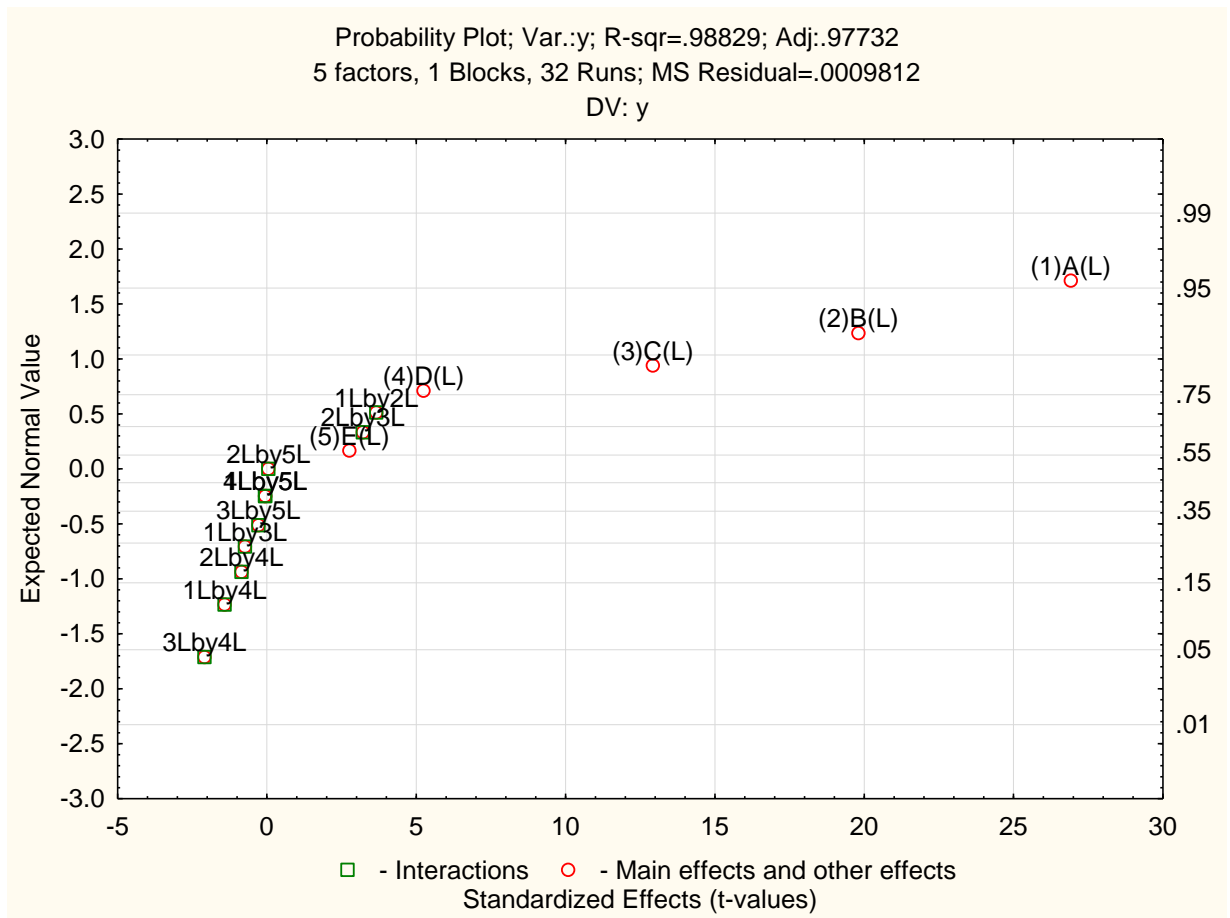


Figure 7.25: Normal probability plot of Catechu applied on PTT using Myrobalan as biomordant.

7.1.4 Optimization with Catechu using Myrobalan as biomordant

The real values of -1 and +1 levels for the five factors used in the normal probability plots for dyeing with Lac using Pomegranate as biomordant were the same when Lac was applied using Catechu as biomordant, as given in Tables 7.1 and 7.2 for PTT and PLA respectively, along with the notations and units.

7.1.4.1 Optimization for PTT

The normal probability plot with Catechu applied on PTT using Myrobalan as biomordant is shown in Figure 7.25. It could be observed that points A, B and C were distinct outliers with positive effects in the probability plot. Also, it could be seen that point 3x4 was also an outlier on the negative side.

It could thus be inferred from Figure 7.25 that temperature (A, 1), time (B, 2) and initial pH of the dye bath (C, 3) were the most significant factors affecting the color strength of PTT with Catechu using Myrobalan as biomordant. Also, the interaction effect between initial pH (3) and material to liquor ratio (4) was more significant than the other factors and their interactions. The R^2 value of 0.98829 and adjusted R^2 value of 0.97732 indicated that the probability plot obtained was statistically significant with a high goodness of fit.

Table 7.23: Average values of experiments used for RSM.

Runs	Dyeing temperature	Initial pH	Dyeing time	Experimental values
	$^{\circ}\text{C}$		min	K/S
	A	B	C	y
1	-1.00	-1.00	-1.00	1.08
2	-1.00	-1.00	1.00	1.32
3	-1.00	1.00	-1.00	1.21
4	-1.00	1.00	1.00	1.39
5	1.00	-1.00	-1.00	1.36
6	1.00	-1.00	1.00	1.48
7	1.00	1.00	-1.00	1.41
8	1.00	1.00	1.00	1.54
9	-1.68	0.00	0.00	1.14
10	1.68	0.00	0.00	1.45
11	0.00	-1.68	0.00	1.39
12	0.00	1.68	0.00	1.59
13	0.00	0.00	-1.68	1.18
14	0.00	0.00	1.68	1.56
15	0.00	0.00	0.00	1.79
16	0.00	0.00	0.00	1.75
17	0.00	0.00	0.00	1.71
18	0.00	0.00	0.00	1.74
19	0.00	0.00	0.00	1.77
20	0.00	0.00	0.00	1.72

With temperature, initial pH of dye bath and time, RSM was done for Catechu with PTT using Myrobalan as biomordant. The levels of the factors chosen for this combination of natural dye and biomordant were the same when Lac was applied with Catechu as biomordant, as given in Table 7.3. Five experiments were done in each run and the average values reported in Table 7.23. The contour plots obtained in the RSM are given in Figures 7.26-7.28. The analysis of variance (ANOVA) for the factors of response is given in Table 7.24 and the same for the quadratic regression model in Table 7.25.

The empirical model equation obtained with the coded variables is as follows:

$$y = 1.747 + 0.096A - 0.163A^2 + 0.047B - 0.094B^2 + 0.096C - 0.136C^2 - 0.011AB - 0.021AC - 0.006BC \quad (7.7)$$

The optimal values were observed as 113⁰C for temperature, 6.2 for initial pH of dye bath and 50 min for dyeing time approximately. The predicted K/S value under these optimal conditions was 1.78.

It was seen from Table 7.24 that the factors A , A^2 , B , B^2 , C and C^2 were the most significant factors with p-values less than 0.05. Thus, temperature (A), initial pH (B) as well as time (C) had significant linear as well as quadratic effects on K/S value.

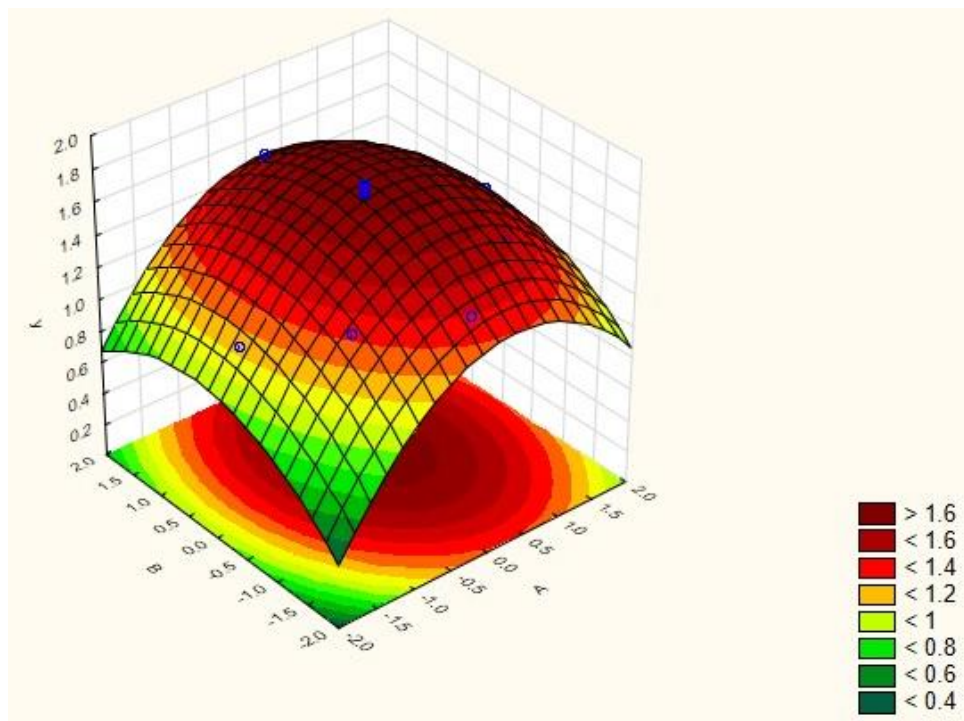
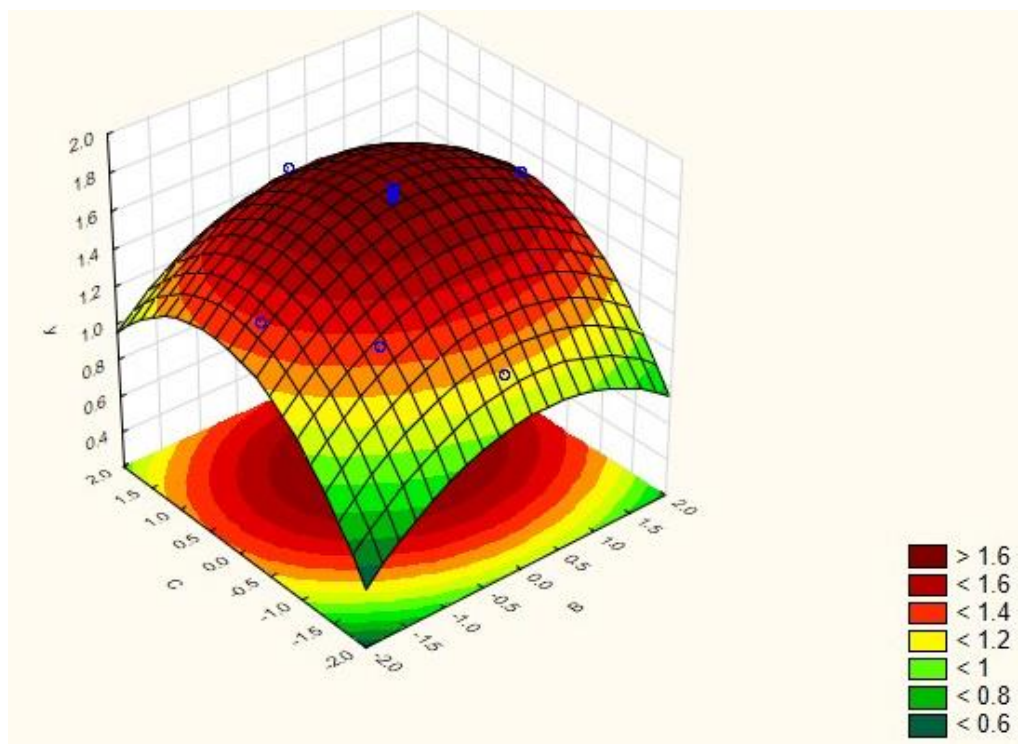


Figure 7.26: Contour plot for K/S value (y) with temperature (A) and initial pH of dye bath (B).



-Figure 7.27: Contour plot for K/S value (y) with initial pH of dye bath (B) and time (C).

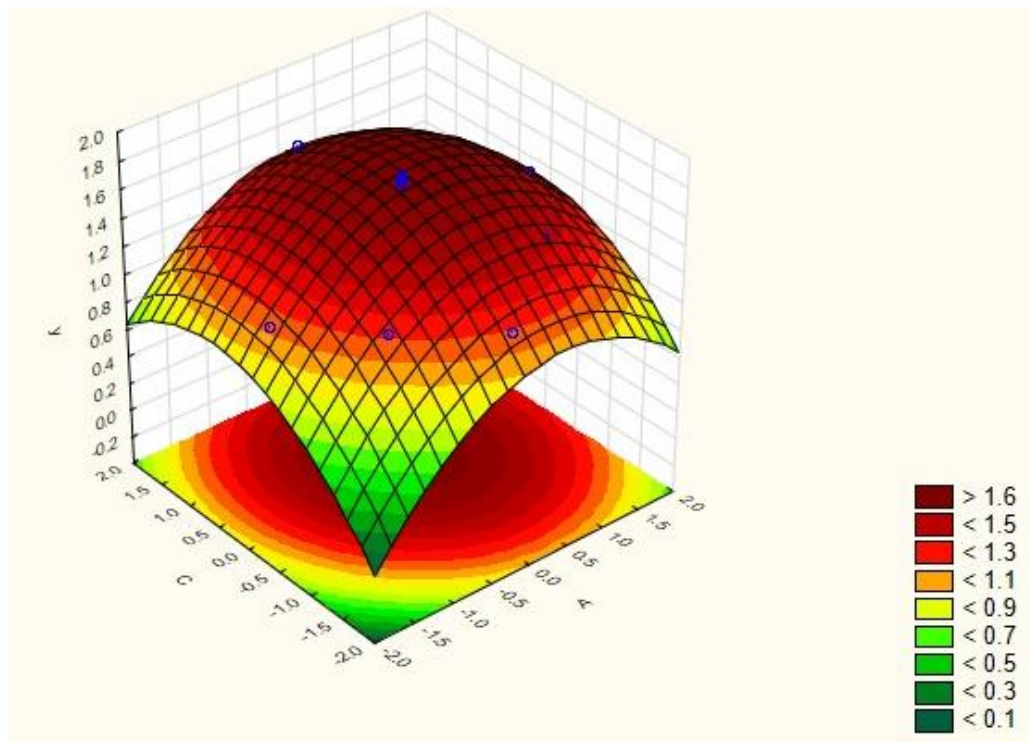


Figure 7.28: Contour plot for K/S value (y) with temperature (A) and time (C).

Table 7.24: Variance analysis (ANOVA) of factors on response.

Factors	Sum of Squares	Degrees of Freedom	Mean Square	F Value	p-Value Prob>F
A	0.126	1	0.126	123.508	0.000
A^2	0.382	1	0.382	374.220	0.000
B	0.031	1	0.031	30.006	0.000
B^2	0.127	1	0.127	124.278	0.000
C	0.125	1	0.125	123.080	0.000
C^2	0.267	1	0.267	262.186	0.000
AxB	0.001	1	0.001	0.993	0.342
AxC	0.004	1	0.004	3.543	0.089
BxC	0.000	1	0.000	0.307	0.592

Table 7.25: Variance analysis (ANOVA) of quadratic regression model.

Source	Sum of Squares	Degrees of Freedom	Mean Square	F Value	p-Value Prob>F
Model	0.9436	9	0.1048	102.836	0.00
Residual	0.0102	10	0.0010		
Lack of fit	0.0057	5	0.01113	1.2489	0.41
Pure error	0.0045	5	0.00091		
Total	0.9538	19			

From Table 7.25, it was observed that at 95% confidence level, the quadratic regression model developed was statistically significant with F-value of 102.836 that was much higher than the F-value of the lack of fit (1.2489). The R^2 value was found to be 0.98931 indicating that 98.93% of the total variations could be explained by the developed model, and 1.07% of the variations could not be explained. The adjusted R^2 value of 0.97969 was reasonably close to the R^2 value, indicating a high goodness of fit for the developed model.

7.1.4.2 Optimization for PLA

The normal probability plot with Catechu applied on PLA using Myrobalan as biomordant is shown in Figure 7.29. It could be observed that points A, B and C were distinct outliers with positive effects in the probability plot. Also, it could be seen that point 1x2 was also an outlier on the negative side.

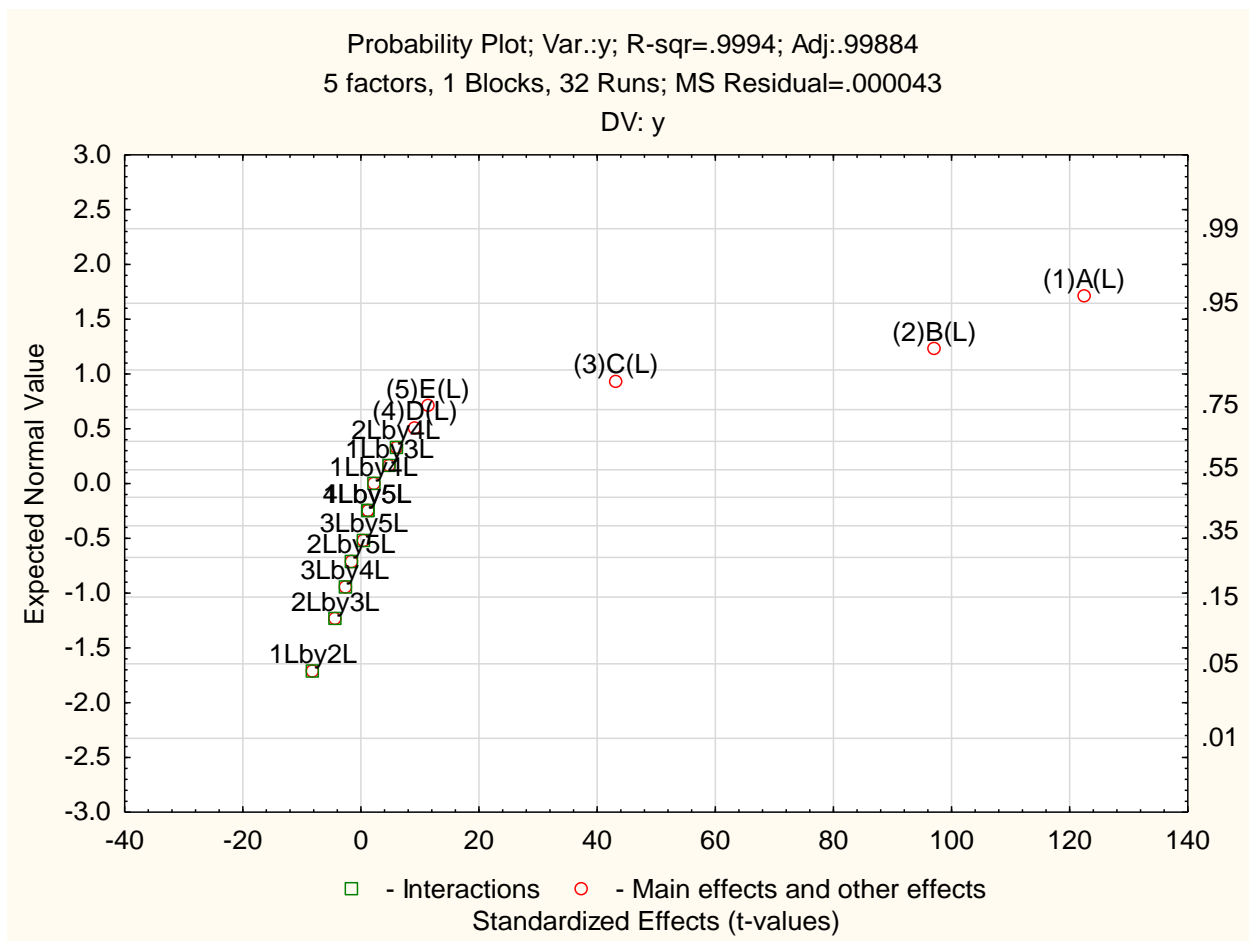


Figure 7.29: Normal probability plot of Catechu applied on PLA using Myrobalan as biomordant.

It could thus be inferred temperature (A, 1), time (B, 2) and initial pH of the dye bath (C, 3) were the most significant factors affecting the color strength of PLA with Catechu using Myrobalan as biomordant. Also, the interaction effect between temperature (1) and time (2) was more significant than the other factors and their interactions. The R^2 value of 0.9994 and adjusted R^2 value of 0.99884 indicated that the probability plot obtained was statistically significant with a high goodness of fit.

Table 7.26: Average values of experiments used for RSM.

Runs	Dyeing temperature	Initial pH	Dyeing time	Experimental values
	^o C		min	K/S
	A	B	C	y
1	-1.00	-1.00	-1.00	0.67
2	-1.00	-1.00	1.00	0.98
3	-1.00	1.00	-1.00	0.89
4	-1.00	1.00	1.00	1.15
5	1.00	-1.00	-1.00	1.09
6	1.00	-1.00	1.00	1.23
7	1.00	1.00	-1.00	1.11
8	1.00	1.00	1.00	1.26
9	-1.68	0.00	0.00	0.84
10	1.68	0.00	0.00	1.19
11	0.00	-1.68	0.00	1.04
12	0.00	1.68	0.00	1.24
13	0.00	0.00	-1.68	0.87
14	0.00	0.00	1.68	1.21
15	0.00	0.00	0.00	1.41
16	0.00	0.00	0.00	1.45
17	0.00	0.00	0.00	1.39
18	0.00	0.00	0.00	1.46
19	0.00	0.00	0.00	1.37
20	0.00	0.00	0.00	1.42

With temperature, initial pH of dye bath and time, RSM was done for Catechu with PLA using Myrobalan as biomordant. The levels of the factors chosen for this combination of natural dye and biomordant were the same when Lac was applied with Catechu as biomordant, as given in Table 7.7. Five experiments were done in each run and the average values reported in Table 7.26. The contour plots obtained in the RSM are given in Figures 7.30-7.32. The analysis of variance (ANOVA) for the factors of response is given in Table 7.27 and the same for the quadratic regression model in Table 7.28.

The empirical model equation obtained with the coded variables is as follows:

$$y = 1.416 + 0.116A - 0.141A^2 + 0.057B - 0.097B^2 + 0.105C - 0.132C^2 - 0.043AB - 0.035AC - 0.005BC \quad (7.8)$$

The optimal values were observed as 113^oC for temperature, 6.2 for initial pH of dye bath and 35 min for dyeing time approximately. The predicted K/S value under these optimal conditions was 1.46.

It was seen from Table 7.27 that the factors A , A^2 , B , B^2 , C , C^2 , AB and AC were the most significant factors with p-values less than 0.05. Thus, temperature (A), initial pH (B) as well as time (C) had significant linear as well as quadratic effects on K/S value. The interaction effects between temperature (A) and initial pH (B) as well as temperature (A) and time (C) also leave significant effects on the K/S value.

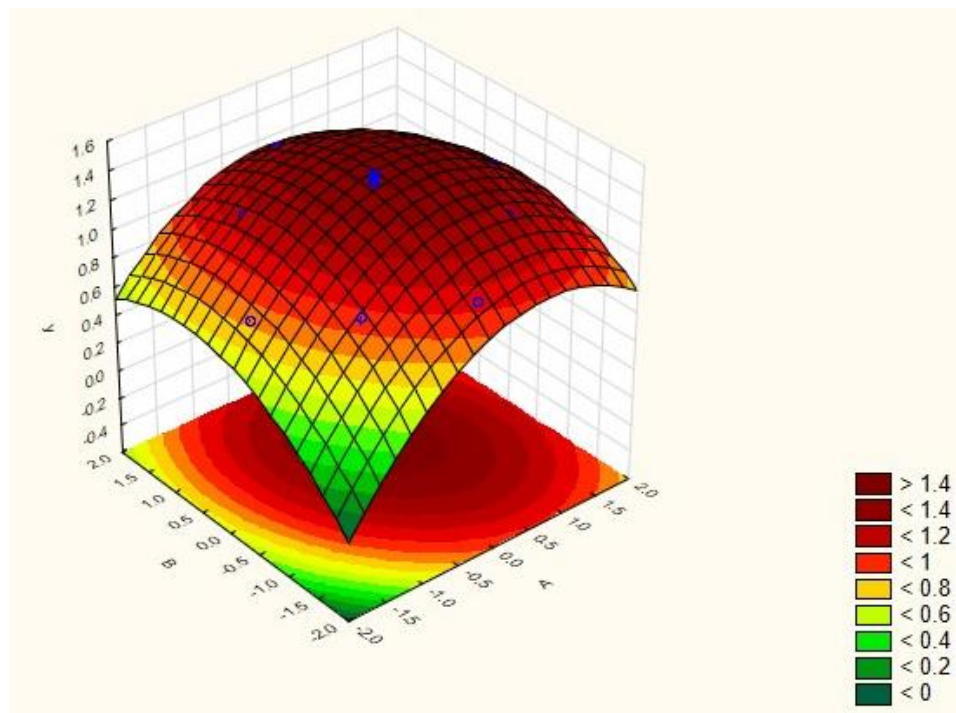


Figure 7.30: Contour plot for K/S value (y) with temperature (A) and initial pH of dye bath (B).

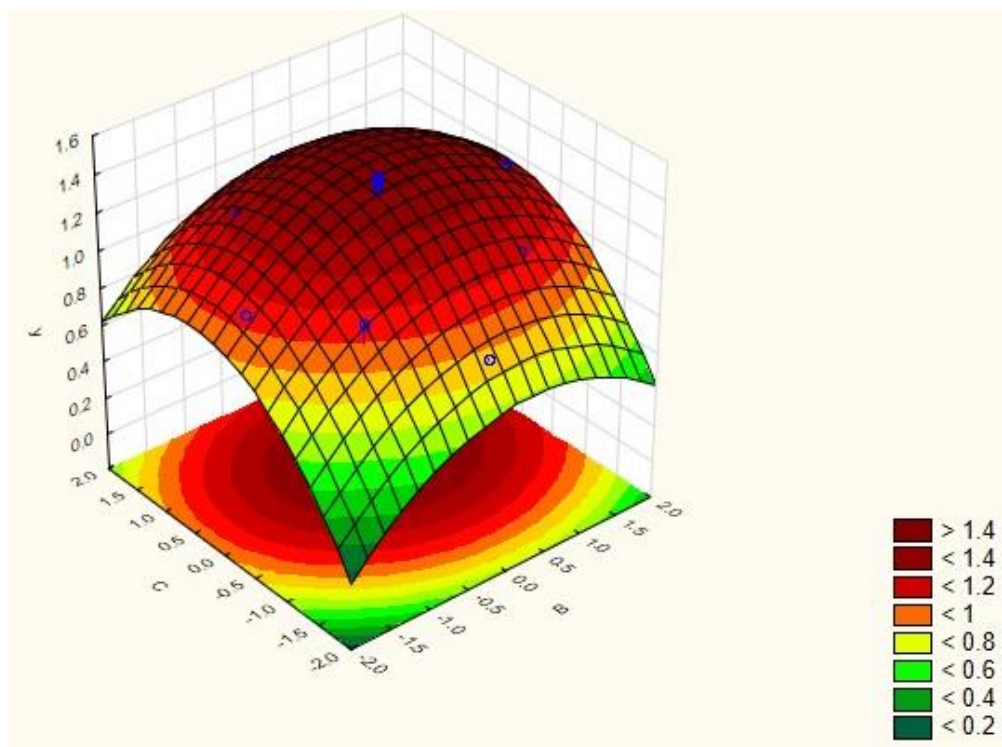


Figure 7.31: Contour plot for K/S value (y) with initial pH of dye bath (B) and time (C).

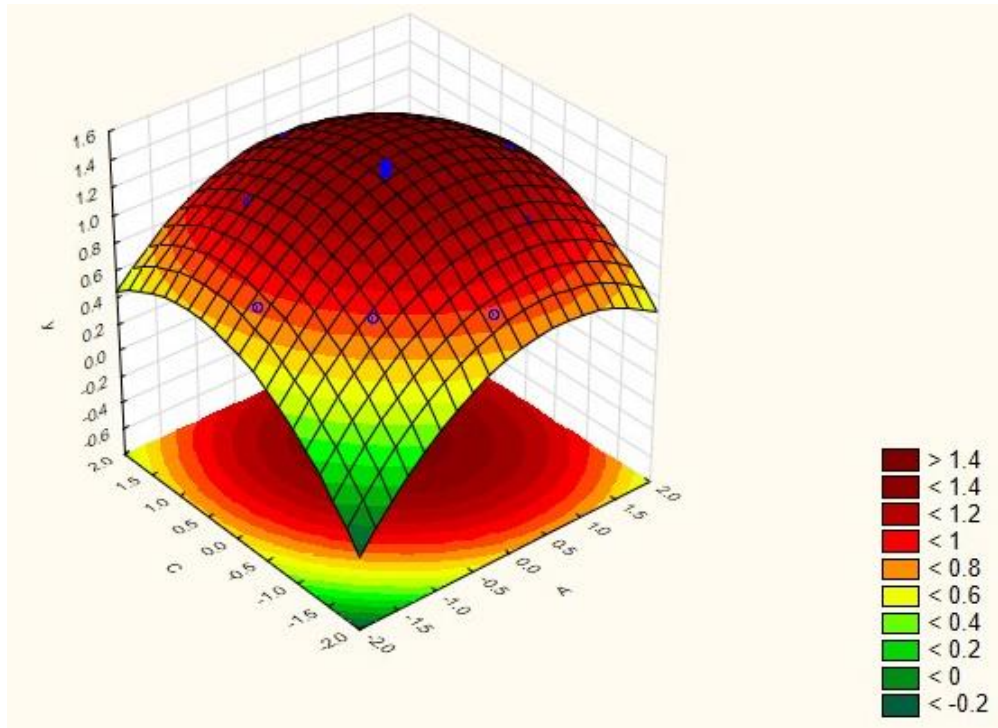


Figure 7.32: Contour plot for K/S value (y) with temperature (A) and time (C).

Table 7.27: Variance analysis (ANOVA) of factors on response.

Factors	Sum of Squares	Degrees of Freedom	Mean Square	F Value	p-Value Prob>F
A	0.185	1.000	0.185	228.532	0.000
A^2	0.287	1.000	0.287	355.335	0.000
B	0.044	1.000	0.044	54.579	0.000
B^2	0.136	1.000	0.136	167.714	0.000
C	0.150	1.000	0.150	185.641	0.000
C^2	0.252	1.000	0.252	312.241	0.000
AxB	0.014	1.000	0.014	17.870	0.002
AxC	0.010	1.000	0.010	12.119	0.006
BxC	0.000	1.000	0.000	0.247	0.630

Table 7.28: Variance analysis (ANOVA) of quadratic regression model.

Source	Sum of Squares	Degrees of Freedom	Mean Square	F Value	p-Value Prob>F
Model	0.9714	9	0.1079	133.473	0.00
Residual	0.0081	10	0.0008		
Lack of fit	0.0022	5	0.00043	0.3629	0.85
Pure error	0.0059	5	0.00119		
Total	0.9795	19			

From Table 7.28, it was observed that at 95% confidence level, the quadratic regression model developed was statistically significant with F-value of 133.473 that was much higher than the F-value of the lack of fit (0.3629). The R^2 value was found to be 0.99174 indicating that 99.17% of the total variations could be explained by the developed model, and 0.83% of the variations could not be explained. The adjusted R^2 value of 0.98431 was reasonably close to the R^2 value, indicating a high goodness of fit for the developed model.

7.1.5 Optimization with Catechu using Pomegranate as biomordant

The real values of -1 and +1 levels for the five factors used in the normal probability plots for dyeing with Catechu using Pomegranate as biomordant were the same when Lac was applied using Catechu as biomordant, as given in Tables 7.23 and 7.24 for PTT and PLA respectively, along with the notations and units.

7.1.5.1 Optimization for PTT

The normal probability plot with Catechu applied on PTT using Pomegranate as biomordant is shown in Figure 7.33. It could be observed that points A, B and C were distinct outliers with positive effects in the probability plot. Also, it could be seen that point 3x4 was also an outlier on the negative side.

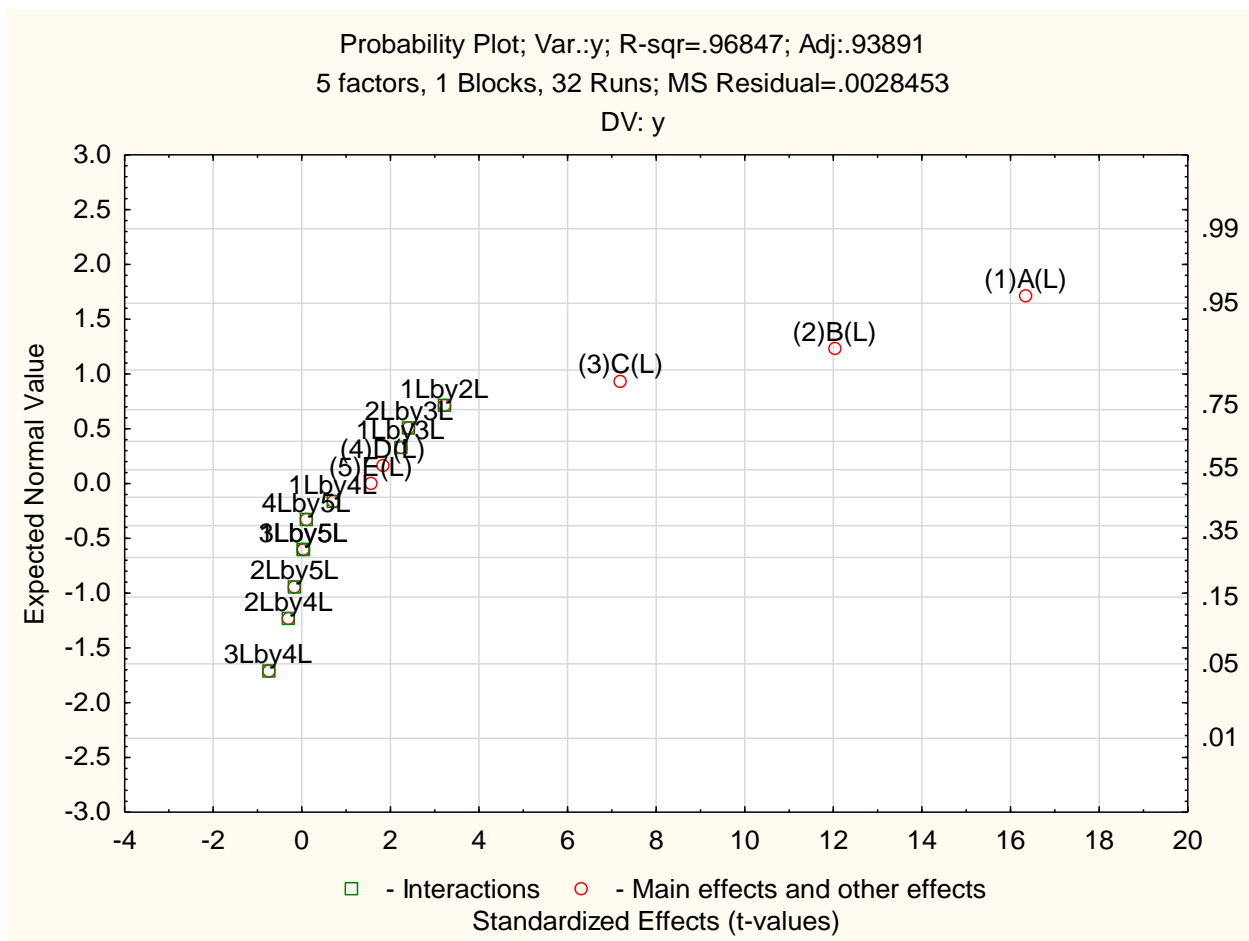


Figure 7.33: Normal probability plot of Catechu applied on PTT using Pomegranate as biomordant.

It could thus be inferred temperature (A, 1), time (B, 2) and initial pH of the dye bath (C, 3) were the most significant factors affecting the color strength of PTT with Catechu using Myrobalan as biomordant. Also, the interaction effect between initial pH (3) and material to liquor ratio (4) was more significant than the other factors and their interactions. The R^2 value of 0.96847 and adjusted R^2 value of 0.93891 indicated that the probability plot obtained was statistically significant with a high goodness of fit.

Table 7.29: Average values of experiments used for RSM.

Runs	Dyeing temperature	Initial pH	Dyeing time	Experimental values
	°C		min	K/S
	A	B	C	y
1	-1.00	-1.00	-1.00	0.82
2	-1.00	-1.00	1.00	1.04
3	-1.00	1.00	-1.00	0.94
4	-1.00	1.00	1.00	1.23
5	1.00	-1.00	-1.00	1.11
6	1.00	-1.00	1.00	1.29
7	1.00	1.00	-1.00	1.13
8	1.00	1.00	1.00	1.34
9	-1.68	0.00	0.00	0.89
10	1.68	0.00	0.00	1.27
11	0.00	-1.68	0.00	1.09
12	0.00	1.68	0.00	1.33
13	0.00	0.00	-1.68	0.96
14	0.00	0.00	1.68	1.32
15	0.00	0.00	0.00	1.59
16	0.00	0.00	0.00	1.61
17	0.00	0.00	0.00	1.65
18	0.00	0.00	0.00	1.63
19	0.00	0.00	0.00	1.59
20	0.00	0.00	0.00	1.62

With temperature, initial pH of dye bath and time, RSM was done for Catechu with PTT using Pomegranate as biomordant. The levels of the factors chosen for this combination of natural dye and biomordant were the same when Lac was applied with Catechu as biomordant, as given in Table 7.3. Five experiments were done in each run and the average values reported in Table 7.29. The contour plots obtained in the RSM are given in Figures 7.34-7.36. The analysis of variance (ANOVA) for the factors of response is given in Table 7.30 and the same for the quadratic regression model in Table 7.31.

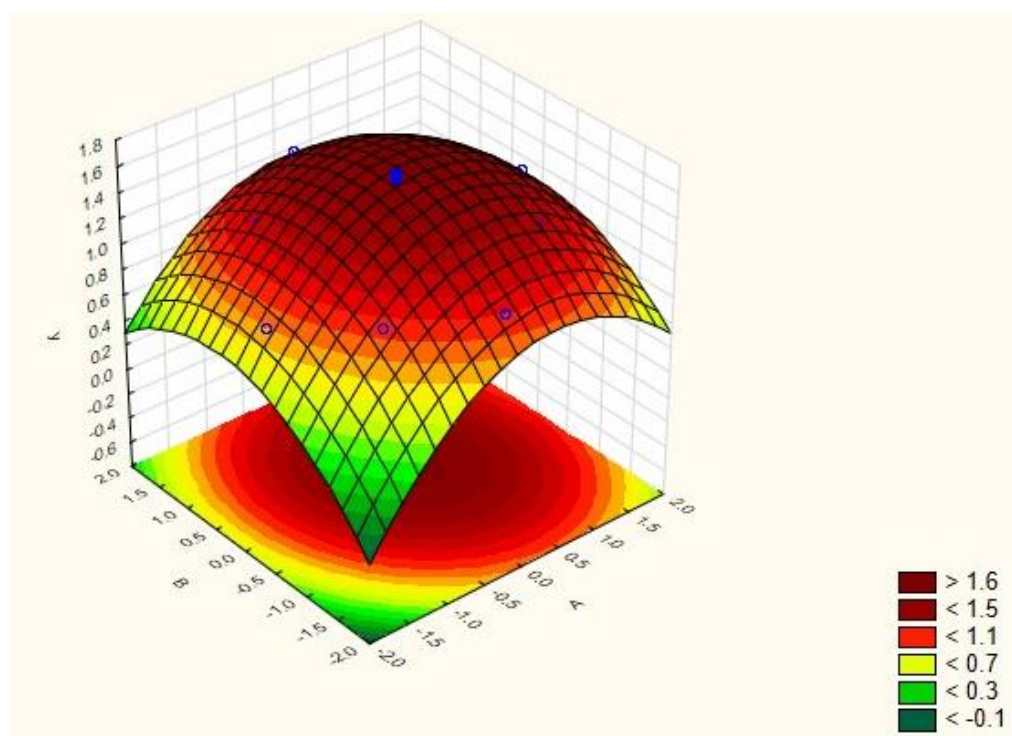


Figure 7.34: Contour plot for K/S value (y) with temperature (A) and initial pH of dye bath (B).

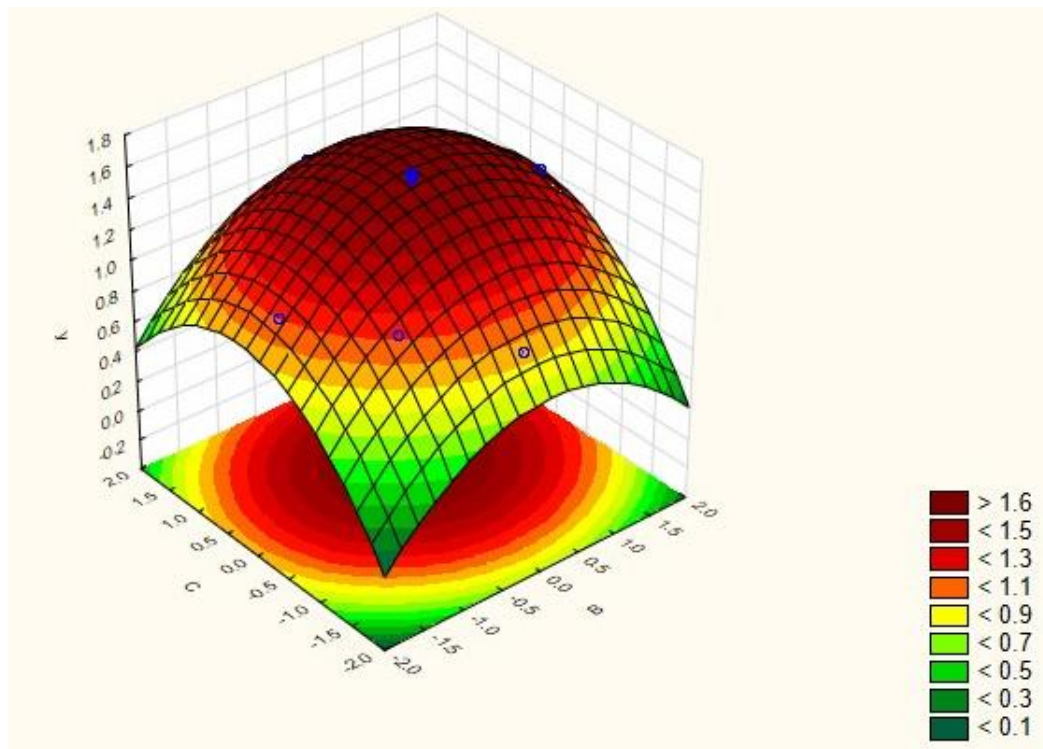


Figure 7.35: Contour plot for K/S value (y) with initial pH of dye bath (B) and time (C).

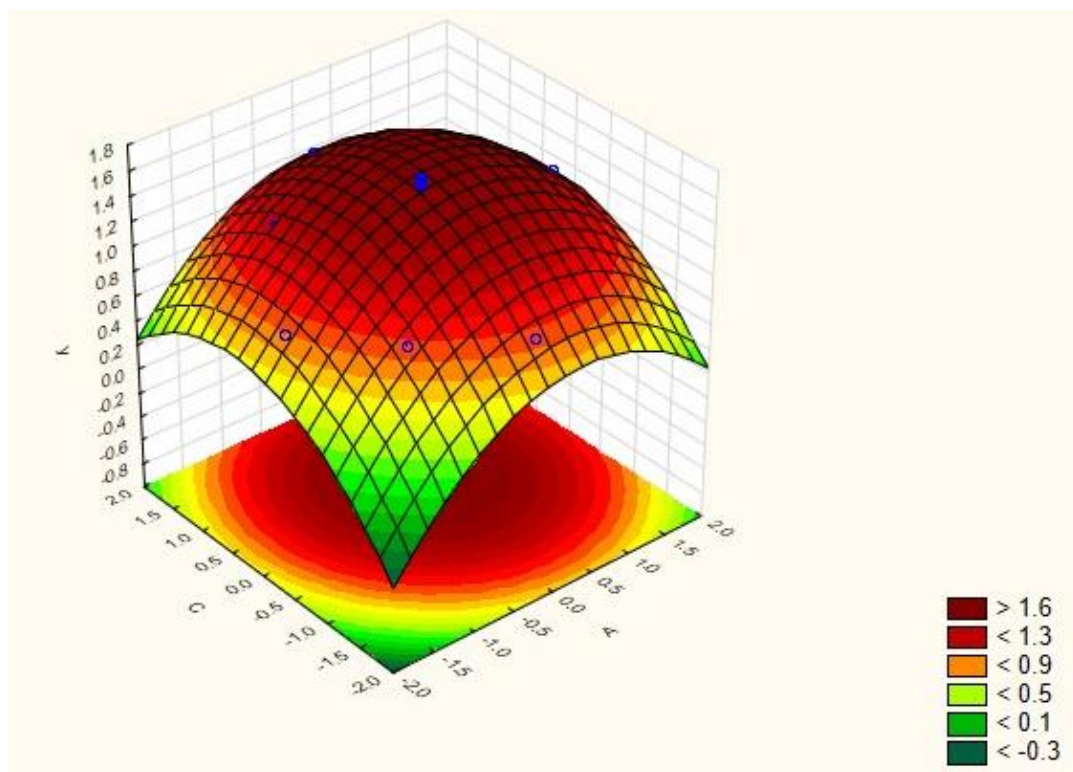


Figure 7.36: Contour plot for K/S value (y) with temperature (A) and time (C).

The empirical model equation obtained with the coded variables is as follows:

$$y = 1.615 + 0.108A - 0.190A^2 + 0.057B - 0.144B^2 + 0.110C - 0.168C^2 - 0.030AB - 0.015AC - 0.013BC \quad (7.9)$$

The optimal values were observed as 113⁰C for temperature, 6.2 for initial pH of dye bath and 50 min for dyeing time approximately. The predicted K/S value under these optimal conditions was 1.65.

Table 7.30: Variance analysis (ANOVA) of factors on response.

Factors	Sum of Squares	Degrees of Freedom	Mean Square	F Value	p-Value Prob>F
<i>A</i>	0.160	1	0.160	310.384	0.000
<i>A</i> ²	0.518	1	0.518	1004.008	0.000
<i>B</i>	0.045	1	0.045	87.124	0.000
<i>B</i> ²	0.297	1	0.297	576.274	0.000
<i>C</i>	0.166	1	0.166	321.548	0.000
<i>C</i> ²	0.409	1	0.409	791.932	0.000
<i>AxB</i>	0.007	1	0.007	13.951	0.004
<i>AxC</i>	0.002	1	0.002	3.488	0.091
<i>BxC</i>	0.001	1	0.001	2.422	0.151

It was seen from Table 7.30 that the factors *A*, *A*², *B*, *B*², *C*, *C*² and *AB* were the most significant factors with p-values less than 0.05. Thus, temperature (*A*), initial pH (*B*) as well as time (*C*) had significant linear as well as quadratic effects on K/S value. The interaction effect of temperature and initial pH was also found to be significant in affecting the K/S value.

Table 7.31: Variance analysis (ANOVA) of quadratic regression model.

Source	Sum of Squares	Degrees of Freedom	Mean Square	F Value	p-Value Prob>F
Model	1.4070	9	0.1563	302.916	0.00
Residual	0.0052	10	0.0005		
Lack of fit	0.0024	5	0.00048	0.8767	0.56
Pure error	0.0028	5	0.00055		
Total	1.4122	19			

From Table 7.31, it was observed that at 95% confidence level, the quadratic regression model developed was statistically significant with F-value of 302.916 that was much higher than the F-value of the lack of fit (0.8767). The R^2 value was found to be 0.99635 indicating that 99.64% of the total variations could be explained by the developed model, and 0.36% of the variations could not be explained. The adjusted R^2 value of 0.99306 was reasonably close to the R^2 value, indicating a high goodness of fit for the developed model.

7.1.5.2 Optimization for PLA

The normal probability plot with Catechu applied on PLA using Pomegranate as biomordant is shown in Figure 7.37. It could be observed that points A and B were distinct outliers with positive effects in the probability plot. Also, it could be seen that point 1x2 was also an outlier on the negative side.

It could thus be inferred temperature (A, 1) and time (B, 2) were the most significant factors affecting the color strength of PLA with Catechu using Pomegranate as biomordant. Also, the interaction effect between them (1x2) was more significant than the other factors and their interactions. The R^2 value of 0.99072 and adjusted R^2 value of 0.98202 indicated that the probability plot obtained was statistically significant with a high goodness of fit.

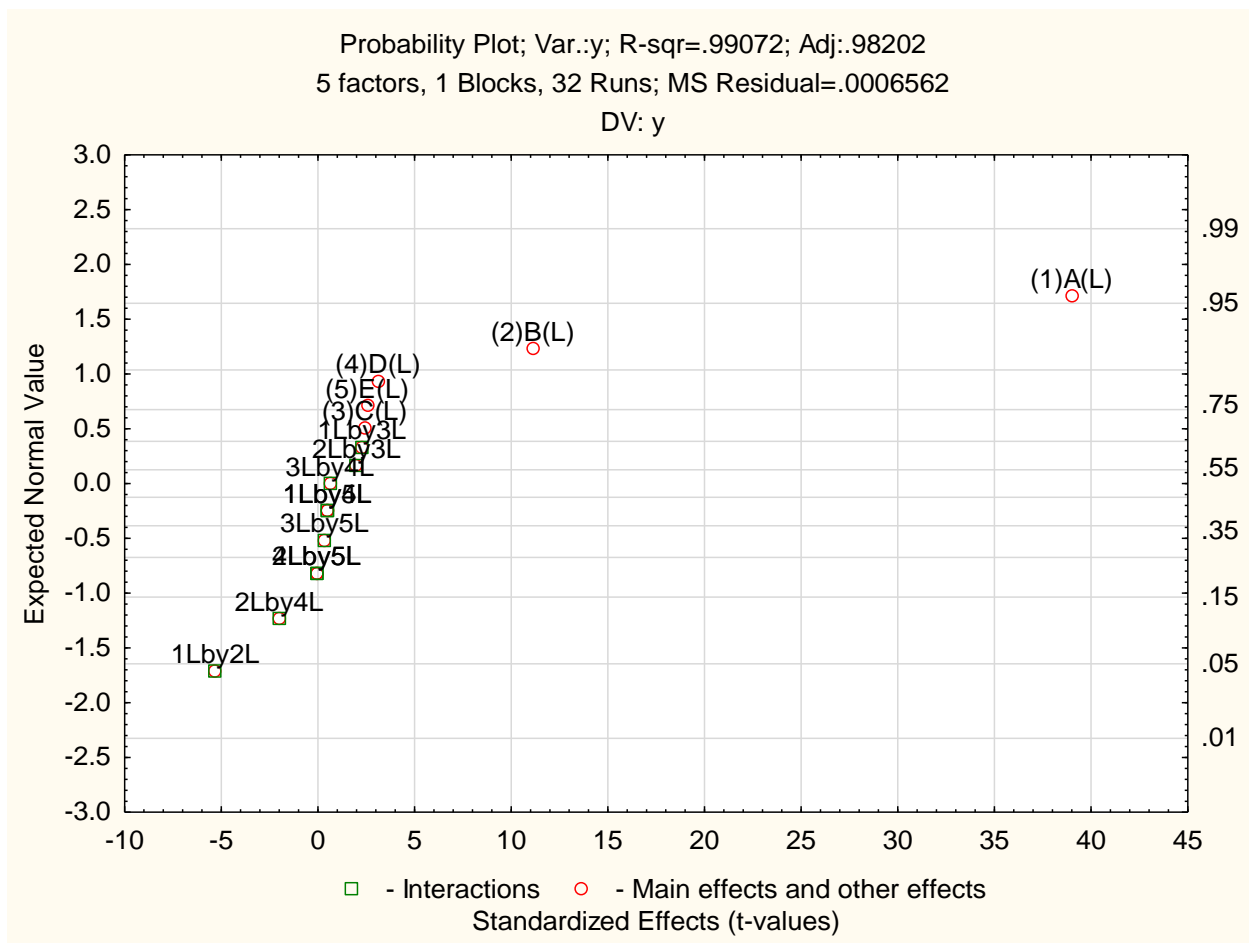


Figure 7.37: Normal probability plot of Catechu applied on PLA using Pomegranate as biomordant.

With temperature, initial pH of dye bath and time, RSM was done for Catechu with PLA using Pomegranate as biomordant. The levels of the factors chosen for this combination of natural dye and biomordant were the same when Lac was applied with Catechu as biomordant, as given in Table 7.7. Five experiments were done in each run and the average values reported in Table 7.32. The contour plots obtained in the RSM are given in Figures 7.38-7.40. The analysis of variance (ANOVA) for the factors of response is given in Table 7.33 and the same for the quadratic regression model in Table 7.34.

Table 7.32: Average values of experiments used for RSM.

Runs	Dyeing temperature	Initial pH	Dyeing time	Experimental values
	$^{\circ}\text{C}$		min	K/S
	A	B	C	y
1	-1.00	-1.00	-1.00	0.62
2	-1.00	-1.00	1.00	0.84
3	-1.00	1.00	-1.00	0.74
4	-1.00	1.00	1.00	1.12
5	1.00	-1.00	-1.00	1.06
6	1.00	-1.00	1.00	1.15
7	1.00	1.00	-1.00	1.04
8	1.00	1.00	1.00	1.34
9	-1.68	0.00	0.00	0.69
10	1.68	0.00	0.00	1.18
11	0.00	-1.68	0.00	1.15
12	0.00	1.68	0.00	1.37
13	0.00	0.00	-1.68	0.86
14	0.00	0.00	1.68	1.25
15	0.00	0.00	0.00	1.48
16	0.00	0.00	0.00	1.52
17	0.00	0.00	0.00	1.56
18	0.00	0.00	0.00	1.49
19	0.00	0.00	0.00	1.51
20	0.00	0.00	0.00	1.55

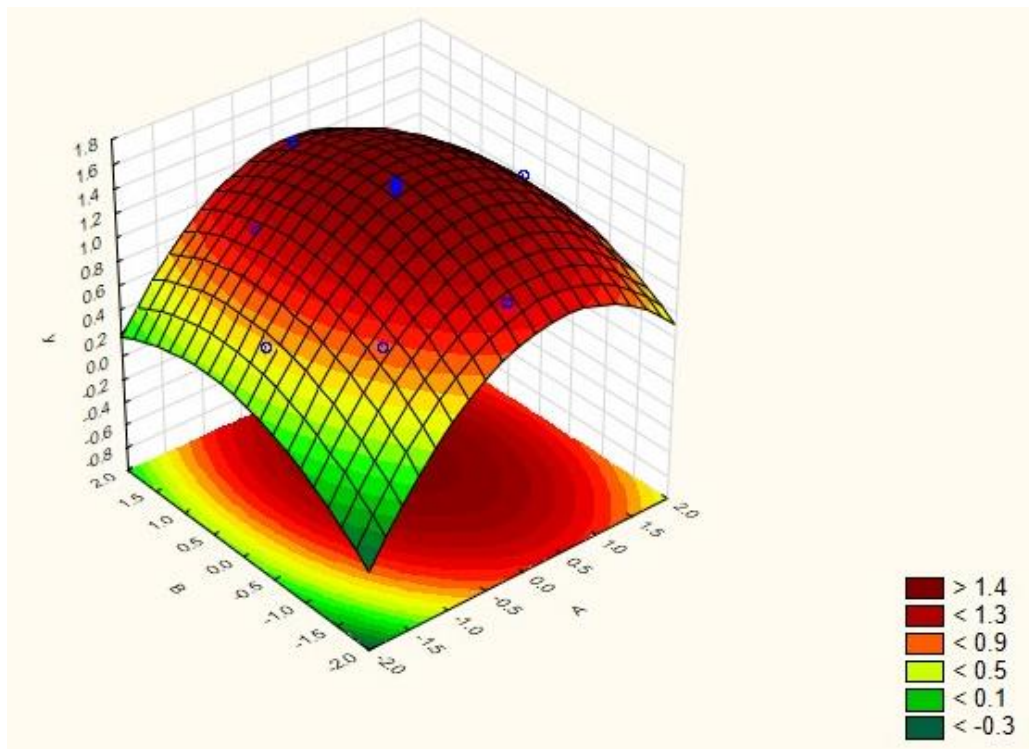


Figure 7.38: Contour plot for K/S value (y) with temperature (A) and initial pH of dye bath (B).

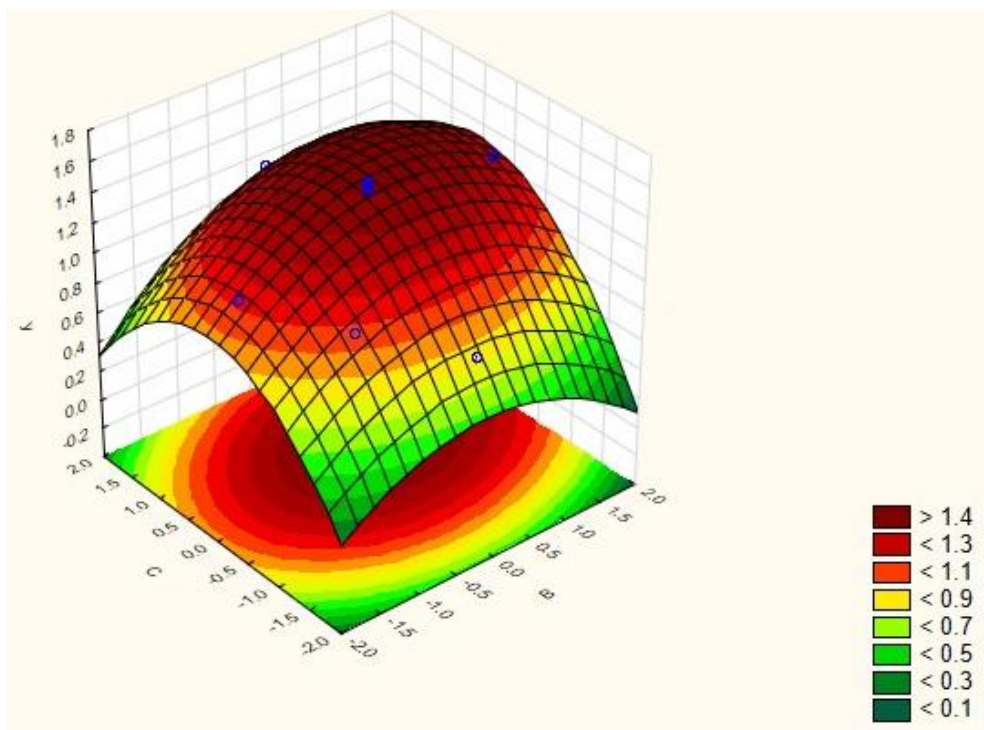


Figure 7.39: Contour plot for K/S value (y) with initial pH of dye bath (B) and time (C).

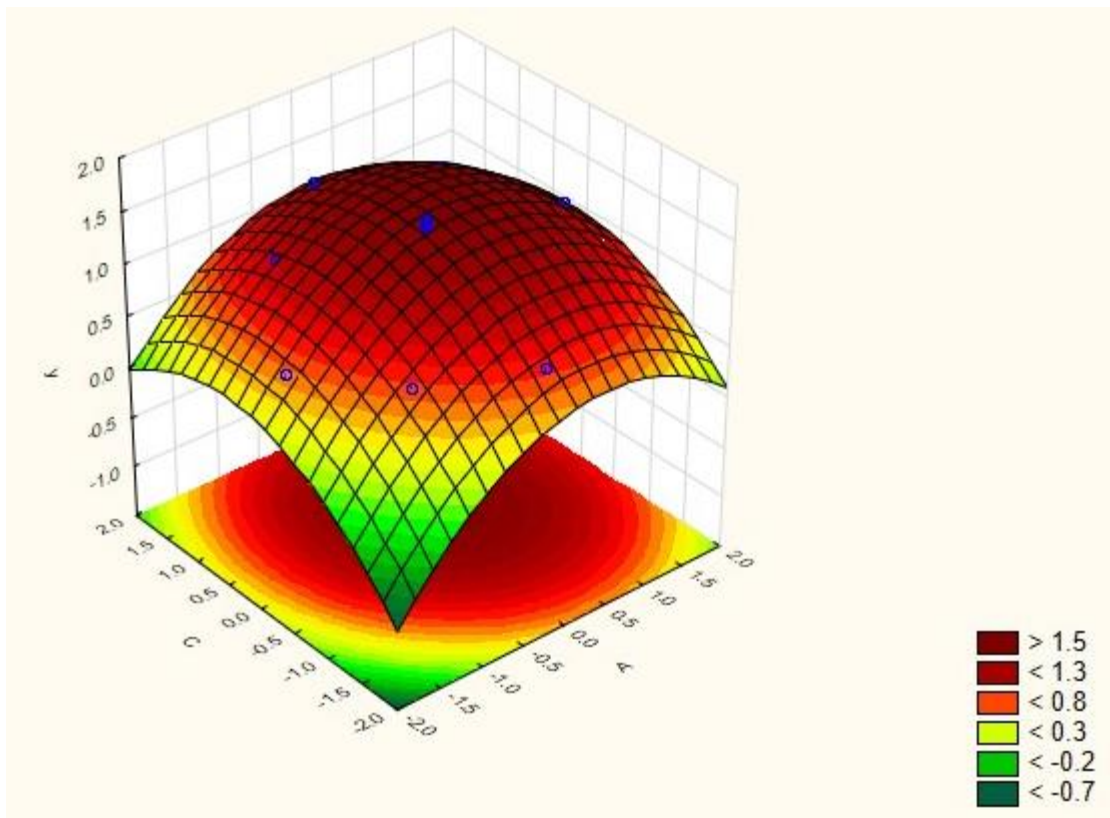


Figure 7.40: Contour plot for K/S value (y) with temperature (A) and time (C).

Table 7.33: Variance analysis (ANOVA) of factors on response.

Factors	Sum of Squares	Degrees of Freedom	Mean Square	F Value	p-Value Prob>F
<i>A</i>	0.321	1.000	0.321	151.962	0.000
<i>A</i> ²	0.702	1.000	0.702	331.996	0.000
<i>B</i>	0.065	1.000	0.065	30.620	0.000
<i>B</i> ²	0.161	1.000	0.161	76.236	0.000
<i>C</i>	0.198	1.000	0.198	93.876	0.000
<i>C</i> ²	0.458	1.000	0.458	216.589	0.000
<i>AxB</i>	0.007	1.000	0.007	3.129	0.107
<i>AxC</i>	0.006	1.000	0.006	2.609	0.137
<i>BxC</i>	0.017	1.000	0.017	8.099	0.017

Table 7.34: Variance analysis (ANOVA) of quadratic regression model.

Source	Sum of Squares	Degrees of Freedom	Mean Square	F Value	p-Value Prob>F
Model	1.7417	9	0.1935	91.589	0.00
Residual	0.0211	10	0.0021		
Lack of fit	0.0160	5	0.00321	3.1567	0.12
Pure error	0.0051	5	0.00102		
Total	1.7629	19			

The empirical model equation obtained with the coded variables is as follows:

$$y = 1.521 + 0.153A - 0.221A^2 + 0.069B - 0.106B^2 + 0.121C - 0.178C^2 - 0.029AB - 0.026AC - 0.046BC \quad (7.10)$$

The optimal values were observed as 113⁰C for temperature, 6.4 for initial pH of dye bath and 35 min for dyeing time approximately. The predicted K/S value under these optimal conditions was 1.58.

It was seen from Table 7.33 that the factors A , A^2 , B , B^2 , C , C^2 and BC were the most significant factors with p-values less than 0.05. Thus, temperature (A), initial pH (B) as well as time (C) had significant linear as well as quadratic effects on K/S value. The interaction effect of initial pH and time was also found to be significant in affecting the K/S value.

From Table 7.34, it was observed that at 95% confidence level, the quadratic regression model developed was statistically significant with F-value of 91.589 that was much higher than the F-value of the lack of fit (3.1567). The R^2 value was found to be 0.98801 indicating that 98.80% of the total variations could be explained by the developed model, and 1.20% of the variations could not be explained. The adjusted R^2 value of 0.97723 was reasonably close to the R^2 value, indicating a high goodness of fit for the developed model.

7.1.6 Optimization with Myrobalan using Pomegranate as biomordant

The real values of -1 and +1 levels for the five factors used in the normal probability plots for dyeing with Myrobalan using Pomegranate as biomordant were the same when Lac was applied using Catechu as biomordant, as given in Tables 7.1 and 7.2 for PTT and PLA respectively, along with the notations and units.

7.1.6.1 Optimization for PTT

The normal probability plot with Myrobalan applied on PTT using Pomegranate as biomordant is shown in Figure 7.41. It could be observed that points A and B were distinct outliers with positive effects in the probability plot. Also, it could be seen that point 1x5 was also an outlier on the negative side.

It could thus be inferred temperature (A, 1) and time (B, 2) were the most significant factors affecting the color strength of PLA with Myrobalan using Pomegranate as biomordant. Also, the interaction effect between temperature (1) and mordant concentration (5) was more significant than the other factors and their interactions. The R^2 value of 0.98688 and adjusted R^2 value of 0.97458 indicated that the probability plot obtained was statistically significant with a high goodness of fit.

With temperature, initial pH of dye bath and time, RSM was done for Myrobalan with PLA using Pomegranate as biomordant. The levels of the factors chosen for this combination of natural dye and biomordant were the same when Lac was applied with Catechu as biomordant, as given in Table 7.3. Five experiments were done in each run and the average values reported in Table 7.35. The contour plots obtained in the RSM are given in Figures 7.42-7.44. The analysis of variance (ANOVA) for the factors of

response is given in Table 7.36 and the same for the quadratic regression model in Table 7.37.

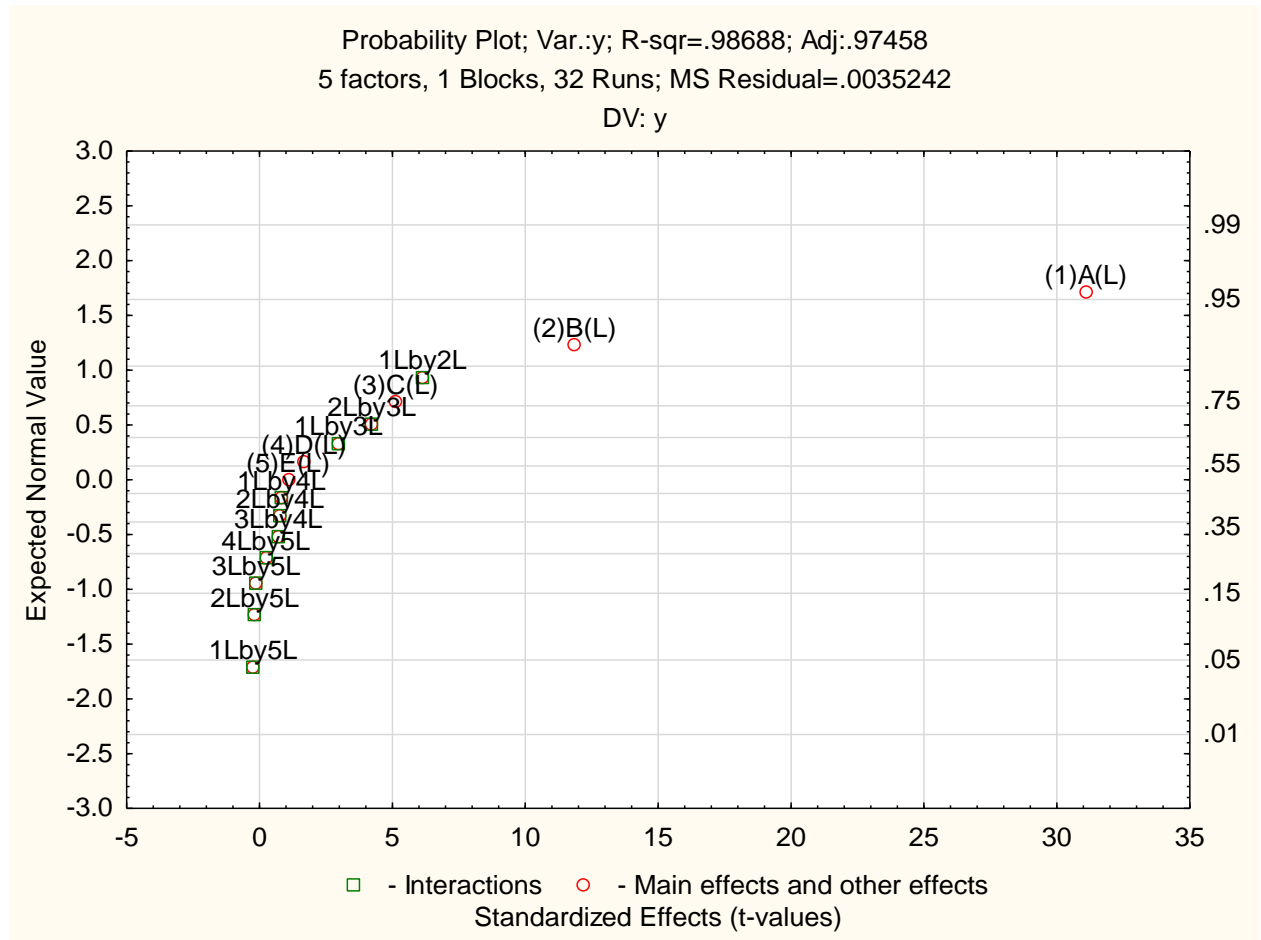


Figure 7.41: Normal probability plot of Myrobalan applied on PTT using Pomegranate as biomordant.

The empirical model equation obtained with the coded variables is as follows:

$$y = 2.050 + 0.172A - 0.237A^2 + 0.089B - 0.103B^2 + 0.133C - 0.174C^2 - 0.035AB - 0.055AC - 0.010BC \quad (7.11)$$

The optimal values were observed as 113⁰C for temperature, 6.4 for initial pH of dye bath and 50 min for dyeing time approximately. The predicted K/S value under these optimal conditions was 2.12.

Table 7.35: Average values of experiments used for RSM.

Runs	Dyeing temperature	Initial pH	Dyeing time	Experimental values
	$^{\circ}\text{C}$		min	K/S
	A	B	C	y
1	-1.00	-1.00	-1.00	1.02
2	-1.00	-1.00	1.00	1.44
3	-1.00	1.00	-1.00	1.29
4	-1.00	1.00	1.00	1.68
5	1.00	-1.00	-1.00	1.56
6	1.00	-1.00	1.00	1.69
7	1.00	1.00	-1.00	1.62
8	1.00	1.00	1.00	1.86
9	-1.68	0.00	0.00	1.09
10	1.68	0.00	0.00	1.71
11	0.00	-1.68	0.00	1.64
12	0.00	1.68	0.00	1.92
13	0.00	0.00	-1.68	1.39
14	0.00	0.00	1.68	1.77
15	0.00	0.00	0.00	2.02
16	0.00	0.00	0.00	1.97
17	0.00	0.00	0.00	2.11
18	0.00	0.00	0.00	2.06
19	0.00	0.00	0.00	2.04
20	0.00	0.00	0.00	2.09

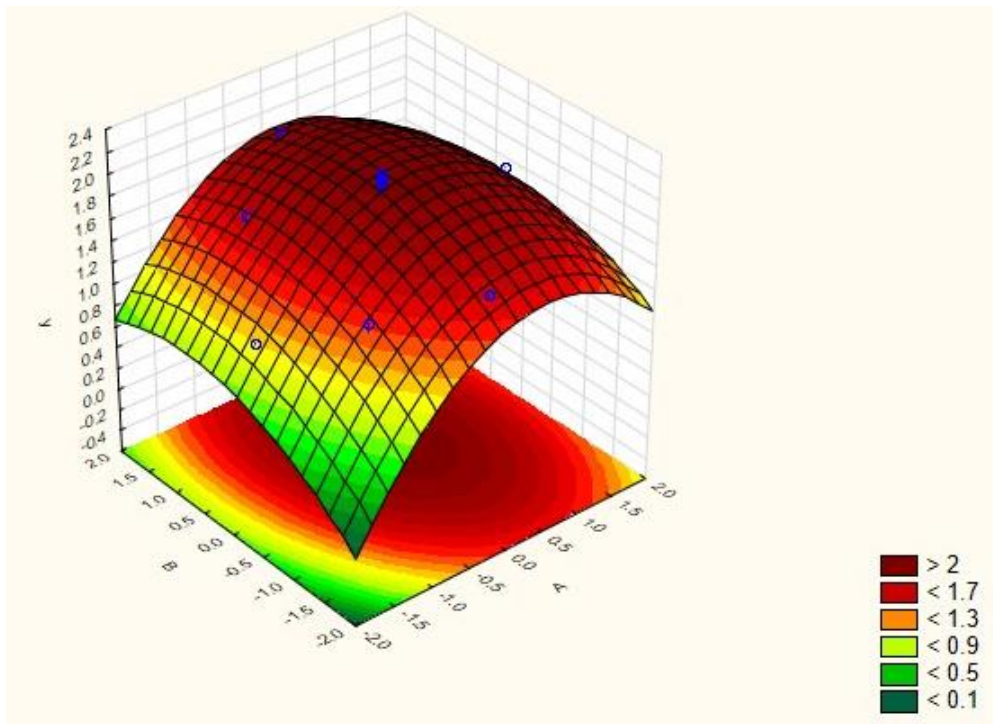


Figure 7.42: Contour plot for K/S value (y) with temperature (A) and initial pH of dye bath (B).

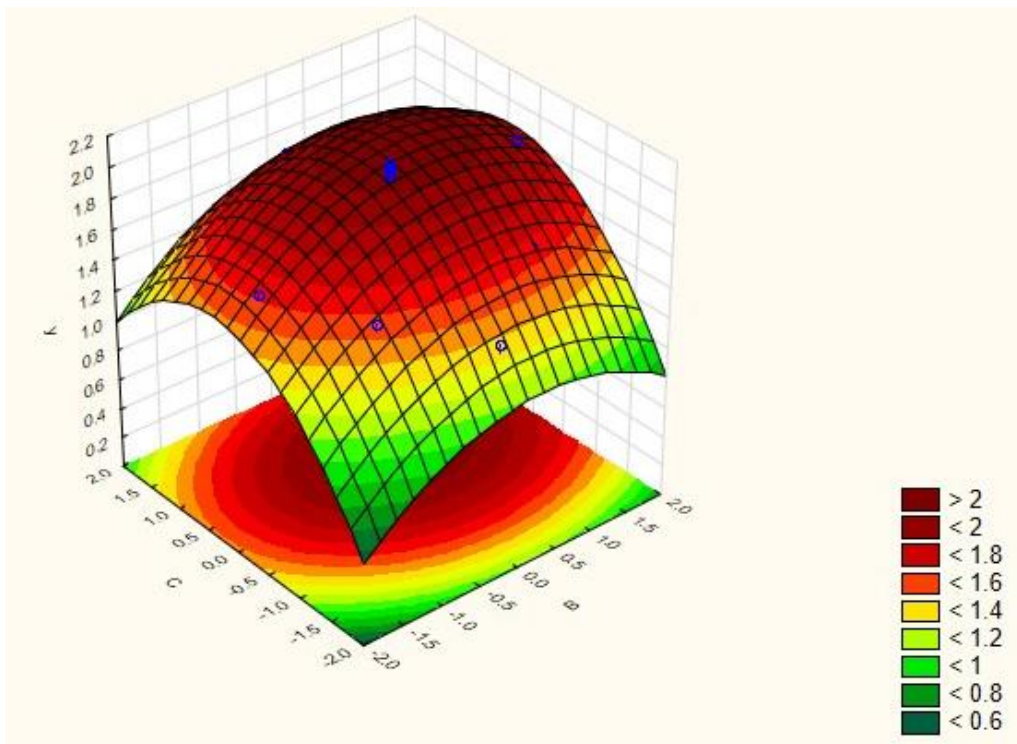


Figure 7.43: Contour plot for K/S value (y) with initial pH of dye bath (B) and time (C).

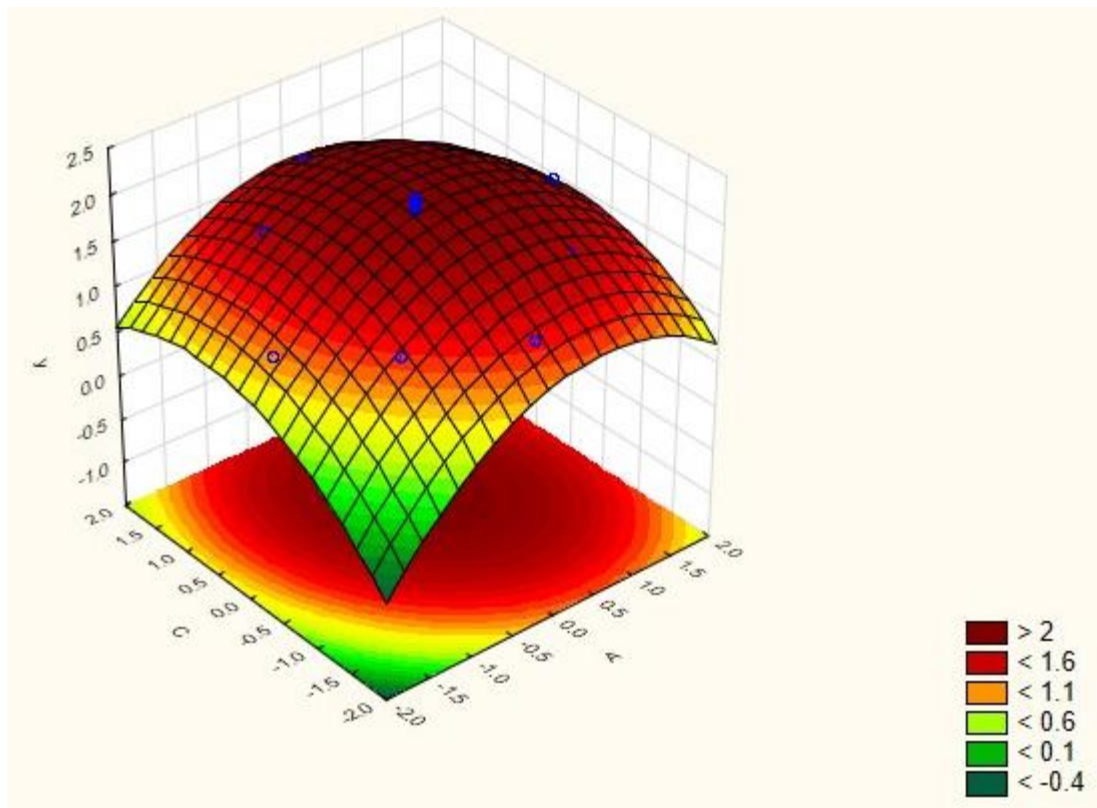


Figure 7.44: Contour plot for K/S value (y) with temperature (A) and time (C).

Table 7.36: Variance analysis (ANOVA) of factors on response.

Factors	Sum of Squares	Degrees of Freedom	Mean Square	F Value	p-Value Prob>F
A	0.402	1.000	0.402	156.251	0.000
A^2	0.812	1.000	0.812	315.735	0.000
B	0.107	1.000	0.107	41.745	0.000
B^2	0.153	1.000	0.153	59.478	0.000
C	0.242	1.000	0.242	94.208	0.000
C^2	0.435	1.000	0.435	169.135	0.000
AxB	0.010	1.000	0.010	3.810	0.079
AxC	0.024	1.000	0.024	9.409	0.012
BxC	0.001	1.000	0.001	0.311	0.589

It was seen from Table 7.36 that the factors A , A^2 , B , B^2 , C , C^2 and AC were the most significant factors with p-values less than 0.05. Thus, temperature (A), initial pH (B) as well as time (C) had significant linear as well as quadratic effects on K/S value. The interaction effect of temperature and time was also found to be significant in affecting the K/S value.

Table 7.37: Variance analysis (ANOVA) of quadratic regression model.

Source	Sum of Squares	Degrees of Freedom	Mean Square	F Value	p-Value Prob>F
Model	1.9903	9	0.2211	95.984	0.00
Residual	0.0257	10	0.0025		
Lack of fit	0.0130	5	0.00261	1.0278	0.49
Pure error	0.0127	5	0.00254		
Total	2.0161	19			

From Table 7.37, it was observed that at 95% confidence level, the quadratic regression model developed was statistically significant with F-value of 95.984 that was much higher than the F-value of the lack of fit (1.0278). The R^2 value was found to be 0.98724 indicating that 98.72% of the total variations could be explained by the developed model, and 1.28% of the variations could not be explained. The adjusted R^2 value of 0.97576 was reasonably close to the R^2 value, indicating a high goodness of fit for the developed model.

7.1.6.2 Optimization for PLA

The normal probability plot with Myrobalan applied on PLA using Pomegranate as biomordant is shown in Figure 7.45. It could be observed that points A, B and C were distinct outliers with positive effects in the probability plot. Also, it could be seen that point 1x2 was also an outlier on the negative side.

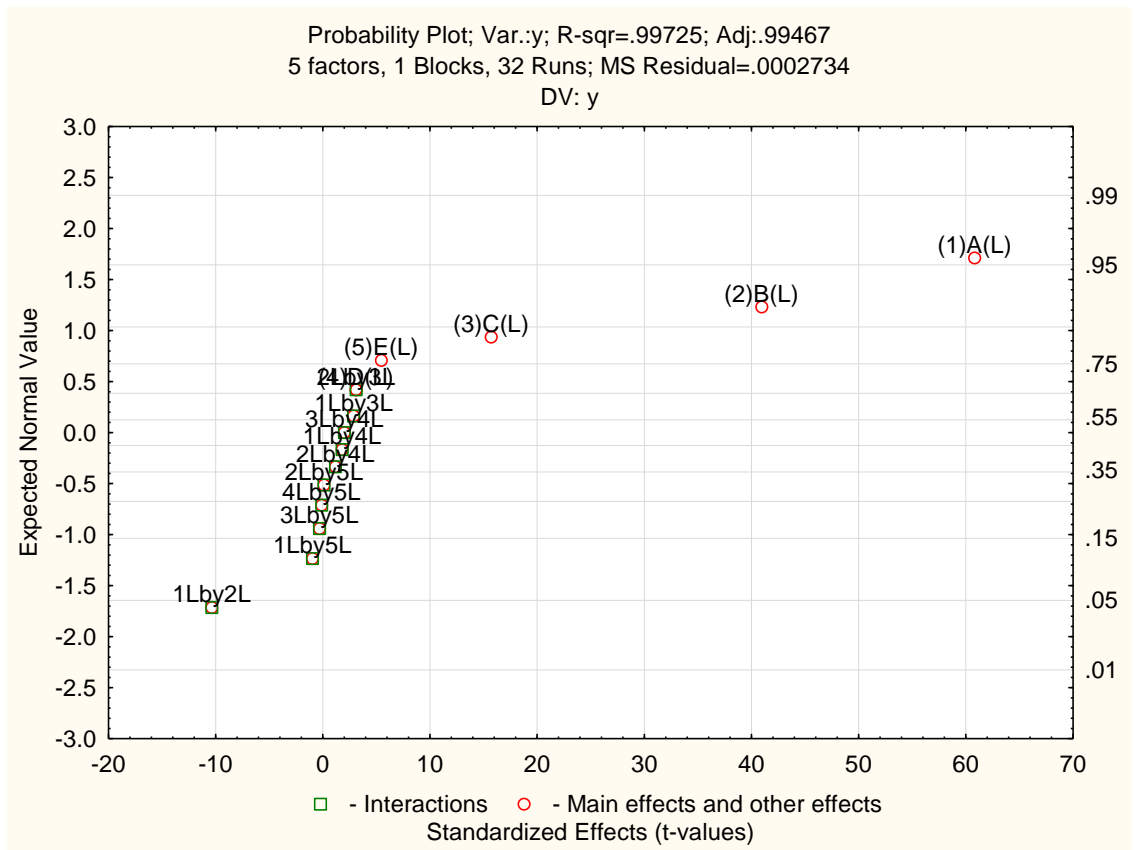


Figure 7.45: Normal probability plot of Myrobalan applied on PLA using Pomegranate as biomordant.

It could thus be inferred temperature (A, 1), time (B, 2) and initial pH (C, 3) were the most significant factors affecting the color strength of PLA with Myrobalan using Pomegranate as biomordant. Also, the interaction effect between them (1x2) was more significant than the other factors and their interactions. The R^2 value of 0.99725 and adjusted R^2 value of 0.99467 indicated that the probability plot obtained was statistically significant with a high goodness of fit.

Table 7.38: Average values of experiments used for RSM.

Runs	Dyeing temperature	Initial pH	Dyeing time	Experimental values
	°C		min	K/S
	A	B	C	y
1	-1.00	-1.00	-1.00	0.82
2	-1.00	-1.00	1.00	1.32
3	-1.00	1.00	-1.00	1.19
4	-1.00	1.00	1.00	1.54
5	1.00	-1.00	-1.00	1.49
6	1.00	-1.00	1.00	1.61
7	1.00	1.00	-1.00	1.58
8	1.00	1.00	1.00	1.77
9	-1.68	0.00	0.00	0.97
10	1.68	0.00	0.00	1.64
11	0.00	-1.68	0.00	1.48
12	0.00	1.68	0.00	1.84
13	0.00	0.00	-1.68	1.15
14	0.00	0.00	1.68	1.86
15	0.00	0.00	0.00	1.98
16	0.00	0.00	0.00	2.11
17	0.00	0.00	0.00	2.06
18	0.00	0.00	0.00	2.16
19	0.00	0.00	0.00	2.13
20	0.00	0.00	0.00	2.1

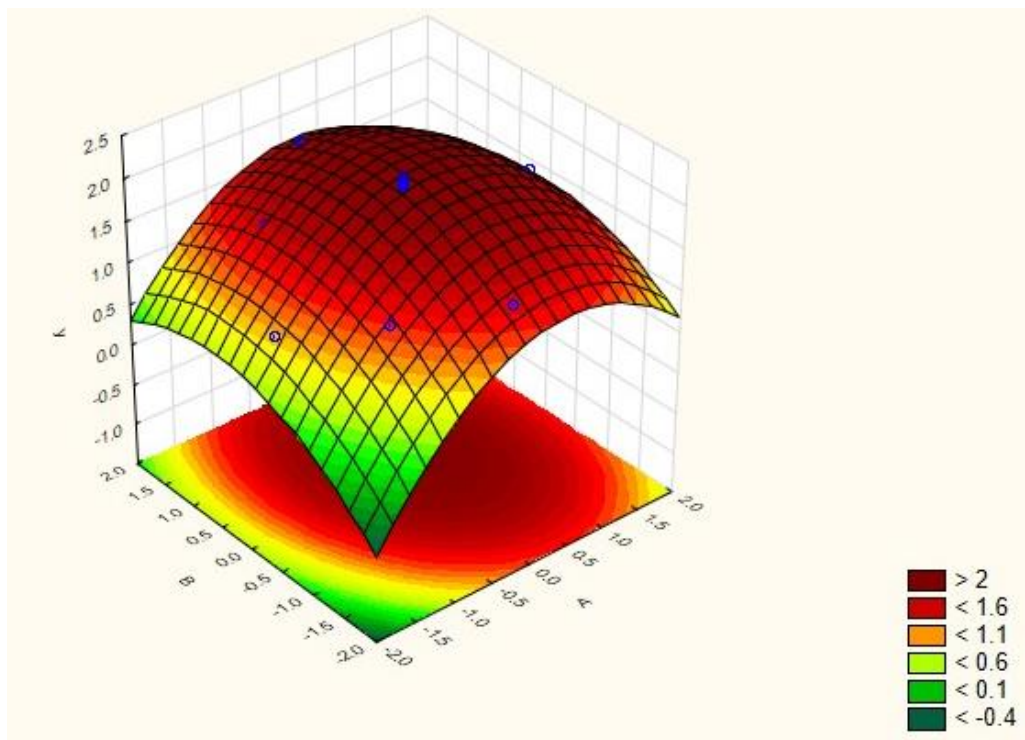


Figure 7.46: Contour plot for K/S value (y) with temperature (A) and initial pH of dye bath (B).

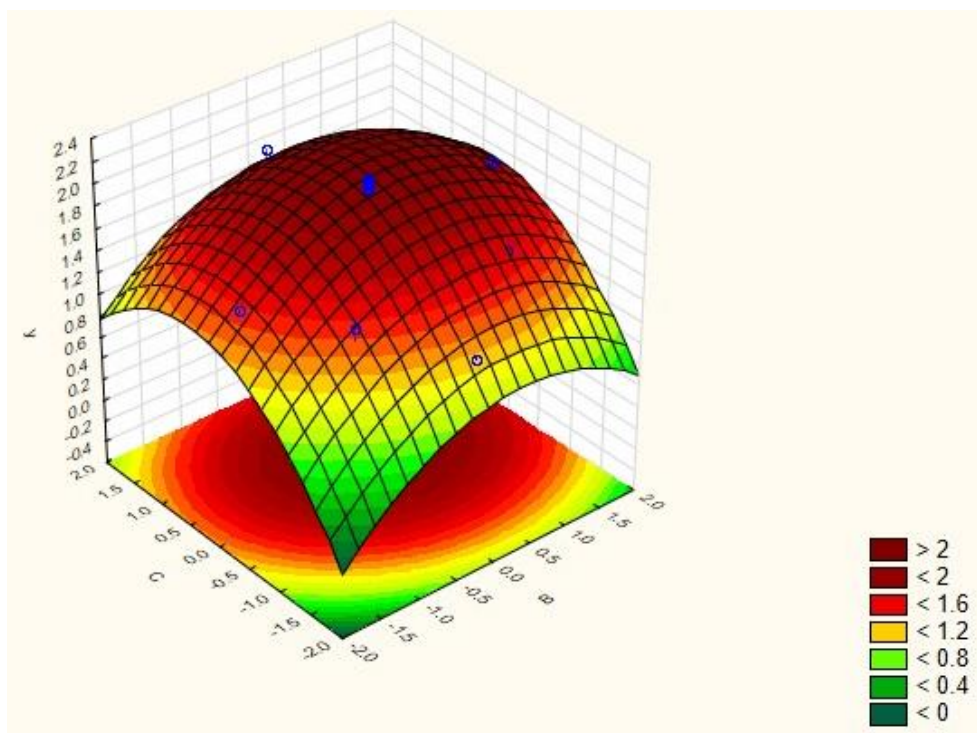


Figure 7.47: Contour plot for K/S value (y) with initial pH of dye bath (B) and time (C).

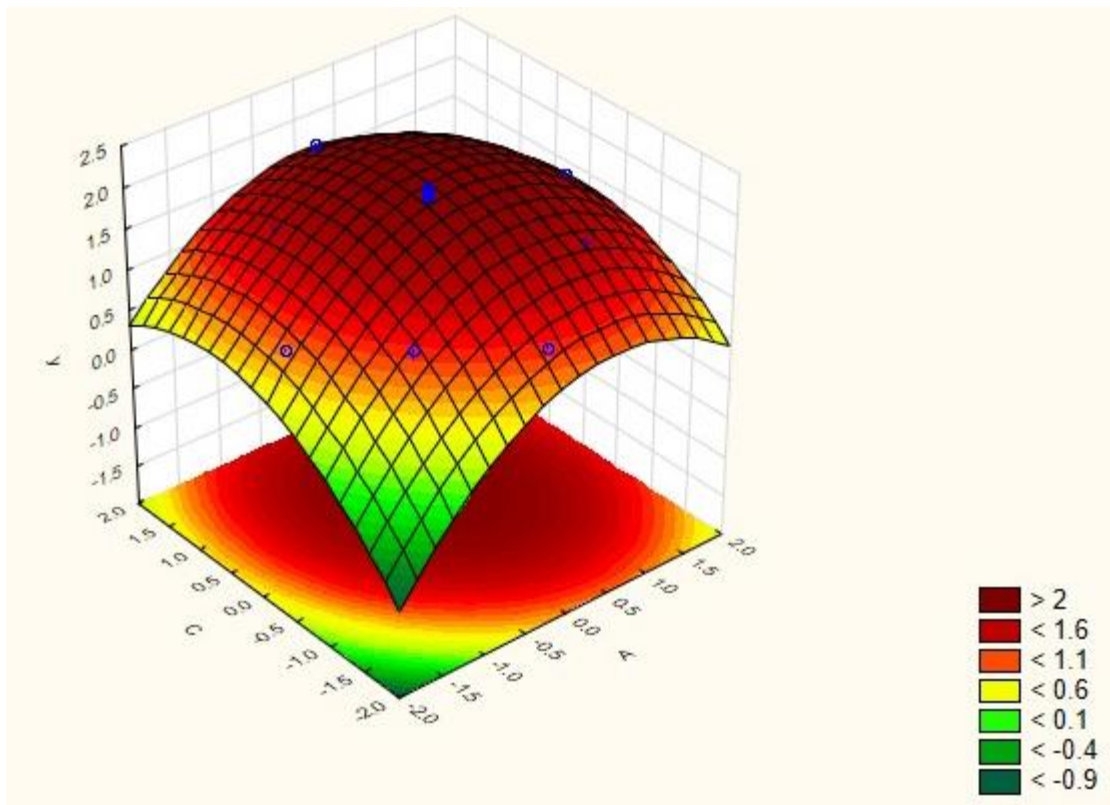


Figure 7.48: Contour plot for K/S value (y) with temperature (A) and time (C).

Table 7.39: Variance analysis (ANOVA) of factors on response.

Factors	Sum of Squares	Degrees of Freedom	Mean Square	F Value	p-Value Prob>F
A	0.536	1	0.536	118.420	0.000
A^2	1.176	1	1.176	259.623	0.000
B	0.153	1	0.153	33.769	0.000
B^2	0.370	1	0.370	81.612	0.000
C	0.406	1	0.406	89.568	0.000
C^2	0.666	1	0.666	147.008	0.000
AxB	0.014	1	0.014	3.190	0.104
AxC	0.036	1	0.036	8.046	0.018
BxC	0.001	1	0.001	0.177	0.683

With temperature, initial pH of dye bath and time, RSM was done for Catechu with PLA using Pomegranate as biomordant. The levels of the factors chosen for this combination of natural dye and biomordant were the same when Lac was applied with Catechu as biomordant, as given in Table 7.7. Five experiments were done in each run and the average values reported in Table 7.38. The contour plots obtained in the RSM are given in Figures 7.46-7.48. The analysis of variance (ANOVA) for the factors of response is given in Table 7.39 and the same for the quadratic regression model in Table 7.40.

The empirical model equation obtained with the coded variables is as follows:

$$y = 2.091 + 0.198A - 0.286A^2 + 0.106B - 0.160B^2 + 0.172C - 0.215C^2 - 0.043AB - 0.068AC - 0.010BC \quad (7.12)$$

The optimal values were observed as 113⁰C for temperature, 6.3 for initial pH of dye bath and 35 min for dyeing time approximately. The predicted K/S value under these optimal conditions was 2.17.

It was seen from Table 7.39 that the factors A , A^2 , B , B^2 , C , C^2 and AC were the most significant factors with p-values less than 0.05. Thus, temperature (A), initial pH (B) as well as time (C) had significant linear as well as quadratic effects on K/S value. The interaction effect of temperature and time was also found to be significant in affecting the K/S value.

Table 7.40: Variance analysis (ANOVA) of quadratic regression model.

Source	Sum of Squares	Degrees of Freedom	Mean Square	F Value	p-Value Prob>F
Model	3.0239	9	0.3359	74.163	0.00
Residual	0.0453	10	0.0045		
Lack of fit	0.0253	5	0.00506	1.2652	0.40
Pure error	0.0200	5	0.00400		
Total	3.0692	19			

From Table 7.40, it was observed that at 95% confidence level, the quadratic regression model developed was statistically significant with F-value of 74.163 that was much higher than the F-value of the lack of fit (1.2652). The R^2 value was found to be 0.98524 indicating that 98.52% of the total variations could be explained by the developed model, and 1.48% of the variations could not be explained. The adjusted R^2 value of 0.97195 was reasonably close to the R^2 value, indicating a high goodness of fit for the developed model.

7.2 Summary

In case of optimization of natural dyes applied to PTT and PLA using biomordants, the observations are summarized as follows:

- (i) The optimal values for PTT with all the natural dyes using biomordants were found to be temperature of 114^oC, initial pH of 6.3 and time of 51 min for Lac and Catechu (biomordant); temperature of 114^oC, initial pH of 6.2 and time of 50 min. for Lac and Myrobalan (biomordant); temperature of 113^oC, initial pH of 6.3 and time of 51 min. for Lac and Pomegranate (biomordant); temperature of 113^oC, initial pH of 6.2 and time of 50 min. for Catechu and Myrobalan (biomordant); temperature of 113^oC, initial pH of 6.2 and time of 50 min. for Catechu and Pomegranate (biomordant); and temperature of

113^oC, initial pH of 6.4 and time of 50 min. for Myrobalan and Pomegranate (biomordant). The K/S values predicted by the model equations derived in case of each of the natural dyes were 3.62 for Lac-Catechu, 2.72 for Lac-Myrobalan, 2.196 for Lac-Pomegranate, 1.78 for Catechu-Myrobalan, 1.65 for Catechu-Pomegranate, and 2.12 for Myrobalan-Pomegranate. It could thus be concluded that the optimal ranges for temperature, initial pH and time were 113-114^oC, 6.2-6.3 and 50-51 min respectively for the combinations of selected natural dyes and biomordants. Also, it could be inferred that Lac with Catechu as biomordant exhibited the highest predicted K/S values. In case of Lac, the K/S value decreased in the sequence of Catechu > Myrobalan > Pomegranate as biomordant. In case of Catechu, Myrobalan as biomordant gave marginally higher K/S value than Pomegranate. The Myrobalan-Pomegranate combination, however, showed higher K/S values than the combinations of Catechu.

- (ii) For PLA, the optimal values with all the natural dyes using biomordants were found to be temperature of 118^oC, initial pH of 6.2 and time of 33 min for Lac and Catechu (biomordant); temperature of 114^oC, initial pH of 6.2 and time of 35 min. for Lac and Myrobalan (biomordant); temperature of 113^oC, initial pH of 6.2 and time of 36 min. for Lac and Pomegranate (biomordant); temperature of 113^oC, initial pH of 6.2 and time of 35 min. for Catechu and Myrobalan (biomordant); temperature of 113^oC, initial pH of 6.4 and time of 35 min. for Catechu and Pomegranate (biomordant); and temperature of 113^oC, initial pH of 6.3 and time of 35 min. for Myrobalan and Pomegranate

(biomordant). The K/S values predicted by the model equations derived in case of each of the natural dyes were 3.11 for Lac-Catechu, 2.48 for Lac-Myrobalan, 1.99 for Lac-Pomegranate, 1.46 for Catechu-Myrobalan, 1.58 for Catechu-Pomegranate, and 2.17 for Myrobalan-Pomegranate. It could thus be concluded that the optimal range for temperature was 113-114°C for all combinations except for Lac with Catechu as biomordant, in which case it was 118°C. For initial pH and time, the optimal ranges were 6.2-6.4 and 33-36 min respectively for all the combinations of selected natural dyes and biomordants. With PLA also, the predicted K/S value for Lac with Catechu as biomordant was found to be highest among the combinations. For Lac, the K/S values decreased in the sequence of Catechu > Myrobalan > Pomegranate. For Myrobalan-Pomegranate combination, the K/S value was higher than the combinations used for Catechu. In case of Catechu, the K/S value with Pomegranate was found to be slightly higher than Myrobalan.

- (iii) The main effects of the factors, both linear as well as quadratic, viz. A, A², B, B², C and C², were found to be statistically significant in affecting the K/S values of the dyed fibers in all the cases where natural dyes were used. This was indicated by their p-values being lesser than 0.05, as well as the high F-values that they displayed. The interaction effects AB, AC and BC were also found to be statistically significant in most of the cases. While the linear effects A, B and C were found to have positive impacts on y (K/S value), all of the other factors left negative impacts on the same. Among all of the factors, the influences of A, A² and C² were found to be the most statistically

significant ones, as signified by their higher F-values as compared to the other factors in almost all of the cases. The F-values of B and B² were also significant in a majority of the dyeing experiments. Thus, it could be concluded that temperature and dyeing time were found to affect the color strength of PTT and PLA dyed with natural dyes with biomordants most significantly, followed by the initial pH.

- (iv) The observed values of optimal temperatures for PTT and PLA were slightly higher than reported in literature (100-110^oC). But it was lower than dyeing temperature for PET (130^oC). In this study, no auxiliary chemicals were used in dyeing other than acetic acid. No dispersing, sequestering or other agents were applied that assist in dyeing. Even the mordants used were biomordants of natural origin that were non-pollutants. Without much assistance from the auxiliary chemicals, the dyeing temperature was higher than as reported in the studies using them. The optimal ranges for pH was same as reported (5-6), while that for dyeing time was again on a slightly higher side. This was also because of the lack of assisting chemicals due to which proper penetration of dyes took longer time. In this study, the dyeing processes presented for PTT and PLA with natural dyes and biomordants without the use of any auxiliary chemicals except for acetic acid, were more eco-friendly than the conventional dyeing processes. Although the values for temperature and time were slightly higher, the effluent did not contain harmful chemicals that were toxic and polluting in nature. Moreover, when compared to conventional dyeing of PET at 130^oC, pH 3-4 and 60 min, the optimal parameters achieved were much

lower or milder. Hence, the dyeing processes described here were more ecofriendly for these fibers with disperse dyes as well as in case of conventional dyeing of PET.

Chapter 8

Conclusion

From the experiments performed in this study, the summary of the results have been discussed at the end of the respective chapters. An overall conclusion from these observations has been discussed here, as follows.

From the characterization of the PTT and PLA fibers, the glass transition temperatures (T_g) and melting points (T_m) for PTT and PLA could be confirmed with the reported values from the thermo-gravimetric analysis performed in this study. The thermally and mechanically stable ranges of temperatures of PTT and PLA could be identified as 80 °C -120 °C and 90 °C -145°C respectively. The presence of a smooth surface with micropores could also be observed from SEM views.

With the experiments for disperse dyes, it was observed that although the color strength and wash fastness of PTT, PLA as well as PET increased with temperature, the tensile properties decreased. High temperature assisted penetration of the dye molecules by increasing their mobility as well as opening up the micropores of the fibers. The reduction in tensile properties was due to the disorientation of the polymer chains because of the increased dye uptake in the amorphous regions of the fibers. The lowering of tensile properties was most marked in case of PLA fibers and least for PET. This was because PLA is highly susceptible to hydrolysis at elevated temperatures which caused a degradation of its polymer chains. Therefore, dyeing at elevated temperatures was not suggested for PTT and PLA, and an optimal range had to be found out. The optimal range of temperature for application of disperse dyes on PTT, PLA and PET were found to be 110-130°C.

Similar observations could be made with dyeing time. More duration of dyeing helped in better penetration of the dye molecules and hence higher color strength and

wash fastness, but at the same time reduced the tensile properties of the fibers. Here also, the decrease was most marked for PLA fibers. The reason for loss in tensile properties was primarily due to the disorientation of the polymer chains in the amorphous regions of the fibers where the dye molecules penetrated. This was also assisted by degradation of the polymer chains at elevated temperatures for prolonged time. In case of PLA, the lowering was more marked as it is susceptible to hydrolysis at high temperatures, and prolonged dyeing time increased the same. Thus, for PLA, optimal dyeing time was identified as 15-45 min whereas it was 30-60 min for the other two fibers.

In case of initial pH values, optimal ranges could be observed for the fibers in which the color strength, wash fastness as well as tensile properties were superior to other conditions. For PTT and PLA, it was 5-6 and for PET, it was 3-4, as reported in literatures. The material to liquor ratio was favorable in the range of 1:20 to 1:40 for all the fibers. Higher ratios made mobility of the dye molecules in solution difficult as a result of lesser volume of the liquor. At ratios lower than the optimal range, the concentration of dye in solution was very low and the equilibrium in its concentration inside the fiber and in solution was achieved earlier. Thus, dye penetration was lower at such ratios. The material to liquor ratio was also found to have no meaningful impact on the tensile properties of the fibers. In case of rate of heating also, the favorable value was found to be 2^oC/min, and its effect on tensile properties was not significant.

In the optimization of dyeing of PTT with disperse dyes, the optimal ranges were observed as temperature of 120^oC, initial pH of 5.6 and time of 58-59 min, whereas with PLA, they were found to be temperature of 120^oC, initial pH of the dye bath of 5.6 and time of 43 min for Disperse Blue 79 and Disperse Red 167. With Disperse Yellow 56,

they were 124^oC, 5.8 and 55 min respectively for PLA. The K/S values predicted by the model equations for PTT were found to be lower than the actual values reported for PET, but higher than the predicted values for PLA.

In application of natural dyes on PTT, PLA and PET fibers, the same trends could be observed for the affecting parameters. With temperature, the color strength increased but the tensile properties decreased. With dyeing time also, the observations were the same. The lowering of tensile properties was most marked for PLA in these cases too. The optimal ranges for temperature and dyeing time were found to be 110-120^oC and 30-45 min respectively. In case of initial pH values, the optimal range was 5-6 for PTT and PLA, and 3-4 for PET. For material to liquor ratio, it was 1:30 to 1:40 for all the fibers.

Studies of the FTIR spectra revealed no chemical bonding of the natural dyes with PTT or PLA. The adsorption isotherms were found to resemble the Nersnt model, indication only physical penetration and binding between the dyes and the fibers. It could thus be inferred that with natural dyes too, dyeing occurred through physical penetration of the dye molecules into the amorphous regions of the polymer matrices of PTT and PLA fibers.

The fastness properties were found to be good to average in case of these fibers with the natural dyes. In order to improve the same, biomordants were applied in dyeing. Out of the three mordanting techniques, meta-mordanting was found to give superior results of fastness properties than the others. The results with pre-mordanting were marginally better than those for post-mordanting. This indicated that during mordanting, the biomordants attached with the dye molecules to form bigger molecular structures with higher molecular weights. This increased the fastness properties of these dyes. In case of

meta-mordanting, the dye and the biomordant were present in solution for a longer duration. This assisted their bonding and hence, the fastness values were superior for meta-mordanting. In case of pre-mordanting and post-mordanting, the bonding could happen inside the amorphous regions of the fiber only. This was hampered due to steric hindrance restricting the movement of the dye molecules and the biomordants inside the fiber polymer matrix. Hence, fastness properties were inferior.

The color strength of the fibers was compared between biomordants and inorganic mordants in the application of natural dyes. It was observed that the values with Catechu as a biomordant were in close proximity to those achieved with stannous chloride. In many cases, the color strength with Catechu was higher than that with stannous chloride. Thus, Catechu could satisfactorily replace stannous chloride as an inorganic mordant in the application of natural dyes on PTT and PLA fibers. Among the inorganic mordants, the color strength was found to decrease in the sequence of alum> ferrous sulfate> stannous chloride for both PTT and PLA. For the biomordants, it followed the sequence Catechu> Myrobalan> Pomegranate in case of both the fibers.

When natural dyes were optimized using biomordants, the optimal dyeing conditions for PTT fiber were observed as temperature of 113-114^oC, initial pH value of 6.2-6.4 and dyeing time of 50-51 min. With PLA, the same were observed as 113-114^oC, 6.2-6.4 and 33-36 min for temperature, initial pH value and dyeing time respectively. For Lac, the K/S values decreased in the sequence of Catechu>Myrobalan>Pomegranate in case of both the fibers. For Myrobalan-Pomegranate combination, the K/S value was higher than the combinations used for Catechu. In case of Catechu, the K/S value with Pomegranate was found to be slightly higher than Myrobalan.

The model equations were found to have very high correlation to the real values due to their very high R^2 values obtained. The proximity of the adjusted R^2 values to the R^2 values indicated a high goodness of fit for the developed models. Temperature and dyeing time were the most statistically significant factors affecting color strength of PTT and PLA with all the dyes, as indicated by their p -values < 0.05 and high F -values. The initial pH was also a significant factor affecting color strength. These three factors not only affected the color strength linearly but quadratically as well for all the dyes. Also, in most cases, the interaction effects among these factors were also found to be statistically significant.

The observed values of optimal temperatures for PTT and PLA were slightly higher than reported in literature (100-110^oC). But it was lower than dyeing temperature for PET (130^oC). In this study, no auxiliary chemicals were used in dyeing other than acetic acid. No dispersing, sequestering or other agents were applied that assist in dyeing. Even the mordants used were biomordants of natural origin that were non-pollutants. Without the auxiliary chemicals, the dyeing temperature was higher than as reported in the studies using them. The optimal ranges for pH was same as reported (5-6), while that for dyeing time was again on a slightly higher side.

In this study, the dyeing processes presented for PTT and PLA with natural dyes and biomordants without the use of any auxiliary chemicals except for acetic acid, were more eco-friendly than the conventional dyeing processes. Although the values for temperature and time were slightly higher, the effluent did not contain harmful chemicals that were toxic and polluting in nature. Moreover, when compared to conventional dyeing of PET at 130^oC, pH 3-4 and 60 min, the optimal parameters achieved were much lower or

milder. Hence, the dyeing processes described here were more ecofriendly for these fibers with disperse dyes as well as in case of conventional dyeing of PET.

It could finally be inferred that the use of natural dyes made the process of dyeing for PTT and PLA possible with milder conditions of temperature, initial pH and dyeing time, as compared to the application of disperse dyes. The natural dyes used in such conditions were suitable for attaining light to medium shades on these two fibers. The use of biomordants further assisted in attaining more ecofriendly dyeing processes by lowering of the dyeing temperature significantly, besides improving the fastness properties. They also substantially increased the K/S values obtained with PTT and PLA for the chosen natural dyes.

Chapter 9

Future Scope of Work

In this study, the effects of various parameters on the color, fastness and tensile properties of PTT and PLA were observed for three selected disperse and natural dyes. In case of natural dyes, the effects were observed both with and without the application of biomordants. The color strength of these fibers was compared between biomordants and inorganic mordants. Optimization of dyeing parameters was also performed in the different cases of disperse and natural dyes. The following suggestions can be made for researches in future related to the work presented here:

- (1) In this study, three disperse dyes were applied on PTT and PLA for observing the effects and optimization. Similar studies can be made with other disperse dyes that are used for dyeing of PTT and PLA in the industry. The effects of various parameters on the application of these dyes without using any auxiliary chemicals on PTT and PLA may be made. Optimization of the dyeing conditions with these dyes can also be made, in order to observe whether satisfactory color strength can be achieved under more eco-friendly conditions than PET when applied for PTT and PLA.
- (2) Besides the three natural dyes used in this study, other natural dyes can also be applied on PTT and PLA. The effects of various factors on color strength and other properties of the dyed fibers in their cases may be studied. Optimization of dyeing conditions may also be studied with these dyes in order to find out the favorable conditions for satisfactory color strength.
- (3) Other than the three biomordants used in this study, newer sets of biomordants may be applied with separate sets of natural dyes. The results may be helpful to

find out if favorable dyeing conditions for these combinations can be achieved for PTT and PLA.

- (4) In the pursuit of ecofriendly dyeing process for PTT and PLA, application of natural dyes and biomordants on these fibers may be explored using non-aqueous media. The use of alkane media, dyeing using supercritical carbon dioxide (CO₂) and ultrasound dyeing techniques may be explored. Optimization of the dyeing parameters using these techniques have the potential of removing wastage of water in dyeing, although the processes may be costlier than the aqueous media used.
- (5) Other than RSM, other statistical tools like artificial neural network (ANN) may be used for optimization with different sets of disperse dyes, natural dyes and biomordants in case of PTT and PLA.

References

References

1. A. K. R. Choudhury, Textile Preparation and Dyeing, 1st edition, Society of Dyers and Colourists, Mumbai (2011) pp. 5-17, 277-298.
2. M. N, Karim, M. Rigout, S. G. Yeates, C. Carr, Surface chemical analysis of the effect of curing conditions on the properties of thermally-cured pigment printed poly (lactic acid) fabrics, Dyes and Pigments, 10 (2014) 168-174; DOI: <http://dx.doi.org/10.1016/j.dyepig.2013.12.010>
3. J. V. Kurian, A new polymer platform for the future- Sorona from corn derived 1,3-propanediol, Journal of Polymers and the Environment, 13(2) (2005) 159-167, DOI: 10.1007/s10924-005-2947-7
4. P. R. Richards, Colour Design, 1st edition, Woodhead Publishing Ltd., London (2012) pp. 471-496.
5. I. Drivas, R. S. Blackburn, C. M. Rayner, Natural anthraquinonoid colorants as platform chemicals in the synthesis of sustainable disperse dyes for polyesters, Dyes and Pigments, 88 (2011) 7-17, DOI:10.1016/j.dyepig.2010.04.009
6. J. E. Booth, Principles of Textile Testing, 3rd edition, CBS, New Delhi (1996), pp. 354.
7. K. Gharanjig, M. Arami, H. Bahrami, B. Movassagh, N. M. Mahmoodi, S. Rouhani, Synthesis, spectral properties and application of novel monoazo disperse dyes derived from *N*-ester-1,8-naphthalimide to polyester, Dyes and Pigments, 76 (2008) 684-689, DOI:10.1016/j.dyepig.2007.01.024

8. J. Seo, W. J. Jo, G. Choi, M. R. Han, S. Y. Lee, S. S. Lee, J. S. Lee, Single crystal X-ray structure of C.I. Disperse Yellow 3, *Dyes and Pigments*, 76 (2008) 530-534, DOI:10.1016/j.dyepig.2006.11.001
9. J.-E. Lee, H. J. Kim, M. R. Han, S. Y. Lee, W. J. Jo, S. S. Lee, J. S. Lee, Crystal structures of C.I. Disperse Red 65 and C.I. Disperse Red 73, *Dyes and Pigments*, 80 (2009) 181-186, DOI:10.1016/j.dyepig.2008.07.001.
10. Y. Zhou, Z. Du, Y. Zhang, Simultaneous determination of 17 disperse dyes in textile by ultra-high performance supercritical fluid chromatography combined with tandem mass spectrometry, *Talanta*, 127 (2014) 108-115, <http://dx.doi.org/10.1016/j.talanta.2014.03.055>.
11. J. Wu, G. Cai, J. Liu, H. Ge, J. Wang, J., Eco-friendly surface modification on polyester fabrics by esterase treatment, *Applied Surface Science*, 295 (2014) 150-157, <http://dx.doi.org/10.1016/j.apsusc.2014.01.019>
12. S. M. Burkinshaw, D. S. Jeong, The dyeing of poly(lactic acid) fibres with disperse dyes using ultrasound: Part 1- Initial studies, *Dyes and Pigments*, 92 (2012) 1025-1030, doi:10.1016/j.dyepig.2011.06.020
13. A. Singh, R. Choi, B. Choi, J. Koh, Synthesis and properties of some novel pyrazolone-based heterocyclic azo disperse dyes containing a fluorosulfonyl group, *Dyes and Pigments* 95 (2012) 580-586, <http://dx.doi.org/10.1016/j.dyepig.2012.06.009>
14. E. R. A. Ferraz, G. A. R. Oliveira, M. D. Grando, T. M. Lizier, M. V. B. Zanoni, D. P. Oliveira, Photoelectrocatalysis based on Ti/TiO₂ nanotubes removes toxic properties of the azo dyes Disperse Red 1, Disperse Red 13 and Disperse

- Orange 1 from aqueous chloride samples, *Journal of Environmental Management*, 124 (2013) 108-114, <http://dx.doi.org/10.1016/j.jenvman.2013.03.033>.
15. K. Wang, Y. Chen, Y. Zhang, Effects of organoclay platelets on morphology and mechanical properties in PTT/EPDM-*g*-MA/organoclay ternary nanocomposites, *Polymer*, 49 (2008) 3301-3309, doi:10.1016/j.polymer.2008.05.025.
16. H. Kaur, *Spectroscopy*, 2nd edition, Pragati Prakashan, Meerut, (2004-'05) pp. 81-174.
17. T. Wu, Y. Li, Q. Wu, L. Song, G. Wu, Thermal analysis of the melting process of poly(trimethylene terephthalate) using FTIR micro-spectroscopy, *European Polymer Journal*, 41 (2005) 2216-2223, doi:10.1016/j.eurpolymj.2005.04.025.
18. A. Eberl, S. Heumann, R. Kotek, F. Kaufmann, S. Mitsche, A. Cavaco-Paulo, G. M. Gubitz, Enzymatic hydrolysis of PTT polymers and oligomers, *Journal of Biotechnology*, 135 (2008) 45-51, doi:10.1016/j.jbiotec.2008.02.015.
19. J. Liu, S. G. Bian, M. Xiao, S. J. Wang, Y. Z. Meng, Thermal degradation and isothermal crystalline behavior of poly(trimethylene terephthalate), *Chinese Chemical Letters*, 20 (2009) pp. 487-491, doi:10.1016/j.ccllet.2008.11.03.
20. H.-B. Chen, Q. Zhou, X. Dong, Y. Zhang, L. Chen, W.-Z. Wang, Pyrolysis study of poly(trimethylene terephthalate) and its phosphorus-containing copolyesters, *Polymer Degradation and Stability*, 97 (2012) 905-913, doi:10.1016/j.polymdegradstab.2012.03.030.
21. <http://www.worlddyevaryety.com/disperse-dyes/> accessed on 27.08.2018.

22. Y.-A.Son, J.-P. Hong, T.-K. Kim, An approach to the dyeing of polyester fiber using indigo and its extended wash fastness properties, *Dyes and Pigments*, 61 (2004) 263-272, doi:10.1016/j.dyepig.2003.11.001
23. S. C. Park, Y. Liang, H. S. Lee, Y. H. Kim, Three-dimensional orientation change during thermally induced structural change of oriented poly(trimethylene terephthalate) films using polarized FTIR-ATR spectroscopy, *Polymer*, 45 (2004) 8981-8988, doi:10.1016/j.polymer.2004.10.079
24. R. G. Ovejero, J. R. Sanchez, J. B. Ovejero, J. Valldeperas, M. J. Lis, Kinetic and Diffusional Approach to the Dyeing Behavior of the Polyester PTT, *Textile Research Journal*, 77(10) (2007) 804-809, DOI: 10.1177/0040517507080665
25. F. F. Yildirim, O. O. Avinc, A. Yavas, Poly(trimethylene terephthalate) fibres part 1: Production, properties, end-use applications, environmental impact, *Tekstil ve Muhendis*, 19(87) 2012 pp. 43-54.
26. J. Jolly, B. Hitzmann, S. Ramalingam, K. B. Ramachandran, Biosynthesis of 1,3-propanediol from glycerol with *Lactobacillus reuteri*: Effect of operating variables, *Journal of Bioscience and Bioengineering*, 118(2) 2014 188-194, <https://doi.org/10.1016/j.jbiosc.2014.01.003>
27. K. Wang, Y. Chen, Y. Zhang, Effects of reactive compatibilizer on the core-shell structured modifiers toughening of poly(trimethylene terephthalate), *Polymer*, 50 (2009) 1483-1490, doi:10.1016/j.polymer.2009.01.046
28. R. K. Saxena, P. Anand, S. Saran, J. Isar, Microbial production of 1,3-propanediol: Recent developments and emerging opportunities, *Biotechnology Advances*, 27 (2009) 895-913, doi:10.1016/j.biotechadv.2009.07.003

29. S. Padee, S. Thumsorn, J. W. On, P. Surin, C. Apawet, T. Chaichalermwong, N. Kaabbuathong, N. O-Charoen, N. Srisawat, Preparation of Poly(lactic acid) and Poly(trimethylene terephthalate) Blend Fibers for Textile Application, *Energy Procedia*, 34 (2013) 534-541, doi: 10.1016/j.egypro.2013.06.782
30. J. Li, W.-Q. Jiang, Z.-B. Wang, P. Chen, Y. Li, J. Zhou, J. Liu, Y.-Z. Wang, Q. Gu, Synthesis, crystallization and hydrolysis of aromatic-aliphatic copolyester: Poly(trimethylene terephthalate)-*co*-poly(L-lactic acid), *Polymer Degradation and Stability*, 96 (2011) 991-999, doi:10.1016/j.polymdegradstab.2011.01.023
31. U. Gurmendi, J. I. Eguiazabal, J. Nazabal, Structure and properties of nanocomposites with a poly(trimethylene terephthalate) matrix, *European Polymer Journal*, 44 (2008) 1686-1695, doi:10.1016/j.eurpolymj.2008.04.001
32. D. Karst, Y. Yang, Molecular modelling study of the resistance of PLA to hydrolysis based on the blending of PLLA and PDLA, *Polymer*, 47 (2006) 4845-4850, doi:10.1016/j.polymer.2006.05.002
33. H. E. Liang, Z. Shufen, T. Bingtao, W. Lili, Y. Jinzong, Dyeability of Polylactide Fabric with Hydrophobic Anthraquinone Dyes, *Chinese Journal of Chemical Engineering*, 17(1) (2009) pp. 156-159.
34. J. Wu, Y. Hu, J. Zhou, W. Qian, X. Lin, Y. Chen, X. Chen, J. Xie, J. Bai, H. Ying, Separation of D-lactic acid from aqueous solutions based on the adsorption technology, *Colloids and Surfaces A: Physicochemical and Engineering Aspects*, 407 (2012) 29-37, <http://dx.doi.org/10.1016/j.colsurfa.2012.04.051>

35. M. B. Bilal, P. Viallier-Raynard, B. Haider, G. Colombe, A. Lallam, A study of the structural changes during the dyeing process of *Ingeo*TM fibers of poly(lactic acid), *Textile Research Journal*, 81(8) (2011) 838-846.
36. M. S. Islam, K. L. Pickering, N. J. Foreman, Influence of alkali treatment on the interfacial and physico-mechanical properties of industrial hemp fibre reinforced polylactic acid composites, *Composites: Part A*, 41 (2010) 596-603, doi:10.1016/j.compositesa.2010.01.006.
37. C. Chuensangjun, C. Pechyen, S. Sirisansaneeyakul, Degradation behaviors of different blends of polylactic acid buried in soil, *Energy Procedia*, 34 (2013) 73-82, doi: 10.1016/j.egypro.2013.06.735.
38. M. Bishai, S. De, B. Adhikari, R. Banerjee, A comprehensive study on enhanced characteristics of modified polylactic acid based versatile biopolymer, *European Polymer Journal*, (2014) <http://dx.doi.org/10.1016/j.eurpolymj.2014.01.027>
39. Y. Dong, A. Ghataura, H. Takagi, H. J. Haroosh, A. N. Nakagaito, K.-T. Lau, Polylactic acid (PLA) biocomposites reinforced with coir fibres: Evaluation of mechanical performance and multifunctional properties, *Composites: Part A*, 63 (2014) 76-84, <http://dx.doi.org/10.1016/j.compositesa.2014.04.003>.
40. O. Avinc, M. Wilding, D. Phillips, D. Farrington, Investigation of the influence of different commercial softeners on the stability of poly(lactic acid) fabrics during storage, *Polymer Degradation and Stability*, 95 (2010) 214-224, doi:10.1016/j.polymdegradstab.2009.11.022

41. H. E. Liang, Z. Shufen, T. Bingtao, W. Lili, Y. Jinzong, Dyeability of Polylactide Fabric with Hydrophobic Anthraquinone Dyes, *Chinese Journal of Chemical Engineering*, 17(1) (2009) 156-159.
42. J. Wu, Y. Hu, J. Zhou, W. Qian, X. Lin, Y. Chen, X. Chen, J. Xie, J. Bai, H. Ying, Separation of D-lactic acid from aqueous solutions based on the adsorption technology, *Colloids and Surfaces A: Physicochemical and Engineering Aspects*, 407 (2012) 29-37, <http://dx.doi.org/10.1016/j.colsurfa.2012.04.051>
43. S. A. Arvidson, K. C. Wong, R. E. Gorga, S. A. Khan, Structure, molecular orientation, and resultant mechanical properties in core/sheath poly(lactic acid)/polypropylene composites, *Polymer*, 53 (2012) 791-800, doi:10.1016/j.polymer.2011.12.042
44. J.-M. Raquez, Y. Habibi, M. Murariu, P. Dubois, Polylactide (PLA)- based nanocomposites, *Progress in Polymer Science*, 38 (2013) 1504-1542, <http://dx.doi.org/10.1016/j.progpolymsci.2013.05.014>
45. K. M. Z. Hossain, A. J. Parsons, C. D. Rudd, I. Ahmed, W. Thielemans, Mechanical, crystallisation and moisture absorption properties of melt drawn polylactic acid fibres, *European Polymer Journal*, 53 (2014) 270-281, <http://dx.doi.org/10.1016/j.eurpolymj.2014.02.001>
46. Y. Dong, A. Ghataura, H. Takagi, H. J. Haroosh, A. N. Nakagaito, K.-T. Lau, Polylactic acid (PLA) biocomposites reinforced with coir fibres: Evaluation of mechanical performance and multifunctional properties, *Composites: Part A*, 63 (2014) 76-84, <http://dx.doi.org/10.1016/j.compositesa.2014.04.003>.

47. O. Monticelli, M. Calabrese, L. Gardella, A. Fina, E. Gioffredi, Silsesquioxanes: Novel compatibilizing agents for tuning the microstructure and properties of PLA/PCl immiscible blends, *European Polymer Journal*, 58 (2014) 69-78, <http://dx.doi.org/10.1016/j.eurpolymj.2014.06.021>
48. D. Cristea, G. Vilarem, Improving light fastness of natural dyes on cotton yarn, *Dyes and Pigments*, 70 (2006) 238-245, doi:10.1016/j.dyepig.2005.03.006
49. L. Fernandes, J. A. Pereira, I. Lopez-Cortes, D. Salazar, J. Gonzalez-Alvarez, E. Ramalhosa, "Physicochemical composition and antioxidant activity of several pomegranate (*Punica granatum* L.) cultivars grown in Spain, *European Food Research Technology*, (2017) DOI 10.1007/s00217-017-2884-4.
50. A. Ujhelyiova, E. Bolhova, J. Oravkinova, R. Tino, A. Marcincin, Kinetics of dyeing process of blend polypropylene/polyester fibres with disperse dye, *Dyes and Pigments*, 72 (2007) 212-216, doi:10.1016/j.dyepig.2005.08.026
51. R. B. Chavan, *Handbook of textile and industrial dyeing*, 1st edition, Woodhead Publishing Ltd., London (2011) pp. 515-561.
52. M. L. Gulrajani, *Handbook of textile and industrial dyeing*, 1st edition, Woodhead Publishing Ltd., London (2011) pp. 365-394.
53. Y. Zhou, Z. Du, Y. Zhang, Simultaneous determination of 17 disperse dyes in textile by ultra-high performance supercritical fluid chromatography combined with tandem mass spectrometry, *Talanta*, 127 (2014) 108-115, <http://dx.doi.org/10.1016/j.talanta.2014.03.055>.

54. C. Radulescu, A. M. Hossu, I. Ionita, Disperse dyes' derivatives from compact condensed system 2-aminothiazolo[5,4-c]pyridine: Synthesis and characterization, *Dyes and Pigments*, 71 (2006) 123-129, doi:10.1016/j.dyepig.2005.06.009
55. C. V. Uliana, G. S. Garbellini, H. Yamanaka, Evaluation of the interactions of DNA with the textile dyes Disperse Orange 1 and Disperse Red 1 and their electrolysis products using an electrochemical biosensor, *Sensors and Actuators B: Chemical*, 178 (2013) 627-635, <http://dx.doi.org/10.1016/j.snb.2013.01.029>
56. S. Sahin, C. Demir, S. Gucer, Simultaneous UV-vis spectrophotometric determination of disperse dyes in textile wastewater by partial least squares and principal component regression, *Dyes and Pigments*, 73 (2007) 368-376, doi:10.1016/j.dyepig.2006.01.045
57. F. Jamal, P. K. Pandey, T. Qidwai, Potential of peroxidase enzyme from *Trichosanthes dioica* to mediate disperse dye decolorization in conjunction with redox mediators, *Journal of Molecular Catalysis B: Enzymatic*, 66 (2010) 177-181, doi:10.1016/j.molcatb.2010.05.005.
58. Z.-H. Cui, X.-H. Cheng, X. Li, H.-H. Lu, X.-D. Wang, Facile synthesis and properties of alkali-clearable azo disperse dye containing a carboxylic ester moiety, *Chinese Chemical Letters*, (2014) <http://dx.doi.org/10.1016/j.ccllet.2014.03.045>
59. S. Nikfar, M. Jaberidoost, "Dyes and Colorants", *Encyclopedia of Toxicology*, 2 (2014) 252-261, <http://dx.doi.org/10.1016/B978-0-12-386454-3.00602-3>

60. T. B. Shah, R. S. Shiny, R. B. Dixit, B. C. Dixit, Synthesis and dyeing properties of new disazo disperse dyes for polyester and nylon fabrics, *Journal of Saudi Chemical Society*, (2011) doi:10.1016/j.jscs.2011.11.022
61. A. Guesmi, N. Ben hamadi, N. Ladhari, F. Sakli, Sonicator dyeing of modified acrylic fabrics with indicaxanthin natural dye, *Industrial Crops and Products*, 42 (2013) 63-69, <http://dx.doi.org/10.1016/j.indcrop.2012.05.022>
62. M. Shahid, S. Islam, F. Mohammad, Recent advancements in natural dye applications: a review, *Journal of Cleaner Production*, 53 (2013) 310-331, <http://dx.doi.org/10.1016/j.jclepro.2013.03.031>
63. S. Islam, M. Shahid, F. Mohammad, Perspectives for natural product based agents derived from industrial plants in textile applications- a review, *Journal of Cleaner Production*, 57 (2013) 2-18, <http://dx.doi.org/10.1016/j.jclepro.2013.06.004>
64. D. Cordon, *Natural Dyes Sources, Tradition, Technology and Science*, 1st edition, Archetype Publications Ltd., Paris (2007) pp. 452-456, 469-472, 481-484, 656-666.
65. J. Shen, P. Gao, H. Ma, The effect of tris(2-carboxyethyl)phosphine on the dyeing of wool fabrics with natural dyes, *Dyes and Pigments*, 108 (2014) 70-75, <http://dx.doi.org/10.1016/j.dyepig.2014.04.027>
66. A. Moiz, M. A. Ahmed, N. Kausar, K. Ahmed, M. Sohail, Study the effect of metal ion on wool fabric dyeing with tea as natural dye, *Journal of Saudi Chemical Society*, 14 (2010) 69-76, doi:10.1016/j.jscs.2009.12.011

67. A. Ujhelyiova, E. Bolhova, J. Oravkinova, R. Tino, A. Marcincin, Kinetics of dyeing process of blend polypropylene/polyester fibres with disperse dye, *Dyes and Pigments*, 72 (2007) 212-216, doi:10.1016/j.dyepig.2005.08.026
68. B. Merzouk, B. Gourich, K. Madani, C. Vial, A. Sekki, Removal of a disperse red dye from synthetic wastewater by chemical coagulation and continuous electrocoagulation. A comparative study, *Desalination*, 272 (2011) 246-253. doi:10.1016/j.desal.2011.01.029
69. C. V. Uliana, G. S. Garbellini, H. Yamanaka, Electrochemical investigations on the capacity of flavonoids to protect DNA against damage caused by textile disperse dyes, *Sensors and Actuators B: Chemical*, 192 (2014) 188-195, <http://dx.doi.org/10.1016/j.snb.2013.10.091>
70. T.-K. Kim, Y.-A. Son, Affinity of disperse dyes on poly(ethylene terephthalate) in non-aqueous media. Part 2: effect of substituents, *Dyes and Pigments*, 66 (2005) 19-25, doi:10.1016/j.dyepig.2004.08.009
71. J. Koh, A. J. Greaves, J. P. Kim, Synthesis and spectral properties of alkali-clearable azo disperse dyes containing a fluorosulfonyl group, *Dyes and Pigments*, 56 (2003) 69-81, PII: S0143-7208(02)00107-9.
72. S. L. Draper, G. A. Montero, B. Smith K. Beck, Solubility relationships for disperse dyes in supercritical carbon dioxide, *Dyes and Pigments*, 45 (2000) 177-183, PII: S0143-7208(00)00008-5
73. Y.-A. Son, J.-P. Hong, T.-K. Kim, An approach to the dyeing of polyester fiber using indigo and its extended wash fastness properties, *Dyes and Pigments*, 61 (2004) 263-272, doi:10.1016/j.dyepig.2003.11.001

74. F. F. Yildirim, O. O. Avinc, A. Yavas, Poly(trimethylene Terephthalate) fibres part 2: Wet Processing, *Journal of Textiles and Engineer*, 19(88) 2012 pp. 28-38.
75. J. Wu, G. Cai, J. Liu, H. Ge, J. Wang, Eco-friendly surface modification on polyester fabrics by esterase treatment, *Applied Surface Science*, 295 (2014) 150-157, <http://dx.doi.org/10.1016/j.apsusc.2014.01.019>
76. H. K. Jang, S. J. Doh, J. J. Lee, Ecofriendly dyeing of poly(trimethylene terephthalate) with temporarily solubilized azo disperse dyes based on pyridone derivatives, *Fibers and Polymers*, 10(3) 2009 315-319.
77. B.-Z. Ke, X.-C. Chai, B.-Q. Wang, Study on the dye diffusion mechanism of PTT fibers, 7th Textile Bioengineering and Informatics Symposium, TBIS (2014) The Hong Kong Polytechnic University, Hong Kong; China, pp. 37-41.
78. D. Karst, D. Nama, D. Y. Yang, Effect of disperse dye structure on dye sorption onto PLA fiber, *Journal of Colloid and Interface Science*, 310 (2007) 106-111, doi:10.1016/j.jcis.2007.01.037
79. Y.-C. Shu, K.-J. Hsiao, Preparation and physical properties of poly(trimethylene terephthalate)/metallocene isotactic polypropylene conjugated fibers, *European Polymer Journal*, 42 (2006) 2773-2780, doi:10.1016/j.eurpolymj.2006.05.003
80. R. M. Rasal, A. V. Janorkar, D. E. Hirt, Poly(lactic acid) modifications, *Progress in Polymer Science*, 35 (2012) 338-356, doi:10.1016/j.progpolymsci.2009.12.003
81. S. M. Burkinshaw, D. S. Jeong, The dyeing of poly(lactic acid) fibres with disperse dyes using ultrasound: Part 2- Fastness, *Dyes and Pigments*, 92 (2012) 988-994, doi:10.1016/j.dyepig.2011.07.005

82. H. E. Liang, Z. Shufen, T. Bingtao, W. Lili, Y. Jinzong, Dyeability of Polylactide Fabric with Hydrophobic Anthraquinone Dyes, *Chinese Journal of Chemical Engineering*, 17(1) (2009) 156-159.
83. G. Seu, Structure-Afinity Relationships in Aminoazo Disperse Dyes. A Multivariate Approach, *Dyes and Pigments*, 37(2) (1998) 103-112.
84. F. M. D. Chequer, T. M. Lizier, R. de Felicio, M. V. B. Zanoni, H. M. Deboni, N. P. Lopes, R. Marcos, D. P. de Oliveira, Analyses of the genotoxic and mutagenic potential of the products formed after the biotransformation of the azo dye Disperse Red 1, *Toxicology in Vitro*, 25 (2011) 2054-2063, doi:10.1016/j.tiv.2011.05.033
85. M. Cinar, A. Coruh, M. Karabacak, FT-IR, UV-vis, H and C NMR spectra and the equilibrium structure of organic dye molecule *disperse red 1 acrylate*: A combined experimental and theoretical analysis, *Spectrochimica Acta Part A: Molecular and Biomolecular Spectroscopy*, 83 (2011) 561-569, doi:10.1016/j.saa.2011.09.003
86. M. Cinar, A. Coruh, M. Karabacak, A comparative study of selected disperse azo dye derivatives based on spectroscopic (FT-IR, NMR and UV-Vis) and nonlinear optical behaviors, *Spectrochimica Acta Part A: Molecular and Biomolecular Spectroscopy*, 122 (2014) 682-689, <http://dx.doi.org/10.1016/j.saa.2013.11.106>
87. M. R. de Giorgi, R. Carpignano, A. Cerniani, Structure Optimization in a Series of Thiadiazole Disperse Dyes using a Chemometric Approach, *Dyes and Pigments*, 37(2) (1998) 187-196.

88. H.-F. Qian, Y.-G. Wang, X.-C. Chen, W.-G. Ruan, W. Huang, Structural and spectral characterizations of C.I. Disperse Blue 148 having a new crystalline form, *Dyes and Pigments*, 99 (2013) 489-495, <http://dx.doi.org/10.1016/j.dyepig.2013.06.002>
89. M. S. Deshmukh, N. Sekar, A combined experimental and TD-DFT investigation of three disperse azo dyes having the nitroterephthalate skeleton, *Dyes and Pigments*, 103 (2014) 25-33, <http://dx.doi.org/10.1016/j.dyepig.2013.10.035>
90. M. S. Tsuboy, J. P. F. Angeli, M. S. Mantovani, S. Knasmuller, G. A. Umbuzeiro, L. R. Ribeiro, Genotoxic, mutagenic and cytotoxic effects of the commercial dye CI Disperse Blue 291 in the human hepatic cell line HepG2, *Toxicology in Vitro*, 21 (2007) 1650-1655, doi:10.1016/j.tiv.2007.06.020.
91. W. Haddar, M. B. Ticha, A. Guesmi, F. Khoffi, B. Durand, A novel approach for a natural dyeing process of cotton fabric with *Hibiscus mutabilis* (Gulzuba): process development and optimization using statistical analysis, *Journal of Cleaner Production*, 68 (2014) 114-120, <http://dx.doi.org/10.1016/j.jclepro.2013.12.066>.
92. F. Rehman, S. Adeel, M. Shahid, I. A. Bhatti, F. Nasir, N. Akhtar, Z. Ahmad, Dyeing of γ -irradiated cotton with natural flavonoid dye extracted from irradiated onion shells (*Allium cepa*) powder, *Radiation Physics and Chemistry*, 92 (2013) 71-75, <http://dx.doi.org/10.1016/j.radphyschem.2013.07.002>
93. F. S. Ghaheh, S. M. Mortazavi, F. Alihosseini, A. Fassihi, A. S. Nateri, D. Abedi, Assessment of antibacterial activity of wool fabrics dyed with natural dyes,

Journal of Cleaner Production, 72 (2014) 139-145,
<http://dx.doi.org/10.1016/j.jclepro.2014.02.050>

94. K. Sinha, P. D. Saha, S. Datta, Response surface optimization and artificial neural network modeling of microwave assisted natural dye extraction from pomegranate rind, *Industrial Crops and Products*, 37 (2012) 408-414, doi:10.1016/j.indcrop.2011.12.032
95. T. Bechtold, A. Turcanu, E. Ganglberger, S. Geissler, Natural dyes in modern textile dyehouses- how to combine experiences of two centuries to meet the demands of the future?, *Journal of Cleaner Production*, 11 (2003) 499-509, doi:10.1016/S0959-6526(02)00077-X
96. M. Yusuf, F. Mohammad, M. Shabbir, M. A. Khan, Eco-dyeing of wool with *Rubia cordifolia* root extract: Assessment of the effect of *Acacia catechu* as biomordant on color and fastness properties, *Textiles and Clothing Sustainability*, 2(10) (2016) 1-9, DOI 10.1186/s40689-016-0021-6
97. R. Mongkholrattansit, C. Saiwan, N. Rungruangkitkrai, N. Punrattanasin, K. Sriharuksa, C. Klaichoi, M. Nakpathom, Ecological dyeing of silk fabric with lac dye by using padding techniques, *The Journal of The Textile Institute*, 106(10) (2015) 1106-1114, <http://dx.doi.org/10.1080/00405000.2014.976957>
98. P. Kongkachuichay, A. Shitangkoon, N. Chinwongamorn, Thermodynamics of adsorption of laccic acid on silk, *Dyes and Pigments*, 53 (2002) 179-185, PII: S0143-7208(02)00014-1

99. B. Wei, Q.-Y. Chen, G. Chen, R.-C. Tang, J. Zhang, Adsorption properties of Lac Dyes on Wool, Silk and Nylon, *Journal of Chemistry*, 2013 (2013) 1-6, <http://dx.doi.org/10.1155/2013/546839>
100. Y. Nishizaki, K. Ishizuki, H. Akiyama, A. Tada, N. Sugimoto, K. Sato, Preparation of a Ammonia-Treated Lac Dye and Structure Elucidation of Its Main Component, *Food Hygiene and Safety Sciences*, 57(6) (2016) 193-200.
101. L. Liu, J. Zhang, R.-C. Tang, Adsorption and functional properties of natural lac dye on chitosan fiber, *Reactive & Functional Polymers*, 73 (2013) 1559-1566, <http://dx.doi.org/10.1016/j.reactfunctpolym.2013.08.007>
102. R. Mongkholrattanasit, C. Saiwan, N. Rungruangkitkrai, N. Punrattanasin, K. Sriharuksa, M. Nakpathom, The effect of Alum, Ferrous, Stannous and NaCl on Silk Fabric Dyed with Natural Dye from *Laccifer lacca* Kerr, *Applied Mechanics and Materials*, 848 (2016) 141-144, [doi:10.4028/www.scientific.net/AMM.848.141](http://dx.doi.org/10.4028/www.scientific.net/AMM.848.141)
103. S. Jose, H. G. Prabu, L. Ammayappan, Eco-Friendly Dyeing of Silk and Cotton Textiles Using Combination of Three Natural Colorants, *Journal of Natural Fibers*, 14(1) (2017) 40-49, DOI: 10.1080/15440478.2015.1137530
104. P. S. Vankar, R. Shanker, Ecofriendly ultrasonic natural dyeing of cotton fabric with enzyme pretreatments, *Desalination*, 230 (2008) 62-69, [doi:10.1016/j.desal.2007.11.016](http://dx.doi.org/10.1016/j.desal.2007.11.016)

105. S. A. Jabasingh, P. Sahu, A. Yimam, Enviro-friendly biofinishing of cotton fibers using *Aspergillus nidulans* AJSU04 cellulases for enhanced uptake of Myrobalan dye from *Terminalia chebula*, *Dyes and Pigments*, 129 (2013) 129-140, <http://dx.doi.org/10.1016/j.dyepig.2016.02.019>
106. M. Shabbir, L. J. Rather, S.-U. Islam, M. N. Bukhari, M. Shahid, M., M. A. Khan, F. Mohammad, An eco-friendly dyeing of woolen yarn by *Terminalia chebula* extract with evaluations of kinetic and adsorption characteristics, *Journal of Advanced Research*, 7 (2016) 473-482, <http://dx.doi.org/10.1016/j.jare.2016.03.006>
107. R. Poorniammal, M. Parthiban, S. Gunasekaran, R. Murugesan, G. Thilagavathi, Natural dye production from *Thermomyces* sp fungi for textile application, *Indian Journal of Fibre & Textile Research*, 38 (2013) 276-279.
108. M. U. Ozgur, Z. O. Acikgoz, B. Y. Sahinbaskan, G. Gumrukcu, Woolen Fabric Dyeing with *Punica granatum* L. Rind by Using Different Mordants, *Asian Journal of Chemistry*, 24(4) (2013) 1956-1964, <http://dx.doi.org/10.14233/ajchem.2013.13251>
109. S. Adeel, S. Ali, I. A. Bhatti, F. Zsila, Dyeing of Cotton Fabric using Pomegranate (*Punica granatum*) Aqueous Extract, *Asian Journal of Chemistry*, 21(5) (2009) 2493-2499.
110. S. Ali, S. Jabeen, T. Hussain, S. Noor, U. H. Siddiqua, Optimization of extraction condition of natural dye from pomegranate peels using response surface methodology, *International Journal of Engineering Sciences and Research Technology*, 5(7) (2016) 542-548.

111. K. Sinha, K. Aikat, P. Das, S. Datta, Dyeing of Modified Cotton Fiber with Natural *Terminalia arjuna* Dye: Optimization of Dyeing Parameters Using Response Surface Methodology, *Environmental Progress and Sustainable Energy*, 35(3) (2016) DOI 10.1002/ep
112. P. Nacowong, S. Saikrasun, Thermo-oxidative and weathering degradation affecting coloration performance of lac dye, *Fashion and Textiles*, 3(18) (2016) 1-16, DOI 10.1186/s40691-016-0070-0
113. A. Johnson, *The Theory of coloration of textiles*, 2nd edition, Society of Dyers and Colourists, Bradford (1989) pp. 53-60, 263-266.
114. AATCC Technical Manual, American Association of Textile Chemists and Colorists, New California (2004).
115. M. A. Bonet-Aracil, P. Diaz-Garcia, E. Bou-Belda, N. Sebastia, A. Montoro, R. Rodrigo, UV protection from cotton fabrics dyed with different tea extracts, *Dyes and Pigments*, 2016, Vol. 134, pp. 448-452, <http://dx.doi.org/10.1016/j.dyepig.2016.07.045>
116. G. K. Priya, M. M. A. Javid, A. George, M. Aarthy, S. D. Anbarasan, N. R. Kamini, M. K. Gowthaman, R. Aravindhani, S. Ganesh, R. Chandrasekar, N. Ayyadurai, Next generation greener leather dyeing process through recombinant green fluorescent protein, *Journal of Cleaner Production*, 126 (2016) 698-706, <http://dx.doi.org/10.1016/j.jclepro.2016.03.105>
117. A. K. Gupta, *Characterization of polymers and fibres*, *Manufactured Fibre Technology*, ed. By Gupta, V.B. and Kothari, V.K., 1st edition, Chapman & Hall, London (1997) pp. 203-247.

118. D. Grifoni, L. Bacci, G. Zipoli, L. Albanese, F. Sabatini, The role of natural dyes in the UV protection of fabrics made of vegetable fibres, *Dyes and Pigments*, 91 (2011) 279-285, doi:10.1016/j.dyepig.2011.04.006
119. M. Yamen, S. Ozkaya, N. Vasanthan, Structural and Conformational Changes During Thermally-Induced Crystallization of Poly(trimethylene terephthalate) by Infrared Spectroscopy, *Journal of Polymer Science: Part B: Polymer Physics*, 46 (2008) 1497-1504, DOI 10.1002/polb
120. M. P. Gashti, A. Pournaserani, H. Ehsani, M. P. Gashti, Surface oxidation of cellulose by ozone-gas in a vacuum cylinder to improve the functionality of fluoromonomer, *Vacuum*, 91 (2013) 7-13, <http://dx.doi.org/10.1016/j.vacuum.2012.10.015>
121. D. C. Montgomery, *Design and Analysis of Experiments*, 8th edition, John Wiley & Sons, Inc., New York (2013) pp. 65-138, 183-303, 440-443 & 478-553.
122. K. C. Bedin, S. P. de Azevedo, P. K. T. Leandro, A. L. Cazetta, V. C. Almeida, Bone char prepared by CO₂ atmosphere: Preparation optimization and adsorption studies of Remazol Brilliant Blue R, *Journal of Cleaner Production*, 161 (2017) 288-298, <http://dx.doi.org/10.1016/j.jclepro.2017.05.093>
123. K. Sinha, S. Chowdhury, P. D. Saha, S. Datta, Modeling of microwave-assisted extraction of natural dye from seeds of *Bixa Orellana* (Annatto) using response surface methodology (RSM) and artificial neural network (ANN), *Industrial Crops and Products*, 41 (2013) 165-171, <http://dx.doi.org/10.1016/j.indcrop.2012.04.004>

124. K. Sinha, P. D. Saha, S. Datta, Extraction of natural dye from petals of Flame of forest (*Butea monosperma*) flower: Process optimization using response surface methodology (RSM), *Dyes and Pigments*, 94 (2012) 212-216, doi:10.1016/j.dyepig.2012.01.008
125. I. Elksibi, W. Haddar, M. B. Ticha, R. Gharbi, M. F. Mhenni, Development and optimisation of a non conventional extraction process from olive solid waste using response surface methodology (RSM), *Food Chemistry*, 161 (2014) 345-352, <http://dx.doi.org/10.1016/j.foodchem.2014.03.108>
126. M. Yolmeh, M. B. H. Najafi, R. Farhoosh, Optimisation of ultrasound-assisted extraction of natural pigment from annatto seeds by response surface methodology (RSM), *Food Chemistry*, 155 (2014) 319-324, <http://dx.doi.org/10.1016/j.foodchem.2014.01.059>
127. Hearle, J. W. S. & Morton, W. E., *Physical properties of textile fibres*, 4th. edition, Woodhead Publishing, London (2008) 274-321.